

**CHARACTERIZATION OF THE ANTILITHIATIC
PROTEINS FROM *TERMINALIA ARJUNA* AND
EVALUATION OF THEIR CYTOPROTECTIVE ROLE
ON OXALATE-INDUCED RENAL TUBULAR
EPITHELIAL CELL INJURY**

**THESIS SUBMITTED IN FULFILLMENT OF THE REQUIREMENT FOR
THE DEGREE OF DOCTOR OF PHILOSOPHY
IN
BIOTECHNOLOGY**

**By
AMISHA MITTAL
Enrollment No.: 126564**



**JAYPEE UNIVERSITY OF INFORMATION TECHNOLOGY
WAKNAGHAT
AUGUST 2016**

Copyright

@

JAYPEE UNIVERSITY OF INFORMATION TECHNOLOGY

WAKNAGHAT

AUGUST 2016

ALL RIGHTS RESERVED

DECLARATION

I hereby declare that:

- a) The work contained in this thesis is original and has been done by me under the guidance of my supervisor and co-supervisor.
- b) The work has not been submitted to any other organization for any degree or diploma.
- c) Wherever, I have used materials (data, analysis, figures or text), I have given due credit by citing them in the text of the thesis.

Amisha Mittal

Date:

Enrollment No.: 126564

Department of Biotechnology and Bioinformatics

Jaypee University of Information Technology,

Waknaghat, H.P.

India

CERTIFICATE

This is to certify that the thesis entitled, “**Characterization of the antilithiatic proteins from *Terminalia arjuna* and evaluation of their cytoprotective role on oxalate-induced renal tubular epithelial cell injury**”, which is being submitted by **Amisha Mittal (Enrollment No.: 126564)** in the fulfillment for the award of degree of **Doctor of Philosophy in Biotechnology at Jaypee University of Information Technology, Waknaghat, India** is the record of candidate’s own work carried out by her under our supervision. This work has not been submitted partially or wholly to any other University or Institute for the award of this or any other degree or diploma.

Dr. Hemant Sood

Date:

(Supervisor)

Assistant Professor (Senior Grade)

Department of Biotechnology and Bioinformatics

Jaypee University of Information Technology

Waknaghat, H.P.

India

Prof. (Dr.) Chanderdeep Tandon

Date:

(Co-Supervisor)

Director and Professor

Amity Institute of Biotechnology

Amity University Campus

Noida, U.P.

India

ACKNOWLEDGEMENT

Well, the list of the people I need to thank will not fit to a single acknowledgement section. Firstly, I would like to offer my prime heartfelt salutations at the lotus feet of the Supreme Being for the strength, courage and perseverance bestowed upon me to accomplish my dreams with such glory and success. This thesis has been kept on track and been seen through to completion with the support and encouragement of numerous people including my parents, well-wishers, friends, colleagues and various institutions. At the end of my thesis, I would like to thank all those people who made this thesis possible and an unforgettable experience for me.

*My first debt of gratitude must go to my Co-supervisor, **Prof. (Dr.) Chanderdeep Tandon**, for all the support and motivation throughout this journey. His positive attitude, deep scientific vision and faith in me inspired me for doing research with a multi-tasking approach. His valuable suggestions enrich my growth as a student, researcher and a person. I would like to extend a word of thanks to **Dr. Simran Tandon**, for all her guidance during my cell line work and also for her timely inputs and moral support. I owe her my heartfelt appreciation.*

*Special thanks to my supervisor, **Dr. Hemant Sood**, for her support, guidance, motivation and helpful suggestions. She encouraged me throughout my Ph.D. work and her guidance has served me well.*

*I express my earnest gratitude to **Prof. (Dr.) R.S. Chauhan** (Dean, Dept. of Biotechnology and Bioinformatics, JUIT), for his constructive comments, support he bestowed and for setting up good standards of research for the department.*

*I earnestly express my deep gratitude to **JUIT administration**, **Prof. (Dr.) S. C. Saxena** (Vice Chancellor, JUIT), **Brig. (Retd.) Balbir Singh** (Director, JUIT), **Prof. (Dr.) T.S. Lamba** (Dean of Academic & Research) for providing opportunity to pursue a Doctorate Degree and advanced lab infrastructure to accomplish this scientific venture of my life.*

*I take this opportunity to sincerely acknowledge **Department of Science and Technology (DST)**, Government of India, for providing financial assistance which helped me to perform my work comfortably.*

*I am thankful to **Dr. S. K. Singh**, Department of Urology (PGIMER, Chandigarh) for providing clinical calcium oxalate stones. I would also express my gratitude to **Prof.***

*S. K. Singla for all his contributions in my research. I would like to thank **Dr. Arshad Jawed** for his endless support, guidance and motivation. Without his support the journey wouldn't have been possible.*

*The help rendered by all **faculty members of Department of Biotechnology and Bioinformatics**, in one way or the other, is thankfully acknowledged. I am also thankful to all the members of technical and non-technical staff of the department, especially **Mrs. Mamta Mishra, Mrs. Somlata Sharma, Mr. Ismail, Mr. Ravikant and Mr. Baleshwar** for their assistance and valuable contributions.*

*I am fortunate to have friends who have always stood beside me. I extend my heartfelt thanks to **all my friends** for their sustained support and ever needed cooperation. It is my pleasure to express my gratitude to **all research scholars** of the Biotechnology and Bioinformatics Department for keeping me blessed with best wishes.*

*Last but not least, I would like to pay high regards to my **grandparents, parents and brother Nimesh Mittal**, for their sincere encouragement and inspiration throughout my research work and lifting me uphill this phase of life. I owe everything to them.*

To all acknowledged, I solemnly owe this work.

I would like to express my heartfelt gratitude to all those who have contributed directly or indirectly towards obtaining my doctorate degree and apologize if I have missed out anyone. Last, but not the least, I thank the one above all of us, omnipresent God, for answering my prayers, for giving me strength to plod on during each and every phase of my life.

All may not be mentioned, but no one is forgotten.

Amisha Mittal

Date:

TABLE OF CONTENT

CONTENT	Page No.
DECLARATION	III
CERTIFICATE	IV
ACKNOWLEDGEMENT	V-VI
LIST OF FIGURES	XV-XX
LIST OF TABLES	XXI
LIST OF ABBREVIATIONS	XXII-XXIV
ABSTRACT	1-3
CHAPTER 1: INTRODUCTION	4-8
CHAPTER 2: REVIEW OF LITERATURE	9-53
2.1 Urolithiasis	9
2.1.1 Overview	9
2.1.2 Renal function	9
2.2 Crystalluria and stone morphology	11
2.2.1 Calcium oxalate stones	12
2.2.2 Calcium phosphate stones	13
2.2.3 Struvite stones	14
2.2.4 Uric acid stones	14
2.2.5 Cystine stones	15
2.2.6 Matrix	15
2.2.7 Other	16
2.3 Epidemiological risk factors for stone disease	16
2.3.1 Age, sex and racial differences	16
2.3.2 Climate and season	16
2.3.3 Geography	17
2.3.4 Occupation	17
2.3.5 Nutritional aspects	18
2.3.5.1 Diet	18
2.3.5.2 Fluid intake	19
2.3.5.3 Body weight	20

2.3.6 Hypertension	20
2.3.7 Metabolic abnormalities	20
2.3.8 Inheritance and family recurrence	20
2.4 Pathophysiological risk factors for stone disease	21
2.4.1 Hypercalciuria	21
2.4.1.1 Absorptive hypercalciuria	22
2.4.1.2 Renal hypercalciuria	22
2.4.1.3 Resorptive hypercalciuria	23
2.4.2 Hypocitraturia	23
2.4.3 Hyperoxaluria	24
2.4.4 Hyperuricosuria	25
2.4.5 Gouty diathesis	26
2.5 Mechanism of renal stone formation	26
2.5.1 Extracellular events	27
2.5.1.1 Urinary supersaturation and crystallization	27
2.5.1.2 Crystal nucleation	28
2.5.1.3 Crystal growth	29
2.5.1.4 Crystal aggregation	30
2.5.1.5 Crystal retention	31
2.5.2 Cellular events to oxalate exposure	31
2.5.2.1 Crystal-cell interaction	32
2.5.2.2 Renal epithelial injury and crystal nucleation	32
2.5.2.3 Attachment of CaOx crystals to renal tubular epithelial cells	33
2.5.2.4 Endocytosis of CaOx crystals by renal tubular epithelial cells and cell proliferation	35
2.5.2.5 Migration of inflammatory cells into the interstitium	37
2.5.2.6 Activation of Phospholipase A ₂	38
2.5.2.7 Activation of Neutral Sphingomyelinase	39
2.5.2.8 Alterations of mitochondrial function and cellular redox state	39
2.5.3 Adaptive response to oxalate	41

2.5.3.1 Increased expression of early response genes and cellular proliferation	41
2.5.3.2 Increased expression of proteins regulating crystal binding	41
2.5.3.3 Apoptotic and necrotic cell death promote crystal nucleation and attachment	42
2.5.4 Signaling pathways	42
2.6 Clinical diagnosis of kidney stones	44
2.6.1 Medical and nutrition evaluation of kidney stones	45
2.6.2 Interpretation of biochemical and urine tests	45
2.6.2.1 The 24-hour urine collection	45
2.7 Treatment of kidney stones	46
2.7.1 Surgical treatment	47
2.7.1.1 Extracorporeal shock wave lithotripsy	47
2.7.1.2 Ureteroscopy	47
2.7.1.3 Percutaneous nephrolithotomy	48
2.7.1.4 Open surgery	48
2.7.2 Dietary management	48
2.7.3 Medical treatment	49
2.8 Phytotherapy	50
2.8.1 Proteins: potent antiurolithiatic biomolecules	50
2.9 Terminalia arjuna	51
2.9.1 Botanical description	51
2.9.2 Geographical distribution	52
2.9.3 Traditional uses	52
2.9.4 Pharmacology	53
CHAPTER 3: MATERIAL AND METHODS	54-80
3.1 Antiurolithiatic potential of aqueous extract of Terminalia arjuna in vitro	54
3.1.1 Plant	54
3.1.2 Preparation of the aqueous extract of Terminalia arjuna	54
3.1.3 Preparation of the aqueous extract of Ayurvedic compound: Cystone drug	54

3.1.4 Calcium oxalate crystallization assay	55
3.1.5 CaOx crystal growth assay	56
3.1.6 Image analysis of crystal morphology	57
3.1.7 Determination of free radical scavenging by DPPH assay	58
3.2 Diminution of oxalate-induced renal tubular epithelial cell injury by aqueous extract of <i>Terminalia arjuna</i>	59
3.2.1 Preparation of the aqueous extract of <i>Terminalia arjuna</i>	59
3.2.2 Cell lines	59
3.2.3 Cell culture	59
3.2.4 Oxalate-induced cell injury	59
3.2.5 Cell viability	59
3.2.5.1 Trypan blue exclusion assay	60
3.2.5.2 MTT assay	61
3.2.5.3 CaOx crystal adhesion	62
3.2.6 Detection of apoptosis	63
3.2.6.1 Hoechst 33258 staining	63
3.2.6.2 Annexin V/Propidium Iodide staining by flow cytometry	64
3.2.6.3 Active Caspase-3 by flow cytometry	65
3.3 Purification of antilithiatic proteins from <i>Terminalia arjuna</i>	67
3.3.1 Materials	67
3.3.2 Extraction	67
3.3.3 Separation of biomolecules on the basis of their molecular weight	67
3.3.4 Protein concentration	67
3.3.5 Anion exchange chromatography	68
3.3.6 Molecular sieve chromatography	71
3.3.7 Electrophoresis	73
3.3.7.1 SDS-PAGE	73
3.3.7.2 Native-PAGE	75
3.3.7.3 Silver staining	77
3.4 Characterization of purified antilithiatic proteins	78
3.4.1 Materials	78

3.4.2 Reverse phase HPLC (RP-HPLC) for protein homogeneity	78
3.4.3 Peptide mass fingerprinting	79
3.4.4 Peptide matching	79
3.4.5 Putative function and domain prediction	79
3.5 Cytoprotective effect of antilithiatic proteins of <i>Terminalia arjuna</i> on oxalate-induced renal tubular epithelial cell injury	80
3.5.1 Sample preparation	80
3.5.2 Cell viability	80
3.5.3 Detection of apoptosis	80
3.6 Statistical analysis	80
CHAPTER 4: RESULTS	81-153
4.1 Antiurolithiatic potential of aqueous extract of <i>Terminalia arjuna</i> in vitro	81
4.1.1 Effect of aqueous extract of <i>Terminalia arjuna</i> on the calcium oxalate (CaOx) crystallization	81
4.1.2 Effect of aqueous extract of <i>Terminalia arjuna</i> on the growth of calcium oxalate (CaOx) crystal	82
4.1.3 Effect of aqueous extract of <i>Terminalia arjuna</i> on the calcium oxalate (CaOx) crystal morphology	83
4.1.4 Effect of aqueous extract of <i>Terminalia arjuna</i> on the scavenging of DPPH radical	84
4.2 Diminution of oxalate-induced renal tubular epithelial cell injury by aqueous extract of <i>Terminalia arjuna</i>	85
4.2.1 Cell viability	85
4.2.1.1 Effect of aqueous extract of <i>Terminalia arjuna</i> on oxalate-induced renal tubular cell injury by trypan blue exclusion assay	86
4.2.1.2 Effect of aqueous extract of <i>Terminalia arjuna</i> on oxalate-induced renal tubular cell injury by MTT assay	88
4.2.1.3 Effect of aqueous extract of <i>Terminalia arjuna</i> on calcium oxalate (CaOx) crystal adherence on	90

oxalate-induced renal tubular epithelial cell injury	
4.2.2 Detection of apoptosis	94
4.2.2.1 Effect of aqueous extract of <i>Terminalia arjuna</i> on induction of apoptosis in oxalate-induced renal cell injury by Hoechst staining	94
4.2.2.2 Effect of aqueous extract of <i>Terminalia arjuna</i> on induction of apoptosis in oxalate-induced renal injury by flow cytometry using Annexin V/PI staining	98
4.2.2.3 Effect of aqueous extract of <i>Terminalia arjuna</i> on induction of apoptosis in oxalate-induced renal cell injury by detecting Active Caspase-3 by flow cytometry	102
4.3 Extraction of proteins from <i>Terminalia arjuna</i> bark	106
4.3.1 Effect of whole protein extract of <i>Terminalia arjuna</i> on the calcium oxalate (CaOx) crystallization	106
4.3.2 Effect of whole protein extract of <i>Terminalia arjuna</i> on the growth of calcium oxalate (CaOx) crystal	107
4.3.3 Effect of <3 kDa fraction of <i>Terminalia arjuna</i> on the calcium oxalate (CaOx) crystallization	108
4.3.4 Effect of <3 kDa of <i>Terminalia arjuna</i> on the growth of calcium oxalate (CaOx) crystal	109
4.3.5 Effect of >3 kDa fraction of <i>Terminalia arjuna</i> on the calcium oxalate (CaOx) crystallization	110
4.3.6 Effect of >3 kDa of <i>Terminalia arjuna</i> on the growth of calcium oxalate (CaOx) crystal	111
4.3.7 SDS-PAGE of >3 kDa fraction of <i>Terminalia arjuna</i>	112
4.4 Purification of antilithiatic proteins from <i>Terminalia arjuna</i>	113
4.4.1 Purification of potent proteins by anion exchange chromatography and their effect on the calcium oxalate (CaOx) crystallization and growth of calcium oxalate (CaOx) crystals	113
4.4.2 Purification of potent proteins by molecular sieve	116

chromatography and their effect on the calcium oxalate (CaOx) crystallization and growth of calcium oxalate (CaOx) crystals	
4.5 Characterization of purified antilithiatic proteins	124
4.6 Cytoprotective effect of >3 kDa fraction and purified proteins of <i>Terminalia arjuna</i> on oxalate-induced renal tubular epithelial cell injury	131
4.6.1 Cell viability	131
4.6.1.1 Effect of >3 kDa fraction and purified proteins of <i>Terminalia arjuna</i> on oxalate-induced renal tubular cell injury by MTT assay	131
4.6.1.2 Effect of >3 kDa fraction and purified proteins of <i>Terminalia arjuna</i> on calcium oxalate (CaOx) crystal adherence on oxalate-induced renal tubular epithelial cell injury	134
4.6.2 Detection of apoptosis	138
4.6.2.1 Effect of >3 kDa fraction and purified proteins of <i>Terminalia arjuna</i> on induction of apoptosis in oxalate-induced renal cell injury by Hoechst staining	138
4.6.2.2 Effect of >3 kDa fraction and purified proteins of <i>Terminalia arjuna</i> on induction of apoptosis in oxalate-induced renal injury by flow cytometry using Annexin V/PI staining	142
4.6.2.3 Effect of >3 kDa fraction and purified proteins of <i>Terminalia arjuna</i> on induction of apoptosis in oxalate-induced renal cell injury by detecting Active Caspase-3 by flow cytometry	148
CHAPTER 5: DISCUSSION	154-165
5.1 Antiurolithiatic potential of aqueous extract of <i>Terminalia arjuna</i> in vitro	156
5.2 Diminution of oxalate-induced renal tubular epithelial cell	157

injury by aqueous extract of <i>Terminalia arjuna</i>	
5.3 Purification and characterization of antilithiatic proteins from <i>Terminalia arjuna</i>	159
CHAPTER 6: CONCLUSION	166-169
REFERENCES	170-198
LIST OF PUBLICATION	199-200

LIST OF FIGURES

Figure No.	Title	Page No.
Figure 1.1	Schematic representation of the bioactivity guided purification and characterization of the antilithiatic proteins from the bark of <i>Terminalia arjuna</i>	8
Figure 2.1	Structure of a kidney	10
Figure 2.2	Oxalate biosynthetic pathway	25
Figure 2.3	Schematic presentation of relationships between various factors, which lead to the formation of idiopathic kidney stones	27
Figure 2.4	Schematic representation of loss of membrane phospholipid asymmetry following cell injury	33
Figure 2.5	Schematic representation of loss of cell polarity following cell or tissue injury	35
Figure 2.6	Oxalate action on renal cells	44
Figure 4.1	Effect of aqueous extract of <i>T. arjuna</i> on nucleation and aggregation of calcium oxalate crystals	82
Figure 4.2	Effect of aqueous extract of <i>T. arjuna</i> on growth of calcium oxalate crystals	83
Figure 4.3	Calcium oxalate crystals, observed under upright microscope at magnification 100X and scale bar 10 microns, formed in the metastable solution of calcium oxalate in the absence (A) and the presence of (B) cysteine (1000 µg/mL) and (C) <i>T. arjuna</i> bark aqueous extract (1000 µg/mL)	84
Figure 4.4	Effect of aqueous extract of <i>T. arjuna</i> on DPPH radicals inhibition	85
Figure 4.5	Effect of aqueous extract of <i>T. arjuna</i> on NRK-52E cell viability assessed by trypan blue exclusion assay	86
Figure 4.6	Effect of aqueous extract of <i>T. arjuna</i> on MDCK cell	87

	viability assessed by trypan blue exclusion assay	
Figure 4.7	Effect aqueous extract of <i>T. arjuna</i> on NRK-52E cell viability assessed by MTT assay	88
Figure 4.8	Effect of aqueous extract of <i>T. arjuna</i> on MDCK cell viability assessed by MTT assay. Data are mean \pm S.D of three independent observations	89
Figure 4.9	Effect of aqueous extract of <i>T. arjuna</i> on CaOx crystal adherence in oxalate induced injury to NRK-52E cells, visualized under polarization and phase contrast at magnification 20X and scale bar 100 microns	91
Figure 4.10	Effect of aqueous extract of <i>T. arjuna</i> on CaOx crystal adherence in oxalate induced injury to MDCK cells, visualized under polarization and phase contrast at magnification 20X and scale bar 100 microns	93
Figure 4.11	Effect of aqueous extract of <i>T. arjuna</i> on induction of apoptosis in oxalate induced injury to NRK-52E cells, visualized under fluorescence microscopy at magnification 20X and scale bar 100 microns	95
Figure 4.12	Effect of aqueous extract of <i>T. arjuna</i> on induction of apoptosis in oxalate induced injury to MDCK cells, visualized under fluorescence microscopy at magnification 20X and scale bar 100 microns	97
Figure 4.13	Flow cytometry analysis showing the effect of aqueous extract of <i>T. arjuna</i> on induction of apoptosis in oxalate induced injury to NRK-52E cells, visualized by AnnexinV/PI staining	99
Figure 4.14	Flow cytometry analysis showing the effect of aqueous extract of <i>T. arjuna</i> on induction of apoptosis in oxalate induced injury to MDCK cells, visualized by AnnexinV/PI staining	101
Figure 4.15	Flow cytometry analysis showing the effect of	103

	aqueous extract of <i>T. arjuna</i> on induction of apoptosis in oxalate induced injury to NRK-52E cells, visualized by Anti-Active Caspase-3 antibody staining	
Figure 4.16	Flow cytometry analysis showing the effect of aqueous extract of <i>T. arjuna</i> on induction of apoptosis in oxalate induced injury to MDCK cells, visualized by Anti-Active Caspase-3 antibody staining	105
Figure 4.17	Effect of whole protein extract of <i>T. arjuna</i> on nucleation and aggregation of calcium oxalate crystals	107
Figure 4.18	Effect of whole protein extract of <i>T. arjuna</i> on growth of calcium oxalate crystals	108
Figure 4.19	Effect of <3 kDa fraction of <i>T. arjuna</i> on nucleation and aggregation of calcium oxalate crystals	109
Figure 4.20	Effect of <3 kDa of <i>T. arjuna</i> on growth of calcium oxalate crystals	110
Figure 4.21	Effect of >3 kDa fraction of <i>T. arjuna</i> on nucleation and aggregation of calcium oxalate crystals	111
Figure 4.22	Effect of >3 kDa of <i>T. arjuna</i> on growth of calcium oxalate crystals	112
Figure 4.23	Separation of proteins. 12% SDS-PAGE of >3 kDa fraction of <i>T. arjuna</i> . Lane 1: Broad range marker (Biorad), Lane 2: >3 kDa fraction	112
Figure 4.24	Elution profile of anion exchange chromatography. Elution profile of >3 kDa protein fraction of <i>T. arjuna</i> loaded on strong anion exchanger. P1, P2 and P3 peaks were collected with a linear gradient of NaCl	114
Figure 4.25	Percentage activity of peaks of anion exchange chromatography on nucleation and aggregation of calcium oxalate crystals	114

Figure 4.26	Percentage activity of peaks of anion exchange chromatography on growth of calcium oxalate crystals	115
Figure 4.27	Separation of proteins. 12% SDS-PAGE of pooled fractions under each peak of <i>T. arjuna</i> after anion exchange chromatography. Lane 1: Broad range marker (Biorad), Lane 2: P1 (Peak1), Lane 3: P2 (Peak 2) and Lane 4: P3 (Peak 3)	115
Figure 4.28	Purification by molecular sieve chromatography. a) Elution profile of fraction Peak 1 (P1) loaded on molecular-sieve chromatography column after anion exchange chromatography; b) Elution profile of fraction Peak 2 (P2) loaded on molecular-sieve chromatography column after anion exchange chromatography; c) Elution profile of fraction Peak 3 (P3) loaded on molecular-sieve chromatography column after anion exchange chromatography	119
Figure 4.29	Bioactivity of eluted peaks of <i>T. arjuna</i> . a) Percentage activity of peaks of molecular sieve chromatography on nucleation and aggregation of calcium oxalate crystals	120
Figure 4.30	Percentage activity of peaks of molecular sieve chromatography on growth of calcium oxalate crystals	120
Figure 4.31	12% SDS-PAGE of pooled fractions under top 4 peaks with maximum activity of <i>T. arjuna</i> after molecular sieve chromatography. Lane 1: Broad range marker (Biorad), Lane 2: A1, Lane 3: B1, Lane 4: B2 and Lane: C1	121
Figure 4.32	12% Native-PAGE of pooled fractions under top 4 peaks with maximum activity of <i>T. arjuna</i> after molecular sieve chromatography. Lane 1: Broad	121

	range marker (Biorad), Lane 2: A1, Lane 3: B1, Lane 4: B2 and Lane: C1	
Figure 4.33	Homogeneity of protein from molecular sieve chromatography	123
Figure 4.34	Identification of novel proteins by MALDI-TOF MS. Peptide mass fingerprinting by MALDI-TOF MS obtained from trypsinized fraction (a) A1 (b) B1 (c) B2 (d) C1	126
Figure 4.35	Effect of >3 kDa fraction and purified proteins of <i>T. arjuna</i> on NRK-52E cell viability assessed by MTT assay	132
Figure 4.36	The effect of >3 kDa fraction and purified proteins of <i>T. arjuna</i> on MDCK cell viability assessed by MTT assay	133
Figure 4.37	Effect of >3 kDa fraction and purified proteins of <i>T. arjuna</i> on CaOx crystal adherence in oxalate induced injury to NRK-52E cells, visualized under polarization and phase contrast at magnification 20X and scale bar 100 microns	135
Figure 4.38	Effect of >3 kDa fraction and purified proteins of <i>T. arjuna</i> on CaOx crystal adherence in oxalate induced injury to MDCK cells, visualized under polarization and phase contrast at magnification 20X and scale bar 100 microns	137
Figure 4.39	Effect of >3 kDa fraction and purified proteins of <i>T. arjuna</i> on induction of apoptosis in oxalate induced injury to NRK-52E cells, visualized under fluorescence microscopy at magnification 20X and scale bar 100 microns	139
Figure 4.40	Effect of >3 kDa fraction and purified proteins of <i>T. arjuna</i> on induction of apoptosis in oxalate induced injury to MDCK cells, visualized under fluorescence	141

	microscopy at magnification 20X and scale bar 100 microns	
Figure 4.41	Flow cytometry analysis showing the effect of >3 kDa and purified proteins of <i>T. arjuna</i> on induction of apoptosis in oxalate induced injury to NRK-52E cells, visualized by AnnexinV/PI staining	144
Figure 4.42	Flow cytometry analysis showing the effect of >3 kDa and purified proteins of <i>T. arjuna</i> on induction of apoptosis in oxalate induced injury to MDCK cells, visualized by AnnexinV/PI staining	147
Figure 4.43	Flow cytometry analysis showing the effect of >3 kDa and purified proteins of <i>T. arjuna</i> on induction of apoptosis in oxalate induced injury to NRK-52E cells, visualized by Anti-Active Caspase-3 antibody staining	150
Figure 4.44	Flow cytometry analysis showing the effect of >3 kDa and purified proteins of <i>T. arjuna</i> on induction of apoptosis in oxalate induced injury to MDCK cells, visualized by Anti-Active Caspase-3 antibody staining	153

LIST OF TABLES

Table No.	Title	Page No.
Table 2.1	Types of stones	12
Table 2.2	Classification of underlying conditions in calcium stone formers	21
Table 3.1	Method used for anion exchange chromatography	70
Table 3.2	Method used for molecular sieve chromatography	72
Table 3.3	Composition of 12% resolving gel	75
Table 3.4	Composition of 5% stacking gel	75
Table 3.5	Composition of 12% resolving gel	77
Table 3.6	Composition of 5% stacking gel	77
Table 4.1	Effect of T.arjuna aqueous extract (AE) on the morphology and dimension of calcium oxalate crystals <i>in vitro</i> at a concentration of 1000 µg/mL as compared to control. Data are mean ± S.D of three independent observations	84
Table 4.2	Molecular weight of the anionic proteins	122
Table 4.3	Identified proteins using the Mascot search engine (http://www.matrixscience.com), from the data obtained from MALDI-TOF of the peaks A1, B1, B2, C1 and domains using online tool ScanProsite for domains and motifs	127
Table 4.4	Biological functions and putative functions of purified proteins	128

LIST OF ABBREVIATIONS

AGT	Alanine Glyoxylate Aminotransferase
AH	Absorptive Hypercalciuria
ALP	Alkaline phosphatase
ANOVA	Analysis of variance
AP-1	Activated protein-1
B.C.	Before Christ
BLAST	Basic local alignment search tool
Ca	Calcium
CaOx	Calcium Oxalate
CaP	Calcium Phosphate
COM	Calcium Oxalate Monohydrate
COD	Calcium Oxalate Dihydrate
c-PLA ₂	Cytosolic Phospholipase A ₂
CT	Computerized Tomography
DEAD	Aspartic acid-Glutamic acid-Alanine-Aspartic acid
DIDS	4'-4' diisothiocyano stilbene-2-2 disulphonic acid
DMEM	Dulbecco's modified Eagles's medium
DMSO	Dimethyl sulfoxide
DPPH	1, 1-diphenyl-2-picrylhydrazyl
EDTA	Ethylene diamine tetra acetic acid
ESWL	Extracorporeal Shockwave Lithotripsy
<i>et al.</i>	<i>et alia</i> (and others)
FBS	Fetal bovine serum
FN	Fibronectin
FTIR	Fourier Transform Infrared Spectroscopy
GAGs	Glycosaminoglycans
GFR	Glomerular Filtration Rate
Gla	γ -carboxyglutamic acid
GO	Glycolate oxidase
GRHPR	Glyoxalate reductase-hydroxypyruvate reductase

G3BP1	GTPase-activating protein SH3 domain binding protein 1
HA	Hyaluronic Acid
HPLC	High Pressure Liquid Chromatography
HS	Heparan Sulfate
IEGs	Immediate early genes
ITI	Inter- α -inhibitor
JNK	c-Jun N-Terminal Kinase
LDH	Lactate dehydrogenase
Lyso-PC	Lysophosphatidylcholine
MALDI-TOF	Matrix-Assisted Laser Desorption/Ionization – Time of Flight
MAPK	Mitogen activated Protein Kinase
MCP-1	Monocyte chemoattractant protein-1
MDCK	Madin-Darby Canine Kidney (Cell line)
MS	Mass Spectrometry
MTT	3-(4,5-dimethylthiazol-2-yl)-2,5-diphenyltetrazolium bromide
NADPH	Nicotinamide adenine dinucleotide phosphate
NCCS	National Centre of Cell Sciences
NPC	Nuclear pore complex
NRK-52E	Normal Rat Kidney Epithelial (Cell line)
NSAIDS	Non-Steroid Anti-Inflammatory Drugs
NUA	Nuclear pore anchor
OPN	Osteopontin
Ox	Oxalate
PCNL	Percutaneous Nephrolithotomy
PH	Primary Hyperoxaluria
PI	Propidium Iodide
PKC	Protein Kinase C
PMF	Peptide Mass Fingerprinting
PMSF	Phenylmethanesulphonylfluoride or Phenylmethylsulphonyl Fluoride
PS	Phosphatidylserine
PTH	Parathyroid Hormone
RGDS	Arginine-Glycine-Aspartic acid-Serine

RH	Renal Hypercalciuria
RP-HPLC	Reverse phase- High Pressure Liquid Chromatography
RTA	Renal Tubular Acidosis
ROS	Reactive oxygen species
SDS-PAGE	Sodium dodecyl sulphate polyacrylamide gel electrophoresis
SS	Supersaturation
<i>T. arjuna</i>	<i>Terminalia arjuna</i>
THP	Tamn-Horsfall Protein
UA	Uric acid
URS	Ureterorenoscopy
UPFT-1	Urinary Prothrombin Fragment-1
USP10	Ubiquitin- specific protease 10
UTI	Urinary Tract Infection

ABSTRACT

Kidney stones are one of the oldest and painful multifactorial disorder caused by metabolic abnormalities influencing the composition of body fluids and urine. Kidney stones are tiny hard masses of minerals that can be lodged in any part of the urinary tract, e.g., kidneys, bladder, urethra and ureter, yet during last century interestingly the incidence of its occurrence has shifted from the lower (bladder and ureter) to the upper (kidneys) urinary tract. Calcium oxalate (CaOx) has been shown to be the main component of about two third of all urinary calculi and exist in two forms as calcium oxalate monohydrate (COM) or Whewellite, and calcium oxalate dihydrate (COD) or Weddellite. COM, the thermodynamically most stable form, is observed more frequently in clinical stones than COD and has greater affinity for renal tubular cells, thus responsible for the formation of stones in the kidney. COM has been found to initiate mineralization followed by the deposition of COD on it. In addition to calcium oxalate, urinary stones have also been found to contain phosphates, uric acid, and magnesium ammonium phosphates with apatite and struvites predominating.

The mechanisms involved in the formation of urinary stones are not fully understood but it is generally agreed that urinary lithiasis is a multifaceted process involving events leading to supersaturation of urine, crystal nucleation, aggregation and growth of insoluble particles. Urine is always supersaturated with common stone forming minerals, however, the crystallization inhibiting capacity of urine does not allow urolithiasis to happen in most of the individuals, whereas, this natural inhibition is in deficit in stone formers. Also, CaOx crystal cell interaction plays a crucial role in the formation of CaOx kidney stones. The retention of microcrystals by the urothelium is considered an essential, critical step in the growth of renal calculi. Moreover, the binding of crystals to kidney epithelial cells in culture has been shown to be enhanced by previous cell injury. Several *in vitro* studies have shown that cell injury and repair, or regeneration, increase the surface expression of phosphatidylserine, sialic acid, hyaluronan, osteopontin, or the glycoprotein receptor CD44, resulting in more crystal adhesion, which may form the nidus for eventual stone formation.

Recurrent stone disease causes not only pain and distress in those affected, but it also imposes a significant economic burden from lost working days and associated healthcare costs. Minimally invasive surgery has revolutionized acute and complex

stone management, but it has not reduced recurrence rates because less invasive therapies, including extracorporeal shockwave lithotripsy (ESWL), percutaneous nephrolithotomy (PCNL) or ureteroscopy (URS), often result in incomplete stone clearance. An alternate, using phytotherapy which is advantageous, safe and culturally acceptable is being sought. Till date, various plant extracts have been studied to reduce the incidence of urolithiasis but the identification of naturally occurring calcium oxalate inhibitory biomolecules from plants was hampered in the past by limitations in identification method.

The bark of *Terminalia arjuna* (*T. arjuna*), very well known in Ayurveda for the treatment of cardiovascular diseases, possess antioxidant activity and diuretic activity. The present study is aimed at investigating the efficacy of potent antilithiatic proteins of *Terminalia arjuna* on calcium oxalate crystallization *in vitro* and their cytoprotective role on oxalate-induced renal tubular epithelial cellular injury.

The activity of aqueous extract of *Terminalia arjuna* was investigated on nucleation, aggregation and growth of the CaOx crystals as well as on oxalate induced cell injury of renal epithelial cells, Normal Rat Kidney Epithelial cells (NRK-52E) and Madin-Darby Canine Kidney cells (MDCK). *Terminalia arjuna* extract exhibited a concentration dependent inhibition of CaOx crystal nucleation and aggregation. The extract also inhibited the growth of CaOx crystals. When NRK-52E and MDCK cells were exposed to 2 mM oxalate for 48 hours, *Terminalia arjuna* extract protected the cells from the injury in a dose-dependent manner. On treatment with the different concentrations of the aqueous extract, the cell viability increased in a concentration dependent manner. Moreover, the extract prevented the interaction of the CaOx crystals with the cell surface and reduced the number of apoptotic cells. The current data suggested that *Terminalia arjuna* aqueous extract not only has a potential to inhibit nucleation, aggregation and growth of the CaOx crystals but also has a cytoprotective role.

To examine the efficacy of antilithiatic proteins of *Terminalia arjuna*, proteins were extracted from the bark of *Terminalia arjuna* as whole protein extract and fractionated into >3 kDa and <3 kDa fractions. The >3 kDa fraction exhibiting highest activity on CaOx crystal nucleation, aggregation and growth assay system was thus chosen for further studies. Also, >3 kDa fraction reduced the oxalate-induced injury to renal epithelial cells (NRK-52E and MDCK). Due to the substantial amount of inhibitory activity exhibited by >3 kDa fraction, it was further subjected to bioactivity guided

purification that included anion exchange chromatography, molecular sieve chromatography and was further validated by High pressure liquid chromatography (HPLC), (Sodium dodecyl sulphate polyacrylamide gel electrophoresis) SDS-PAGE analysis and Native-PAGE analysis. The effect of purified proteins was studied on CaOx crystallization and growth system and on oxalate injured NRK-52E and MDCK cells. These purified proteins were further characterized by Matrix-Assisted Laser Desorption/Ionization-Time of Flight-Mass Spectrometry (MALDI-TOF-MS). Nuclear pore anchor, DEAD Box ATP-dependent RNA helicase 45, Lon protease homolog 1 and Heat shock protein 90-3 were identified as novel purified anionic antilithiatic proteins from the bark of *Terminalia arjuna*. These proteins have an ability to inhibit CaOx crystallization and crystal growth as well as exhibited cytoprotective effect on NRK-52E and MDCK cells w.r.t. cell viability, CaOx crystal adherence to cells and apoptotic changes which was much more in comparison to the cytoprotective potential by aqueous extract, whole protein extract and >3 kDa fraction.

The studies with aqueous extract of *Terminalia arjuna* indicate that it has the potential of inhibiting calcium oxalate crystallization, influencing crystal-cell interaction and preventing and curing kidney stones. The studies also suggest that the purified proteins from *Terminalia arjuna* are endowed with an antilithiatic potential.

CHAPTER 1

INTRODUCTION

Among urinary tract disease, urolithiasis is the third most frequent urological afflictions affecting mankind for millennia [1]. Literature indicates that the occurrence of kidney stones dates back to pre-historic era. The oldest renal stone on record was described by Shattock in 1905 and was found in an Egyptian mummy in a tomb dating to approximately 4400 B.C. [2]. This 1.5 cm calciferous calculi lay beside the first lumbar vertebra. Stone disease affects 2-20% population worldwide with a prevalence rate of 15% in India [3, 4]. After passage of a first stone, the risk of recurrence is 40% at 5 years and 75% at 20 years [5]. The "stone belt regions" of the world are located in countries of Middle East, North Africa, the Mediterranean Regions, North Western state of India and Southern State of USA [6]. In India, two stone belt regions are observed. First, Amritsar in North, passing through Delhi and Agra ends up in UP. Second, Jamnagar in the west coast extends inwards towards Jabalpur in Central India [7]. Changes in socioeconomic conditions over time, and the subsequent changes in dietary habits, have affected not only the incidence but also the site and chemical composition of calculi. Stone composition has changed substantially over the past decades, with a progressive increase in frequency of calcium oxalate and calcium phosphate stones. Recent epidemiology studies from different continents and countries report that calcium oxalate accounts for 70% of stones, followed by calcium phosphate (~10%), struvite (~10%), uric acid (~5%), cystine (~1%), and mixed or miscellaneous (~4%) [6, 8].

It is a well-known fact that water is a pivotal element in digestion, circulation, elimination, and regulation of body temperature. A critical function of the urinary system is the maintenance of normal composition and volume of body fluid; this is accomplished by glomerular filtration, tubular reabsorption, and tubular secretion of soluble and filterable plasma components. As a result of this, urine contains water, electrolytes, minerals, hydrogen ions, electrically active ions, end products of protein metabolism, small and macromolecular organic components and other compounds not useful to the metabolism, energy requirements, or structure of the body [9]. Human urine is a complex solution containing not only calcium (Ca) and oxalate (Ox) but also

other ions and macromolecules that can interact with Ca and/or Ox and modulate crystallization. Under normal circumstances, urine will contain crystals but not stones. Some urinary constituents, referred to as inhibitors of crystal formation, enable the urine to retain more ions in solution than at the level of saturation [9].

In the study of urolithiasis, formation of CaOx kidney stones is the consequence of extracellular as well as cellular events. Extracellular events include supersaturation, crystal nucleation, growth and aggregation and occur in renal tubular lumens and renal pelvises. Cellular events occur in cells of the renal epithelium and interstitium. These include management of acid base balance, urinary citrate, oxalate, calcium, magnesium, and pH as well as response of renal epithelial cells to the changing urinary environment, particularly oxalate overload and the presence of calcium oxalate crystals. The interplay between renal epithelial cells and Ox and/or CaOx crystals alters renal cell functions, changes the extracellular environment and plays a significant role in the formation of CaOx stones [10].

The driving force for crystallization is the development of supersaturation with respect to the precipitating salt. Since most of the ions crystallizing within the urinary tract will be excreted freely, crystal formation is by no means equivalent to symptomatic stone disease. However, when crystals are retained within the kidney, they can grow to become full-size stones [11]. Crystals can be retained at many sites in the kidneys and undergo the size-enhancing process of growth and aggregation. In order for stones to be formed, not only do crystals need to be retained within the kidney, but they must be located at sites from which crystals can cause ulceration at the papillary surface to form a stone nidus. It is thought that renal tubular injury plays an important role at this point. Khan hypothesized that renal tubular injury promotes crystal retention and the development of a stone nidus on the renal papillary surface [12]. In addition, renal tubular injury enhances crystal nucleation at low supersaturation [13]. Crystal–cell interaction is the next step, and is also promoted by renal tubular injury. Since crystal formation is a common phenomenon in human urine and crystalluria per se is harmless, abnormal retention of formed particles must occur when kidney stones form. Thus, crystal–cell interactions may be highly relevant. The crystals that are internalized in the interstitium undergo growth and aggregation, and develop into renal stones.

Despite the major technical achievements for stone removal, the problem of recurrence persists. Management of stone disease depends on the size and location of the stones.

- The foremost treatment which is considered is with pain medication, as the worst pain known as colicky pain is produced in the lower back.
- The formed calculi are most commonly removed by surgical methods, but the rate of recurrence is high in this case.
- The ultrasonic energy is used to break and reduce the size of the stone to make them easily pass in urine, but this is not beneficial in all the cases as some larger stones do not respond to this energy.
- ESWL uses sound waves which are also known as shock waves to break the stones in to small pieces for their easy passage out.
- Many allopathic agents like thiazide diuretics (e.g. Hydrochlorothiazide), alkali (e.g. Potassium citrate), allopurinol, sodium cellulose phosphate (SCP), penicillamine (Cuprimine), analgesic (Diclophenac sodium), bisphosphonates, and potassium phosphate are prescribed for the management of kidney stones and their symptoms.
- *Oxalobacter Formigenes* and other probiotics are used in treating the stones formed which act by decreasing the excretion of stone forming agents such as oxalates, calcium, phosphates etc. [14].
- The ayurvedic medicine used in the treatment are Cystone, Calcuri, Chandraprabha bati, Trinapanchamool, Rencare Capsul, Patherina tablet, Ber Patthar Bhasma, Chander Prabha vati.

Development of modern techniques such as ESWL, PCNL, or URS have revolutionized surgical management of kidney stones in recent years but do not give satisfactory results as these techniques do not prevent the likelihood of new stone formation [15]. Various medicinal plants have been used since ages to treat urinary stones though the rationale behind their use is not well established through systematic and pharmacological studies, except for some composite herbal drugs and plants [16]. In recent years, numerous studies describing the therapeutic properties of extracts from different parts of various medicinal plants have been developed. Indeed, the use of such extracts as complementary and alternative medicine has lately increased, and also serves as an interesting source of drug candidates for the pharmaceutical industrial research [17].

Terminalia arjuna belonging to the family Combretaceae, is a deciduous tree found throughout India and it's thick white to pinkish-grey bark has been used in India's

native Ayurvedic system of medicine for over three centuries, primarily as a cardiac tonic [18] as shown in Figure 1.1. *Terminalia arjuna* bark helps maintain a healthy heart and reduces the effects of stress and nervousness (Himalaya herbal health care). It also promotes effective cardiac functioning and regulates blood pressure. Experimental and clinical studies revealed the beneficial effects of this plant against all sorts of conditions of cardiac failure [19], dropsy, antinfective [20], antiasthmatic and for the treatment of rheumatoid arthritis. *Terminalia arjuna* therapy for two weeks leads to significant regression of the endothelial abnormality amongst smokers [21]. The bark of *Terminalia arjuna* is also reported to inhibit nitric oxide production in murine macrophages [22]. Aqueous extract of the bark of *Terminalia arjuna* is shown to protect the liver and kidney tissues against CCl₄-induced oxidative stress probably by increasing antioxidative defense activities [23]. Casuarinin extracted from *Terminalia arjuna* attenuates H₂O₂-induced oxidative stress, decreases DNA oxidative damage and prevents the depletion of intracellular GSH in MDCK cells [24].

Keeping in view the importance of *Terminalia arjuna* and the complications arising due to the surgical treatment of kidney stones available, the study was designed to further investigate its antilithiatic potential *in vitro* and *in vivo* with the following objectives:

1. To study the aqueous extract of *Terminalia arjuna* on *in vitro* system of nucleation and aggregation for calcium oxalate and kinetics of calcium oxalate crystal growth.
2. To study the effect of the aqueous extract of *Terminalia arjuna* on the oxalate induced renal epithelial cell injury (NRK-52E and MDCK)
3. To purify, characterize and identify antilithiatic proteins from *Terminalia arjuna* by Peptide mass fingerprinting (PMF) using MALDI-TOF-MS.
4. To study the effect of antilithiatic proteins from *Terminalia arjuna* on the oxalate induced cell injury (NRK-52E and MDCK).

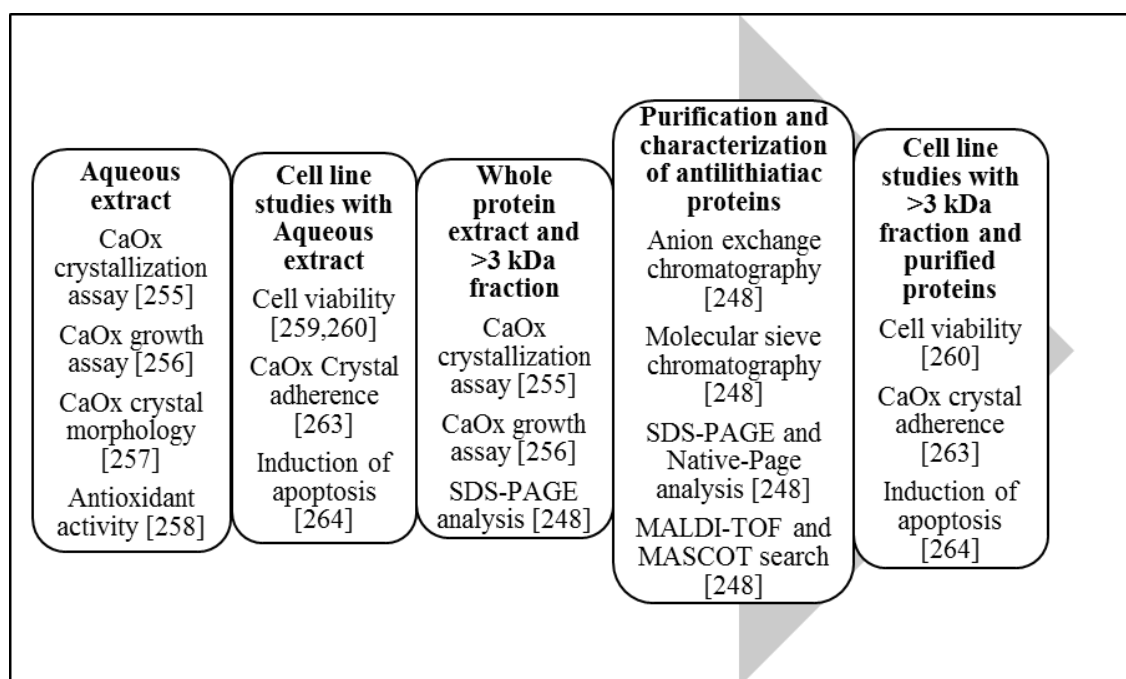


Figure 1.1 Schematic representation of the bioactivity guided purification and characterization of the antilithiatic proteins from the bark of *Terminalia arjuna*

CHAPTER 2

REVIEW OF LITERATURE

2.1 Urolithiasis

2.1.1 Overview

Kidney stone disease is a multi-factorial disorder resulting from the combined influence of epidemiological, biochemical and genetic risk factors. Nephrolithiasis, or kidney stone, is the presence of renal calculi caused by a disruption in the balance between solubility and precipitation of salts in the urinary tract and in the kidneys. The incidence is at peak among white males age 20 and 30 years old. It occurs both in men and women but the risk is generally high in men and is becoming more common in young women. The overall probability of forming stones differ in various parts of the world and is estimated as 1-5% in Asia, 5-9% in Europe, 13% in North America [25] and the recurrence rate of renal stones about 75% in 20 years span [26]. Continuous increase in cases reported in wake of GLOBAL WARMING. The researchers predict that by 2050, higher temperatures will cause an additional 1.6 million to 2.2 million kidney-stone cases, representing up to a 30 percent growth in some areas [27]. Kidney stones develop when urine becomes "supersaturated" with insoluble compounds containing calcium, oxalate (CaOx), and phosphate (CaP), resulting from dehydration or a genetic predisposition to over-excrete these ions in the urine. Kidney stones are of four types. The most common urinary stone types are calcium oxalate, calcium phosphate, uric acid, struvite (magnesium ammonium phosphate), and cystine.

2.1.2 Renal function

The physiological function of the kidneys is to excrete endogenous (e.g. creatinine, urea and oxalate) as well as exogenous (like drugs) waste products and maintaining body homeostasis. The kidneys purify toxic metabolic waste products from the blood in several hundred thousand functionally independent units called nephrons. Nephron is a functional unit of Kidney and human kidneys are composed of 1-2 million nephrons. The nephron is a specialized structure that is involved in concentration and dilution of primary urine. A nephron consists of one glomerulus and one double hairpin-shaped tubule that drains the filtrate into the renal pelvis. The glomeruli located in the kidney cortex are bordered by the Bowman's capsule. They are lined with parietal epithelial

cells and contain the mesangium with many capillaries to filter the blood. The glomerular filtration barrier consists of endothelial cells, the glomerular basement membrane and visceral epithelial cells (also known as podocytes). All molecules below the molecular size of albumin (that is, 68 kDa) pass the filter and enter the tubule, which consists of the proximal convoluted tubule, the loop of Henle and the distal convoluted tubule as shown in Figure 2.1. An intricate countercurrent system forms a high osmotic gradient in the renal medulla that concentrates the filtrate. The tubular epithelial cells reabsorb water, small proteins, amino acids, carbohydrates and electrolytes, thereby regulating plasma osmolality, extracellular volume, blood pressure and acid–base and electrolyte balance. Non-reabsorbed compounds pass from the tubular system into the collecting ducts to form urine. The space between the tubules is called the interstitium and contains most of the intrarenal immune system, which mainly consists of dendritic cells, but also of macrophages and fibroblasts [28].

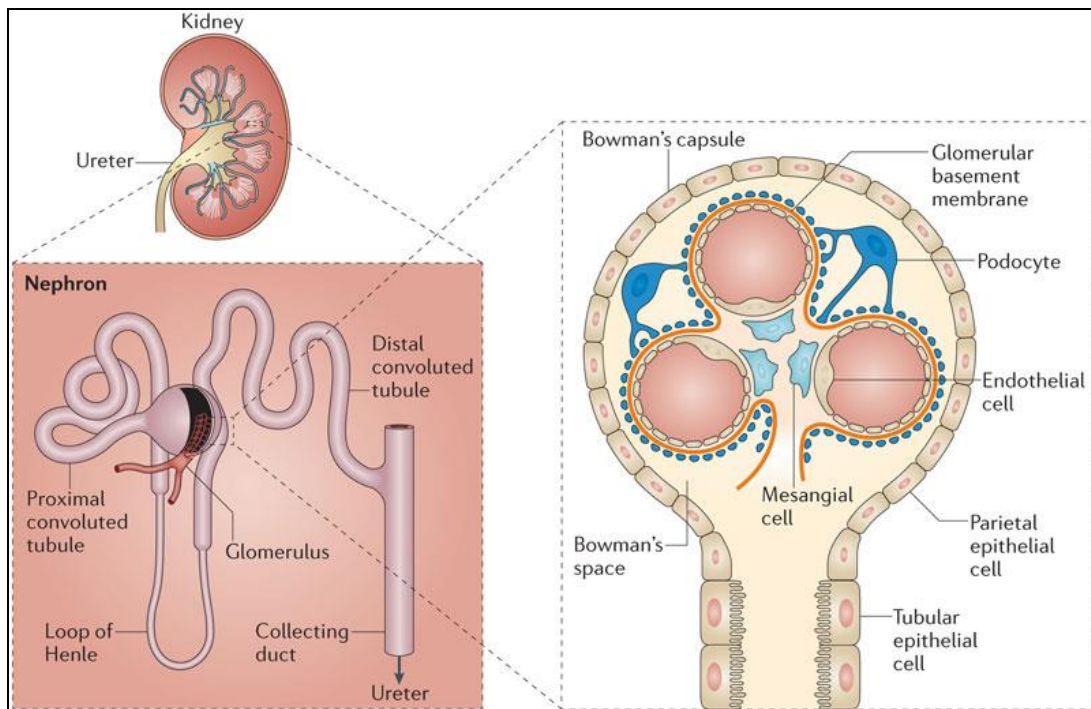


Figure 2.1 Structure of a kidney [28]

2.2 Crystalluria and stone morphology

It is well established that human urine is supersaturated with respect to ions and molecules, which can crystallize as clinical crystalluria with a potential for stone development. Regardless of the specific site of crystallization within the nephron, crystals can either pass from the kidney into the bladder and be excreted or attach to cells in the late collecting duct and grow into mature kidney stones. The crystalline composition of a stone reflects the urine chemistry and abnormalities in tubular physiology during the process of stone development. Crystalline material is the primary constituent of most human urinary tract stones. All stones contain macromolecules and other cellular components from the urine, termed matrix, and the amount of matrix normally approaches 2–5%, although some stones can be composed entirely of matrix. Most human stones contain more than one crystalline component and are termed multicomponent stones. The presence of multicomponent stones suggests multiple physiological conditions that must be unraveled in the process of defining the optimal medical management and the avoidance of stone recurrence. The major crystalline components of human urinary tract stones are listed in Table 2.1.

The levels of urinary supersaturation of different solutes determine the specific types of stones [30-32]. Many of the crystals demonstrate birefringence so observation of growth morphology is often more definitive. Calcium oxalate monohydrate can be observed as ovals or dumbbells and calcium oxalate dihydrate as bipyramids. Apatite crystals usually appear as an amorphous precipitate, and frequently grow as clumps of very small crystallites. Struvite crystals grow in a characteristic coffin lid shape. Uric acid crystals appear as flat parallelepiped plates, and cystine crystals appear as hexagonal plates.

Table 2.1 Types of stones [29]

Type	Frequency (%)	Gender (M: Male, F: Female)	Crystals shape
Calcium oxalate, mix	70-75	M	Hexagon; Dumbbell shaped; Bipyramidal envelope
Calcium phosphate (Brushite)	~10	F>M	Amorphous: Alkaline urine
Uric acid	5-10	M=F	Diamond; Acid urine
Struvite (Magnesium ammonium phosphate)	~10	F	Coffin lid; Infection/urea splitter
Cystine	~1	M=F	Hexagon

2.2.1 Calcium oxalate stones

When CaOx concentration is 4 times above the normal solubility a crystal starts to form. If the CaOx concentration is 7 to 11 times higher than normal solubility the nucleation begins. In low urine volume, the presence of high calcium and high oxalate the supersaturation (SS) of CaOx is increased. Citrate in the urine forms soluble complex with urinary Ca. If urine has low citrate concentration SSCaOx is promoted to form CaOx stone. If urine pH is less than 6.5, proportion of divalent and trivalent ions are increased then SSCaP is favorable. The levels of urinary supersaturation of the different solutes determine the specific types of stones [30-32].

Dietary oxalate may be important in stone development; spinach, beets and rhubarb in particular, contain large amounts of oxalate and they may increase urinary oxalate excretion and predispose to the development of calcium oxalate stones. High dose vitamin C therapy can also lead to increased oxalate generation as vitamin C (ascorbic acid) is metabolized. Oxalate reabsorption in the colon is reduced by the formation of insoluble calcium oxalate [33-35].

These stones are frequently hard, dark brown, and often have a dull gray exterior. Pure dihydrate stones are usually small and spherical consisting of a tan or yellow cluster of platelets. The platelets are sharp and are arranged in various orientations. Admixed monohydrate/dihydrate stones frequently have many of the characteristics of a dihydrate stone because dihydrate most frequently appears on the exterior of the admixed stone. These stones are normally larger than pure dihydrate stones, are often spherical, and have a cluster of yellow platelets surrounding a hard dark brown interior.

2.2.2 Calcium phosphate stones

Stones that contain more than 50% CaP are uncommon [36]. The major determinants of CaP supersaturation are alkaline urine pH > 6.3 combined with hypercalciuria [37]. Treatment of CaP stones is similar to that of CaOx stones in that reduced dietary sodium and protein, high fluid intake, and thiazides are effective in our experience [38], although few trials deal specifically with this group of stone formers. The role of alkali therapy in the treatment of patients with CaP stone disease is highly controversial, as the balance of risks and benefits is likely patient-dependent. Potassium alkali can raise urine citrate levels, and may reduce urine calcium, with additional direct inhibitory effects on CaP crystal formation [39]. Citrate also inhibits individual crystal growth and aggregation, a beneficial effect not reflected in supersaturation calculations. These positive effects, however, are usually accompanied by a rise in urine pH which can predispose to CaP crystallization and worsening of stone disease. Which effect will be predominant in any given patient is difficult to predict. If treatment with alkali is undertaken, completion of follow up 24 hour urines to assess these differential effects is paramount.

Pure apatite stones are usually small, white in color with a very fine granular surface. Occasionally, these stones are also light brown with a smooth shiny surface. The most frequently occurring stone admixture of apatite or calcium oxalate monohydrate and calcium oxalate dihydrate is generally smooth, spherical, and has light brown platelets on the surface. Pure brushite stones are normally clusters of beige, nodular material surrounding a crystalline interior with a cauliflower-like growth pattern. Occasionally, the surface has a yellow or white tinge [52].

2.2.3 Struvite stones

Struvite stones (also sometimes known as triple phosphate stones or infection stones) are composed of calcium magnesium ammonium phosphate and form in the presence of upper urinary tract infections with urease-producing bacteria (most commonly *Proteus*, *Providencia*, and sometimes *Klebsiella*, *Pseudomonas*, and *enterococci*). Because of their potential for rapid growth and substantial morbidity, early detection and eradication are essential [40]. Normal urine is undersaturated with ammonium phosphate; struvite stone formation occurs only when ammonia production is increased and the urine pH is elevated, which decreases the solubility of phosphate. Bacterial urease is essential for the development of struvite stones because it leads to an elevation in ammonium, carbonate and urinary pH all at the same time. The stones may also occur on infected calcium, uric acid or cystine stones, especially after instrumental procedures. Struvite stones are three times more common in women than men, presumably because urinary tract infections are more common in women. They are typically very large and may be so large as to fill the renal pelvis (forming a "Staghorn calculus"). Their growth is rapid and they often grow back after surgical removal because infected fragments of stone have been left behind [41-43]. Struvite stones are difficult to treat, and require collaboration with an expert urologist. Treatment requires both removal of all stone material and effective antibiotic therapy. Antibiotic therapy should be guided by culture of the stone itself (or renal pelvic urine obtained at the time of surgery) as well as the bladder urine [44].

Pure struvite stones are usually off-white to light brown in color with a rough textured surface. Struvite stones frequently grow in a staghorn shape. Admixed struvite/apatite stones are usually light brown in color with a coarse, granular surface. The interior is normally intermixed with white and light brown layers [52].

2.2.4 Uric acid stones

The three major factors in the development of uric acid stones are low urine volume, hyperuricosuria, and abnormally acidic urine pH. However, low urinary pH is the principle determinant in uric acid crystallization [45]. At a urinary pH of less than 5.5, uric acid is poorly soluble, but solubility increases at a pH greater than 6.5. The solubility of undissociated uric acid is only 90 mg/L. Uric acid is a weak organic acid with a pKa of 5.5. Therefore, at low urine pH, undissociated uric acid precipitates to form uric acid stones [46]. A diet rich in animal protein, because of its high purine

content, which produces uric acid in its catabolism, may increase the risk of uric acid stone formation [47, 48]. The main treatment is to increase the solubility of uric acid in urine and to reduce its concentration. Urinary alkalinization is the cornerstone of medical management of uric acid stones. Patients with known uric acid stones without significant obstruction or infection can receive a trial of oral medical dissolution, which will also serve as preventative therapy. Both potassium and sodium alkali treatment can effectively raise urinary pH, but potassium citrate is preferred over sodium citrate because sodium loads increase urinary calcium excretion.

Pure uric acid calculi are radiolucent on plain radiographs but visible on ultrasonography or computerized tomography (CT). Uric acid stones are spherical with a smooth yellow-orange surface. The surface of uric acid dihydrate stones is often dark orange and the stone is composed of small spherical regions [52].

2.2.5 Cystine stones

Cystine is an amino acid formed by the linkage of two cysteine molecules via a disulfide bond. The limited solubility of cystine can result in stone formation. Stones are generally composed of pure cystine although admixtures with calcium salts can occur rarely. Cystine solubility increases at higher urine pH [49, 50]. Urine dilution, alkalinization and chelating therapy have remained the cornerstone of the therapeutic approach. Cystine excretion may fall modestly on a sodium-restricted (<100 mmol/day) and protein-restricted (0.8 g/kg/day) diet. If stones recur despite adequate hydration and alkaline urine pH, a cysteine-binding drug should be added. Cysteine-binding drugs have sulfhydryl groups that allow them to form mixed disulfides with cysteine that are more soluble than the homodimer [51]. Recurrent stones should be analyzed, because therapy may need to be adjusted to prevent the formation of stones containing CaP due to the alkaline urine pH. Pure L-cystine stones are homogeneously composed of very small yellow spheroids.

2.2.6 Matrix

Matrix stones are noncrystalline and take on a variety of shapes and colors. The stones are composed of a variety of organic molecules including urinary macromolecules and membrane fragments [52].

2.2.7 Other

Other substances that have been reported in stones include the drugs sulfamethoxazole, crixivan, guaifenesin, triamterene and 5-fluorocytosine, xanthine, 2,8-dihydroxyadenine, gypsum, and silicates following antacid therapy. Growth morphology for these components is often variable [53].

2.3 Epidemiological risk factors for stone disease

2.3.1 Age, sex and racial differences

Men are at greatest risk of developing kidney stones with incidence and prevalence rates between two and four times that of women [54, 55]. Baker *et al.* found that the peak age for the development of calcium oxalate stones was between 50 and 60 years. Uric acid stones tended to occur in an older population with an average age of 60–65 years. Infection stones, however, occurred in younger people, most commonly in women between the ages of 20 and 55 years. A second peak is seen, particularly in men, between 55 and 70 years of age. This study also found that 70% of all stones analyzed were from men. Men were at greater risk of producing calcium oxalate stones (73% were in men) and uric acid stones (79% were in men). Women were at greater risk of infection stones (58% occur in women) [56]. Several groups have reported racial differences in the risk of developing kidney stones. Soucie *et al.* in a large cross-sectional survey in the United States found that the prevalence of kidney stones was highest among White people and lowest in Black people. Hispanic and Asian people had an intermediate prevalence [57].

2.3.2 Climate and season

Many epidemiological studies have recorded a geographic variability in the prevalence of stone disease. It has been postulated that this variability may be owing to variations in climate and sun exposure, although others have questioned the role of diet and water quality as well. The most convincing evidence to date, however, reveals temperature and sun exposure to play important roles in the geographic variability of stone disease. It has been well documented that the incidence of urinary stones is higher in countries with warm or hot climates, probably due to low urinary output and scant fluid intake. Also, in a given population, stone recurrence is higher in summer and fall than in winter and spring. It is believed that individuals living in hot climates have an increased lifetime prevalence of stone disease secondary to dehydration. Further, individuals

living in areas with increased sun exposure are likely to have absorptive Hypercalciuria secondary to elevated vitamin D synthesis [57, 58].

2.3.3 Geography

Kidney stone incidence varies in different parts of the world, high incidence areas are Scandinavian countries, Mediterranean countries, British Isles, northern Australia, central Europe, portions of the Malayan Peninsula, China, Pakistan and northern India whereas the incidence of kidney stone formation is lower in areas like Central and South America, some parts of Africa. In Asia stone-forming belt has been reported to stretch across Sudan, Saudi Arabia, the United Arab Emirates, the Islamic Republic of Iran, Pakistan, India, Myanmar, Thailand, Indonesia and Philippines [59]. In India, with a prevalence rate of 15%, two high incidence stone belts have been found to occur. The first belt starts from Amritsar in North and while passing through Delhi and Agra ends up in U.P. The other belt which starts from Jamnagar in west coast extends inwards towards Jabalpur in central India. Very low incidence areas have been in West Bengal and coastal areas of Maharashtra, Karnataka, Kerala, Tamil Nadu, Andhra Pradesh [4, 7]. The effect of geography on the incidence of stone formation may be direct, through its effect on temperature, high temperatures increase perspiration, which may result in concentrated urine, which in turn promotes increased urinary crystallization.

2.3.4 Occupation

The role of occupation in stone formation is highly debated. Kidney-related complications are on the increase because of geographic factors: residence in the stone belt, occupation related lifestyle changes - in case of indoor occupation - sedentary habits, stress, unhealthy dietary plan in terms of healthy or over healthy food intake, irregular food habits and fluid intake (intake of juices and beverages instead of water) or the other spectrum of physical manual labor - involving working outside exposed to heat and sun, low socioeconomic status, malnutrition and reduced fluid intake. Some experts speculated that this increased risk might be due to a hormone called vasopressin, which is released during stress, which increases the concentration of urine. A report suggested that manual workers had a higher incidence of urolithiasis when compared to sedentary workers [60].

2.3.5 Nutritional aspects

An unbalanced diet or particular sensitivity to various foods in stone formers can lead to urinary alterations such as hypercalciuria, hyperoxaluria, hyperuricosauria, hypocitrauria and excessive acid urinary pH. Over the course of time, these conditions contribute to the formation or recurrence of kidney stones, due to the effect they exert on the lithogenous salt profile. The fundamental aspects of the nutritional approach to the treatment of idiopathic nephrolithiasis are diet, water intake and body weight.

2.3.5.1 Diet

Diet has long been suspected to affect the incidence of stone disease. Specific dietary factors, which have been shown to have a role in stone disease, include animal protein, supplemental calcium, sodium, oxalate, and fruit juices. Excessive animal protein intake has been shown to lead to an increase in urinary excretion of calcium and uric acid, and a decrease in urinary citrate. Additionally, a recent study suggests that a diet rich in animal protein leads to an increase in urinary oxalate excretion in recurrent idiopathic calcium stone formers [61]. Animal protein induces stone formation, reports indicated operation of different mechanisms. (a) Protein contains amino acids composed of sulfur, such as cystine and methionine, which are more prevalent in animal protein. Sulfur is oxidized, yielding sulfate, which generates an acid load that is buffered by bone. The resultant osseous dissolution provides more calcium to be excreted [62, 63]. (b) Sulfate also forms a soluble complex with calcium in the nephron and limits the reabsorption of this cation. (c) Increased protein consumption augments glomerular filtration, thus delivering more calcium to the nephron [64-66]. (d) Animal protein has a high purine content, which explains the associated increase in uric acid excretion. This is a risk factor for the development of uric acid stones and may play a role in calcium stone formation. (e) Chronic metabolic acidosis induced by the increased acid load decreases calcium reabsorption within the nephron [67]. (f) The decreased urinary pH may potentiate uric acid lithiasis, and it enhances citrate reabsorption in the proximal tubules, thus decreasing the excretion of this important inhibitor of crystallization [68]. (g) The augmented oxalate excretion with increasing dietary protein reported by some investigators may be caused by generation of more glycolate, an oxalate precursor [69]. Studies investigating the role of calcium intake and stone formation differentiate dietary calcium intake from supplemental calcium, used most commonly by women [70]. In contrast to traditional belief, recent studies have

shown an inverse relationship between dietary calcium intake and the incidence of stone disease [71]. However, there also seems to be a direct relationship between the use of supplemental calcium in women and the incidence of urolithiasis. These studies hypothesize that dietary calcium binds to dietary oxalate and reduces the intestinal absorption of oxalate, thus reducing the risk for calcium oxalate stone formation. Based on this hypothesis, women are advised to take supplemental calcium only with meals. Other epidemiological studies implicate sodium and certain fruit juices with an increase in the incidence of nephrolithiasis. Increased sodium intake has been linked to increased urinary calcium excretion, and thus to increased calcium stone formation. Increases in sodium intake of 100 mmol may produce an increase in urinary calcium of 1 mmol [72]. An inverse relationship occurs between renal potassium and calcium excretion, which brings attention to the role of potassium-rich foods such as vegetables and fruits in the prevention of stone formation [73]. Potassium consumption augments renal tubular phosphate absorption, which inhibits the synthesis of 1,25-dihydroxyvitamin [74]. This results in decreased intestinal absorption of calcium, which reduces urinary calcium excretion. Another potential benefit is that foods high in potassium content are usually replete with alkali, which reflects the dietary intake of actual bicarbonate or potential bicarbonate that reduces net acid excretion and stimulates urinary citrate excretion [66].

2.3.5.2 Fluid Intake

Supersaturation of the urinary environment with stone -forming constituents is a prerequisite for calculus formation and increased fluid consumption results in excretion of higher volume of urine, which is less supersaturated with stone-forming constituents. High fluid intake is associated with a lower risk of developing kidney stones in men and women [75]. Certain beverages also appear to provide additional protection with coffee, tea, beer and wine consumption associated with reduced risk of kidney stones while grapefruit juice consumption was associated with an increased risk [75, 76]. Increased fluid intake has been demonstrated to have a positive effect on two urinary inhibitors, citrate and Tamm-Horsfall protein. Hydration augments urinary citrate excretion, which was thought to result from an increased fluid flux in the proximal tubule to the cells of this portion of the nephron. The ensuing intracellular alkalosis blunts citrate reabsorption, leading to increased excretion of citrate. Urinary dilution has been found to increase the inhibitory activity of Tamm-Horsfall protein in calcium oxalate crystal aggregation in the urine of stone patients [77, 78].

2.3.5.3 Body weight

Overweight condition and obesity was found in 59.2% of the men and 43.9% of the women and both these conditions were strongly associated with an elevated risk of stone formation in both genders due to increased urinary excretion of promoters but not inhibitors of calcium oxalate stone formation and further concluded that overweight and obese men are more prone to stone formation than overweight women. Excess body weight may be associated with various functional /structural lesions of the kidney and will lead to nephrolithiasis, glomerulomegaly, diabetic nephropathy, carcinoma of the kidney [79].

2.3.6 Hypertension

A modest association has been reported between hypertension and nephrolithiasis in both sexes. In prospective studies, people with a history of nephrolithiasis are more likely to develop hypertension [80, 81] and those with hypertension are more likely to develop kidney stones, especially when they are overweight [82].

2.3.7 Metabolic abnormalities

People who form kidney stones often have metabolic or other abnormalities detectable on urinary testing. The common abnormalities include low urinary volume, hypercalcuria (25–40%), hyperoxaluria (10–50%), hyperuricosuria (8–30%) and hypocitraturia (5–30%). There is, however, significant overlap with healthy controls who also often have biochemical ‘abnormalities’, albeit less frequently [83, 84].

2.3.8 Inheritance and family recurrence

Autosomal recessive inheritance was defined for cystinuria and primary hyperoxaluria. The reported prevalence for cystinuria is 1–5% of all patients with urolithiasis and much lower for primary hyperoxaluria (~2 per million populations) [85]. Cystinuria and primary hyperoxaluria, as well as renal tubular acidosis and Dent’s disease, are some of the different monogenic conditions that have been identified to date as etiologies for urolithiasis. However, all of these rare conditions probably account for less than 2% of renal stones. A familial occurrence has also been suggested for hypercalciuria, one of the main risk factors for idiopathic urolithiasis. However, familial recurrence does not necessarily imply an inherited transmission, as it may be an effect of environmental factors shared by family members, mainly those related to dietary habits [86].

2.4 Pathophysiological risk factors for stone disease

The basis for calcium stone formation is supersaturation of urine with stone-forming calcium salts. A number of dietary factors and metabolic abnormalities can change the composition or saturation of the urine so as to enhance stone-forming propensity. Among the metabolic conditions are hypercalciuria, hypocitraturia, hyperoxaluria, hyperuricosuria, and gouty diathesis as shown in Table 2.2, and these conditions are reviewed in detail. Dietary factors also play a role in stone occurrence, and are discussed with regard to their role in preventing stone formation [87].

Table 2.2 Classification of underlying conditions in calcium stone formers [87]

Condition	Metabolic/environmental defect	Prevalence
Hypercalciuria		
Absorptive hypercalciuria	Increased GI calcium absorption	20-40%
Renal hypercalciuria	Impaired renal calcium reabsorption	5-8%
Resorptive hypercalciuria	Primary hyperparathyroidism	3-5%
Hyperuricosuric calcium nephrolithiasis	Dietary purine excess, uric acid overproduction or overexcretion	10-40%
Hypocitraturic calcium nephrolithiasis		
Chronic diarrheal syndrome	GI alkali loss	-
Distal RTA	Impaired renal tubular acid excretion	-
Thiazide-induced	Hypokalemia and intracellular acidosis	10-50%
Hyperoxaluric calcium nephrolithiasis		
Primary hyperoxaluria	Genetic oxalate overproduction	-
Dietary hyperoxaluria	Excessive dietary intake	2-15%
Enteric hyperoxaluria	Increased GI oxalate absorption	-
Gouty Diathesis	Low urine pH	10-30%

2.4.1 Hypercalciuria

Hypercalciuria is the most common pathophysiologic risk factor in calcium stone formation. Urinary calcium raises ionic calcium concentration and increases urinary saturation of stone-forming calcium salts (CaP and CaOx). In addition, complexation of calcium with urinary inhibitors such as citrate and glycosaminoglycans reduces urinary inhibitory activity, thereby increasing stone risk. Hypercalciuria can be more precisely

classified according to the site of primary metabolic derangement, whether intestine, kidney, or bone. Accordingly, hypercalciuria can be divided into three distinct subtypes: (1) absorptive Hypercalciuria (AH), characterized by intestinal hyperabsorption of calcium; (2) renal Hypercalciuria (RH), resulting from impaired renal tubular calcium reabsorption; or (3) resorptive hypercalciuria, caused by bone demineralization [88].

Although hypercalciuria is classified according to the site of the primary defect in calcium transport, secondary changes can occur at other sites; that is, renal calcium leak leads to secondary hyperparathyroidism, which results in bone resorption and increased intestinal calcium absorption. Hypercalciuria has a rich genetic predisposition. Nearly half of patients who have Hypercalciuria have a family history of stone disease [89].

2.4.1.1 Absorptive hypercalciuria

This condition, previously referred to as idiopathic hypercalciuria, results from intestinal hyperabsorption of calcium. This increases the renal calcium load resulting in hypercalciuria and formation of stones predominantly composed of calcium oxalate or mixed calcium oxalate and calcium phosphate [90]. The disease is heterogenous and multifactorial. The positive calcium balance suppresses parathyroid hormone (PTH) secretion and increases the renal filtered load of calcium, leading to increased urinary calcium excretion. AH is classified as Type I or II, according to the response to dietary calcium restriction. AH Type I is diet-unresponsive, whereas in AH Type II, urinary calcium normalizes in response to a low calcium diet.

2.4.1.2 Renal hypercalciuria

RH is caused by impaired renal tubular reabsorption of calcium. Renal loss of calcium reduces serum calcium and secondarily stimulates PTH secretion. Consequently, increased intestinal calcium absorption caused by enhanced 1,25-[OH]₂D synthesis and mobilization of calcium from bone caused by increased PTH lead to hypercalciuria. Serum calcium remains normal because the loss of calcium in the urine is offset by enhanced intestinal calcium absorption and bone resorption. The pathogenesis of renal calcium leak is unknown. Several factors have been implicated in RH, including salt abuse and excessive urinary prostaglandins [91]. RH is relatively uncommon, occurring in approximately 9% of stone formers.

2.4.1.3 Resorptive hypercalciuria

Resorptive hypercalciuria is a rare cause of stone disease that is most commonly associated with primary hyperparathyroidism. Excessive PTH secretion from a parathyroid adenoma leads to bone resorption, increased renal synthesis of 1,25-[OH]₂D (calcitriol), and enhanced intestinal absorption of calcium [92].

2.4.2 Hypocitraturia

Citrate is the most abundant organic anion in human urine, and is a well-recognized inhibitor of stone formation. Hypocitraturia is defined as urinary citrate excretion of less than 320 mg daily, although this is a somewhat arbitrary cutoff, because the acid-base status of the patient strongly determines total citrate excretion. Hypocitraturia is a well-known risk factor for calcium nephrolithiasis, and has been identified in 20% to 60% of calcium stone formers [93].

The protective effect of citrate is threefold, arising from its buffering capacity, its ability to complex with calcium in solution, and its inhibitory activity [94]. The buffering action of citrate is manifest during an alkali challenge, such that only a small rise in urinary pH occurs with an alkali load, thereby mitigating against calcium phosphate precipitation. Secondly, as an anion, citrate forms a soluble complex with calcium, reducing the ionic activity of calcium and decreasing urinary saturation of stone-forming calcium salts (CaOx and CaP). Finally, citrate directly inhibits crystallization, aggregation, and agglomeration of CaOx and CaP, thereby further reducing stone formation.

A variety of pathologic states associated with acidosis leads to hypocitraturia. Distal renal tubular acidosis (RTA) is associated with systemic acidosis, and is characterized by high urine pH 6.8 and low serum bicarbonate and potassium [95]. Chronic diarrheal states are also associated with systemic acidosis because of alkali loss in the stool. Excessive animal protein provides an acid load that promotes bone loss and causes hypocitraturia [96]. A recent study investigating the effects of a high protein, low carbohydrate diet, typified by the Atkins' diet, demonstrated a significant reduction in urine pH and citrate during both the induction and maintenance phases of the diet. Other causes of acidosis associated with hypocitraturia are thiazide-induced hypokalemia, which produces intracellular acidosis, and vigorous exercise, which produces lactic acidosis [97]. Finally, idiopathic hypocitraturia may represent an isolated abnormality, unrelated to an acidotic state.

2.4.3 Hyperoxaluria

Hyperoxaluria is defined as urinary oxalate excretion of greater than 40 mg daily. Hyperoxaluria is thought to increase the risk of stone formation by increasing urinary saturation of CaOx. The effect of oxalate on stone formation depends on the interaction between calcium and oxalate that takes place in the intestine and urine. In the intestine, oxalate absorption is modulated by dietary oxalate and the formation of a poorly absorbed calcium-oxalate complex. In the setting of dietary calcium restriction, calcium-oxalate complex formation is reduced, thereby increasing luminal free oxalate that is absorbed from the intestine and excreted in the urine. In the urine, calcium-oxalate interaction results in formation of a soluble complex that lowers ionic oxalate concentration.

Hyperoxaluria can be associated with primary disorders in biosynthetic pathways as shown in Figure 2.2 (primary hyperoxaluria), malabsorptive states (enteric hyperoxaluria), excessive dietary oxalate intake (dietary hyperoxaluria), or high substrate levels (excessive vitamin C). Primary hyperoxaluria Type 1 is caused by a rare inherited autosomal recessive disorder in glyoxalate metabolism by which the normal conversion of glyoxalate to glycine is prevented due to the deficiency of peroxisomal enzyme AGT (Alanine Glyoxylate Aminotransferase), leading to oxidative conversion of excess glyoxalate to oxalate in the peroxisome by glycolate oxidase or by lactate dehydrogenase in the cytoplasm. Primary hyperoxaluria type 2 is a rare monogenic disorder caused by a deficiency of the enzyme glyoxylate reductase GRHPR (D-glycerate dehydrogenase or hydroxypyruvate reductase), which catalyzes the conversion of glyoxylate to glycolate. When GRHPR is deficient, more glyoxylate is oxidized to oxalate. Systemic oxalosis ensues, and leads to excretion of markedly high levels of urinary oxalate, increasing urinary saturation of CaOx and causing stone formation and nephrocalcinosis.

Oxalate-degrading bacteria such as *Oxalobacter formigenes* have been shown to colonize the intestine of normal individuals, and may reduce intestinal oxalate. Absence of these bacteria has been linked to increased urinary oxalate levels and higher rates of stone formation in stone formers [98]. The contribution of oxalate-degrading bacteria to CaOx stone formation has not been fully elucidated.

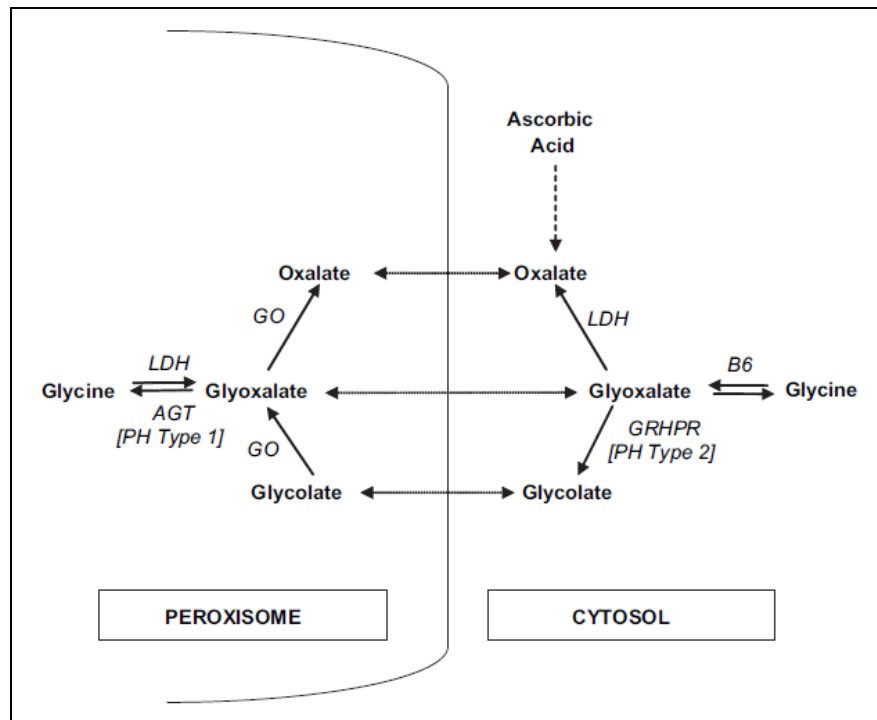


Figure 2.2 Oxalate biosynthetic pathway. Type 1 primary hyperoxaluria is caused by a deficiency in peroxisomal alanine glyoxalate aminotransferase. Type 2 primary hyperoxaluria is caused by a defect in cytosolic glyoxalate reductase/hydroxypyruvate reductase. AGT, alanine-glyoxalate aminotransferase; GRHPR, glyoxalate reductase-hydroxypyruvate reductase, GO, glycolate oxidase; LDH, Lactate dehydrogenase [87]

2.4.4 Hyperuricosuria

Hyperuricosuria can lead to CaOx stone formation by heterologous nucleation on the surface of monosodium urate crystals [99]. Hyperuricosuria is defined as urinary uric acid exceeding 600 mg daily. The most common cause of hyperuricosuria is increased dietary purine intake, because uric acid is the end product of purine metabolism. Numerous other acquired and hereditary diseases can lead to hyperuricosuria, however, including gout, myelo- and lymphoproliferative disorders, multiple myeloma, hemolytic disorders, and hemoglobinopathies.

The pathophysiology of hyperuricosuric CaOx nephrolithiasis is intimately related to urinary pH. At pH less than 5.5, poorly soluble undissociated uric acid precipitates, leading to uric acid or CaOx stone formation. At pH greater than 5.5, uric acid is found predominantly in its dissociated form, increasing urinary saturation of monosodium urate and promoting CaOx stone formation through heterogeneous nucleation [100]. Furthermore, monosodium urate has been shown to bind to urinary inhibitors, thereby

reducing urinary inhibitory activity and indirectly promoting CaOx crystallization [101].

2.4.5 Gouty diathesis

Gouty diathesis refers to uric acid stone formation associated with primary gout [102]. The invariant feature of this disorder is low urine pH, which promotes the precipitation of the sparingly soluble, undissociated form of uric acid, leading to uric acid stone formation. Gouty diathesis is also a risk factor for CaOx stone formation, however. Although uric acid, which is favored at low pH, is not as efficient as monosodium urate in promoting CaOx stone formation, it too leads to CaOx crystallization by way of heterogeneous nucleation [87].

2.5 Mechanism of renal stone formation

Formation of calcium oxalate kidney stones is the result of cellular as well as extracellular events. The interplay between renal epithelial cells and Ox and/or CaOx crystals alters renal cell functions, changes the extracellular environment and plays a significant role in the formation of CaOx stones [10]. The formation of renal stones is a consequence of increased urinary supersaturation with subsequent formation of crystalline particles. Since most of the solid particles crystallizing within the urinary tract will be excreted freely [11]. However, when solid particles are retained within the kidney, they can grow to become full-size stones. Crystals can be retained at many sites in the kidneys and undergo the size- enhancing process of growth and aggregation. In order for stones to be formed, not only do crystals need to be retained within the kidney, but they must be located at sites from which crystals can cause ulceration at the papillary surface to form a stone nidus. It is thought that renal tubular injury plays an important role at this point. Khan hypothesized that renal tubular injury promotes crystal retention and the development of a stone nidus on the renal papillary surface [12]. In addition, renal tubular injury enhances crystal nucleation at low supersaturation [13]. Crystal–cell interaction is the next step, and is also promoted by renal tubular injury. The crystals that are internalized in the interstitium undergo growth and aggregation, and develop into renal stones. Persistent mild hyperoxaluria by itself or through crystallization of CaOx is injurious to the renal epithelium [103].

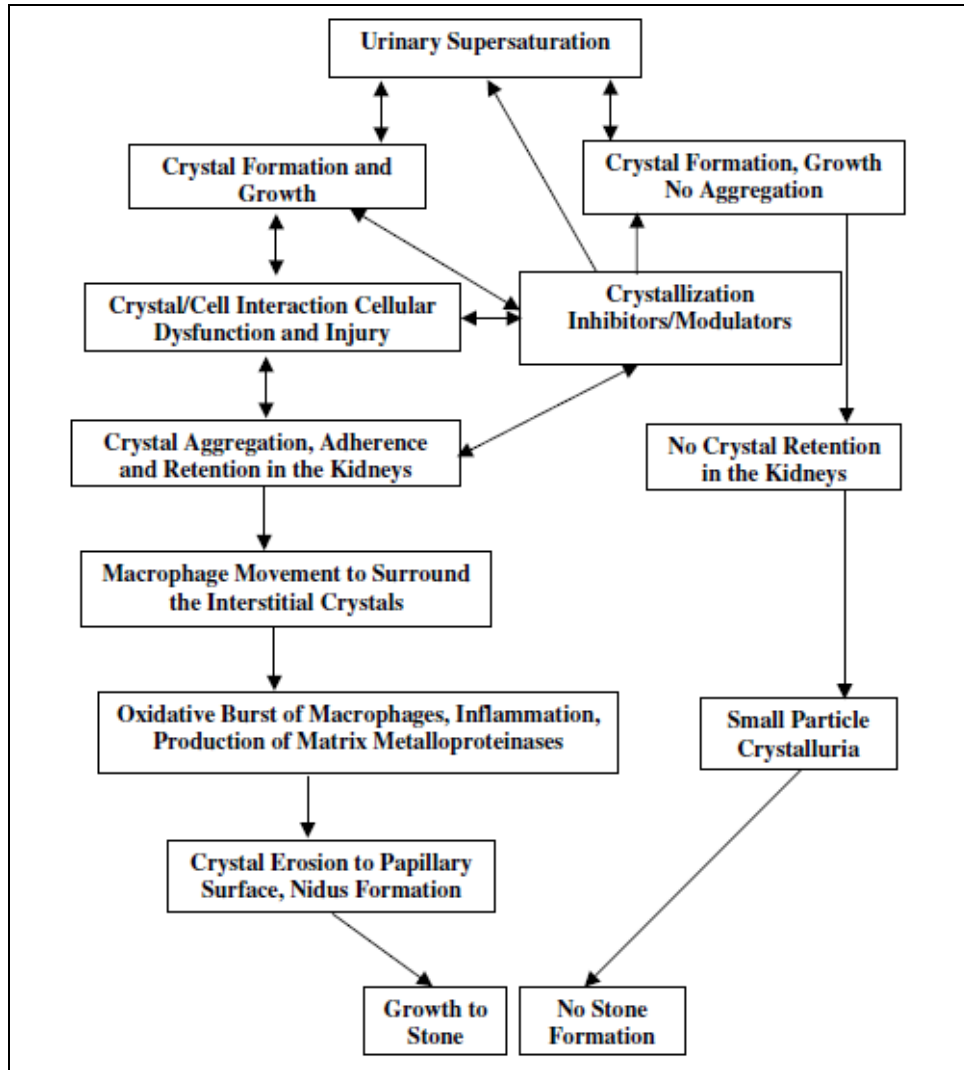


Figure 2.3 Schematic presentation of relationships between various factors, which lead to the formation of idiopathic kidney stones [104]

2.5.1 Extracellular events

Extracellular events include supersaturation, crystal nucleation, growth and aggregation and occur in renal tubular lumens and renal pelvises.

2.5.1.1 Urinary supersaturation and crystallization

The formation of kidney stones or nephrolithiasis is a result of crystal formation in the kidneys. The driving force for crystallization is the development of supersaturation with respect to the precipitating salt. Stone formers tend to excrete urine that is more supersaturated than that of non-stone formers [105-107]. It has been suggested that with a transit time across the kidney of 5–10 min, residence time is too short for crystals to nucleate and grow large enough to be trapped. The inner diameter of the various

segments of the renal tubules ranges from 15 to 60 μm . CaOx crystals, growing at the rate of 1–2 $\mu\text{m}/\text{min}$, cannot grow larger than a few microns and are therefore excreted with urine without causing stone development. In tubular fluid and urine, crystallization processes are largely dependent on solution composition. Human urine is a complex solution containing not only Ca and Ox but also other ions and macromolecules that can interact with Ca and/or Ox and modulate crystallization because of their activity as chelators. For instance, by forming soluble complexes with calcium and oxalate, respectively, citrate and magnesium reduce free ion activity and the relative supersaturation of calcium oxalate [108]. Crystals can precipitate in the urinary tract when the urine is supersaturated, i.e. when the concentration of salts is higher than what can be kept in solution. CaP can precipitate already in the loop of Henle or distal part of distal tubules, while CaOx supersaturation usually occurs later in the nephron, in the collecting ducts. CaP that is precipitated in the earlier parts of the nephron dissolves as it travels through the tubules to the collecting ducts, where the pH is lower. At that site, CaP can act as nucleation site for CaOx crystals [109-111]. On the basis of supersaturation, CaOx nucleation can first occur in the loops of juxtamedullar nephrons [112].

2.5.1.2 Crystal nucleation

The initial step in the transformation from a liquid to a solid phase in a supersaturated solution i.e. when the concentration product of the ions of the stone components is greater than the formation product, ions begin to cluster close together to form the earliest non soluble crystal structure, is called nucleation. This process begins with the coalescence of stone salts in solution into loose clusters that may increase in size by addition of new components or clusters [113]. There are two types of nucleation: homogeneous and heterogeneous. When the process occurs spontaneously in a pure solution, homogeneous nucleation results. Because impurities are always present in human urine, homogeneous nucleation is unlikely to occur *in vivo*. The surfaces provided by the impurities can serve as a nidus in the nucleation process, leading to heterogeneous nucleation.

Crystallization of calcium oxalate is thought to start through the process of heterogeneous nucleation, which is facilitated by a good fit for the calcium oxalate lattice. Formed crystals either can be excreted in the urine as crystalluria or grow and/or aggregate to become clinically significant stones. Finlayson and Reid calculated the

required time for free crystals to nucleate and grow, and concluded that before free calcium oxalate particles could grow large enough to be trapped within the renal tubules, they would be excreted in the urine rather than develop into calculi [114]. Based on the concentration profile of calcium and oxalate in the urine, tubular fluid and renal tissue, it was suggested that interstitium of the inner medulla had the highest Ox concentration and the best chance of being the primary nucleation site for CaOx [115]. CaOx crystals can, however, migrate from tubular location to the interstitium [12]. Different types of crystals tend to nucleate in different parts of the nephron. Crystal nucleation of calcium carbonate, calcium phosphate, and calcium oxalate are more likely to occur in the loop of Henle, the late distal tubule, and the collecting ducts, respectively [116].

In vitro and *in vivo* studies have shown that renal tubular cell injury can promote crystallization of CaOx crystals by providing substances for their heterogeneous nucleation. *In vitro* cell degradation following renal tubular cell injury produces numerous membrane vesicles, which have been shown to be good nucleators of calcium crystals. *In vivo* crystals observed in the renal tubules of hyperoxaluric rats are always associated with cellular degradation products [13, 117]. The stone matrix contains both membrane vesicles and lipids. Phospholipids of the cell membranes are proposed to help crystal nucleation [118]. Lipids isolated from the kidney stone matrix also promoted the nucleation of CaOx crystals. Interestingly, membranes of injured but intact cells also showed the capacity to nucleate CaOx crystals. Direct nucleation on cell surface can also promote crystal retention within the tubule [119]. Although crystal nucleation is thought to be one of the prerequisites for urolithiasis, it alone cannot explain stone disease, in which the stones are much larger than the crystal nuclei. There must, therefore, be other mechanisms for crystals to grow and be retained in the kidney to form stones before they are excreted in the urine.

2.5.1.3 Crystal growth

Crystal growth, defined as the rate of deposition of ions onto a crystal nidus, occurs at the interface between the liquid and solid phases and involves both solute transfer and interfacial processes [120]. Growth of crystals is influenced by the rate of diffusion of various solutes and by properties of the crystal surface, including surface charge. Moreover, analysis of extracts of kidney stones confirms that the urinary macromolecules are indeed incorporated into the crystal lattices of stones [121-124].

These considerations suggest that the kinetics of crystal growth *in vivo* likely differ from those *in vitro* when growth occurs in pure solutions of inorganic chemicals. Moreover, the kinetics *in vivo* may differ in different segments of the nephron since urine concentrations and composition vary in different parts of the nephron [125, 126] and since different macromolecules are produced in different regions. For example, crystals formed in the early portion of the nephron may be coated with nephrocalcin, which is produced only in proximal tubules and in the thick ascending limb of the loop of Henle [127], or with inter-alpha-inhibitor (bikunin), found in both proximal and distal tubules [128, 129]. Crystals forming later in the nephron may interact with Tamm-Horsfall glycoprotein [77], urinary prothrombin fragment 1 [130, 131] and/or osteopontin [130, 132], which are produced in the thick ascending limb of the loop of Henle and/or in the distal convoluted tubules. Since the rate of CaOx crystal growth is low and the transit time of tubular fluid through the kidney amounts to only several minutes, it has been calculated that the probability of a single particle achieving a pathophysiologically relevant size by the process of crystal growth alone is extremely low, even if growth proceeds at an uninhibited rate of 2 μm per minute [112].

2.5.1.4 Crystal aggregation

The process whereby crystals in solution stick together to form larger particles is called aggregation. According to Randolph and Drach, aggregation is the grouping of two or more particles held together by strong intermolecular forces, which cannot be dispersed by shear forces [133]. Robertson *et al.* found that recurrent calcium stone formers tend to excrete larger calcium oxalate crystals (10–20 μm in diameter) than those (3–4 μm in diameter) in nonstone formers [134]. Although crystal growth is definitely a step in CaOx renal stone formation, the process of growth is so slow that crystals cannot become large enough to obstruct the renal tubules and be retained there by this mechanism alone, as several minutes are required for the tubular fluid to pass through the kidney. For this reason, the more critical step is thought to be crystal aggregation. Kok *et al.* demonstrated that the urines from stone formers had a similar effect on the solubility, but a significantly lower ability to inhibit the crystal growth and the crystal aggregation [135]. They concluded that defective inhibition of the kinetic process of crystal aggregation constitutes a major physiochemical mechanism of calcium oxalate renal stone formation, which appears to be modulated by urinary citrate concentrations but the speed of aggregation is rapid enough to allow development of significantly sized particles within

seconds. These observations reveal the potential role of crystal aggregation in urinary stone formation. Ultrastructural examination of crystal aggregates in the kidneys, as well as urine, displays membranous cellular material closely associated with the crystals [118]. It is our understanding that cell debris, formed as a result of exposure to high concentration of Ox and CaOx crystals, collects with the crystals resulting in the formation of larger particles. Membrane lipids with properly aligned calcium-binding head groups bridge crystals together and promote crystal aggregation.

2.5.1.5 Crystal retention

Randall proposed that the calcific deposits originate in damaged renal tubule epithelial basement membranes and later erode into the urinary collecting system. These plaques, now known as Randall's plaques, are thought to serve as a nidus for urinary stone formation [136]. The exact mechanism of action is unknown but it has been postulated that the sulfur groups on glycosaminoglycan molecules will bind large quantities of water molecules forming a "water barrier" on the cell surface thereby inhibiting calcium oxalate crystal and bacterial adherence [137]. It has been postulated that the crystal adherence reaction is mediated through cell surface substances, termed crystal-binding molecules [138]. Several compounds, including phosphatidylserine (PS) [139, 140], sialic acid [141], collagen type IV [142], osteopontin [143], and hyaluronan [138], have been shown to be candidates of crystal-binding molecules. The crystal–renal cell interaction is supported by clinical observations and laboratory studies [144]. For example, endocytosis of calcium oxalate crystals was observed in a patient with type 1 primary hyperoxaluria [145]. In studies using monkey renal epithelial cells as a model of the distal tubular epithelium, COM crystals were endocytosed by the cells and cellular proliferation was induced [146, 147]. Crystals can reside in the kidneys by crystal formation in the renal interstitium, aggregating with other crystals, attachment to the renal epithelial cells after their formation in the renal tubules and not moving with the urinary flow, and growing large enough to be trapped.

2.5.2 Cellular events to oxalate exposure

Cellular events occur in cells of the renal epithelium and interstitium. These include management of acid base balance, urinary citrate, oxalate, calcium, magnesium, and pH as well as response of renal epithelial cells to the changing urinary environment, particularly oxalate overload and the presence of calcium oxalate crystals.

2.5.2.1 Crystal–cell interaction

Before crystals can turn into an actual stone, they have to be retained in the kidney. Crystals grow and aggregate to the point at which they become too large to pass through the tubular lumen and become trapped. Crystal retention in the kidney could be dependent on the interaction between crystals and the epithelium lining the renal tubules, even when crystals are small [110, 111, 114, 148]. It is hypothesized that this occurs when the epithelium lining the renal tubules becomes susceptible to crystal binding. Under pathological conditions, crystal binding molecules that are normally absent from the cell surface might be expressed, enabling crystal–cell interaction. The interaction is influenced by the type of crystal, the presence of a crystal coat, the type of cell surface, and the surface electric charge [141, 149]. Once adhered, the crystals are subsequently internalized into the epithelial cells through endocytosis; altered gene expression, cytoskeletal alterations, and cellular proliferation can then occur [144]. The process of attachment or endocytosis of crystals to renal tubular cells is what is generally meant by crystal–cell interactions. The structural characteristics of the binding and uptake of COM crystals by BSC-1 cells have been characterized by scanning electron microscopy (SEM). Microvilli on the apical cell surface appear to make initial contact with the crystal before its internalization. Transmission electron microscopy (TEM) confirmed that endocytosis of COM crystals by BSC-1 cells occurs as early as 30 min after exposure. These structural and functional studies of crystal–cell interactions in culture indicate that COM crystals rapidly adhere to microvilli on the cell surface and are subsequently internalized [150, 154].

2.5.2.2 Renal epithelial injury and crystal nucleation

Both animal models as well as tissue culture studies indicate that exposure to high levels of oxalate and CaOx crystals is injurious to renal epithelial cells [12, 155]. These effects are additive and concentration dependent leading to both apoptosis and necrosis [156]. Death, degradation, and detachment of many epithelial cells are results of cell injury. Dead epithelial cells disintegrate into membranous vesicles. *In vivo*, injury causes exposure of the basal lamina, which often becomes a site for crystal attachment. Urinary crystals are frequently associated with the membranes of cellular degradation products suggesting their involvement in crystal formation. Cell membranes are further implicated in crystallization by *in vitro* studies, which show production of CaOx crystals by incubating vesicles of isolated renal brush border membrane in metastable

solutions [157]. Cellular degradation products may also be involved in crystal retention by slowing urinary movement through the renal tubules as well as by promoting crystal aggregation and increasing the size of crystal aggregates.

2.5.2.3 Attachment of CaOx crystals to renal tubular epithelial cells

In vivo and *in vitro* studies have provided evidence for crystal retention within the kidneys via attachment to renal epithelial cells. A number of studies have demonstrated that renal epithelial cell injury promotes crystal attachment as a consequence of changes in the surface properties of affected cells and/or unmasking of attachment sites beneath or between cells. The animal model studies showed that CaOx crystals attach to cellular surfaces and basement membranes [12]. The reasons for their attachment include crystal-PS interaction and crystal-basement membrane interaction. The crystal-PS interactions could occur as a result of redistribution of PS on the cell surface of renal cells [158] that have lost their membrane lipid asymmetry as depicted in Figure 2.4. Studies indicated that redistribution of the phospholipid, phosphatidylserine (PS), to the surface of the cell can promote crystal binding. This phospholipid is normally restricted to the inner leaflet of the membrane via an ATP-dependent process that may involve the actin cytoskeleton [159]. When cells are damaged, membrane PS redistributes to the surfaces of cells, where it can serve as a binding site for CaOx crystal attachment and recognition signal for engulfment and removal by macrophages [160].

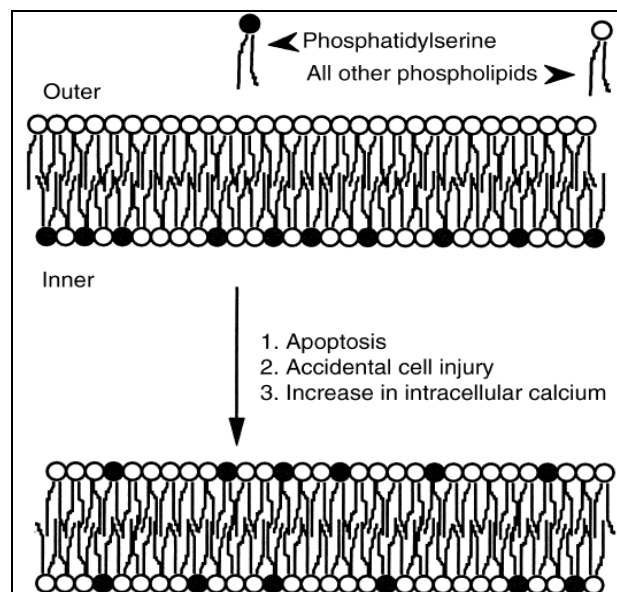


Figure 2.4 Schematic representation of loss of membrane phospholipid asymmetry following cell injury [140]

The second mechanism of the crystal interaction with basolateral or basement membrane components could be a result of the loss of cell polarity, as illustrated in Figure 2.5. This type of injury may allow cell membrane components that are usually sequestered to the basolateral surface or in the tight junction region to migrate to the apical surface of the cell. Studies by Mandel and his collaborators [161-163, 139, 140] were among the first to demonstrate this linkage, showing an increase in crystal binding following treatments that disrupt tight junctions, allowing crystal access to membrane constituents normally restricted to basolateral membranes [161]. When primary cultures of inner medullary collecting duct cells were exposed to crystals of CaOx, uric acid or hydroxyapatite, crystals preferentially adhered to cells with impaired tight junctions. Recently, similar conclusions were made when MDCK-b1 cell monolayers were first physically injured by removal of a strip of cells and then exposed to CaOx crystals. Crystals specifically adhered to residues on the growth substrate and surfaces of injured and regenerating cells. It was concluded that both mature and immature cells surfaces express crystal binding molecules but, while they are available on surfaces of immature cells, in mature cells these molecules become available only after injury. These results strongly support the suggestions that epithelial damage promotes crystal adherence to the renal epithelium. Molecules, which become available on cell surfaces on exposure to high Ox and CaOx crystals, include phosphatidylserine, CD44, osteopontin, hyaluronan. All of them have been shown to promote crystal adherence to renal epithelial cell surfaces. Khan *et al.* observed crystal attachment to the brush border of proximal tubules in rats. Some urinary macromolecules have an inhibitory effect on CaOx crystal attachment. Lieske *et al.* reported that diverse polyanionic molecules in urine, such as specific glycosaminoglycans, glycoproteins, and citrate, block the binding of COM crystals to the cell membrane. One common feature of molecules that inhibit COM crystal adhesion to cells is their polyanionic character. They mentioned that although polyanions present in tubular fluid may coat crystals and thereby inhibit their adhesion to tubular cells, a distinct and separate set of signals acts on the cells to regulate their response to crystals that do bind [164, 165]. Related studies suggested that the crystal attachment may also involve extracellular matrix proteins and/or cellular binding sites for these proteins, which are normally masked in intact monolayers. Studies by Lieske and colleagues [141, 146] demonstrated an attenuation of crystal attachment in BSC-1 cells by treatment with arginine-glycine-aspartic acid-serine (RGDS, a tetrapeptide that bind to integrins), or by pretreatment with

fibronectin, a connective tissue protein containing this peptide sequence. Similarly, Verkoelen *et al.* [166] demonstrated that crystal attachment to wounded MDCK monolayers could be attenuated by enzymatic removal of hyaluronic acid [167], expressed by subconfluent cultures of renal epithelial cells *in vitro* and by damaged renal epithelial cells *in vivo* [168].

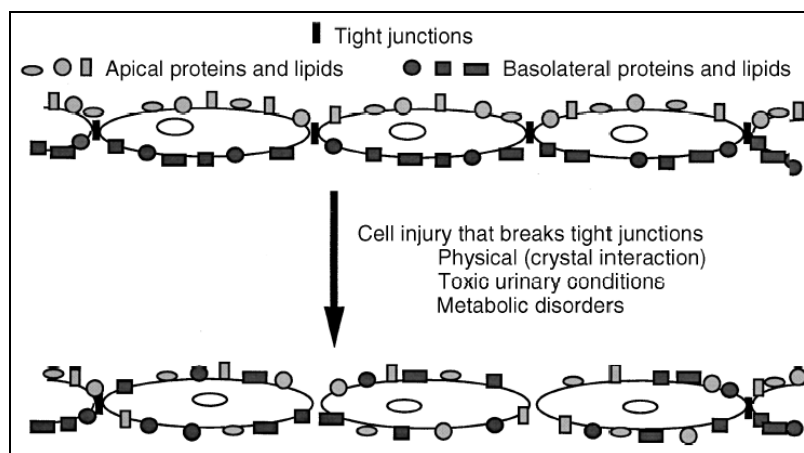


Figure 2.5 Schematic representation of loss of cell polarity following cell or tissue injury [140]

2.5.2.4 Endocytosis of CaOx crystals by renal tubular epithelial cells and cell proliferation

CaOx crystals binding to renal epithelium often leads to endocytosis followed by DNA synthesis and cell proliferation as indicated by an increase in the incorporation of thymidine into DNA, increase in cell number and enhanced expression of immediate early genes *c-jun*, *c-myc*, *Egr-1* and *nur 77* [12, 147, 169]. The proliferative response could serve to promote further crystal attachment as the dividing cells round up and detach, unmasking new attachment sites on the underlying basement membrane [147]. In particular, both *in vivo* [170] and *in vitro* [146, 147, 171-173] studies provided evidence that the adherence of crystals may activate endocytic pathways that bring about an internalization of attached crystals. This uptake involves an active engulfment of surface particles, following attachment to specific sites on the cell surface.

After attachment, the crystals are internalized, eventually moving to a basolateral location where they become anchored to the basement membrane. It was suggested that disruption of tight junctions, which leads to migration of adhesive basolateral molecules to cell surfaces, increases crystal binding [174]. Internalized crystals are

transported into the lysosomes where they appear to dissolve because of extremely low pH [175] or released at the basolateral surface, a process that may account for the appearance of crystals in the renal interstitium in experimental stone disease [170]. This may promote crystal retention by exposing attachment sites on the ensuing immature cells as well as the basal lamina. CD44 is generally expressed at the basolateral membrane of the confluent renal epithelial cells and at their apical membrane during proliferation [176]. Cells are susceptible to crystal adherence during proliferation but lose this feature after the development of functional tight junctions and attaining confluency. Tubular epithelial cells of the injured kidneys also express CD44 *in vivo*. In addition to CD44, its two ligands, OPN and hyaluronic acid (HA), are also implicated in crystal binding. Crystal binding is significantly reduced by enzymatic removal of HA. Pretreatment of MDCK cells with polyclonal antibodies against OPN as well as transfection of NRK-52E cells with antisense OPN cDNA also reduces adhesion of CaOx crystals [177]. Other molecules, which support CaOx crystal attachment to the renal epithelial cells include PS, sialic acid containing glycoproteins, collagen, and nucleolin and/or glycosaminoglycans such as HA [149, 167]. However, pretreatment with annexin V significantly reduces the attachment by annexin binding to superficial PS [178]. Neuraminidase pretreatment reduces crystal attachment indicating a role for sialic acid containing glycoproteins [179]. In addition, the presence of free bikunin, osteopontin, fibronectin, heparan sulfate and matrix Gla protein inhibits crystal attachment.

The presence of nephrocalcin inhibits DNA synthesis [147]. Both attached and internalized crystals promote adhesion of additional crystals to the cell surface. Crystal endocytosis is an active process and can be enhanced by treatments that stimulate cell migration and/or proliferation, such as ADP and cytokines [146] and inhibited by agents that interact with cell adhesion sites including Tamn-Horsfall Protein (THP), tetrapeptide RGDS, fibronectin, heparin and transforming growth factor (TGF β 2) [146, 171, 172]. The inhibitory effect of arachidonic acid and its metabolites PGE1 and PGE2 on crystal endocytosis is mediated by cAMP. In addition, endocytosis is inhibited by an increase in intracellular calcium. There is generalized reorganization of intermediate filaments and concentration of F actin at the sites of internalized crystals [173]. Furthermore, prevention of cytoskeleton assembly by cytochalasin B and colchicine inhibits CaOx crystal internalization by MDCK cells. Crystal endocytosis is also attenuated by treatments that inhibit protein kinase C or that disrupt the

cytoskeleton [173]. Lieaske *et al.* reported that the internalization of CaOx crystals by BSC-1 and MDCK cells is a regulated event that can be modified by various signals [146]. In addition, they reported that the adsorption of nephrocalcin, a urinary glycoprotein of renal cell origin, to COM crystals prevented attachment of the crystal to the plasma membrane, engulfment, or both, and thereby prevented mitogenic effects.

2.5.2.5 Migration of inflammatory cells into the interstitium

Diverse inflammatory cells are present in the interstitium next to the tubules that contain crystals [180]. Interstitial crystals are surrounded by inflammatory cells positive for CD45 (antigen which identifies all leukocytes), ED1 (specific for monocytes and macrophages) and MHCII (major histocompatibility class II antigen). Some crystals are seen inside multinucleated giant cells which are also positive for CD45, ED1 and occasionally for MHCII as well. In addition, global assessment of gene expression in kidneys of hyperoxaluric rats has shown differential regulation of many genes linked with immune response and inflammation [181]. Renal tubules, the interstitium, and crystal-associated material also stain positive for the monocyte chemoattractant protein-1 (MCP-1), a key regulator of the inflammatory response known to attract cells of the inflammatory cascade such as monocytes. Renal epithelial cells express MCP-1 mRNA and protein, and their levels are increased following exposure to Ox and CaOx crystal [182]. Many crystallization modulators, whose production is upregulated by exposure to Ox and CaOx crystals, are also participants in the inflammatory and repair processes. OPN is a specific monocyte chemoattractant for renal interstitium and its production is increased prior to monocyte infiltration. Acute inflammatory conditions are known to up- or down-regulate transcription of inter- α -inhibitor (ITI) genes. Bikunin, a plasma protease inhibitor, is associated with inflammation and stabilizes the extracellular matrix. THP is seen in the renal interstitium in several forms of tubulointerstitial diseases. The administration of THP is shown to produce interstitial inflammation and scarring, can activate alternate pathways, interact with neutrophils and bind to certain cytokines. Prothrombin is the precursor of thrombin and fragments 1 and 2. Thrombin is involved in platelet aggregation and blood coagulation and plays a major role in the recruitment and activation of infiltrating immune cells. Other studies have provided evidence for the activation of renin-angiotensin system during the development of tubulointerstitial lesions of CaOx crystals [183, 184]. Reduction of angiotensin production by inhibiting

angiotensin- converting enzyme as well as blocking angiotensin receptor reduced crystal deposition and ameliorated the associated inflammatory response. We have recently shown that CaOx crystal deposition in rat kidneys activates the renin-angiotensin system and increases renin expression in the kidneys and serum.

2.5.2.6 Activation of Phospholipase A₂

However, both the process of endocytosis and the processes regulating membrane phospholipid asymmetry involve the actin filament lattice, which is intimately linked to a number of membrane bound signaling molecules, including tyrosine kinases, phospholipases, phosphoinositide kinases, etc. [159]. These signaling molecules control multiple pathways within cells including those regulating the activity of cytosolic phospholipase A₂ (cPLA₂), an enzyme that hydrolyzes the acyl group from the sn-2 position of phospholipids. This enzyme produces a number of active byproducts including arachidonic acid and assorted lysophospholipids that can, in turn, stimulate other signaling pathways within cells [185]. Activation of PLA₂ has been observed in a number of pathologies involving injury of renal epithelial cells [186-188]. In addition, patients with active stone disease show elevations in plasma arachidonate levels and in the arachidonate content of red cell membranes [189, 190], suggesting a role for PLA₂ in the etiology of stone disease. Thus, it was of interest to discover that cPLA₂ is also activated in renal epithelial cells following exposure to elevated concentrations of oxalate [191, 192]. Studies on MDCK cells demonstrated that oxalate produces a time- and concentration-dependent increase in the activity of cPLA₂ [191] that may be responsible for many of the other cellular actions of oxalate. Indeed activation of this enzyme may be responsible for the induction of a number of immediate early genes that are involved in cellular proliferation, since inhibition of PLA₂ activity blocked the oxalate-induced increases in *Egr-1*, *c-jun* and *c-myc* mRNAs [192]. The induction of several early response genes appears to be mediated by specific lysophospholipid byproducts of PLA₂ activation, since lysophosphatidylcholine (Lyso-PC), but not arachidonic acid or lysophosphatidic acid, mimicked the effects of oxalate on gene expression [192]. Lysophospholipids released by PLA₂ activation have also been implicated in the proliferative responses of OK cells [193], vascular smooth muscle cells [194] and mouse renal proximal tubular cells [195].

2.5.2.7 Activation of Neutral Sphingomyelinase

Renal cell exposure to oxalate also increases the cellular levels of ceramide, another lipid signaling molecule [196, 197]. Oxalate-induced increase in ceramide are of interest because in other cells, ceramide has been shown to mediate a variety of responses, including proliferation, differentiation, cytotoxicity and death [198]. The nature of the stimulus for neutral sphingomyelinase activation in response to oxalate exposure is not completely understood. Oxalate may exert a direct effect, but it is also likely that oxalate works indirectly, via PLA₂ activation in renal epithelial cells, since pretreating MDCK cells with AACOCF₃, a selective inhibitor of cytosolic PLA₂, blocked the oxalate-induced increase in ceramide production [197]. Moreover, arachidonic acid, a lipid signal generated by PLA₂ activation, mimics oxalate actions on ceramide production in renal cells [197]. A similar link between the PLA₂ and the ceramide pathways also occurs in HL-60 (human leukemia) cells [199]. Several studies in neural cells have suggested that the cross-talk between these two pathways may also occur in the opposite direction, namely, ceramide may enhance the activation of PLA₂ [200, 201]. This possibility has not yet been confirmed in renal epithelial cells. Irrespective of the trigger(s) eliciting ceramide production, it is clear that increased availability of this lipid can exert multiple effects on cellular function, including apoptosis [198, 202]. Several studies have linked oxalate toxicity to apoptotic renal cell death [196, 203], although the precise links between ceramide and renal cell death have not yet been completely elucidated.

2.5.2.8 Alterations of mitochondrial function and cellular redox state

Two lines of evidence support the notion that alterations in mitochondrial function are responsible for many of the effects of oxalate (and by extension for the effects of its lipid mediators). First, many studies indicate that mitochondria are the major source of oxidants in mammalian cells. Second, in whole kidney and in isolated kidney cells there is evidence supporting an increase in oxidant stress following oxalate exposure [204]. Early evidence came from studies on experimental animals which found that experimental increase in urinary oxalate loads also increased the excretion of lipid peroxides [205-207] and decreased the levels/activities of renal antioxidant enzymes [208, 209]. To determine whether oxalate exposure could elicit a direct, acute oxidant stress in renal cells, a number of studies have used monolayer cultures of renal epithelial cells to identify oxalate-induced changes in mitochondrial production of

reactive oxygen molecules. Many studies have observed that oxalate exposure in a variety of kidney cell lines increases free radical production [210, 216] and induces toxicity [196, 211, 212, 216-219]. In other studies, oxalate treatment of renal cell cultures increased production of lipid peroxides and increased the release of intracellular enzymes [212]. Moreover, oxalate-induced toxicity and free radical production could be attenuated by pretreatment with various antioxidants [211-213, 217, 219], by treatments that disrupt electron transport in mitochondria [210], and by genetic manipulations that enhance expression of bcl-2 [196], a protein that modulates mitochondrial permeability [214].

Recent studies have examined mitochondrial responses to oxalate and its lipid mediators in more detail. Treatment of renal epithelial cells with oxalate, ceramide, arachidonic acid or lyso-PC evoked a number of changes in mitochondrial function, including depolarization of the mitochondrial membrane [220]. The changes in mitochondrial membrane potential were accompanied by an increase in the production of reactive oxygen molecules in isolated mitochondria, by an increase in the oxidation of mitochondrial thiols and by an increase in the peroxidation of mitochondrial membranes [210]. These findings provide support for earlier studies in which oxalate exposure was shown to increase the permeability of the inner mitochondrial membrane that led to release of mitochondrial factors cyto-c required for activation of caspases, cysteine proteases that are involved in apoptotic cell death [215] and to increase the oxidation of mitochondrial glutathione [208]. Interestingly, the effects on mitochondrial membrane potential could be blocked by AACOCF₃, an inhibitor of cPLA₂. Thus, it seems likely that the increase in renal oxidant stress caused by exposure to high levels of oxalate *in vitro* [211, 212] or *in vivo* [205-207, 209] are due to changes in mitochondrial function mediated by lipid signaling molecules. Moreover, Angiotensin II induces oxidative stress by activating membrane-associated nicotinamide adenine dinucleotide phosphate-oxidase (NADPH oxidase), which leads to the production of superoxide. Reactive oxygen species (ROS) generated through the activation of NADPH oxidase are also involved in the production of MCP-1, which causes the recruitment of monocytes and/or macrophages to the interstitium.

2.5.3 Adaptive response to oxalate

2.5.3.1 Increased expression of early response genes and cellular proliferation

Oxalate exposure to renal cells also elicits adaptive responses that may enhance the survival of the remaining renal epithelial cells. For example, oxalate exposure activates pathways leading to proliferation of renal cells (a process that facilitates replacement of damaged/dead cells), producing increased expression of several immediate early genes (IEGs). Many of these IEGs are transcription factors that, in turn, regulate expression of downstream genes involved in proliferation, increased DNA synthesis, and increased number of renal epithelial cells [220].

In cultured kidney cells, oxalate exposure leads to rapid increases in expression of several IEGs. For example, in LLC-PK1 cells (a line of porcine proximal tubular epithelial cells), oxalate exposure leads to an increase in *c-myc* expression and an increase in cellular proliferation [216]. Treatments that block expression of the c-Myc protein (e.g., treatment of cells with an antisense oligonucleotide directed against *c-myc*) abolished the oxalate-induced increases in c-Myc expression, DNA synthesis, and cell number [216]. Other IEGs induced by exposure to oxalate or to calcium oxalate crystals, include *Egr-1*, *c-jun*, and *nur-77* [219, 221]. Oxalate-induced upregulation of IEGs was attenuated by concomitant exposure to antioxidants [219], suggesting that this process was dependent upon prior generation of reactive oxygen species. Lipid-signaling molecules may initiate this process, since inhibition of PLA₂ selectively blocks the effects of oxalate on IEGs induction [191].

2.5.3.2 Increased expression of proteins regulating crystal binding

When renal epithelial cells are exposed to oxalate ions and CaOx crystals, there is an increase in gene expression and production of several urinary macromolecules, which modulate the nucleation, growth, aggregation and retention of crystals in the kidneys. The calcium binding property of these molecules enables them to interact with calcium containing crystals. Some of them, such as OPN, Fibronectin, have specific domains to interact with cell membranes, which facilitate their immobilization and promotion of crystal attachment. Almost all of the modulators are produced by the kidneys and excreted in the urine [222, 223].

Fibronectin (FN) is one of the macromolecules over secreted from renal tubular cells as a result of stimulation by COM crystals [224]. It has also been reported that FN protected against renal tubular cell injury caused by oxalate and COM crystals, as

shown by MTT [3-(4,5-dimethylthiazol-2-yl)-2,5-diphenyl-tetrazoliumbromide] assay and morphological examination. We speculate that FN has an inhibitory effect on the adhesion of COM crystals in renal tubular cell injury [225]. The adaptive effects of oxalate, like the toxic effects, appear to be mediated by PLA₂ and subsequent ROS production [220].

2.5.3.3 Apoptotic and necrotic cell death promote crystal nucleation and attachment

Perturbations in mitochondrial function are often accompanied by an increase in mitochondrial permeability and a release of pro-apoptotic factors. These factors in turn trigger the activation of cellular caspases, serine proteases that have been linked to apoptotic cell death [226]. Exposure to high levels of oxalate *in vitro* [196] and *in vivo* [203] leads to an increase in the abundance of apoptotic (and necrotic) renal epithelial cells by a process involving increased oxidant stress [219].

Damaged cells exhibit membrane alterations that can promote adherence of crystals to the cell surface. These membrane alterations include exposure of annexin binding phosphatidylserine to the cell surface. Clusters of negatively charged headgroups of phosphatidylserine attract calcium and can act as sites for attachment of calcific crystals to cell surfaces. Such clusters on the surface of apoptotic bodies and membranous cellular degradation products can promote crystal nucleation [117].

In addition, damaged cells can foster crystal growth and deposition in another way, by providing cellular debris for crystal nucleation. Crystals formed *in vivo* all contain an organic core with a composition similar to that found in cellular membranes [227], and the addition of cellular membranes to artificial urine has been shown to increase crystal formation *in vitro* [228]. Therefore, cellular damage that leads to shedding of dead cells and the generation of cellular debris within the tubular lumen would foster crystal nucleation. It would also foster the growth of crystals via agglomeration.

2.5.4 Signaling pathways

- Ox and CaOx crystals induce oxidative stress in the kidneys, a condition in which either more ROS such as superoxide and H₂O₂ are produced that can be dealt with or endogenous antioxidant defenses are depleted. Renal cell cultures exposed to oxalate leads to a reduction in the activity of antioxidant enzymes, an increased production of lipid peroxides [219] and caused apoptotic and necrotic cell death.

- Exposure to oxalate elicits a number of membrane changes, including a redistribution of phosphatidylserine (PS), altering the membrane surface in such a way to enhance crystal binding. Attached crystals may then be internalized by endocytosis.
- Oxalate-induced membrane perturbations also causes activation of at least two lipid signaling cascades, one involving phospholipase A₂ (and resulting in increased release of arachidonic acid and formation of lysophospholipids [191] and the other involving sphingomyelinase (and resulting in increased levels of ceramide and decreased levels of sphingomyelin) [197].
- NADPH oxidase is also a major source of ROS in the kidneys [229] and Reactive oxygen species (ROS) may be produced by the activation of NADPH oxidase located at the plasma membrane or by the activation of PLA₂ and neutral sphingomyelinase (N-Smase).
- Even though mitochondria have been shown to be a source of free radicals and ROS [230]. Lipid signals (arachidonic acid, lysophospholipid and ceramide) act on mitochondria, disrupting mitochondrial membrane potential, promoting mitochondrial dysfunction, increasing oxidation of mitochondrial thiols, increasing peroxidation of mitochondrial membranes, increasing oxidation of mitochondrial glutathione and increasing permeability of the inner mitochondrial membrane that led to release of mitochondrial factors cyto-c required for activation of caspases, cysteine proteases that are involved in apoptotic cell death [208, 220, 230] and thereby, increasing production of reactive oxygen species (ROS).
- Many signaling molecules such as protein kinase C (PKC), c-Jun N-terminal kinase (JNK) and p38 mitogenactivated protein kinase (MAPK), and transcription factors such as NF- κ B and activated protein-1 (AP-1), are activated by ROS. They lead to upregulation of early response genes (*c-jun*, *c-myc*, *Egr-1*, *nur 77*) to replace damaged cells, and proteins such as MCP-1, OPN, fibronectin, bikunin and TGF- β 1 to modulate crystal formation, that may serve as adaptive functions [231].
- ROS also promote cell damage which may unmask additional crystal binding sites. Attached crystals may form centers for nucleation of new crystals, which would favor stone development. Crystal uptake by endocytosis may exacerbate cell damage; alternatively crystals may dissolve within lysosomes or re-emerge at the basolateral surface, again providing centers for stone growth in the renal interstitium [231].

- Cell death produced by oxalate exposure may leave cellular debris that forms a nidus for additional crystal growth, also promoting stone formation [231].

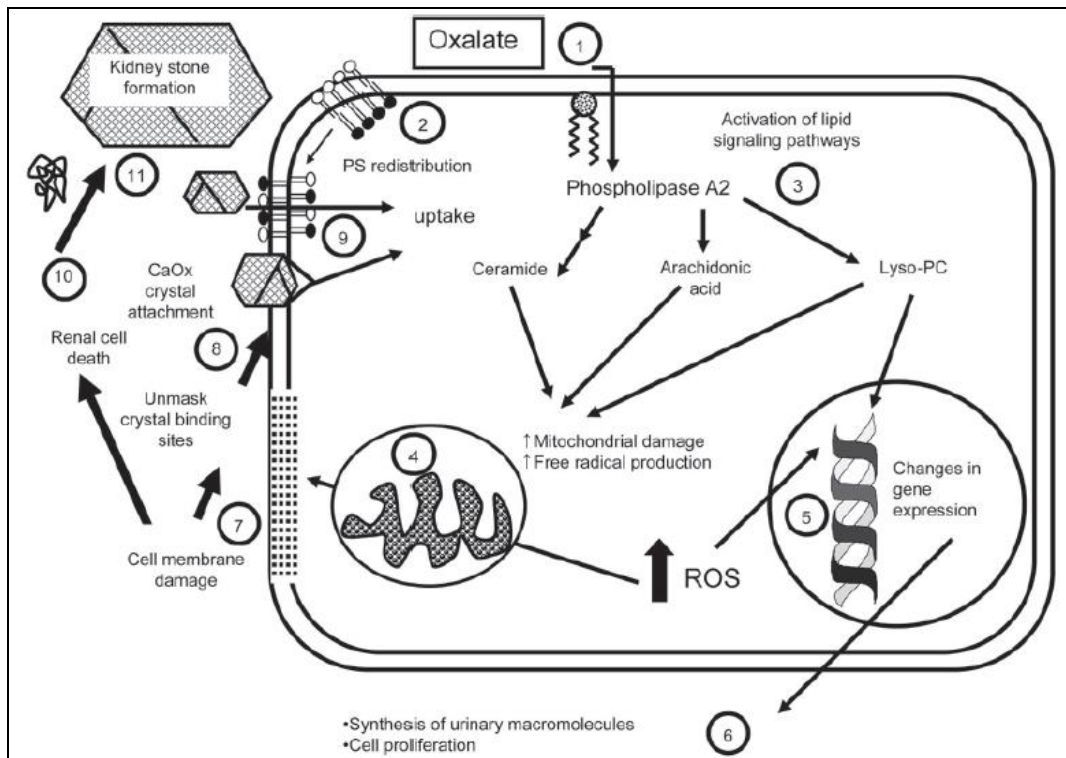


Figure 2.6 Oxalate action on renal cells [231]

2.6 Clinical diagnosis of kidney stones

Non-obstructing kidney stones produce no symptoms or signs apart from hematuria. However, the kidney stone may cause severe pain, usually accompanied by nausea, vomiting and hematuria (renal colic) when it passes into the ureter. Patients may also complain of urinary frequency and urgency. These signs and symptoms lead to many emergency department visits and hospitalization. The pattern of the pain from stone depends on its location: a stone in the upper ureter leads to pain in the flank that may radiate to the upper abdomen. When the stone is in the lower ureter, pain may radiate to the ipsilateral testicle in men or labium in women. If the stone is lodged at the ureterovesical junction, the main symptoms will be urinary frequency or urgency. Symptoms quickly improve after passing the stone. On physical examination, the patient is often in excruciating pain, and is unable to achieve a comfortable position. Ipsilateral costovertebral angle tenderness may also be present.

Laboratory tests may show a leukocytosis which may be due to a stress response or infection. Serum creatinine is often elevated if the patient is volume depleted, or if there is bilateral ureteral obstruction or unilateral obstruction in a patient with a solitary kidney. The urinalysis will have red blood cells, white blood cells and occasionally crystals. However, because of the often non-specific physical examination and laboratory findings, imaging studies are critical in making the diagnosis.

Initial evaluation includes obtaining a non-contrast helical CT, which can accurately visualize the size and location of the stones. A kidney, ureter and bladder (KUB) film, although it is insensitive to uric acid stones since they are radiolucent and therefore are not visualized. However, it can visualize calcium – containing, struvite and cystine stones in the kidney or ureter. Complete ureteral obstruction and upper urinary tract infection (UTI) are indications for stone removal by ESWL or surgery [36, 232]

2.6.1 Medical and nutrition evaluation of kidney stones

A comprehensive history should be taken by one of the health care providers, and the following items should be covered: prior kidney stones, composition of prior stones if known, dietary history including an estimate of typical daily fluid intake, social history including details regarding occupation and lifestyle, and family history. The medical history should focus on identifying diseases that increase stone risk including conditions that lead to hypercalciuria, gout, chronic diarrhea and malabsorptive gastrointestinal disorders.

2.6.2 Interpretation of biochemical and urine tests

2.6.2.1 The 24-hour urine collection

The best way to evaluate stone risk is a 24-hour urine collection and analysis [232]. Two 24-hour urine collections are recommended for the initial evaluation for an accurate analysis and to determine variability [233]. The 24-hour urine collection should be several weeks after any procedures (i.e. 6-8 weeks after lithotripsy) in order to minimize the risk of result be being influenced by infection or presence of blood due to these causes. Infection can change the pH and citrate levels.

It is very important that patients continue with their usual diet and activities during the collection period. The 24-hour urine creatinine excretion can give information about the adequacy of the urine collection. In general, adult males produce 18–24 mg creatinine/kg/d and females 15-20 mg/kg/d [232]. 24-hour urine collection is not

accurate as the urinary creatinine levels will be higher than normal for over collection and lower than normal for under-collection [233].

The 24-hour urine sample should include volume, and the solutes calcium, phosphorus, oxalate, citrate, pH, creatinine and uric acid to provide an estimate of supersaturation and the risk of stone formation. Creatinine is tested to ensure full collection and to normalize solute excretion to the more constant amount of creatinine. Dietary factors include sulfates which are mostly from animal protein and sodium since they are related to calcium, potassium, and magnesium excretion. Urea nitrogen is used to estimate protein catabolic rate (PCR). The PCR is usually indicative of dietary protein intake in an individual who is not in a catabolic state. The relationship between urinary nitrogen appearance rate and estimated dietary protein intake is then calculated. The value of the 24-hour urine is to evaluate dietary nutrients and fluid intakes and to provide guidance for the patient's management. For example, normal urinary calcium levels are <250 mg/d for men and <200 mg/d for women. High urinary calcium may be caused by idiopathic hypercalciuria, or diet high in sodium or protein. Low urinary calcium is often due to malabsorption or underlying bone disease. A normal urinary oxalate level is 20-40 mg/d. High levels are due to high oxalate diet, increased endogenous production, high vitamin C consumption and irritable bowel disease. Normal urinary citrate levels are >450 mg/d for men and >550 mg/d for women. High animal protein diets and renal tubular acidosis (RTA) can increase acid production affecting urinary pH so that it declines citrate levels.

2.7 Treatment of kidney stones

Urgent surgical intervention is indicated in a patient with an obstructed, infected urinary tract, worsening renal function, intractable pain or vomiting or obstruction of a solitary or transplanted kidney. Analgesia is essential and parenteral Non-Steroid Anti-Inflammatory Drugs (NSAIDs: Ketorolac) are as effective as narcotics. NSAIDS are less likely to cause nausea, but should be avoided if the patient has impaired renal function. Pain is due to renal capsule dilatation, and so intractable pain may require decompression of the obstruction. If urgent intervention is not required, the treating physician needs to decide if the stone can be passed spontaneously. The likelihood of spontaneous passage decreases as the size of the stone increases and stones >5-6 mm are not likely to pass spontaneously.

Patients who are having repeated stone attacks should be instructed to strain their urine and submit the stone for composition analysis. Repeated imaging (plain abdominal radiography (KUB) for radiopaque stones and CT for radiolucent stones) is warranted to confirm stone passage. If follow-up imaging reveals no movement after a month, urologic intervention is generally warranted [234].

2.7.1 Surgical treatment

Larger and more proximal ureteral stones are less likely to pass spontaneously and usually require urologic evaluation. If the stone does not pass rapidly, the patient can be sent home with oral analgesia and instructions to return for fever or uncontrollable pain. Infection in the setting of obstruction is a surgical emergency and mandates emergency drainage.

2.7.1.1 Extracorporeal shock wave lithotripsy

The introduction of shock wave lithotripsy in the early 1980s revolutionized the treatment of nephrolithiasis. A shock wave is generated by a source external to the patient that propagates through the body before being focused on a kidney stone. Shock waves cause stone fragmentation directly by producing mechanical stresses or indirectly by the collapse of cavitation bubbles which pass spontaneously days or weeks later [235]. Although shock wave lithotripsy is the most common treatment for urolithiasis, it can have side effects. In human and animal models it can cause acute renal injury [236]. Obese patients may not be effectively treated with ESWL. Cystine stones are very hard and are often not effectively treated with ESWL.

2.7.1.2 Ureteroscopy

Ureteroscopy involves retrograde visualisation of the collecting system using a rigid, semi-rigid, or flexible endoscope. Improved fibreoptics and deflectability and the reduced size of ureteroscopes have expanded the use of ureteroscopy for stones in the upper urinary tract. The ureteroscope has a working channel that allows the introduction of a variety of instruments for stone fragmentation and removal. A retrospective study showed that ureteroscopy is useful when lithotripsy fails; when complex or lower pole renal calculi are present; or when patient factors such as pregnancy, coagulopathy, or morbid obesity preclude lithotripsy. One disadvantage of ureteroscopy is that a ureteral stent, which causes considerable discomfort in some

patients, is often necessary to prevent obstruction from ureteral oedema or stone fragments [237].

2.7.1.3 Percutaneous nephrolithotomy

Percutaneous nephrolithotomy involves creating an access tract into the renal collecting system through which nephroscopy can be performed. The nephroscope has a working channel through which an intracorporeal lithotripsy device (lithotrite or laser) can be introduced. Stone fragments are removed using suction, graspers, or basket extraction. The technique enables stones to be retrieved for analysis, and all stone material can be removed so that the patient does not have to pass any fragments, as is common with shock wave lithotripsy and ureteroscopy. Although percutaneous nephrolithotomy is thought to be more invasive than other treatments, a large meta-analysis has demonstrated its safety and efficacy, particularly when stones are large, multiple, or complex [237].

2.7.1.4 Open surgery

Open surgery for renal stone disease has decreased considerably because of the adoption of non-invasive and minimally invasive techniques. The commonest current and acceptable indications for open surgery include complex stones in kidneys with a dilated collecting system, failure of percutaneous, endourological or ESWL, and stones in a kidney with anatomical abnormalities, e.g. PUJ obstruction, infundibular stenosis, ureteric strictures and concomitant open surgery [238].

2.7.2 Dietary management

Dietary modifications could play an important part in the management of stone disease in the region; keeping in perspective the social and cultural environment of the stone-formers, the following modifications should be advised in the long term.

- High fluid intake: a minimum of 10-12 glasses of water (250 mL each).
- Oxalate restriction: restrict the use of spinach, okra, green vegetables, tea, and green and black pepper.
- Fat-rich foods: reduce the consumption of oily or fat-rich food, especially animal-fat products.
- Sodium: avoid the use of salt shakers and salty food.

- Increase citrus fruits: promote the consumption of lemon juice, orange juice, and especially potassium-rich products.
- Increase the fibre intake, e.g. bran bread.
- Increase calcium intake by having at least two cups of milk/milk products per day.

2.7.3 Medical treatment

Medical treatment should be used on assessing 24 hour urinary metabolic abnormalities. Drug treatment is advised after a high fluid intake (>3 L/day) and dietary modifications in the long term fail to correct abnormalities or prevent recurrence. In cases of Hypercalciuria with normal parathyroid hormone levels, the treatment is thiazide diuretics and potassium citrate, with a reduction of sodium in the diet [239]. Patients with hyperoxaluria not related to diet should be investigated for underlying bowel disease. Therapy should include a reduction in oxalate-rich diet, with pyridoxine supplements and lemon juice. For severe hypocitraturia investigations should be directed to detect gastrointestinal disorders and renal tubular acidosis. Here the mainstay of treatment is lemon juice or potassium citrate. Hyperuricosuria with hyperuricaemia is treated by allopurinol 300 mg/day and potassium citrate or orange juice as an alternative [240]. Most patients with stone disease present with more than one risk factor; in our studies, 10% presented with several metabolic or environmental risk factors. Medical therapy thus requires a combination, depending on the individual patient profile and the type of stone formation.

2.8 Phytotherapy

Treatment and prevention of kidney stones has considerably evolved during the last two decades by combination of dietary procedures, surgical treatments and medicaments, side effects of these methods and recurrence remain as problems to overcome. Thus, an adjunct to these conventional methods, phytotherapy is highly recommended. Medicinal plants have been known for millennia and are being used as a rich source of therapeutic agents worldwide. WHO reported that ~75% global population, most in the developing world, depends on botanical medicines for their basic healthcare needs with around 800 plants being used in indigenous system of medicines [241]. The use of herbal medicine is becoming popular due to toxicity and side effects of allopathic medicines.

Urolithiasis has been a matter of concern to clinicians since the time of Hipocrates. Many remedies have been employed during the ages to treat urinary stones. In the traditional system of medicine, most of the remedies were taken from plants and they proved to be useful though the rationale behind their use is not well established through systematic pharmacological and clinical studies except for some composite herbal drugs. The various marketed composite antiurolithiatic herbal formulations, Cystone (Himalaya Drug Company, India), Calcury (Charak Pharmaceuticals, Mumbai, India), Chandraprabhabati (Baidyanath, India), Neeri (Aimil Pharmaceuticals, India), Uriflow (BioNeutrix Healthcare, USA), Uriflush (Global Pharmaceuticals, India) have been used worldwide [242].

2.8.1 Proteins: potent antiurolithiatic biomolecules

Until recently, pharmaceuticals used are being largely synthesized by organic chemistry. As knowledge about sources of many diseases and how body fights these diseases is available, focus is on developing the therapeutics that mimic or enhance the actions of body's arsenal. Protein based drugs, as proteins are one of the main macronutrients in food, are one of the most important and rapidly growing segments of the pharmaceutical market with reduced immunogenicity, improved safety and greater effectiveness [242]. Insulin [243], plant lectins, Lunasin from soy [244], Bromelain from Pineapple [245], MAP30 (*Momordica* anti-HIV protein of 30 kDa) and GAP31 (*Gelonium* anti-HIV protein of 31 kDa) [246], are few bioactive plant protein and peptides being explored.

Till date not many reports are available about antilithiatic plant proteins and peptides, even though urolithiasis has afflicted mankind since antiquity and there are many herbal formulations available in market. The antilithiatic plant proteins isolated, purified and characterized till date are anionic, rich in acidic amino acids and have EF Hand domain, a characteristic feature of various calcium binding protein like calgranulin , osteopontin [247]. Acidic amino acids interact with calcium ions thus making them unavailable for oxalate to bind. A 98 kDa dimeric antilithiatic protein was purified from seeds *Dolichos biflorus* having abundant acidic amino acids. This protein showed similarity with Calnexin of *Pisum sarivum* [248]. A CaOx growth inhibitor with two EF hand domains was purified and characterized from seeds of *Trachyspermum ammi* [249]. The protein maintained renal functioning, reduced renal injury and decreased crystal excretion in urine and retention in renal tissues [250]. A CaOx growth inhibitory protein isolated from *Tribulus terrestris* (~60 kDa), anionic with EF hand domain, was found to be cytoprotective in comparison to cystone [251]. These proteins and peptides can be produced on large scale using recombinant DNA technology, taking into consideration potential toxicity, allergenicity and stability of peptides.

2.9 Terminalia arjuna

Classification:

Kingdom: Plantae

Division: Magnoliophyta

Class: Magnoliopsida

Order: Myrtales

Family: Combretaceae

Genus: *Terminalia*

Species: *arjuna*

Common name:

Arjuna, Dhavala, Kakubha, Nadisarja, Veeravriksha, Partha, Indradru

Part used: Bark

2.9.1 Botanical description

The tree is about 60-80 feet height. Arjuna is large, evergreen with a spreading crown and dropping branches. The bark of *Terminalia arjuna* is smooth, pinkish-grey from

outside and flakes off in large, curved and rather flat pieces. The histology of *Terminalia arjuna* bark reveals the presence of single layered epidermis with hair like projections and few scattered lenticels. Underlying the epidermis is a thin layer of cortex. Periderm and secondary phloem are present in the old bark. Leaves are simple, borne sub-opposite coriaceous, often crenulating, oblong or elliptic. Their upper face is pale or dark green and the lower face is pale brown. The tree bears white sessile flowers arranged in short axillary spikes or in terminal pannicule. The flowers are bisexual. Linear, lanceolate-like bracteoles are present. Calyx is glabrous. Its fruit is a drupe, 2.5–5 cm long, ovoid or oblong, fibrous-woody, smooth-skinned with five hard angles or wings. The lines of the wings are oblique and curved upwards [252].

2.9.2 Geographical distribution

Terminalia arjuna (Roxb.) Wt. and Am. is a large evergreen tree distributed throughout the greater part of the Indian Peninsula along rivers and found in Sub-Himalayan tract, Chota Nagpur, Orissa, Bihar, Madhya Pradesh, West Bengal, Punjab, Deccan and Konkan.

2.9.3 Traditional uses

In the Indian system of Medicine, its bark decoction is being used as an astringent, cooling, urinary astringent, cardi tonic, in fractures, ulcers, spermatorrhoea, leucorrhoea, diabetes, cough, tumour, excessive perspiration, asthma, inflammation and skin disorders, dyslipidemia, hypertension, angina pain and congestive heart failure. Bark stem possesses diuretic, inotropic and chronotropic. Its useful phytoconstituents are: Triterpenoids, β -sitosterol, flavonoids and glycosides. Triterpenoids and flavonoids are considered to be responsible for its beneficial antioxidant cardiovascular properties. Chakradatta, the great ancient physician, recommended it to be given as a decoction of bark with milk or as a ghrita (a preparation with ghee or butter). Decoction of the bark has been used as ulcer wash, while bark ashes have been prescribed for snakebite and scorpion sting. When bark powder boiled in water and inhaled, cure headache and to kill worms in teeth. The fruit paste was also used on wounds. Fresh leaf juice is used for the treatment of earache and bark powder for treating heart ailments. Dried bark along with rice washed water was also used to treat blood in urine. Moreover, the fresh bark was chewed and swallowed the juice as an antacid [252].

2.9.4 Pharmacology

Terminalia arjuna bark helps maintain a healthy heart and reduces the effects of stress and nervousness (Himalaya herbal health care). It also promotes effective cardiac functioning and regulates blood pressure. *Terminalia arjuna* therapy for two weeks leads to significant regression of the endothelial abnormality amongst smokers [21]. The bark of *Terminalia arjuna* is also reported to inhibit nitric oxide production in murine macrophages [22] and is traditionally used to prevent kidney stone formation.

Aqueous extract of the bark of *Terminalia arjuna* is shown to protect the liver and kidney tissues against CCl₄-induced oxidative stress probably by increasing antioxidative defense activities [23]. Casuarinin extracted from *Terminalia arjuna* attenuates H₂O₂-induced oxidative stress, decreases DNA oxidative damage and prevents the depletion of intracellular GSH in MDCK cells [24]. In a recent study, both alcoholic and aqueous extracts of the bark attenuated H₂O₂-mediated reactive oxygen species generation in human monocytic cells by promoting catalase and glutathione peroxidase activities and by sustaining cellular reducing power. Moreover, the extracts inhibited lipid peroxidation and 3-hydroxy-3-methyl-glutaryl-CoA, but had no effect on lipoprotein lipase. Arjunolic acid has been found to prevent the decrease in the levels of superoxide dismutase, catalase, glutathione peroxidase, ceruloplasmin, α -tocopherol, reduced glutathione, ascorbic acid, lipid peroxide and myeloperoxidase.

CHAPTER 3

MATERIAL AND METHODS

3.1 Antiurolithiatic potential of aqueous extract of *Terminalia arjuna* in vitro

3.1.1 Plant

The dried bark of *Terminalia arjuna* were purchased from Natural Remedies Pvt. Ltd., Bangalore, India. A collection of voucher specimen is available at the company.

3.1.2 Preparation of the aqueous extract of *Terminalia arjuna*

The dried fine powdered *Terminalia arjuna* bark was soaked in distilled water for 24 hours at 4°C. The extract was then filtered through muslin cloth followed by centrifugation at 10,000 rpm for 20 minutes at 4°C and the filtrate was lyophilized to obtain the dried powder referred to as aqueous extract of *Terminalia arjuna* bark. The dried aqueous extract (AE) was stored in labeled sterile bottles and kept at -20°C [253].

3.1.3 Preparation of the aqueous extract of Ayurvedic compound: Cystone drug

One tablet of the Ayurvedic compound preparation (Cystone-from The Himalaya Drug Company, Bombay) was powdered and dissolved in 5 ml of distilled water. Each tablet according to the information provided by the manufacturers contains the following ingredients. *Didymocarpus pedicellata* (65 mg), *Saxifraga ligulata* (49 mg), *Rubia cordifolia* (16 mg), *Cyperus scarious* (16 mg), *Achyranthes aspera* (16 mg), *Onosma bracteatum* (16 mg), *Vernonia cinerea* (16 mg), Shillajeet (purified) (13 mg), and Hajrul yahood (Unani drug; 16 mg). Hajrul yahood bhasma (ash) is prepared with *Ocimum basilicum*, *Tribulus terrestris*, *Mimosa pudica*, *Dolichos biflorus*, *Pavonia odorata*, *Equisetum arvense* and *Tectona grandis* seeds. This solution was thoroughly mixed for 3-4 hours and centrifuged at 3,000 rpm for 15 minutes at 4°C. The supernatant was lyophilized to obtain the dried powder referred to as the aqueous extract of Cystone (AEC). The dried aqueous extract of cystone was stored in labeled sterile bottles and kept at -20°C [254].

3.1.4 Calcium oxalate crystallization assay

• Principle:

Crystals in the urine result from nucleation, the initial step whereby the urinary constituent transforms from a liquid to a solid phase in a supersaturated solution. When the concentration product of the ions of the stone components is greater than the formation product, ions begin to cluster close together to form the earliest nonsoluble crystal structure. This cluster structure is a loose association and is initially not compact. Gradually the structure becomes more and more organized and finally resembles an orderly crystal lattice structure. The process whereby crystals in solution stick together to form larger particles is called aggregation. The aggregation of small particles into large aggregates by strong intermolecular forces which cannot be dispersed by shear forces, is favored from a thermodynamic perspective [133].

• Reagents:

1. 10.0 mM calcium chloride (CaCl_2)
2. 1.0 mM sodium oxalate ($\text{Na}_2\text{C}_2\text{O}_4$)
3. Sodium acetate buffer (containing 200 mM NaCl and 10 mM sodium acetate, pH 5.7)
4. Distilled water
5. Test sample
6. Cystone

• Methodology:

Stock solutions of CaCl_2 (10.0 mM) and $\text{Na}_2\text{C}_2\text{O}_4$ (1.0 mM), containing 200 mM NaCl and 10 mM sodium acetate, were adjusted to pH 5.7. All chemicals were of the highest purity grade available. Before being used in crystallization experiments, solutions were filtered through Millex-GV membranes with a pore diameter of 0.22 μm and warmed up to 37°C in a water bath. For crystallization experiments, 1.0 mL of the CaCl_2 solution was transferred into a 10 mm light path quartz cuvette and an additional 1.0 mL of the $\text{Na}_2\text{C}_2\text{O}_4$ solution was then added to final assay concentrations of 5.0 mM for calcium and 0.5 mM for oxalate, respectively. In the cuvette, the final solutions were stirred continuously and maintained at 37°C [255].

Control experiment was performed with calcium/oxalate concentration ratio, i.e., 5.0/0.5 mM/mM. After addition of the oxalate-containing solution, automated time-course measurements of optical density at 620 nm (Chemito Spectroscan UV-2700, Thermo Scientific) were performed, i.e., OD_{620} was recorded every 60 seconds over 40

minutes, experiments with added test sample (100 μ L), where rates of nucleation and aggregation were considerably lower, had to be extended to 60 minutes. All crystallization experiments have to be performed at least in triplicate [255].

• **Calculations:**

Percentage inhibition produced by the plant extract was calculated as:

$$\text{Percentage nucleation inhibition} = [1 - (S_{Ni}/S_{Nc})] \times 100$$

$$\text{Percentage aggregation inhibition} = [1 - (S_{Ai}/S_{Ac})] \times 100$$

Where, i stands for inhibitor and c for control.

3.1.5 CaOx crystal growth assay

• **Principle:**

Crystal growth, defined as the rate of deposition of ions onto a crystal nidus, occurs at the interface between the liquid and solid phases and involves both solute transfer and interfacial processes. Once a crystal nucleus has achieved a critical size and relative supersaturation remains above 1, overall free energy is decreased by adding new crystal components to the nucleus leading to growth of crystal [120].

• **Reagents:**

1. 4.0 mM calcium chloride (CaCl_2)
2. 4.0 mM sodium oxalate ($\text{Na}_2\text{C}_2\text{O}_4$)
3. Tris-Cl buffer buffer (containing 10 mM Tris-HCl containing 90 mM NaCl, pH 7.2)
4. 1.5 mg/ml stone slurry
5. 50 mM sodium acetate buffer (pH 5.7)
6. Distilled water
7. Test sample
8. Cystone

• **Methodology:**

Inhibitory activity against CaOx crystal growth was measured using the seeded, solution-depletion assay described previously by Nakagawa and colleagues [256]. Briefly, an aqueous solution of 10 mM Tris-HCl containing 90 mM NaCl was adjusted to pH 7.2 with 4 N HCl. Stone slurry (1.5 mg/mL) was prepared in 50 mM sodium acetate buffer (pH 5.7). CaOx monohydrate crystal seed (from Fourier Transform Infrared Spectroscopy (FTIR) identified clinical kidney stones) was added to a solution containing 1 mM CaCl_2 and 1 mM $\text{Na}_2\text{C}_2\text{O}_4$. The reaction of CaCl_2 and $\text{Na}_2\text{C}_2\text{O}_4$ with crystal seed led to deposition of CaOx (CaC_2O_4) on the crystal surfaces, thereby

decreasing free oxalate that is detectable by spectrophotometry at $\lambda 214$ nm (Multiskan 2GO, Thermo Scientific). When test sample is added into this solution, depletion of free oxalate ions will decrease if the test sample inhibits CaOx crystal growth. Rate of reduction of free oxalate was calculated using the baseline value and the value after 60 seconds incubation for 20 minutes, with or without test sample [256].

• **Calculations:**

The relative inhibitory activity was calculated as follows: % Relative inhibitory activity = $[(C-S)/C] \times 100$, where C is the rate of reduction of free oxalate without any test sample and S is the rate of reduction of free oxalate with a test sample.

3.1.6 Image analysis of crystal morphology

• **Principle:**

The formation of renal stones is a consequence of increased urinary supersaturation with subsequent formation of crystalline particles. Crystals in the urine result from nucleation of the urinary constituent in a supersaturated solution. These crystals undergo size enhancing processes of aggregation and growth and develop into a renal stone. Calcium oxalate is the major component of renal calculi. Calcium oxalate may exist in the monohydrate (COM) or dihydrate (COD) configurations. COM being most stable and least soluble, COD can exist in urine for a prolonged time since several factors in urine, however, favor the presence of the COD [120, 133].

• **Reagents:**

1. 12.75 mM calcium chloride (CaCl_2)
2. 2.25 mM sodium oxalate ($\text{Na}_2\text{C}_2\text{O}_4$)
3. Distilled water
4. Test sample
5. Cystone

• **Methodology:**

The stock solutions of 12.75 mM CaCl_2 and 2.25 mM $\text{Na}_2\text{C}_2\text{O}_4$ were used to observe the size and morphology of the crystals and to verify the effect of incubation with the test material on CaOx crystal formation. 50 μL of CaCl_2 solution was added to wells in a 96-well plate. To each of the wells, 50 μL of test sample and $\text{Na}_2\text{C}_2\text{O}_4$ solution were added to obtain final concentrations of 4.25 mM calcium and 0.75 mM oxalate [257]. The plates were then incubated at 37°C for 45 minutes. Cystone was used as a positive control. Crystal morphology was examined in five randomly selected fields at 100X

magnification under an upright microscope (BX53, Olympus Corporation, Japan). Images were captured from different fields.

• **Calculations:**

The measurement parameters in terms of area, perimeter, length and width of CaOx crystals in the absence and presence of various concentrations of test sample were measured using the inbuilt software ‘Image-Pro Plus 7.0’ to show the efficacy of *Terminalia arjuna*.

3.1.7 Determination of free radical scavenging by DPPH assay

• **Principle:**

The free radical scavenging activity is based on principle, when DPPH (1, 1-diphenyl-2-picrylhydrazyl) reacts with phenolic compounds, it reduces to 1,1-diphenyl-2-picrylhydrazine due its ability to donate H atom. This change in color was measured at 517 nm wavelength. The DPPH method is described as a simple, rapid and the most convenient method. It is independent of sample polarity for screening of two or more samples for free radical scavenging activity. (D) + (H-A) purple D-H + (A) yellow, where H-A is Hydrogen donor and D is DPPH radical.

• **Reagents:**

1. 0.135 mM DPPH reagent prepared in methanol
2. 70% Methanol
3. Test sample in methanol

• **Methodology:**

To 1.0 mL of test sample, 0.135 mM DPPH dissolved in methanol was added in a ratio of 1:1. This mixture was then vortexed thoroughly and incubated in dark at 37°C for 30 minutes. The absorbance of the mixture was taken at a wavelength of 517 nm (Chemito Spectroscan UV-2700, Thermo Scientific). Ascorbic acid was used as reference [258].

• **Calculations:**

The IC₅₀ value is defined as the concentration (µg/mL) of extract that scavenges the DPPH radicals by 50%. The IC₅₀ value was calculated from concentration versus percent inhibition curve and formula used to calculate percent (%) inhibition was:

$$\text{DPPH radical scavenging activity (\%)} = [(A_{\text{control}} - A_{\text{sample}})/A_{\text{control}}] \times 100$$

where A_{control} is the absorbance of DPPH radical plus methanol; A_{sample} is the absorbance of DPPH radical plus sample extract/standard. Here, methanol was used as a blank.

3.2 Diminution of oxalate-induced renal tubular epithelial cell injury by aqueous extract of *Terminalia arjuna*

3.2.1 Preparation of the aqueous extract of *Terminalia arjuna*

For cell culture studies a stock solution of the dried aqueous extract of *Terminalia arjuna* was dissolved in dimethyl sulfoxide (DMSO) [final concentration of the DMSO in the highest concentration of plant extract tested did not exceed 0.4% (v/v) and did not affect the cell proliferation]. Further dilutions of the stock were done using serum free DMEM (Dulbecco's Modified Eagles's Media) and filtered by 0.22 µm syringe filter [259].

3.2.2 Cell lines

Experimental studies were done using *in vitro* models of Normal rat epithelial derived renal tubular epithelial (NRK-52E) and Madin-Darby Canine Kidney (MDCK) cell lines. Both the cell lines were obtained from NCCS (National centre for cell science), Pune, India.

3.2.3 Cell culture

The cells were maintained as monolayers in Dulbecco's Modified Eagle's Medium (DMEM) with 2.0 mM L-glutamine adjusted to contain 3.7 g/L sodium bicarbonate, 4.5 g/L glucose. Media was supplemented with 1% Penicillin (100 units/mL)-Streptomycin (10,000 µg/mL) and 10% fetal bovine serum. Cells were cultured in 25 cm² tissue-culture treated flasks at 37°C and 5% CO₂ in humidified chambers [259, 260].

3.2.4 Oxalate-induced cell injury

NRK-52E and MDCK cells were incubated in DMEM containing 2 mM sodium oxalate in the presence of different concentrations of the plant extract for 48 hours [261]. Cystone drug was used as a positive control.

3.2.5 Cell viability

The cytoprotective potential of the aqueous extract of *Terminalia arjuna* was assessed by cell viability using trypan blue exclusion method and MTT assay.

3.2.5.1 Trypan blue exclusion assay

• Principle:

Direct counting of live and dead cells was evaluated by trypan blue exclusion assay. Trypan blue is a diazo dye, which is a vital stain to selectively color dead cells blue. This dye is impermeant to live cells but enters the compromised membranes of dead cells. It is based on the principle that live cells possess intact cell membranes excluding certain dyes, such as trypan blue, Eosin, or propidium, whereas dead cells do not. Since live cells are excluded from staining, this staining method is also described as a dye exclusion method. By using a 58 Neubauer haemocytometer, the cells can be directly counted and the cell count obtained using a standard formula.

• Reagents:

1. 0.4% Trypan blue dye
2. Test sample
3. Cystone
4. 2.0 mM Oxalate
5. 1X PBS
6. Complete media
7. 0.25% Trypsin-EDTA

• Methodology:

For the determination of cell viability, cells were plated at the density of 1×10^5 cells/well in a 12 well plate and incubated for 24 hours at 37°C and 5% CO₂ in humidified chambers to obtain 70 - 80% confluency. The effect of *Terminalia arjuna* in the presence of oxalate injury was assessed by adding test sample at various concentrations (10 µg/mL, 20 µg/mL, 30 µg/mL and 40 µg/mL) to the cells and incubated for 48 hours at 37°C. After the treatment period, the medium was removed and cells were washed twice with 1X PBS (500 µL) and trypsinized with 0.25% trypsin-EDTA (250 µL) for 2-3 minutes. To neutralize the action of trypsin, 500 µL of complete medium was added and centrifuged at 100 g for 5 minutes. Cell pellet was resuspended in 1 mL of complete medium. Cell count (viable and non-viable) was performed by mixing 1 part cell suspension with 1 part of 0.4% trypan blue using a Neubauer haemocytometer (Sigma chemicals, 99% TLC and CAS number 68941-95-7) and an inverted microscope (CKX31, Olympus). Cystone drug at a concentration of 40 µg/mL was used as a positive control [259].

Cell count (cells/ml) = (total cells counted X dilution factor X 10⁴)/ Number of squares observed

Where, dilution factor = 2,

Number of squares observed = 4

• **Calculations:**

The percentage viability of the cells was calculated as follows:

Percentage viability = (live cells/total cells) x 100

Where, Total cells = Live cells + Dead cells

3.2.5.2 MTT assay

• **Principle:**

Determination of cell cytotoxicity by spectrophotometric method was done by performing MTT assay. The underlying principle behind this technique is reduction of MTT (3-(4,5-dimethylthiazol-2-yl)-2,5-diphenyl tetrazolium bromide) by mitochondrial dehydrogenase enzyme into purple colored formazan products in case of normal healthy cells. These products are solubilized by dissolving them with DMSO (Dimethyl sulfoxide) or acidic isopropanol. Since MTT is only reduced in metabolically active cells, therefore the level of metabolically active and metabolically inactive cells can be estimated through this assay.

• **Reagents:**

1. MTT (5 mg/mL dissolved in 1X PBS)
2. DMSO
3. Test sample
4. Cystone
5. 2.0 mM Oxalate

• **Methodology:**

1 x 10⁴ cells were seeded into each well of a 96-well microplate and incubated for 24 hours at 37°C and 5% CO₂ in humidified chambers. At 70-80% confluency, the effect of *Terminalia arjuna* in the presence of oxalate injury was assessed by adding test sample at various concentrations (10 µg/mL, 20 µg/mL, 30 µg/mL and 40 µg/mL) to the cells and incubated for 48 hours at 37°C. At the end of the treatment period, 25 µL of MTT reagent (final concentration of 0.5 mg/ml) was added to each well and incubated for 4 hours at 37°C. Supernatant was discarded and 200 µL DMSO was added to each well after the incubation was over to solubilize the formazan product and

kept at room temperature for 15-20 minutes. Absorbance values (A) were determined at a 570 nm test wavelength and a 630 nm reference wavelength to test the cell viability using a microplate reader (Model 680, Bio-Rad). Cystone drug at a concentration of 40 µg/mL was used as a positive control [260, 262].

• **Calculations:**

An increase in absorbance in this assay measures the extent of increase in the number of viable cells on exposure to oxalate in the presence of test sample. The cell viability was calculated by using the following formula:

$$\% \text{ Cell viability} = (A_{\text{sample}} - A_{\text{blank}} / A_{\text{control}} - A_{\text{blank}}) \times 100$$

where A_{control} is the absorbance of untreated cells; A_{sample} is the absorbance of extract treated cells and A_{blank} is the absorbance of media only. Here, DMEM was used as blank.

3.2.5.3 CaOx crystal adhesion

• **Principle:**

This experiment gives the idea about crystal-cell interaction and that this interaction led to cell death either due to apoptosis or necrosis.

• **Reagents:**

1. Complete medium
2. 1X PBS
3. Test sample
4. Cystone
5. 2.0 mM Oxalate
6. 4% Paraformaldehyde (prepared in 1X PBS)

• **Methodology:**

Cells were seeded onto coverslips at a density of 2×10^5 cells/coverslip in a 6-well plate and incubated for 24 hours at 37°C and 5% CO₂ in humidified chambers. At 70-80% confluency, the effect of *Terminalia arjuna* in the presence of oxalate injury was assessed by adding test sample at a concentration of 40 µg/mL to the cells and incubated for 48 hours at 37°C. At the end of the treatment period, medium was removed and the cells were fixed with 4% paraformaldehyde for 30 minutes. After washing twice with 1X PBS, cells were observed under phase contrast and polarization upright microscope (BX53, Olympus Corporation, Japan) at a magnification of 20X to

study cell-crystal interactions [263]. Cystone drug at a concentration of 40 µg/mL was used as a positive control.

3.2.6 Detection of apoptosis

Apoptosis is a suicidal programme characterized by morphological and biochemical alterations such as membrane blebbing, cell shrinkage, chromatin condensation, flip-flop translocation and DNA fragmentation. Loss of plasma membrane is one of the earliest features. In apoptotic cells, the membrane phospholipid phosphatidylserine (PS) is translocated from the inner to the outer leaflet of the plasma membrane, thereby exposing PS to the external cellular environment. Various *in vitro* assays were performed to detect apoptosis mediated cell death on treatment with test samples.

3.2.6.1 Hoechst 33258 staining

• **Principle:**

The DNA-specific fluorochrome Hoechst 33258 dye is used to identify the morphological changes in an apoptotic cell. This dye binds the DNA and distinguishes densely stained, condensed apoptotic nuclei from weakly stained healthy nuclei. The apoptotic cells appeared to be bright blue colored, showing signs of chromatin condensation, while healthy cells appeared to be faint blue colored cells with intact membranes.

• **Reagents:**

1. Complete medium
2. 1X PBS
3. Test sample
4. Cystone
5. 2.0 mM Oxalate
6. 4% Paraformaldehyde (prepared in 1X PBS)
7. 5 µg/mL Hoechst dye (prepared in 1X PBS)

• **Methodology:**

Cells were seeded onto coverslips at a density of 2×10^5 cells/coverslip in a 6-well plate and incubated for 24 hours at 37°C and 5% CO₂ in humidified chambers. At 70-80% confluency, the effect of *Terminalia arjuna* in the presence of oxalate injury was assessed by adding test sample at a concentration of 40 µg/mL to the cells and incubated for 48 hours at 37°C. At the end of the treatment period, medium was

removed and the cells were fixed with 4% paraformaldehyde for 30 minutes. After washing twice with 1X PBS, cells were stained with 5 µg/mL of Hoechst 33258 dye for 10 minutes at room temperature in the dark. After washing twice with 1X PBS, stained nuclei were observed under fluorescence upright microscope (BX53, Olympus Corporation, Japan) at a magnification of 20X [264]. Cystone drug at a concentration of 40 µg/mL was used as a positive control.

3.2.6.2 Annexin V/Propidium Iodide staining by flow cytometry

• Principle:

In an apoptotic cell, the cellular disturbance causes relocation of phosphatidylserine from internal leaflet to the external leaflet of the cell membrane. Annexin V is a 35-36 kDa Ca^{2+} dependent phospholipid-binding protein that has a high affinity for phosphatidylserine, and binds to cells with exposed phosphatidylserine and identifies apoptotic cells. FITC Annexin V staining can identify apoptosis at an earlier stage. FITC Annexin V staining precedes the loss of membrane integrity which accompanies the latest stages of cell death resulting from either apoptotic or necrotic processes. Therefore, staining with FITC Annexin V is typically used in conjunction with a vital dye such as propidium iodide (PI) to identify early apoptotic cells (PI negative, FITC Annexin V positive). Viable cells with intact membranes exclude PI, whereas the membranes of dead and damaged cells are permeable to PI distinguishing apoptotic cells from necrotic cells.

Cells that are considered viable are FITC Annexin V and PI negative; cells that are in early apoptosis are FITC Annexin V positive and PI negative; cells that are in late apoptosis or already dead are both FITC Annexin V and PI positive and cells that are in necrosis are FITC Annexin V negative and PI positive. This assay does not distinguish between cells that have undergone apoptotic death versus those that have died as a result of a necrotic pathway because in either case, the dead cells will stain with both FITC Annexin V and PI.

• Reagents:

1. Complete medium
2. 0.25% Trypsin-EDTA
3. 1X PBS
4. 10X Annexin V Binding buffer (component no. 51-66121E, diluted 10 times with distilled water)

5. FITC Annexin V (component no. 51-65874X)
6. Propidium Iodide (PI) (component no. 51-66211E)
7. Test sample
8. Cystone
9. 2.0 mM Oxalate

• **Methodology:**

6×10^5 cells were seeded into 60 mm dishes and incubated for 24 hours at 37°C and 5% CO₂ in humidified chambers. At 70-80% confluency, the effect of *Terminalia arjuna* in the presence of oxalate injury was assessed by adding test sample at a concentration of 40 µg/mL to the cells and incubated for 48 hours at 37°C. At the end of the treatment period, the subsequent procedure followed was in accordance to the instructions of BDPharminogen™ FITC ANNEXIN V Apoptosis Detection Kit 1 (catalogue no. 556547), where, cell suspension and cells from monolayer were pooled together and centrifuged at 1000 x g for 5 minutes. The supernatant was decanted and cells were washed with cold 1X PBS twice. The pellet was resuspended in 100 µL of 1X binding buffer and 2 µL of FITC annexin V and 2 µL of Propidium iodide were added to it. The cells were gently vortexed and incubated for 15 minutes at room temperature in the dark. 400 µL of 1X binding buffer was added to each group and then the cells were analyzed by flow cytometry (BD Accuri C6, BD Biosciences). Cystone drug at a concentration of 40 µg/mL was used as a positive control.

3.2.6.3 Active Caspase-3 by flow cytometry

• **Principle:**

The caspase family of cysteine proteases plays a key role in apoptosis and inflammation. Caspase-3 is a key protease that is activated during the early stages of apoptosis and, like other members of the caspase family, is synthesized as an inactive pro-enzyme that is processed in cells undergoing apoptosis by self-proteolysis and/or cleavage by another protease. The processed forms of caspases consist of large (17-22 kDa) and small (10-12 kDa) subunits which associate to form an active enzyme. Active caspase-3, a marker for cells undergoing apoptosis, consists of a heterodimer of 17 and 12 kDa subunits which is derived from the 32 kDa pro-enzyme. Active caspase-3 proteolytically cleaves and activates other caspases, as well as relevant targets in the cytoplasm, e.g., D4-GDI and Bcl-2, and in the nucleus (e.g. PARP). This antibody has

been reported to specifically recognize the active form of caspase-3 in human and mouse cells. It has not been reported to recognize the pro-enzyme form of caspase-3.

• **Reagents:**

1. Complete medium
2. 0.25% Trypsin-EDTA
3. 1X PBS
4. FITC Rabbit Anti-Active Caspase-3 antibody (CPP32; Yama; Apopain) (component no. 51-68654X)
5. Cytofix/Cytoperm™ Fixation and Permeabilization Solution (1X) (component no. 51-6896KC)
6. 10X Perm/Wash™ Buffer (diluted 10 times with distilled water) (component no. 51-6897KC)
7. Test sample
8. Cystone
9. 2.0 mM Oxalate

• **Methodology:**

6×10^5 cells were seeded into 60 mm dishes and incubated for 24 hours at 37°C and 5% CO₂ in humidified chambers. At 70-80% confluency, the effect of *Terminalia arjuna* in the presence of oxalate injury was assessed by adding test sample at a concentration of 40 µg/mL to the cells and incubated for 48 hours at 37°C. At the end of the treatment period, the subsequent procedure followed was in accordance to the instructions of BDPharminogen™ FITC Active Caspase-3 Apoptosis Kit (catalogue no. 550480), where, cell suspension and cells from monolayer were pooled together and centrifuged at 1000 x g for 5 minutes. Cells were washed with cold PBS twice and resuspended in BD Cytofix/Cytoperm solution at a final concentration of 1×10^6 cells/0.5 mL and incubated cells for 20 minutes on ice. The cells were pelleted and BD Cytofix/Cytoperm solution was aspirated and discarded. The cells were washed twice with 1X BD Perm/Wash buffer at a volume of 0.5 mL buffer/ 1×10^6 cells at room temperature. The cells were then resuspended in the 1X BD Perm/Wash buffer plus 10 µL of antibody and incubated for 30 minutes at room temperature. The cells were washed with 0.5 mL of 1X BD Perm/Wash buffer and then resuspended in 0.5 mL of 1X BD Perm/Wash buffer for analysis by flow cytometry (BD Accuri C6, BD Biosciences). Cystone drug at a concentration of 40 µg/mL was used as a positive control.

3.3 Purification of antilithiatic proteins from *Terminalia arjuna*

The fractions obtained after each step of purification were assayed for their antilithiatic properties by *in vitro* calcium oxalate (CaOx) crystallization [133, 255] and crystal growth [120, 256]. The protein content was determined by Bradford assay and the extent of purity of the active fractions was determined by SDS-PAGE analysis.

3.3.1 Materials

Materials required were Q Sepharose strong anion exchanger (GE Healthcare), Bio gel® P-100 gel (Medium, 90-180 µm) molecular sieve support (Bio- Rad laboratories), Solvents used were of HPLC grade.

3.3.2 Extraction

The dried bark of *Terminalia arjuna* was ground to fine powder. To obtain crude protein extract, 100 grams of bark powder was then extracted with extraction buffer (50 mM Tris-Cl buffer (pH 7.4), containing 0.25 M NaCl, 1 mM PMSF, 0.01% sodium azide and 5% PVP). The slurry so formed was then stirred continuously for 24 hours at 4°C. After 24 hours of continuous stirring, the slurry was centrifuged at 10,000 g for 20 minutes at 4°C. The supernatant was removed and stored at -20°C for further experimentation [248, 249]. This supernatant was referred to as the whole extract of *Terminalia arjuna*.

3.3.3 Separation of biomolecules on the basis of their molecular weight

Whole extract of *Terminalia arjuna* was separated into >3 kDa and <3 kDa fractions and dialyzed against 10 mM Tris-Cl buffer at pH 7.4 by centrifugation with the help of Amicon Ultra-4 centrifugal separating tubes (Millipore) of 3 kDa cut off molecular weight. Thus, two fractions >3 kDa and <3 kDa were obtained [260].

3.3.4 Protein concentration

Total protein concentration of the whole extract, >3 kDa and <3 kDa fraction was determined using a commercial Bradford assay reagent (Bio-Rad Laboratories, Hercules CA). The subsequent procedure followed was in accordance to the instructions of Bio-Rad Protein Assay manual.

• Principle:

The assay (Bradford 1976) is based on the observation that the absorbance maximum for an acidic solution of Coomassie Brilliant Blue G-250 shifts from 465 nm to 595 nm when binding to protein occurs. Both hydrophobic and ionic interactions stabilize the anionic form of the dye, causing a visible color change. The assay is useful since the extinction coefficient of a dye-albumin complex solution is constant over a 10-fold concentration range.

• Reagents:

1. Bradford reagent: 100 mg Coomassie Brilliant Blue G-250 was dissolved in 50 mL of 95% ethanol. To this solution 100 mL of 85% (w/v) phosphoric acid was added. Resultant solution was diluted to 1 liter and filtered through Whatman #1 paper just before use.

• Methodology:

10 μ L of test solution was taken in a well of 96 well plate. 200 μ L of 1X Bradford reagent was added and the solution was mixed and incubated at room temperature for 5 minutes. Similarly standard and blank tubes were prepared and absorbance of all samples was measured at 595 nm. Distilled water was used as a blank and BSA as a standard protein [265].

• Calculations:

The concentration of protein (μ g/mL) in test sample was calculated using the standard curve of BSA plotted with various concentrations of BSA on Y axis *versus* their respective absorbance on X axis.

3.3.5 Anion exchange chromatography**• Principle:**

In anion exchange chromatography, negatively charged molecules are attracted to a positively charged solid support. To optimize binding of all charged molecules, the mobile phase is generally a low to medium conductivity (i.e., low to medium salt concentration) solution. The adsorption of the molecules to the solid support is driven by the ionic interaction between the oppositely charged ionic groups in the sample molecule and in the functional ligand on the support. The strength of the interaction is determined by the number and location of the charges on the molecule and on the functional group. By increasing the salt concentration (generally by using a linear salt gradient) the molecules with the weakest ionic interactions start to elute from the

column first. Molecules that have a stronger ionic interaction require a higher salt concentration and elute later in the gradient.

• **Reagents:**

1. Buffer A (10 mM Tris-Cl buffer, pH 7.4)
2. Buffer B (10 mM Tris-Cl containing 1.0 M NaCl, pH 7.4)
3. Distilled water
4. Protein sample
5. Q Sepharose strong anion exchanger
6. Column (XK 16/20)

• **Methodology:**

➤ **Sample preparation**

The active fraction which exhibited activity against calcium oxalate crystallization assay system i.e. >3 kDa was used for further analysis. The active >3 kDa fraction was dialyzed against 10 mM Tris-Cl buffer at pH 7.4 to maintain the equilibration, sample loading and washing conditions. The >3 kDa fraction was centrifuged at 10,000 rpm for 15 minutes at 4°C to remove insoluble material and then filtered by 0.22 µm syringe filter.

➤ **Preparation of column**

▪ **Washing of slurry**

The Q Sepharose strong anion exchanger was supplied hydrated in 20% (v/v) ethanol respectively. 100 mL of exchanger was taken into a beaker and was allowed to settle down for 2-3 hours. The ethanol solution was decanted. Slurry was washed 4-5 times with 2-3 column volumes of deionized water.

▪ **Equilibration of slurry**

After ethanol removal, the slurry was washed with the starting buffer i.e. 10 mM Tris-Cl buffer at pH 7.4. After 2-3 washes with starting buffer, the pH of slurry was checked with pH strips. When the color of pH strip matched with that of pH of 7-7.5, equilibration was confirmed.

▪ **Column packing**

The degassed slurry was resuspended in starting buffer in a ratio of 1:1. One fourth of the column (XK 16/20) was filled with starting buffer. A funnel was kept at top of column. The slurry was mixed well and poured over it slowly until the slurry reached the bottom of the column. For even packing, bottom lid of the column was opened for the flow of buffer and slurry was poured with constant speed. When the one-third

column was packed, funnel was removed and slurry was poured continuously poured till the desired level. The bottom lid was closed and the top of the column was filled with the starting buffer. The slurry was allowed to settle down for 7-8 hours.

➤ **Sample loading and separation of biomolecules**

The column (XK 16/20) was packed with pre-equilibrated strong anion exchanger and washed with same buffer by five column volumes of strong anion exchanger. Total 50.8 mg of protein sample was loaded into injecting loop. The loading and washing under similar conditions. After washing, the total bound protein was eluted in a linear gradient of 0.0-1.0 M NaCl (buffer A to B) in 10 mM Tris-Cl buffer (pH 7.4) at a flow rate of 1.0 mL/min using automated Aktaprime plus system (GE Healthcare). Fractions of 2 ml were collected. The absorbance at 280 nm for each fraction was read and the elution profile was made using the software Primeview 5.0. The method used for anion exchange chromatography is illustrated in Table 3.1.

The fractions under each peak were pooled and were dialyzed against the buffer A to remove the excess salt. The concentration of each peak was quantified by Bradford assay. These peaks were checked for their inhibitory potential towards calcium oxalate crystallization and crystal growth followed by SDS-PAGE. The peaks which showed maximum activity and few bands were then lyophilized and preserved for further purification [248, 249, 260].

Table 3.1 Method used for anion exchange chromatography

Steps	Column volume (CV)	Flow rate (ml/min)
Equilibration	5	1.0
Sample injection	-	0.5
Buffer A wash	5	0.5
0-100% Linear gradient of buffer A to B	10	0.5
Buffer B wash	5	0.5
Re-equilibration with Buffer A	5	0.5

3.3.6 Molecular sieve chromatography

• Principle:

To perform a separation, gel filtration medium is packed into a column to form a packed bed. The medium is a porous matrix of spherical particles with chemical and physical stability and inertness (lack of reactivity and adsorptive properties). The packed bed is equilibrated with buffer which fills the pores of the matrix and the space between the particles. The liquid inside the pores, or stationary phase, is in equilibrium with the liquid outside the particles, or mobile phase. For high resolution fractionation, a sample volume from 0.5% to 4% of the total column volume is recommended. Samples are eluted isocratically so there is no need to use different buffers during the separation. The largest molecule is eluted first from the column and the smallest molecule is more delayed than the largest molecule. However, a wash step using the running buffer is usually included at the end of a separation to remove molecules that may have been retained on the column and to prepare the column for a new run.

• Reagents:

1. Buffer A (10 mM Tris-Cl buffer, pH 7.4)
2. Distilled water
3. Protein sample
4. Bio-Gel P-100 Gel (Medium)
5. Column (XK 16/70)

• Methodology:

➤ Sample preparation

The lyophilized powder of the active peaks with the highest calcium oxalate crystallization and growth inhibitory activities obtained after anion exchange chromatography was reconstituted in 2.5 mL of 10 mM Tris-Cl buffer at pH 7.4 to maintain the equilibration, sample loading and washing conditions. The active peak was centrifuged at 10,000 rpm for 15 minutes at 4°C to remove insoluble material and then filtered by 0.22 µm syringe filter.

➤ Preparation of column

▪ Preparation of the Gel

10 gram of Bio-Gel P-100 Gel (Medium) was added to 10 mM Tris-Cl buffer at pH 7.4 in a beaker. It was allowed to hydrate for 12 hours at 20°C. After hydration was completed, half of the supernatant was decanted to remove fines and the hydrated gel

was degassed for 10-15 minutes with occasional swirling. Two bed volume of degassed buffer was added to degassed gel.

- **Equilibration of slurry**

After ethanol removal, the slurry was washed with the starting buffer i.e. 10 mM Tris-Cl buffer at pH 7.4. After 2-3 washes with starting buffer, the pH of slurry was checked with pH strips. When the color of pH strip matched with that of pH of 7-7.5, equilibration was confirmed.

- **Column packing**

Column packing was done by using the same method as described in section 3.3.5. Column packing for anion exchange chromatography.

- **Sample loading and separation of biomolecules**

The molecular sieve resin [Bio gel® P-100 gel (Medium, 90- 180 μm), Bio-Rad laboratories] was equilibrated with five column volume of above mentioned buffer. A total of 432.2 μg , 461.4 μg and 496.1 μg of proteins were loaded on the molecular sieve column (XK 16/70) separately, and eluted with same buffer using Automated Aktaprime plus system (GE Healthcare) at a flow rate of 0.1 ml/min. Fractions of 2 ml were collected throughout the elution. The absorbance at 280 nm for each fraction was read and the elution profile was made using the software Primeview 5.0. The method used for molecular sieve chromatography is illustrated in Table 3.2.

Fractions under each peak which eluted out based on their molecular weights were pooled to study their calcium oxalate crystallization and growth inhibitory activities. The concentration of each peak was quantified by Bradford assay. Peaks with calcium oxalate crystallization and growth inhibitory activities were dialyzed against distilled water and lyophilized. Also, their activity was tested on oxalate injured NRK-52E and MDCK renal epithelial cells. Potent peaks thus obtained were subjected to 1-D SDS-PAGE, Native-PAGE and reverse phase HPLC (RP-HPLC) [248, 249, 260].

Table 3.2 Method used for molecular sieve chromatography

Buffer	Column volume (CV)	Flow rate (ml/min)
Buffer A	2	0.2

3.3.7 Electrophoresis

Polyacrylamide gel electrophoresis separates molecules in complex mixtures according to size and charge. During electrophoresis there is an intricate interaction of samples, gel matrix buffers, and electric current resulting in separate bands of individual molecules. Gel pores are created by the crosslinking of polyacrylamide with bis-acrylamide (bis) to create a network of pores. This structure allows the molecular sieving of molecules through the gel matrix. The buffer system determines the power requirements and affects separation. The buffer system is composed of the buffer used in the gel and the running buffer.

3.3.7.1 SDS-PAGE

• **Principle:**

The Laemmli buffer system is a discontinuous buffer system that incorporates SDS in the buffer. In this system, proteins are denatured by heating them in buffer containing sodium dodecyl sulfate (SDS) and a thiol reducing agent such as 2-mercaptoethanol. The resultant denatured polypeptides take on a rod-like shape and a uniform charge-to-mass ratio proportional to their molecular weights. Proteins are separated according to their molecular weight, making this system extremely useful for calculating molecular weights.

• **Reagents:**

➤ **30% Stock Acrylamide**

- 29.2 g Acrylamide
- 0.8 g Bis Acrylamide
- Make upto 100 mL with distilled water

➤ **10% SDS solution**

- 10 g SDS
- Make upto 100 mL with distilled water

➤ **1.5 Tris-Cl pH 8.8 (Lower gel buffer)**

- 18.15 g Tris-base
- Adjust the pH with conc. HCl and raise the volume upto 100 mL with distilled water

➤ **Tris-Cl pH 6.8 (Upper gel buffer)**

- 12.11 g Tris-base
- Adjust the pH with conc. HCl and raise the volume upto 100 mL

- **10X Running buffer**
 - 30.3 g Tris-base
 - 144 g Glycine
 - 10 g SDS
 - Make the volume upto 1000 mL with distilled water. For 1X running buffer, take 50 mL of 10X running buffer and make upto 450 mL with distilled water
- **2X Sample buffer**
 - 4 mL SDS (10% w/v)
 - 2 mL Glycerol
 - 2 mg Bromophenol Blue (0.02%)
- 1.2 mL Tris-Cl buffer pH 6.8 (1M)
 - Make upto 10 mL with distilled water
- **10% (w/v) Ammonium persulfate (APS)**
 - Dissolve 100 mg of APS in 1 mL of distilled water
- **Fixative solution (for silver staining)**
 - 40 mL Methanol
 - 10 mL glacial acetic acid
 - 50 mL distilled water
 - Make upto 100 mL with distilled water

• **Methodology:**

For SDS-PAGE, protein samples (active fraction obtained after fractionation based on molecular weight, anion exchange and molecular sieve chromatography) were reconstituted in reducing sample buffer and analyzed by one-dimensional discontinuous SDS-PAGE using 1 mm thick, 12% resolving (Table 3.3) and 5% stacking (Table 3.4) gels with a Mini-Protean III apparatus (Bio-Rad) at 100 V for an average of 2.0 hour [248,249,260]. Protein bands were silver stained. Broad range molecular weight marker (catalog # 161-0317, Bio-Rad) were used as standard [248, 249, 260].

Table 3.3 Composition of 12% resolving gel

Components	Stock concentration	Volume (mL)
Distilled water	-	3.175
Acrylamide	30%	4
Tris-base buffer (pH 8.8)	1.5 M	2.503
SDS	10%	0.1
APS	10%	0.1
TEMED	-	4 μ L

Table 3.4 Composition of 5% stacking gel

Components	Stock concentration	Volume (mL)
Distilled water	-	6.8
Acrylamide	30%	1.66
Tris-base buffer (pH 6.8)	1.0 M	1.26
SDS	10%	0.1
APS	10%	0.1
TEMED	-	10 μ L

3.3.7.2 Native-PAGE

• Principle:

Native PAGE is a technique for separating biologically active proteins. In contrast to SDS-PAGE, the mobilities of proteins in a native PAGE system depend on both size and charge. There is no single electrophoresis buffer system that will optimally purify all native proteins. Key parameters for separating proteins in a native PAGE system are pI of the protein of interest and the pH of the electrophoresis buffer.

• Reagents:

- **30% Stock Acrylamide**
 - 29.2 g Acrylamide
 - 0.8 g Bis Acrylamide
 - Make upto 100 mL with distilled water
- **10% SDS solution**
 - 10 g SDS
 - Make upto 100 mL with distilled water

- **1.5 Tris-Cl pH 8.8 (Lower gel buffer)**
 - 18.15 g Tris-base
 - Adjust the pH with conc. HCl and raise the volume upto 100 mL
- **Tris-Cl pH 6.8 (Upper gel buffer)**
 - 12.11 g Tris-base
 - Adjust the pH with conc. HCl and raise the volume upto 100 mL
- **10X Running buffer**
 - 30.3 g Tris-base
 - 144 g Glycine
 - Make the volume upto 1000 mL with distilled water. For 1X running buffer, take 50 mL of 10X running buffer and make upto 450 mL with distilled water
- **2X Sample buffer**
 - 3 mL Glycerol
 - 0.2 mL Bromophenol Blue (0.5% w/v)
 - 1.25 mL Tris-Cl buffer pH 6.8 (0.5 M)
 - Make upto 10 mL with distilled water
- **10% (w/v) Ammonium persulfate (APS)**
 - Dissolve 100 mg of APS in 1 mL of distilled water
- **Fixative solution (for silver staining)**
 - 40 mL Methanol
 - 10 mL glacial acetic acid
 - 50 mL distilled water
 - Make upto 100 mL with distilled water

• **Methodology:**

The electrophoresis of the peak obtained after molecular sieve chromatography was performed maintaining the native configuration of protein biomolecule(s). The purified proteins were reconstituted in non-reducing sample buffer i.e. without using SDS or 2-mercaptoethanol (reducing agent) and analyzed by one-dimensional discontinuous Native-PAGE using 1 mm thick, 10% resolving (Table 3.5) and 5% stacking (Table 3.6) gels with a Mini-Protean III apparatus (Bio-Rad) at 100 V for an average of 2.0 hour. The molarity of the electrophoresis buffer used for native gels was 50 mM Tris-Cl and 284 mM glycine. The gels were over-run for 15 minutes and silver stained [248, 249, 260].

Table 3.5 Composition of 12% resolving gel

Components	Stock concentration	Volume (mL)
Distilled water	-	4.2
Acrylamide	30%	3.3
Tris-base buffer (pH 8.8)	1.5 M	2.5
APS	10%	50 μ L
TEMED	-	4 μ L

Table 3.6 Composition of 5% stacking gel

Components	Stock concentration	Volume (mL)
Distilled water	-	2.66
Acrylamide	30%	1.7
Tris-base buffer (pH 6.8)	1.0 M	1.25
APS	10%	50 μ L
TEMED	-	10 μ L

3.3.7.3 Silver staining

- **Principle:**

In silver staining, polyacrylamide gels are impregnated with soluble silver ion (Ag^+) and developed by treatment with a reductant. Macromolecules in the gel promote the reduction of silver ion to metallic silver (Ag^0), which is insoluble and visible, allowing bands containing protein or nucleic acid to be seen. The initial deposition of metallic silver promotes further deposition in an autocatalytic process, resulting in exceptionally high sensitivity.

- **Reagents:**

- **Farmer's reagent**

- 0.3 g Potassium ferricyanide
- 0.7 g Sodium thiosulfate
- g Sodium carbonate
- Make the volume upto 250 mL with distilled water

- **Silver nitrate solution**

- 0.2 g of AgNO_3
- Make the volume upto 200 ml with distilled water

- **2.5% Sodium carbonate solution**
 - 5 g Na₂CO₃
 - Make the volume upto 200 mL with distilled water
- **Developer**
 - 5 g Na₂CO₃
 - 217 μL Formaldehyde
- **10% Ethanol**
 - 20 mL Ethanol
 - Make the volume upto 200 ml with distilled water
- **Stop solution (i.e. 2% Acetic acid solution)**
 - 4 mL Acetic acid
 - Make the volume upto 200 mL with distilled water
- **Methodology:**

The polyacrylamide gel was washed with 10% ethanol solution for 10 minutes twice. The gel was washed with distilled water for 30 minutes, though changing the water after every 2 minutes. The gel was dipped in farmer's reagent for 30-50 seconds and rinsed with distilled water thrice for 5 minutes each. The polyacrylamide gel was again dipped in silver nitrate solution for 4-5 minutes and followed by rinsing with 2.5% sodium carbonate solution for 4-5 minutes. The gel was dipped in developer solution for 30 seconds and as the bands started to appear, the reaction was stopped adding stop solution i.e. 2% acetic acid solution.

3.4 Characterization of purified antilithiatic proteins

3.4.1 Materials

HPLC column used was Pico Tag (Waters). Solvents used were HPLC grade. MASCOT, ScanProsite and BLASTp were online tools used.

3.4.2 Reverse phase HPLC (RP-HPLC) for protein homogeneity

Waters Spherisorb® C18 (5 μ, 4.6 X 250 mm) column with solvent A (0.1% TFA in water) and solvent B (100% acetonitrile containing 0.1% TFA) was used for determining the homogeneity of purified protein. Flow rate was maintained at 1 mL/min at the time of protein injection. The column was washed with solvent A and brought to 20% acetonitrile in 5 minutes. The bound protein was eluted with a linear gradient of acetonitrile (20-70%) over a period of 50 minutes. The detection was monitored at 280 nm using Waters 2996 photodiode array detector [248, 249].

3.4.3 Peptide mass fingerprinting

Peptide mass fingerprinting was done using Matrix-Assisted Laser Desorption/Ionization –Time of Flight Mass Spectrometry. It is a very sensitive technique and can determine the molecular mass of a protein even in a pico mole amount. In Peptide mass fingerprinting, protein is digested with trypsin and various small peptides thus obtained are subjected to MALDI-TOF-MS which determines the molecular weight of each peptide of the trypsinized protein.

The differentially expressed bands identified after the image analysis were excised and cut into small pieces of approximately 1 mm followed by destaining of the pieces in a freshly prepared 1:1 (v/v) mixture of potassium ferricyanide and sodium thiosulphate. The gel pieces were then sequentially incubated with reducing and alkylating reagents and with modified trypsin (Sigma). Peptides were eluted and reextracted in 50% trifluoroacetic acid (TFA) containing 0.1% acetonitrile (ACN). The samples were purified using ZipTip and mixed with α -cyano-4-hydroxycinnamic acid (4-HCCA) matrix in 1:1 ratio followed by plating onto a MALDI plate. After air drying, the plate was analysed using MALDI TOF/TOF ultraflex III instrument and further analysis was done with flex analysis software for obtaining the peptide mass fingerprint.

3.4.4 Peptide matching

Peptide matching was performed using MASCOT search engine (<http://www.matrixscience.com>) assuming that the peptides were monoisotopic, carbamidomethylated at cysteine residues and oxidised at methionine residues. A mass tolerance was 120 parts per million and only 1 maximal cleavage was allowed for peptide matching. Probability-based MOWSE (Molecular Weight Search) score was calculated using the formula $[-10 \log (P)]$, where P was the probability that the observed match was a random event.

3.4.5 Putative function and domain prediction

The amino acid sequences of protein were subjected to BLASTp analysis to determine putative function and family of protein using all non-redundant GenBank. The presence of the active domains in the random hit was found using the online tool, ScanProsite. The amino acid sequence of the hit was used as an input and the presence of the domains were searched.

3.5 Cytoprotective effect of antilithiatic proteins of *Terminalia arjuna* on oxalate-induced renal tubular epithelial cell injury

3.5.1 Sample preparation

For cell culture studies, the >3 kDa fraction and purified protein samples obtained after molecular sieve chromatography as described in section 3.3.7 were dialyzed against distilled water by centrifugation through Amicon Ultra-4 centrifugal separating tubes (Millipore) of 3 kDa cut off molecular weight and then lyophilized. The lyophilized >3 kDa fraction and purified protein samples obtained after molecular sieve chromatography were reconstituted in serum free DMEM and filtered by 0.22 µm syringe filter.

3.5.2 Cell viability

Cytotoxicity was assessed by MTT assay as discussed earlier (Section 3.2.5.2 and 3.2.5.3) with test sample at various concentrations of 4 µg/mL, 6 µg/mL, 8 µg/mL and 10 µg/mL in the presence of oxalate for >3 kDa fraction and purified proteins obtained after molecular sieve chromatography. A positive control, cysteine at a concentration of 10 µg/mL, was also tested for its protective potential towards oxalate injured renal epithelial cells (NRK-52E and MDCK).

3.5.3 Detection of apoptosis

Apoptosis and necrosis was assessed as discussed earlier (Section 3.2.6.1, 3.2.6.2 and 3.2.6.3) with test sample at a concentration of 10 µg/mL in the presence of oxalate for >3 kDa fraction and purified proteins obtained after molecular sieve chromatography. A positive control, cysteine at a concentration of 10 µg/mL, was also tested for its protective potential towards oxalate injured renal epithelial cells (NRK-52E and MDCK).

3.6 Statistical analysis

Statistical procedures were performed with GraphPad Prism software version 6.01. The statistically different groups were identified by one way analysis of variance (ANOVA), followed by Dunnett's multiple comparison tests. Results were expressed as the mean ± SD. A p-value of <0.05 was considered significant. All the experiments were performed three times, each time in triplicate.

CHAPTER 4

RESULTS

4.1 Antiurolithiatic potential of aqueous extract of *Terminalia arjuna* in vitro

For *in vitro* antiurolithiatic potential studies a stock solution was prepared by dissolving the dried aqueous extract of *Terminalia arjuna* in distilled water. Further dilutions of the stock were done using the distilled water and filtered by 0.22 μm syringe filter. The various concentrations of aqueous extract of *Terminalia arjuna* tested for their inhibitory activity were 10 $\mu\text{g}/\text{mL}$, 25 $\mu\text{g}/\text{mL}$, 50 $\mu\text{g}/\text{mL}$, 100 $\mu\text{g}/\text{mL}$, 200 $\mu\text{g}/\text{mL}$, 500 $\mu\text{g}/\text{mL}$ and 1000 $\mu\text{g}/\text{mL}$ which were prepared at the time of experiment.

4.1.1 Effect of aqueous extract of *Terminalia arjuna* on the calcium oxalate (CaOx) crystallization

At final concentrations of 5.0 mmol/L calcium and 0.5 mmol/L oxalate, the CaOx crystallization inhibitory activity of *Terminalia arjuna* aqueous extract increased with increasing concentrations of the extract in a dose-dependent manner from 10 $\mu\text{g}/\text{mL}$ to 1000 $\mu\text{g}/\text{mL}$ as shown in Figure 4.1. The cystone drug at a concentration of 1000 $\mu\text{g}/\text{mL}$ was used as a positive control.

For CaOx crystal nucleation, the percentage inhibition shown by the *Terminalia arjuna* bark aqueous extract at 10 $\mu\text{g}/\text{mL}$, 25 $\mu\text{g}/\text{mL}$ and 50 $\mu\text{g}/\text{mL}$ were found to be $20.77 \pm 3.61\%$, $27.34 \pm 2.84\%$ and $31.06 \pm 2.47\%$ respectively. As the concentration of aqueous extract was increased to 100 $\mu\text{g}/\text{mL}$, the percentage inhibition increased to $42.63 \pm 1.41\%$. The inhibition was almost constant in the range of 45-50% at 200 $\mu\text{g}/\text{mL}$ and 500 $\mu\text{g}/\text{mL}$ and increased upto $61.36 \pm 0.58\%$ at 1000 $\mu\text{g}/\text{mL}$ when compared to the control (with no plant extract). Addition of 1000 $\mu\text{g}/\text{mL}$ cystone resulted in a nucleation percentage inhibition of $57.53 \pm 3.54\%$.

For CaOx crystal aggregation, the percentage inhibition shown by the *Terminalia arjuna* bark aqueous extract at 10 $\mu\text{g}/\text{mL}$ was found to be $31.05 \pm 5.34\%$ which remained almost constant at 25 $\mu\text{g}/\text{mL}$ and 50 $\mu\text{g}/\text{mL}$. As the concentration of aqueous extract was increased to 100 $\mu\text{g}/\text{mL}$, 200 $\mu\text{g}/\text{mL}$ and 500 $\mu\text{g}/\text{mL}$, the percentage inhibition increased to $34.47 \pm 2.67\%$, $39.9 \pm 2.27\%$ and $44.65 \pm 2.38\%$ respectively. The percentage inhibition increased to $49.8 \pm 2.4\%$ at 1000 $\mu\text{g}/\text{mL}$ when compared to

the control (with no plant extract). Addition of 1000 $\mu\text{g/mL}$ cystone resulted in an aggregation percentage inhibition of $69.66 \pm 4.25\%$.

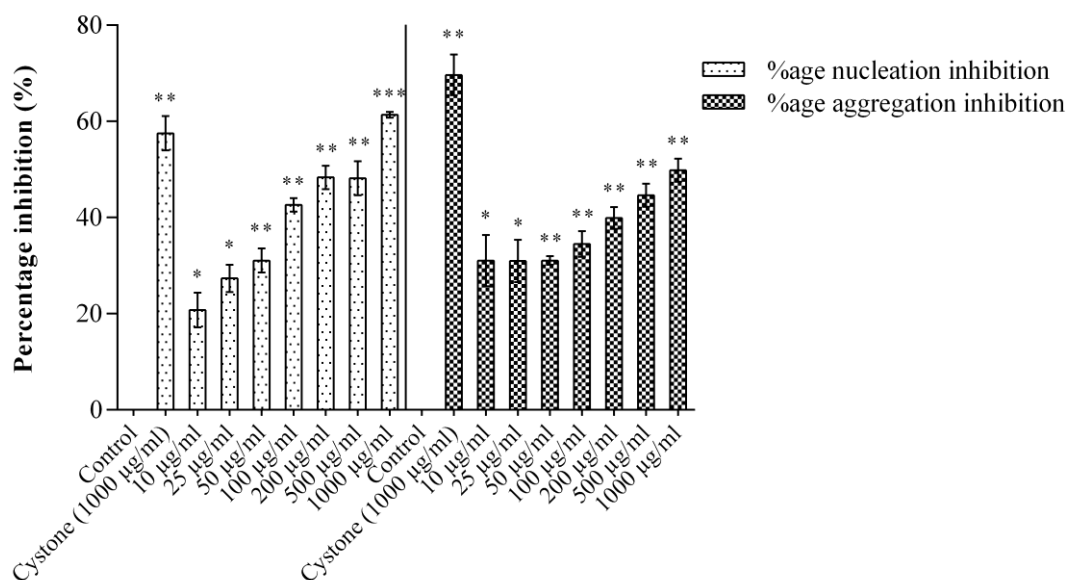


Figure 4.1 Effect of aqueous extract of *T. arjuna* on nucleation and aggregation of calcium oxalate crystals. Data are mean \pm S.D of three independent observations. * $p < 0.05$, ** $p < 0.005$, *** $p < 0.0005$

4.1.2 Effect of aqueous extract of *Terminalia arjuna* on the growth of calcium oxalate (CaOx) crystal

The aqueous extract of *Terminalia arjuna* bark showed the inhibitory effect on the growth of CaOx crystals as shown in Figure 4.2. When compared to the control (with no plant extract), the percentage inhibition at 10 $\mu\text{g/mL}$ was found to be $13.78 \pm 1.86\%$, which increased to $30.34 \pm 0.4\%$ and $34.34 \pm 4.48\%$ at 25 $\mu\text{g/mL}$ and 50 $\mu\text{g/mL}$ aqueous extract respectively. As the concentration of aqueous extract was increased to 100 $\mu\text{g/mL}$, the percentage inhibition decreased to $24.97 \pm 4.61\%$. The percentage inhibition was significantly increased to $41.82 \pm 2.03\%$ and $96.41 \pm 1.36\%$ at 200 $\mu\text{g/mL}$ and 500 $\mu\text{g/mL}$ respectively and again reduced to $86.89 \pm 1.87\%$ at 1000 $\mu\text{g/mL}$. The cystone drug at a concentration of 1000 $\mu\text{g/mL}$ was used as a positive control. Addition of 1000 $\mu\text{g/mL}$ cystone resulted in a growth percentage inhibition of $90.67 \pm 5.9\%$.

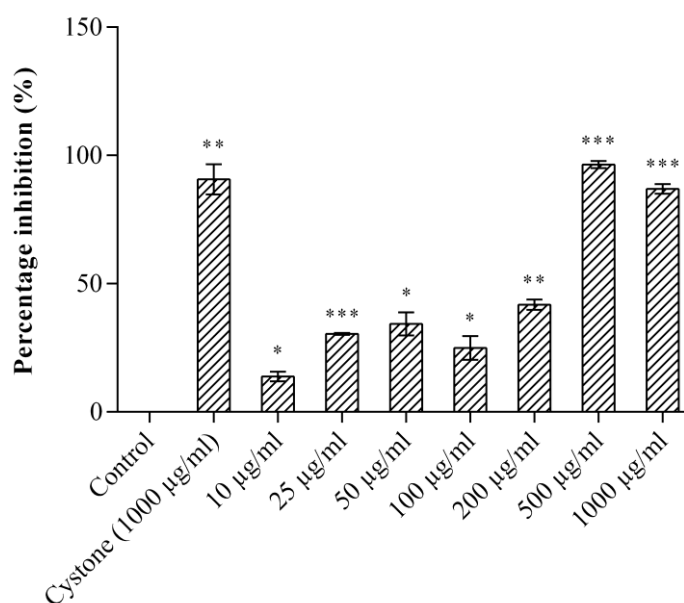


Figure 4.2 Effect of aqueous extract of *T. arjuna* on growth of calcium oxalate crystals. Data are mean \pm S.D of three independent observations. * $p < 0.05$, ** $p < 0.005$, *** $p < 0.0005$

4.1.3 Effect of aqueous extract of *Terminalia arjuna* on the calcium oxalate (CaOx) crystal morphology

Incubating the metastable solutions of 4.25 mM calcium and 0.75 mM oxalate resulted in the formation of CaOx crystals composed predominately of hexagonal CaOx monohydrate as shown in Figure 4.3A. Microphotography studies showed that the aqueous extract of *Terminalia arjuna* bark resulted in the formation of rounded CaOx crystals. When compared to control (with no plant sample), the aqueous extract of *Terminalia arjuna* bark modified the morphology of CaOx crystals from hexagonal to spherical shape at a concentration of 1000 $\mu\text{g/mL}$ aqueous extract as shown in Figure 4.3C and reduced the dimensions such as area, perimeter, length and width of CaOx crystals as shown in Table 4.1. The CaOx crystal area, perimeter, length and width was reduced from 0.3 μm^2 , 2.31 μm , 0.85 μm and 0.54 μm to 0.06 μm^2 , 0.85 μm , 0.31 μm and 0.23 μm by the addition of 1000 $\mu\text{g/mL}$ of aqueous extract respectively. The cystone drug at a concentration of 1000 $\mu\text{g/mL}$ was used as a positive control. Addition of 1000 $\mu\text{g/mL}$ of cystone also rounded the edges of hexagonal CaOx monohydrate crystals (Figure 4.3B) and decreased the area, perimeter, length and width of CaOx crystals to 0.23 μm^2 , 1.73 μm , 0.64 μm and 0.41 μm respectively.

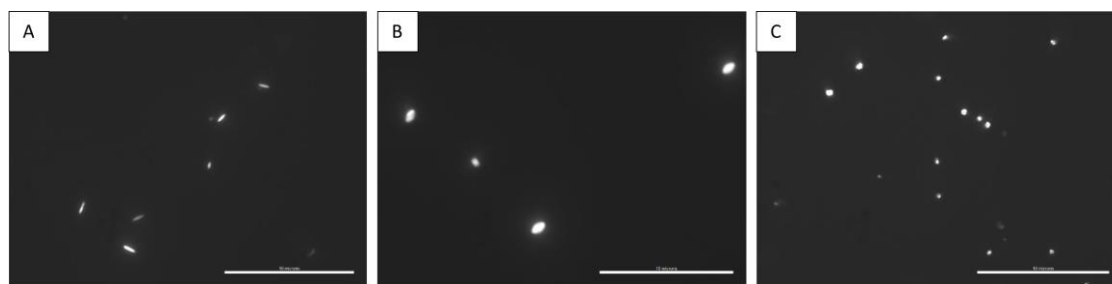


Figure 4.3 Calcium oxalate crystals, observed under upright microscope at magnification 100X and scale bar 10 microns, formed in the metastable solution of calcium oxalate in the absence (A) and the presence of (B) cystone (1000 $\mu\text{g}/\text{mL}$) and (C) *T. arjuna* bark aqueous extract (1000 $\mu\text{g}/\text{mL}$)

Table 4.1 Effect of *T. arjuna* aqueous extract (AE) on the morphology and dimension of calcium oxalate crystals *in vitro* at a concentration of 1000 $\mu\text{g}/\text{mL}$ as compared to control. Data are mean \pm S.D of three independent observations

	Control (A)	Cystone 1000 $\mu\text{g}/\text{ml}$ (B)	AE 1000 $\mu\text{g}/\text{ml}$ (C)
Area (μm^2)	0.30 \pm 0.05	0.23 \pm 0.14	0.06 \pm 0.001
Perimeter (μm)	2.31 \pm 0.21	1.73 \pm 0.72	0.85 \pm 0.007
Length (μm)	0.85 \pm 0.0	0.64 \pm 0.29	0.31 \pm 0.01
Width (μm)	0.54 \pm 0.07	0.41 \pm 0.15	0.23 \pm 0.02
Shape	Hexagonal	Hexagonal with rounded edges	Spherical

4.1.4 Effect of aqueous extract of *Terminalia arjuna* on the scavenging of DPPH radical

The antioxidant activity of aqueous extract of *Terminalia arjuna* was determined by measuring the DPPH radical scavenging activity. The aqueous extract of *Terminalia arjuna* bark displayed the DPPH radical scavenging activity. The ability to scavenge the DPPH radical increased with increasing concentrations of the extract in a dose-dependent manner as shown in Figure 4.4. The percentage of DPPH radical inhibition ranged from 25.82% at 5 $\mu\text{g}/\text{mL}$ to 93.87% at 50 $\mu\text{g}/\text{mL}$. The aqueous extract caused scavenging of DPPH radical with IC_{50} value of 13.11 $\mu\text{g}/\text{mL}$. The chemical, ascorbic

acid was used as a standard and similarly inhibited DPPH with IC₅₀ value of 5.84 µg/mL.

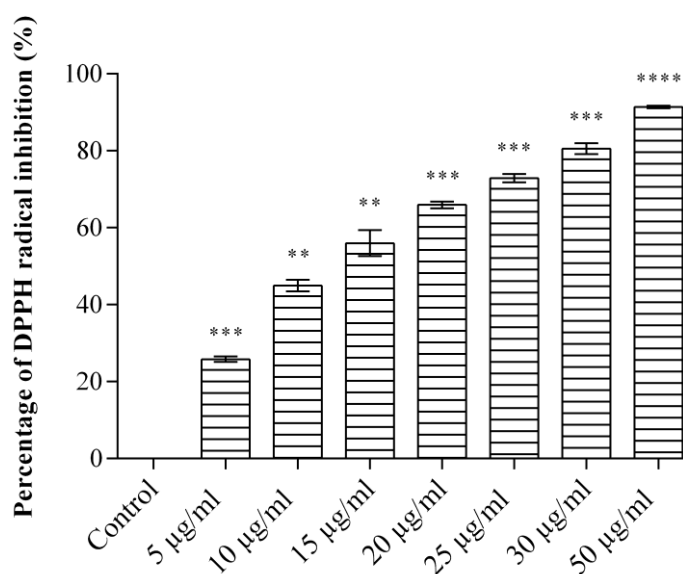


Figure 4.4 Effect of aqueous extract of *T. arjuna* on DPPH radicals inhibition. Data are mean \pm S.D of three independent observations. ** $p < 0.005$, *** $p < 0.0005$, **** $p < 0.0001$

4.2 Diminution of oxalate-induced renal tubular epithelial cell injury by aqueous extract of *Terminalia arjuna*

For cell culture studies a stock solution was prepared by dissolving the dried aqueous extract of *Terminalia arjuna* in dimethyl sulfoxide (DMSO) [final concentration of the DMSO in the highest concentration of plant extract tested did not exceed 0.4% (v/v) and did not affect the cell proliferation]. Further dilutions of the stock were done using serum free DMEM (Dulbecco's Modified Eagle's Media) and filtered by 0.22 µm syringe filter.

The various concentrations of aqueous extract of *Terminalia arjuna* tested for their inhibitory potential were 10 µg/mL, 20 µg/mL, 30 µg/mL and 40 µg/mL which were prepared at the time of experiment.

4.2.1 Cell viability

The cytoprotective potential of aqueous extract of *Terminalia arjuna* was assessed by cell viability using trypan blue exclusion method and MTT assay.

4.2.1.1 Effect of aqueous extract of *Terminalia arjuna* on oxalate-induced renal tubular epithelial cell injury by trypan blue exclusion assay

The protective effect of aqueous extract of *Terminalia arjuna* towards the renal tubular epithelial cells, NRK-52E is displayed in Figure 4.5. The oxalate induced a significant injury to the cells which could be ascertained by a decrease in viability from 100% in the controls (untreated cells) to $23.4 \pm 1.75\%$. However, the injury due to oxalate was significantly reduced in those cells treated with the aqueous extract *Terminalia arjuna* bark. As the concentration of the extract increased from $10 \mu\text{g/mL}$ to $40 \mu\text{g/mL}$, the percentage viability improved showing that the plant has a protective effect towards the oxalate caused injury to the renal cells in a concentration dependent manner. The solvent system (0.4% DMSO) and plant extract alone ($40 \mu\text{g/mL}$, containing 0.4% DMSO) had no effect on the cell with a viability percentage of $96.51 \pm 1.19\%$ and $82.76 \pm 2.26\%$ respectively, indicating that there was no cytotoxicity to the cells. The percentage viability with $10 \mu\text{g/mL}$, $20 \mu\text{g/mL}$, $30 \mu\text{g/mL}$ and $40 \mu\text{g/mL}$ was $26.2 \pm 1.88\%$, $33.53 \pm 1.32\%$, $39.61 \pm 2.26\%$ and $47.41 \pm 3.03\%$ respectively. The effect of $40 \mu\text{g/mL}$ of Cystone on oxalate treated NRK-52E cells also exhibited cytoprotective effect with viability percentage of $42.93 \pm 2.61\%$ as compared to oxalate treated cells.

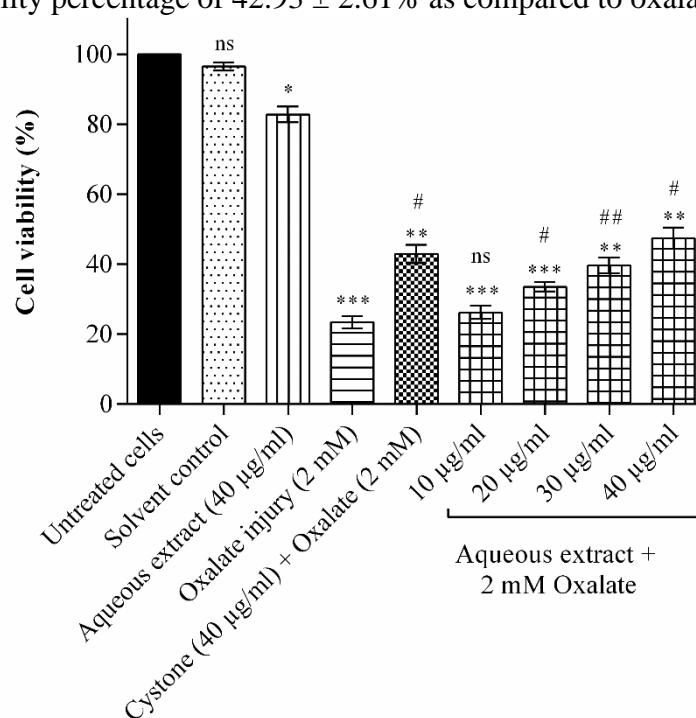


Figure 4.5 Effect of aqueous extract of *T. arjuna* on NRK-52E cell viability assessed by trypan blue exclusion assay. Data are mean \pm S.D of three independent observations. ns: not significant. * $p < 0.05$, ** $p < 0.005$, *** $p < 0.001$ versus untreated control; and # $p < 0.05$, ## $p < 0.005$ versus oxalate injury control

The protective effect of aqueous extract of *Terminalia arjuna* towards the renal tubular epithelial cells, MDCK is displayed in Figure 4.6. The oxalate caused injury to the cells which could be ascertained by a decrease in viability from 100% in the controls (untreated cells) to $24.33 \pm 0.81\%$. The solvent system (0.4% DMSO) and plant extract alone (40 $\mu\text{g}/\text{mL}$, containing 0.4% DMSO) had no effect on the cell with a viability percentage of $97.22 \pm 1.26\%$ and $83.71 \pm 1.83\%$ respectively, indicating that there was no cytotoxicity to the cells. However, the injury due to oxalate exposure was significantly reduced in those cells treated with the aqueous extract *Terminalia arjuna* bark. As the concentration of the extract increased from 10 $\mu\text{g}/\text{mL}$ to 40 $\mu\text{g}/\text{mL}$, the percentage viability improved showing that the plant has a protective effect towards the oxalate caused injury to the renal cells in a concentration dependent manner. The percentage viability with 10 $\mu\text{g}/\text{mL}$, 20 $\mu\text{g}/\text{mL}$, 30 $\mu\text{g}/\text{mL}$ and 40 $\mu\text{g}/\text{mL}$ was $25.73 \pm 2.72\%$, $36.4 \pm 1.83\%$, $44.1 \pm 2.33\%$ and $51.3 \pm 2.65\%$ respectively. The addition of 40 $\mu\text{g}/\text{mL}$ of Cystone to oxalate treated MDCK cells also exhibited cytoprotective effect with viability percentage of $44.77 \pm 2.32\%$ as compared to oxalate treated cells.

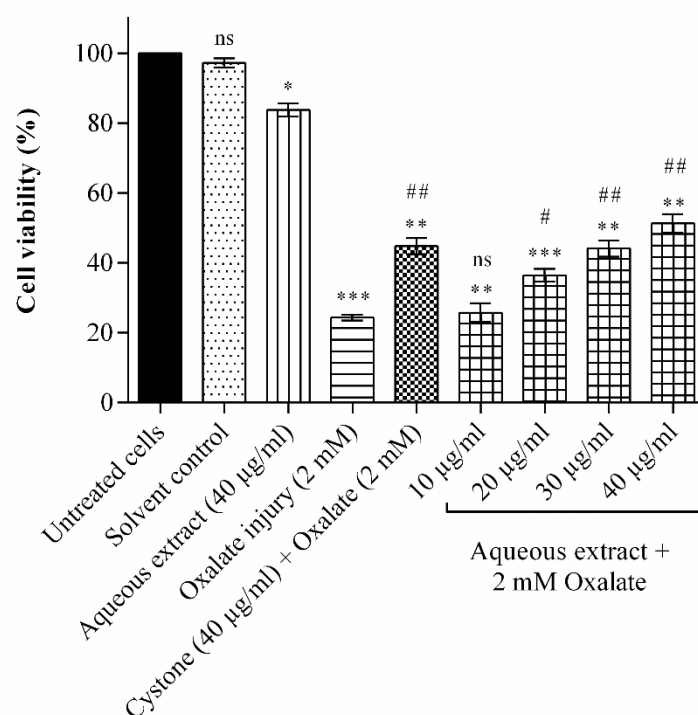


Figure 4.6 Effect of aqueous extract of *T. arjuna* on MDCK cell viability assessed by trypan blue exclusion assay. Data are mean \pm S.D of three independent observations. ns: not significant. * $p < 0.05$, ** $p < 0.005$, *** $p < 0.001$ versus untreated control; and # $p < 0.05$, ## $p < 0.01$ versus oxalate injury control

4.2.1.2 Effect of aqueous extract of *Terminalia arjuna* on oxalate-induced renal tubular epithelial cell injury by MTT assay

The cytoprotective potential of aqueous extract of *Terminalia arjuna* towards the oxalate induced injury to renal tubular epithelial cells, NRK-52E is displayed in Figure 4.7. The oxalate caused injury to the cells which could be ascertained by a decrease in viability from 100% in the controls (untreated cells) to $23.75 \pm 1.66\%$. The solvent system (0.4% DMSO) and plant extract alone (40 $\mu\text{g}/\text{mL}$ containing 0.4% DMSO) had no effect on the cell with a viability percentage of $96.99 \pm 1.69\%$ and $80.84 \pm 1.27\%$ respectively, indicating that there was no cytotoxicity to the cells. However, the injury due to oxalate was significantly reduced in those cells treated with the aqueous extract *Terminalia arjuna* bark. As the concentration of the extract increased from 10 $\mu\text{g}/\text{mL}$ to 40 $\mu\text{g}/\text{mL}$, the percentage viability improved in a concentration dependent manner. The percentage viability with 10 $\mu\text{g}/\text{mL}$, 20 $\mu\text{g}/\text{mL}$, 30 $\mu\text{g}/\text{mL}$ and 40 $\mu\text{g}/\text{mL}$ of extract was $25.89 \pm 1.44\%$, $33.22 \pm 1.57\%$, $39.71 \pm 1.37\%$ and $48.47 \pm 1.83\%$ respectively. The addition of 40 $\mu\text{g}/\text{mL}$ of Cystone on oxalate treated NRK-52E cells also exhibited cytoprotective effect with viability percentage of $45.88 \pm 1.61\%$ as compared to oxalate treated cells.

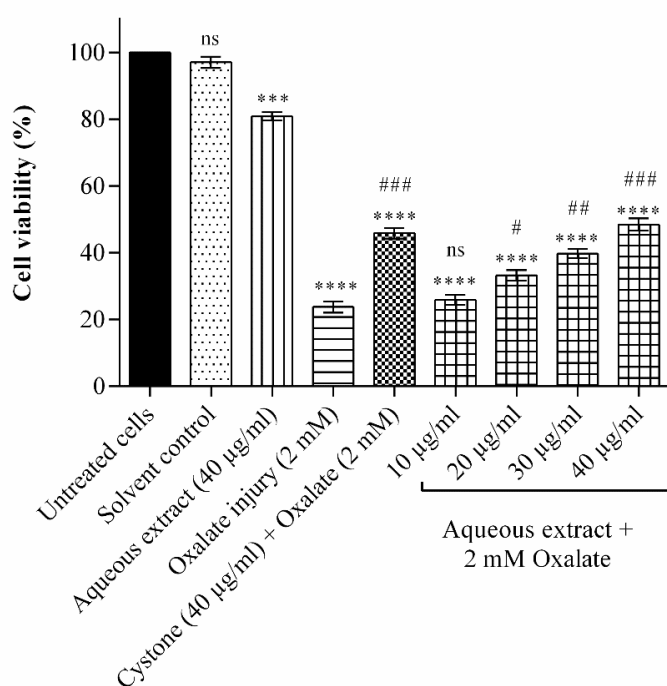


Figure 4.7 Effect aqueous extract of *T. arjuna* on NRK-52E cell viability assessed by MTT assay. Data are mean \pm S.D of three independent observations. ns: not significant. *** $p < 0.0005$, **** $p < 0.0001$ versus untreated control; and # $p < 0.05$, ## $p < 0.005$, ### $p < 0.001$ versus oxalate injury control

The aqueous extract of *Terminalia arjuna* protected the MDCK cells from oxalate induced injury to renal tubular epithelial cells as displayed in Figure 4.8. The oxalate caused significant cell death which could be ascertained by a decrease in viability from 100% in the control (untreated cells) to $24.18 \pm 1.17\%$. The solvent system (0.4% DMSO) and aqueous extract alone (40 $\mu\text{g}/\text{mL}$ containing 0.4% DMSO) had no adverse effect on the cells with a viability percentage of $97.95 \pm 1.11\%$ and $82.7 \pm 1.86\%$ respectively. However, the injury caused by oxalate was significantly reduced in those cells treated with the aqueous extract *Terminalia arjuna* bark. As the concentration of the extract increased from 10 $\mu\text{g}/\text{mL}$ to 40 $\mu\text{g}/\text{mL}$, the percentage viability improved showing that the plant has a protective effect towards the oxalate caused injury to the renal cells in a concentration dependent manner. The percentage viability with 10 $\mu\text{g}/\text{mL}$, 20 $\mu\text{g}/\text{mL}$, 30 $\mu\text{g}/\text{mL}$ and 40 $\mu\text{g}/\text{mL}$ was $26.64 \pm 0.88\%$, $34.98 \pm 1.79\%$, $42.7 \pm 1.51\%$ and $50.04 \pm 1.44\%$ respectively. The treatment of 40 $\mu\text{g}/\text{mL}$ of Cystone on oxalate exposed MDCK cells also reduced the injury caused to cells by oxalate with viability percentage of $45.6 \pm 1.69\%$ as compared to oxalate treated cells.

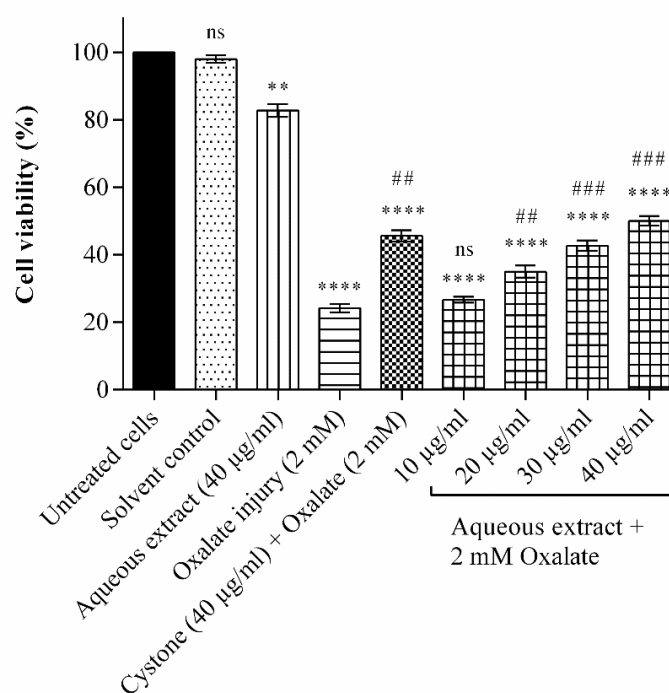


Figure 4.8 Effect of aqueous extract of *T. arjuna* on MDCK cell viability assessed by MTT assay. Data are mean \pm S.D of three independent observations. ns: not significant. ** $p < 0.005$, **** $p < 0.0001$ versus untreated control; and ## $p < 0.01$, ### $p < 0.0005$ versus oxalate injury control

4.2.1.3 Effect of aqueous extract of *Terminalia arjuna* on calcium oxalate (CaOx) crystal adherence on oxalate-induced renal tubular epithelial cell injury

The NRK-52E and MDCK cells were microscopically studied for cell-crystal interactions under phase contrast polarized microscope to demonstrate crystal adhesion on the cell surface as shown in Figure 4.9 and 4.10 respectively.

After incubation of the NRK-52E cells with 2 mM oxalate for 48 hours at 37°C, hexagonal COM crystals and smaller granules were observed. These crystals internalized and remained adhered to the cells even after several washes using PBS depicting that CaOx crystals adhered tightly to renal cells with subsequent detrimental effects to the cells (Figure 4.9D). These crystals caused cell damage and cell death which is evident by lesser number of cells. Crystal adhesion and internalization into the cells were observed; showing the mechanism of renal cellular injury by CaOx. The cells treated with the solvent system (0.4% DMSO) and plant extract alone (40 µg/mL containing 0.4% DMSO) showed healthy cellular morphology (Figure 4.9B and 4.9C), indicating that there is no adverse effect to the cells. The effect of 40 µg/mL of aqueous extract on oxalate treated NRK-52E cells (Figure 4.9F) was assessed and compared to oxalate treated cells (Figure 4.9D), more viable cells and smaller crystals were observed, showing loss of crystal adherence to cells and dissolution of crystals in presence of 40 µg/mL of aqueous extract of *Terminalia arjuna* and thus, indicating cell-crystal interaction. Cystone drug used as a positive control at a concentration of 40 µg/mL also exhibited cytoprotective effect with more viable cells and loosely bound crystals (Figure 4.9E) as compared to oxalate treated cells.

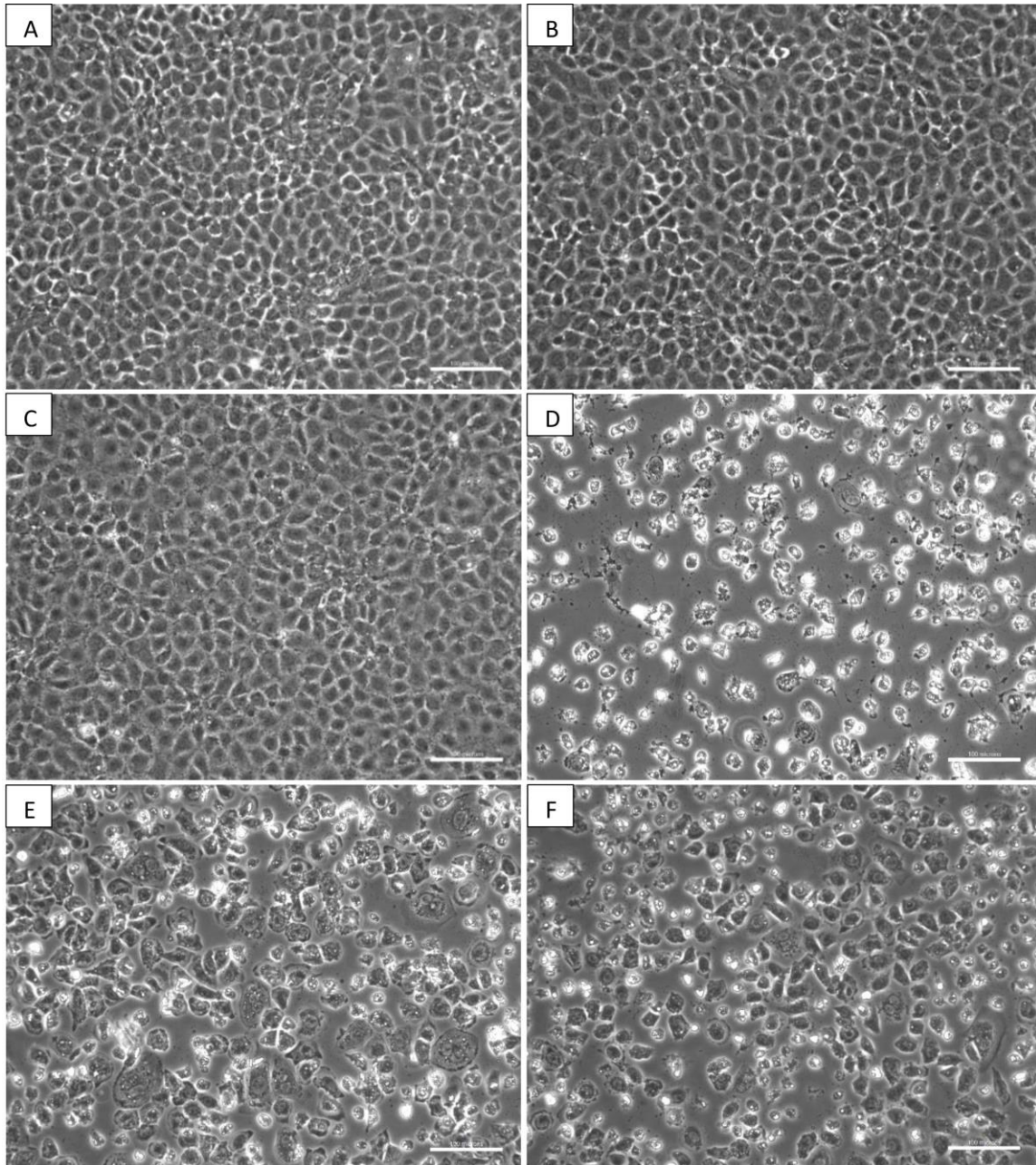


Figure 4.9 Effect of aqueous extract of *T. arjuna* on CaOx crystal adherence in oxalate induced injury to NRK-52E cells, visualized under polarization and phase contrast at magnification 20X and scale bar 100 microns. Labels are as follow: A: Untreated cells; B: Solvent control (0.4% DMSO); C: Only 40 µg/mL Aqueous extract (AE); D: 2 mM Oxalate injury; E: Positive control (40 µg/mL Cystone + 2 mM Oxalate) and F: 40 µg/mL AE + 2 mM Oxalate

After incubation of the MDCK cells with 2 mM oxalate for 48 hours at 37°C, hexagonal COM and bipyramidal COD crystals were observed. Some of these crystals internalized and some remained adhered to the cells even after several washes using PBS depicting that CaOx crystals adhered tightly to renal cells with subsequent detrimental effects to the cells (Figure 4.10D). These crystals caused cell damage and cell death which is evident by lesser number of cells. Crystal adhesion and internalization into the cells were observed; showing the mechanism of renal cellular injury by CaOx. The cells treated with the solvent system (0.4% DMSO) and aqueous extract (40 µg/mL containing 0.4% DMSO) showed healthy cellular morphology (Figure 4.10B and 4.10C), indicating that there is no harmful effect to the cells. The effect of 40 µg/mL of aqueous extract on oxalate treated MDCK cells (Figure 4.10F) was evaluated and compared to oxalate treated cells (Figure 4.10D), more viable cells were observed showing loss of crystal adherence to cells and dissolution of crystals in presence of 40 µg/mL of aqueous extract of *Terminalia arjuna* and thus, indicating cell-crystal interaction. Cystone drug at a concentration of 40 µg/mL was used as a positive control. The effect of 40 µg/mL of Cystone on oxalate treated MDCK cells (Figure 4.10E) also exhibited protective effect with more viable cells and loosely bound crystals as compared to oxalate treated cells.

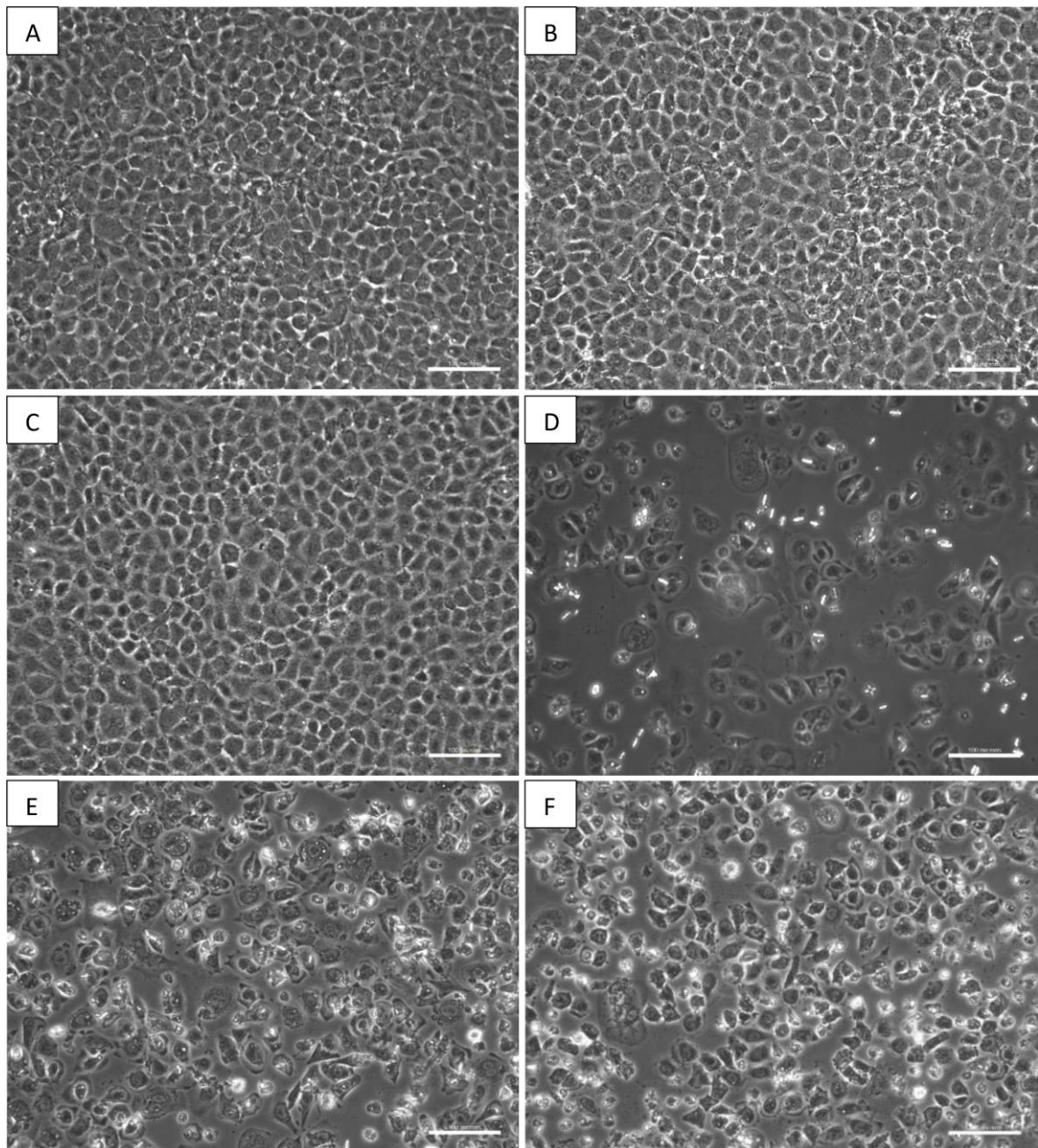


Figure 4.10 Effect of aqueous extract of *T. arjuna* on CaOx crystal adherence in oxalate induced injury to MDCK cells, visualized under polarization and phase contrast at magnification 20X and scale bar 100 microns. Labels are as follow: A: Untreated cells; B: Solvent control (0.4% DMSO); C: Only 40 µg/mL Aqueous extract (AE); D: 2 mM Oxalate injury; E: Positive control (40 µg/mL Cystone + 2 mM Oxalate) and F: 40 µg/mL AE + 2 mM Oxalate

4.2.2 Detection of apoptosis

4.2.2.1 Effect of aqueous extract of *Terminalia arjuna* on induction of apoptosis in oxalate-induced renal cell injury by Hoechst staining

The morphological changes in cell nuclei were determined by fluorescence microscopy by staining NRK-52E and MDCK cells with Hoechst 33258 dye as shown in Figure 4.11 and 4.12 respectively. This dye binds to (A-T) regions of the major groove of DNA and shows distinct fluorescence emission spectra as per dye:base pair ratios.

The untreated NRK-52E cells appeared to be intact in healthy morphology and showed intact chromatin (Figure 4.11A), indicating that there was no significant cell death in the untreated cells. The cells treated with the solvent system (0.4% DMSO) and plant extract alone (40 µg/mL containing 0.4% DMSO) showed healthy cellular morphology (Figure 4.11B and 4.11C), indicating that there was no adverse effect to the cells. After incubation of the NRK-52E cells with 2 mM oxalate for 48 hours at 37°C, a substantial level of cell death w.r.t. control was observed. The cells showed marked changes in morphology such as irregular shape, membrane blebbing, apoptotic bodies and condensed and fragmented chromatin (Figure 4.11D). The effect of 40 µg/mL of aqueous extract on oxalate treated NRK-52E cells (Figure 4.11F) was assessed and compared to oxalate treated cells (Figure 4.11D), more viable cells with intact cellular membrane and fewer apoptotic bodies were observed, showing reduced level of cells undergoing apoptosis w.r.t. the oxalate injured cells. Cystone drug at a concentration of 40 µg/mL was used as a positive control. The effect of 40 µg/mL of Cystone on oxalate treated NRK-52E cells (Figure 4.11E) also showed cytoprotective effect with more viable cells and reduced level of apoptosis and necrosis as compared to oxalate treated cells.

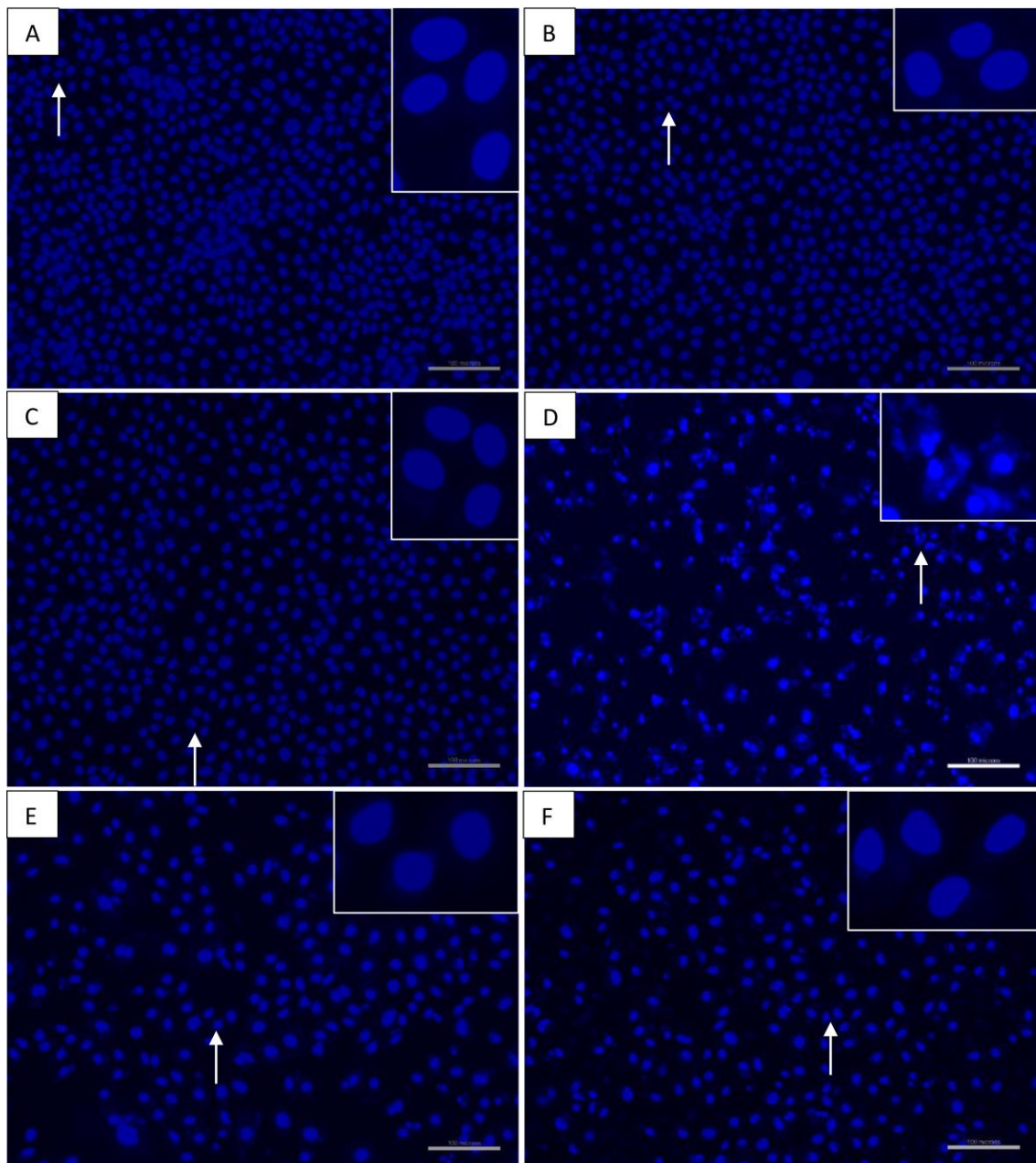


Figure 4.11 Effect of aqueous extract of *T. arjuna* on induction of apoptosis in oxalate induced injury to NRK-52E cells, visualized under fluorescence microscopy at magnification 20X and scale bar 100 microns. Labels are as follow: A: Untreated cells; B: Solvent control (0.4% DMSO); C: Only 40 µg/mL Aqueous extract (AE); D: 2 mM Oxalate injury; E: Positive control (40 µg/mL Cystone + 2 mM Oxalate) and F: 40 µg/mL AE + 2 mM Oxalate

The untreated MDCK cells appeared to be intact in healthy morphology and showed intact chromatin (Figure 4.12A), indicating that there was no cell death in the untreated cells i.e. all the cells were live. The cells treated with the solvent system (0.4% DMSO) and plant extract alone (40 µg/mL containing 0.4% DMSO) showed healthy cellular morphology (Figure 4.12B and 4.12C), indicating that there was no adverse effect to the cells. When MDCK cells were treated with 2 mM oxalate for 48 hours at 37°C, a substantial level of cells undergoing apoptosis w.r.t. control was observed. The cells showed marked changes in morphology such as irregular shape, membrane blebbing, apoptotic bodies and condensed and fragmented chromatin (Figure 4.12D). The effect of 40 µg/mL of aqueous extract on oxalate treated MDCK cells (Figure 4.12F) was assessed and compared to oxalate treated cells (Figure 4.12D), more viable cells with intact cellular membrane and fewer apoptotic bodies were observed, showing reduced level of apoptosis and necrosis w.r.t. the oxalate injured cells. Cystone drug at a concentration of 40 µg/mL was used as a positive control and protected the cells from injury caused by oxalate (Figure 4.12E) thus, exhibited cytoprotective effect with more viable cells and reduced level of apoptosis as compared to oxalate treated cells.

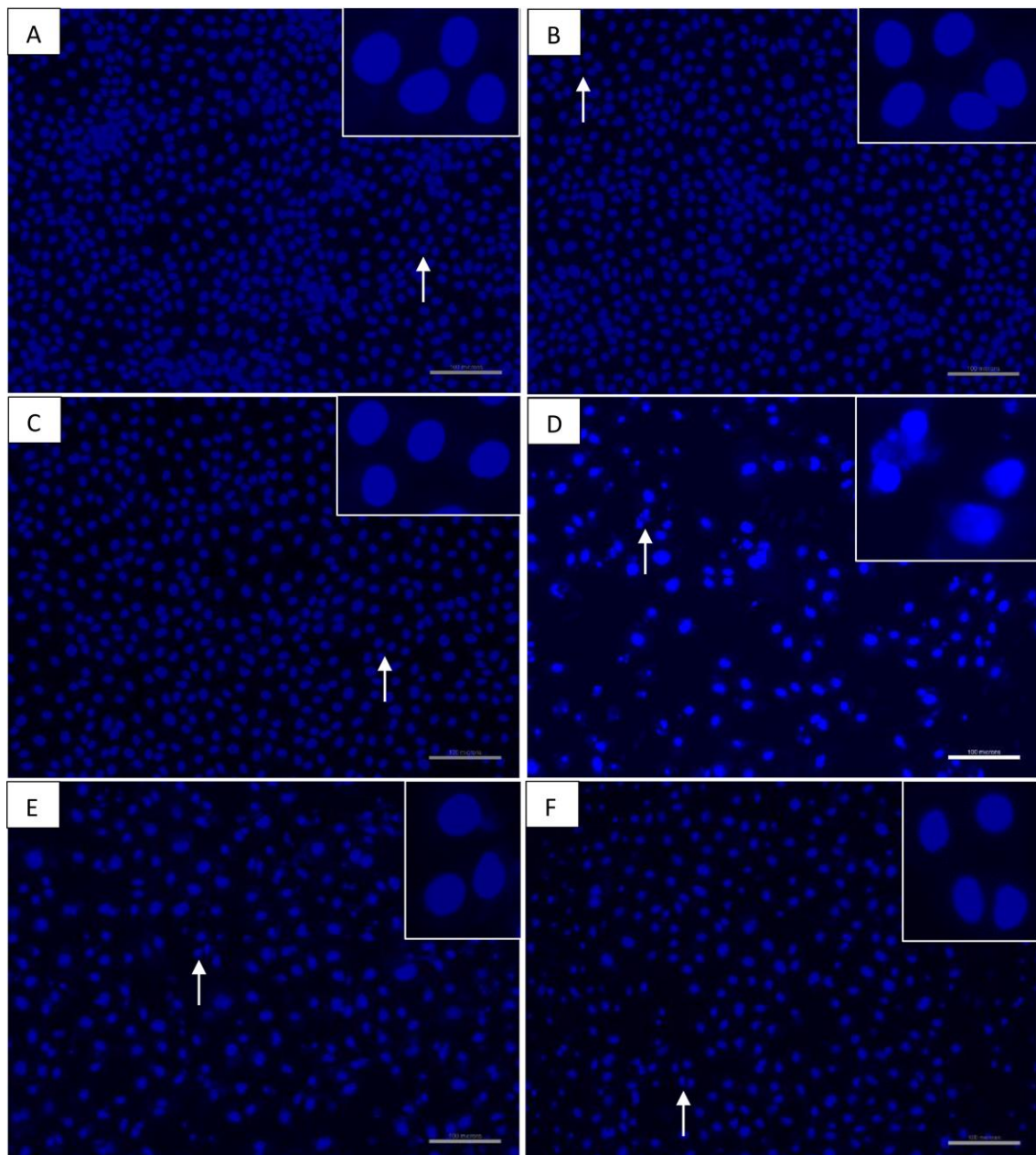


Figure 4.12 Effect of aqueous extract of *T. arjuna* on induction of apoptosis in oxalate induced injury to MDCK cells, visualized under fluorescence microscopy at magnification 20X and scale bar 100 microns. Labels are as follow: A: Untreated cells; B: Solvent control (0.4% DMSO); C: Only 40 µg/mL Aqueous extract (AE); D: 2 mM Oxalate injury; E: Positive control (40 µg/mL Cystone + 2 mM Oxalate) and F: 40 µg/mL AE + 2 mM Oxalate

4.2.2.2 Effect of aqueous extract of *Terminalia arjuna* on induction of apoptosis in oxalate-induced renal cell injury by flow cytometry using Annexin V/PI staining

Oxalate-induced apoptosis in NRK-52E and MDCK cells was detected by flow cytometry by identification of staining with annexin V and Propidium iodide (PI) as depicted in Figure 4.13 and 4.14 respectively.

There was no significant apoptosis and necrosis in the untreated NRK-52E cells i.e. control with a cell viability of 94.3% (Figure 4.13A). Treatment of cells with the solvent system (0.4% DMSO) and aqueous extract alone (40 µg/mL containing 0.4% DMSO) did not lead to any significant alteration in cell viability w.r.t. control with the percentage viability of 89.2% and 87.8% respectively (Figure 4.13B and 4.13C). After treatment of the NRK-52E cells with 2 mM oxalate for 48 hours at 37°C, a substantial level of cell death w.r.t. control was observed (Figure 4.13D). Time-course cell death assay using annexin V/propidium iodide staining showed that percent of cells undergoing apoptosis was gradually increased in cells exposed to oxalate from 0.3% in control to 50%. The effect of 40 µg/mL of aqueous extract on oxalate treated NRK-52E cells (Figure 4.13F) was evaluated and compared to oxalate treated cells (Figure 4.13D), the number of apoptotic cells was significantly reduced to 37.4%, indicating that aqueous extract protected the cells from oxalate induced apoptosis. Cystone drug at a concentration of 40 µg/mL was used as a positive control. The effect of 40 µg/mL of Cystone on oxalate treated NRK-52E cells (Figure 4.13E) also exhibited cytoprotective effect with reduced level of apoptosis to 42.8% as compared to oxalate treated cells.

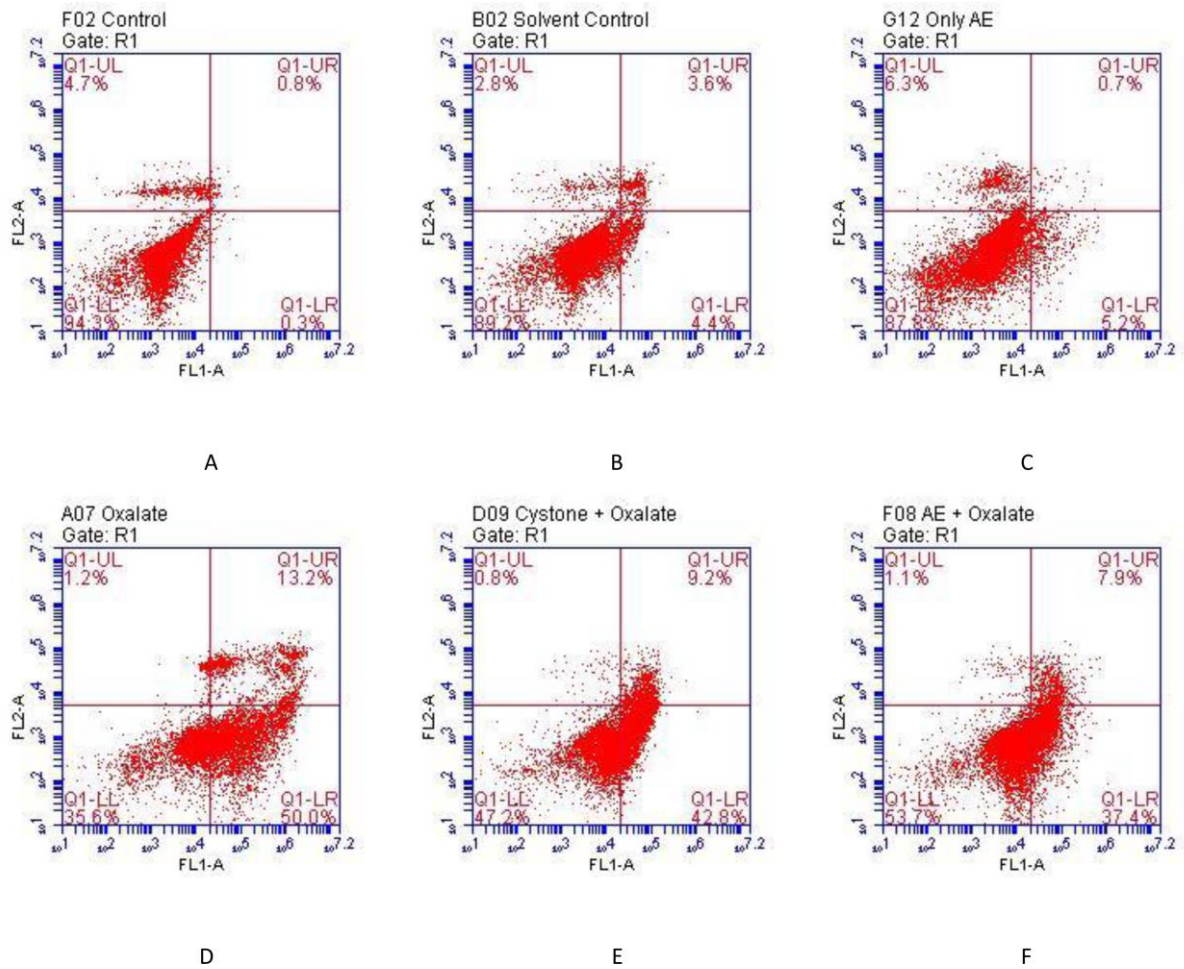


Figure 4.13 Flow cytometry analysis showing the effect of aqueous extract of *T. arjuna* on induction of apoptosis in oxalate induced injury to NRK-52E cells, visualized by AnnexinV/PI staining. Labels are as follow: A: Untreated cells; B: Solvent control (0.4% DMSO); C: Only 40 $\mu\text{g}/\text{mL}$ Aqueous extract (AE); D: 2 mM Oxalate injury; E: Positive control (40 $\mu\text{g}/\text{mL}$ Cystone + 2 mM Oxalate) and F: 40 $\mu\text{g}/\text{mL}$ AE + 2 mM Oxalate

There was an insignificant apoptosis and necrosis in the untreated MDCK cells i.e. control with a cell viability of 93.7% (Figure 4.14A). Treatment of cells with the solvent system (0.4% DMSO) and extract alone (40 µg/mL containing 0.4% DMSO) caused no adverse effects to the cells w.r.t. control with the percentage viability of 90% and 89.6% respectively (Figure 4.14B and 4.14C). When the MDCK cells were incubated with 2 mM oxalate for 48 hours at 37°C, a substantial level of cell death by apoptosis w.r.t. control was observed (Figure 4.14D). Time-course cell death assay using annexin V/propidium iodide double staining showed that the percentage of cells undergoing apoptosis was gradually increased in cells exposed to oxalate from 1.7% in control to 60.2%. The effect of 40 µg/mL of aqueous extract on oxalate treated MDCK cells (Figure 4.14F) was assessed and compared to oxalate treated cells (Figure 4.14D), the number of apoptotic cells was significantly reduced to 33.8%, indicating that aqueous extract protected the cells from oxalate induced apoptosis. Cystone drug at a concentration of 40 µg/mL was used as a positive control. The treatment of 40 µg/mL of Cystone to oxalate exposed MDCK cells (Figure 4.14E) also protected the cells and reduced level of apoptosis to 38.2% as compared to oxalate treated cells.

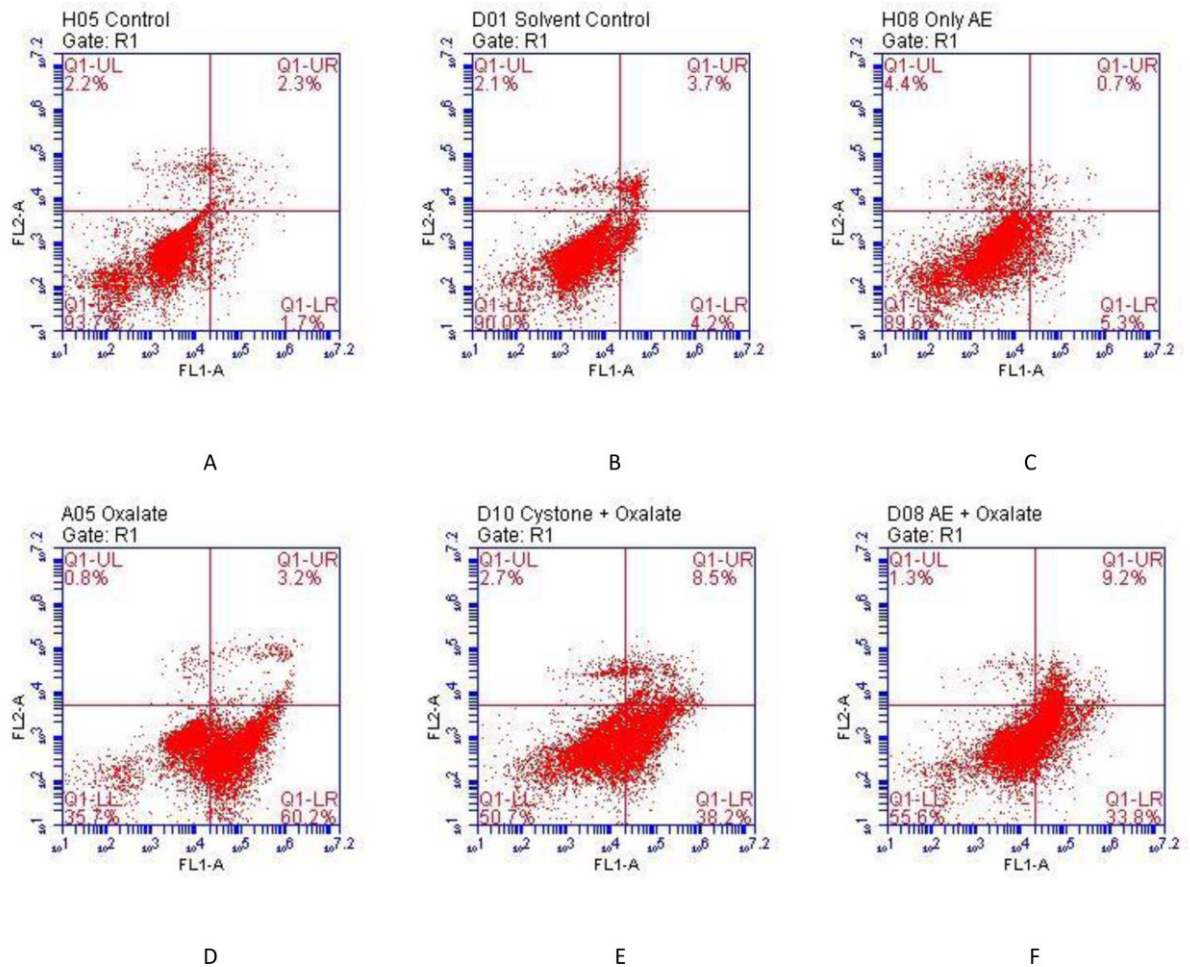


Figure 4.14 Flow cytometry analysis showing the effect of aqueous extract of *T. arjuna* on induction of apoptosis in oxalate induced injury to MDCK cells, visualized by Annexin V/PI staining. Labels are as follow: A: Untreated cells; B: Solvent control (0.4% DMSO); C: Only 40 $\mu\text{g}/\text{mL}$ Aqueous extract (AE); D: 2 mM Oxalate injury; E: Positive control (40 $\mu\text{g}/\text{mL}$ Cystine + 2 mM Oxalate) and F: 40 $\mu\text{g}/\text{mL}$ AE + 2 mM Oxalate

4.2.2.3 Effect of aqueous extract of *Terminalia arjuna* on induction of apoptosis in oxalate-induced renal cell injury by detecting Active Caspase-3 by flow cytometry

Oxalate-induced apoptosis in NRK-52E and MDCK cells was assessed by flow cytometry by using Anti-Active Caspase-3 antibody staining as depicted in Figure 4.15 and 4.16 respectively.

The untreated NRK-52E cells showed no substantial apoptosis and necrosis of cells with a cell viability of 79.1% (Figure 4.15A). Treatment of cells with the solvent system (0.4% DMSO) and aqueous extract alone (40 µg/mL containing 0.4% DMSO) caused no significant alteration in cell viability w.r.t. control with the percentage viability of 74.9% and 66.9% respectively (Figure 4.15B and 4.15C). After incubation of the NRK-52E cells with 2 mM oxalate for 48 hours at 37°C, a significant level of cell death by apoptosis w.r.t. control was observed (Figure 4.15D). Time-course cell death assay using Anti-Active Caspase-3 antibody staining showed that the cells undergoing apoptosis was gradually increased in cells exposed to oxalate from 22.3% in control to 72.9%. The effect of 40 µg/mL of aqueous extract on oxalate treated NRK-52E cells (Figure 4.15F) was evaluated and compared to oxalate treated cells (Figure 4.15D), the number of apoptotic cells was significantly decreased to 58.7%, indicating that aqueous extract reduced oxalate induced apoptosis. Cystone drug at a concentration of 40 µg/mL was used as a positive control. The effect of 40 µg/mL of Cystone on oxalate treated NRK-52E cells (Figure 4.15E) also exhibited cytoprotective effect with reduced level of apoptosis to 61.1% as compared to oxalate treated cells.

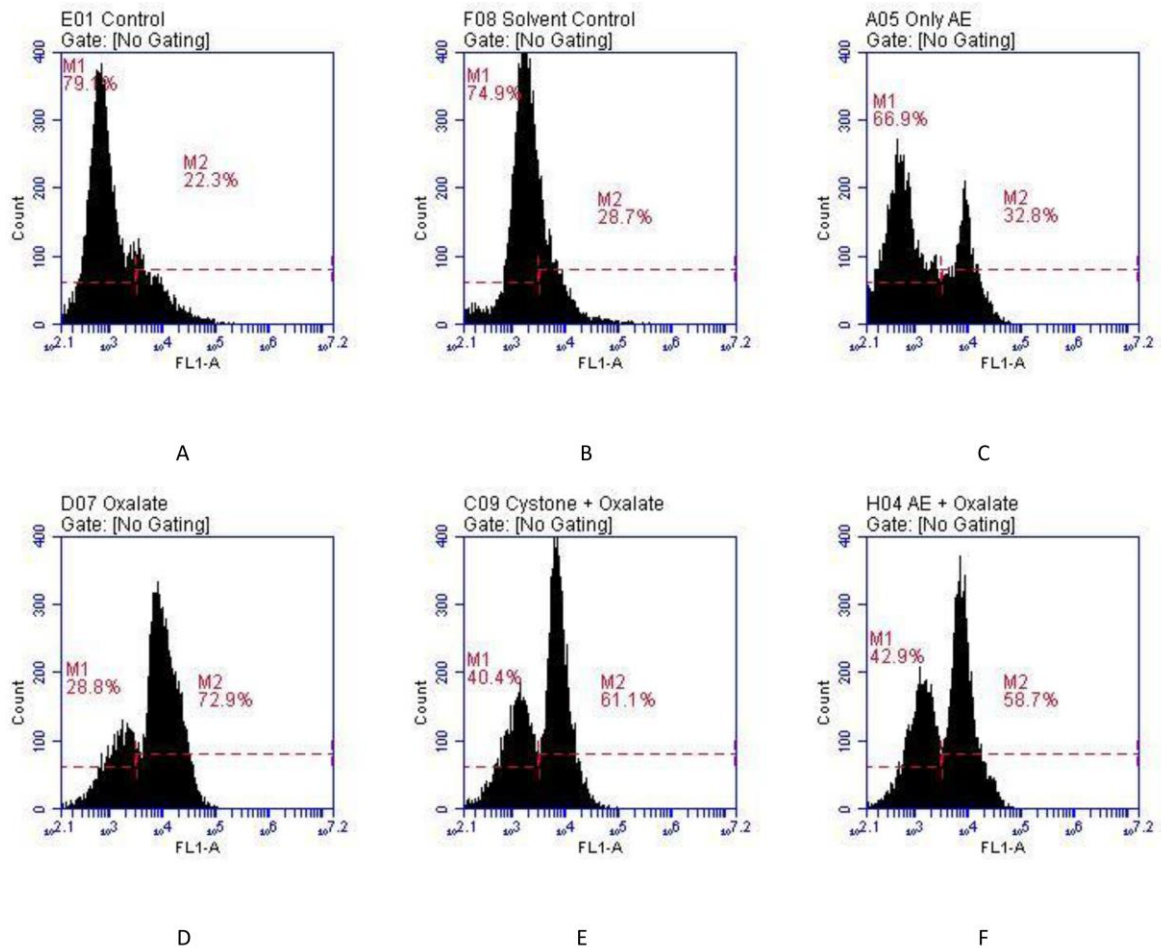


Figure 4.15 Flow cytometry analysis showing the effect of aqueous extract of *T. arjuna* on induction of apoptosis in oxalate induced injury to NRK-52E cells, visualized by Anti-Active Caspase-3 antibody staining. Labels are as follow: A: Untreated cells; B: Solvent control (0.4% DMSO); C: Only 40 $\mu\text{g}/\text{mL}$ Aqueous extract (AE); D: 2 mM Oxalate injury; E: Positive control (40 $\mu\text{g}/\text{mL}$ Cystone + 2 mM Oxalate) and F: 40 $\mu\text{g}/\text{mL}$ AE + 2 mM Oxalate

There was an insignificant percentage of apoptosis and necrosis in the untreated MDCK cells i.e. control with a cell viability of 79.4% (Figure 4.16A). Treatment of cells with the solvent system (0.4% DMSO) and extract alone (40 µg/mL containing 0.4% DMSO) did not lead to any significant alteration in cell viability w.r.t. control with the percentage viability of 75.8% and 68.5% respectively (Figure 4.16B and 4.16C). When MDCK cells were treated with 2 mM oxalate for 48 hours at 37°C, a substantial level of cell death by apoptosis w.r.t. control was observed (Figure 4.16D). Time-course cell death assay using Anti-Active Caspase-3 antibody staining showed that percentage of cells undergoing apoptosis was gradually increased in cells exposed to oxalate from 22.4% in control to 71.1%. The effect of 40 µg/mL of aqueous extract on oxalate treated MDCK cells (Figure 4.16F) was assessed and compared to oxalate treated cells (Figure 4.16D), the number of apoptotic cells was significantly reduced to 57.5%, indicating that aqueous extract protected the cells from oxalate induced apoptosis. Cystone drug at a concentration of 40 µg/mL was used as a positive control. The addition of 40 µg/mL of Cystone on oxalate treated MDCK cells (Figure 4.16E) also protected the cells with reduced level of apoptosis to 60.4% as compared to oxalate treated cells.

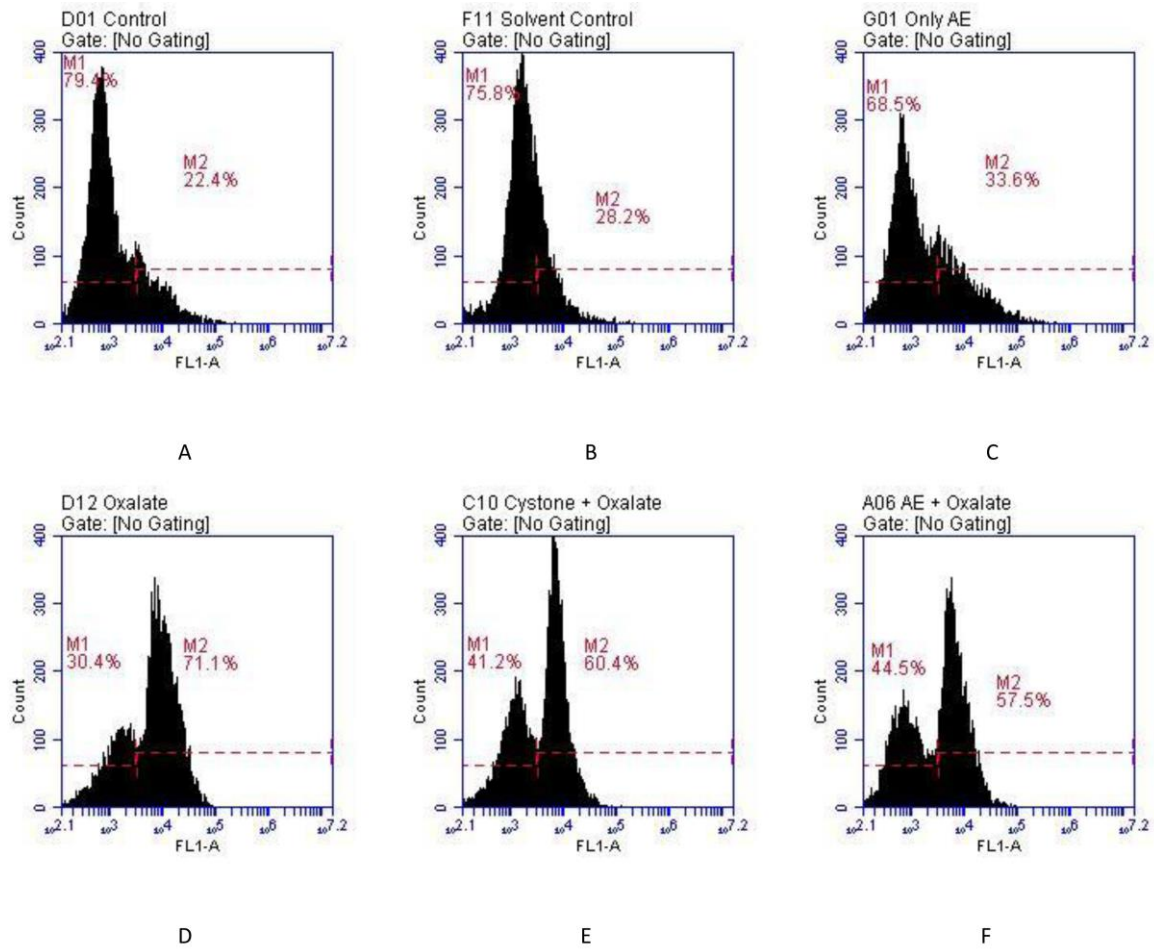


Figure 4.16 Flow cytometry analysis showing the effect of aqueous extract of *T. arjuna* on induction of apoptosis in oxalate induced injury to MDCK cells, visualized by Anti-Active Caspase-3 antibody staining. Labels are as follow: A: Untreated cells; B: Solvent control (0.4% DMSO); C: Only 40 $\mu\text{g}/\text{mL}$ Aqueous extract (AE); D: 2 mM Oxalate injury; E: Positive control (40 $\mu\text{g}/\text{mL}$ Cystone + 2 mM Oxalate) and F: 40 $\mu\text{g}/\text{mL}$ AE + 2 mM Oxalate

4.3 Extraction of proteins from *Terminalia arjuna* bark

The dried bark of *Terminalia arjuna* were purchased from Natural Remedies Pvt. Ltd., Bangalore, India. A collection of voucher specimen is available at the company. Proteins were extracted from *Terminalia arjuna* to investigate the antiurolithiatic properties of *Terminalia arjuna*. The whole protein extract of *Terminalia arjuna* was separated into >3 kDa and <3 kDa fractions and dialyzed against 10 mM Tris-Cl buffer at pH 7.4 by centrifugation with the help of Amicon Ultra-4 centrifugal separating tubes (Millipore) of 3 kDa cut off molecular weight. Thus, two fractions >3 kDa and <3 kDa were obtained. The resulting whole protein extract, >3 kDa and <3 kDa were stored at –20°C for further studies.

High molecular weight biomolecules are reported to play role in kidney stone formation. After filtering the whole protein extract through Amicon ultra centrifugal filter device with a molecular weight cut off 3kDa, activities of whole extract, <3 kDa fraction and >3 kDa fraction so obtained were studied individually on CaOx crystal nucleation, aggregation and growth assay system.

4.3.1 Effect of whole protein extract of *Terminalia arjuna* on the calcium oxalate (CaOx) crystallization

At final concentrations of 5.0 mmol/L calcium and 0.5 mmol/L oxalate, the CaOx crystallization inhibitory activity of *Terminalia arjuna* whole extract increased with increasing concentrations of the whole protein extract in a dose-dependent manner from 5 µg/mL to 100 µg/mL as shown in Figure 4.17. The cystone drug at a concentration of 100 µg/mL was used as a positive control.

For CaOx crystal nucleation, the percentage inhibition shown by the *Terminalia arjuna* bark whole extract at 5 µg/mL, 10 µg/mL and 25 µg/mL were found to be $25.20 \pm 3.98\%$, $31.78 \pm 3.26\%$ and $38.67 \pm 2.37\%$ respectively. As the concentration of whole extract was increased to 50 µg/mL and 100 µg/mL, the percentage inhibition increased to $45.25 \pm 2.05\%$ and $53.18 \pm 2.89\%$ respectively when compared to the control (with no plant extract). Addition of 100 µg/mL cystone resulted in a nucleation percentage inhibition of $37.29 \pm 0.93\%$.

For CaOx crystal aggregation, the percentage inhibition shown by the *Terminalia arjuna* bark whole extract at 5 µg/mL was found to be $36.25 \pm 2.03\%$ which remained almost constant at 10 µg/mL with the percentage inhibition of $37.15 \pm 2.06\%$. As the concentration of whole extract was increased to 25 µg/mL, 50 µg/mL and 100 µg/mL,

the percentage inhibition increased to $40.92 \pm 1.66\%$, $45.64 \pm 1.28\%$ and $48.55 \pm 1.34\%$ respectively when compared to the control (with no plant extract). Addition of $100 \mu\text{g/mL}$ cystone resulted in an aggregation percentage inhibition of $44.64 \pm 2.64\%$.

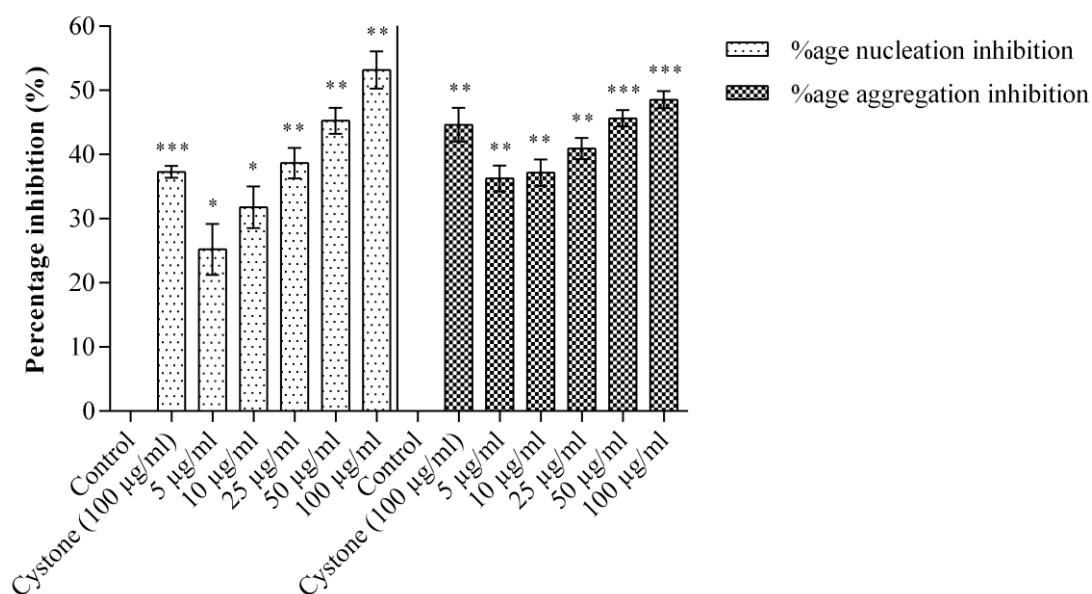


Figure 4.17 Effect of whole protein extract of *T. arjuna* on nucleation and aggregation of calcium oxalate crystals. Data are mean \pm S.D of three independent observations. * $p < 0.05$, ** $p < 0.005$, *** $p < 0.001$

4.3.2 Effect of whole protein extract of *Terminalia arjuna* on the growth of calcium oxalate (CaOx) crystal

The whole protein extract of *Terminalia arjuna* bark showed the inhibitory effect on the growth of CaOx crystals as shown in Figure 4.18. The cystone drug at a concentration of $100 \mu\text{g/mL}$ was used as a positive control. When compared to the control (with no plant extract), the percentage inhibition at $5 \mu\text{g/mL}$ was found to be $15.65 \pm 2.58\%$, which increased to $21.39 \pm 1.71\%$ and $28.14 \pm 2.98\%$ at $10 \mu\text{g/mL}$ and $25 \mu\text{g/mL}$ respectively. As the concentration of whole extract was increased to $50 \mu\text{g/mL}$ and $100 \mu\text{g/mL}$, the percentage inhibition increased to $30.06 \pm 2.25\%$ and $38.85 \pm 1.91\%$ respectively. Addition of $100 \mu\text{g/mL}$ cystone resulted in a growth percentage inhibition of $37.78 \pm 2.78\%$.

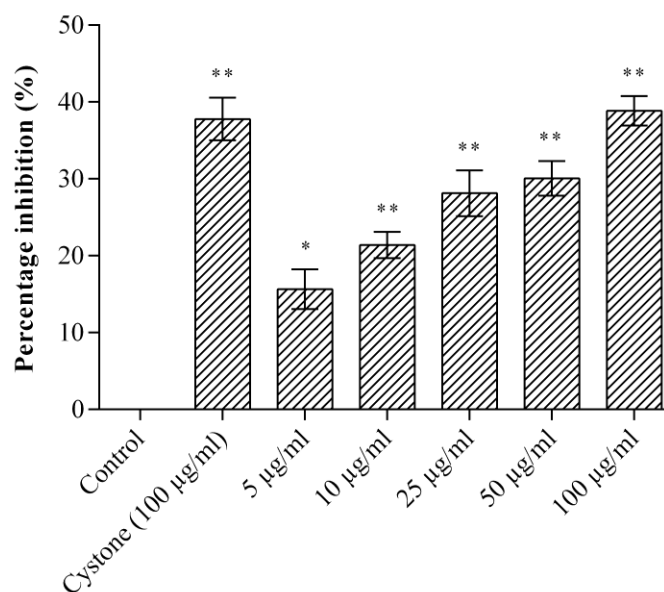


Figure 4.18 Effect of whole protein extract of *T. arjuna* on growth of calcium oxalate crystals. Data are mean \pm S.D of three independent observations. * $p < 0.05$, ** $p < 0.01$

4.3.3 Effect of <3 kDa fraction of *Terminalia arjuna* on the calcium oxalate (CaOx) crystallization

At final concentrations of 5.0 mmol/L calcium and 0.5 mmol/L oxalate, the CaOx crystallization inhibitory activity of <3 kDa fraction of *Terminalia arjuna* increased with increasing concentrations of <3 kDa fraction in a dose-dependent manner from 5 µg/mL to 100 µg/mL as shown in Figure 4.19. The cystine drug at a concentration of 100 µg/mL was used as a positive control.

For CaOx crystal nucleation, the percentage inhibition shown by the *Terminalia arjuna* bark <3 kDa fraction at 5 µg/mL, 10 µg/mL and 25 µg/mL were found to be $7.9 \pm 2.77\%$, $13.11 \pm 2.45\%$ and $17.66 \pm 2.23\%$ respectively. As the concentration of <3 kDa fraction was increased to 50 µg/mL and 100 µg/mL, the percentage inhibition increased to $20.44 \pm 2.93\%$ and $24.04 \pm 1.88\%$ respectively when compared to the control (with no plant extract). Addition of 100 µg/mL cystine resulted in a nucleation percentage inhibition of $37.29 \pm 0.93\%$.

For CaOx crystal aggregation, the percentage inhibition shown by the *Terminalia arjuna* bark <3 kDa fraction at 5 µg/mL and 10 µg/mL was found to be $12.94 \pm 2.48\%$ and $17.96 \pm 2.61\%$. As the concentration of <3 kDa fraction was increased to 25

$\mu\text{g/mL}$, $50 \mu\text{g/mL}$ and $100 \mu\text{g/mL}$, the percentage inhibition significantly increased to $23.12 \pm 2.59\%$, $26.5 \pm 2.29\%$ and $30.46 \pm 1.66\%$ respectively when compared to the control (with no plant extract). Addition of $100 \mu\text{g/mL}$ cystone resulted in an aggregation percentage inhibition of $44.64 \pm 2.64\%$.

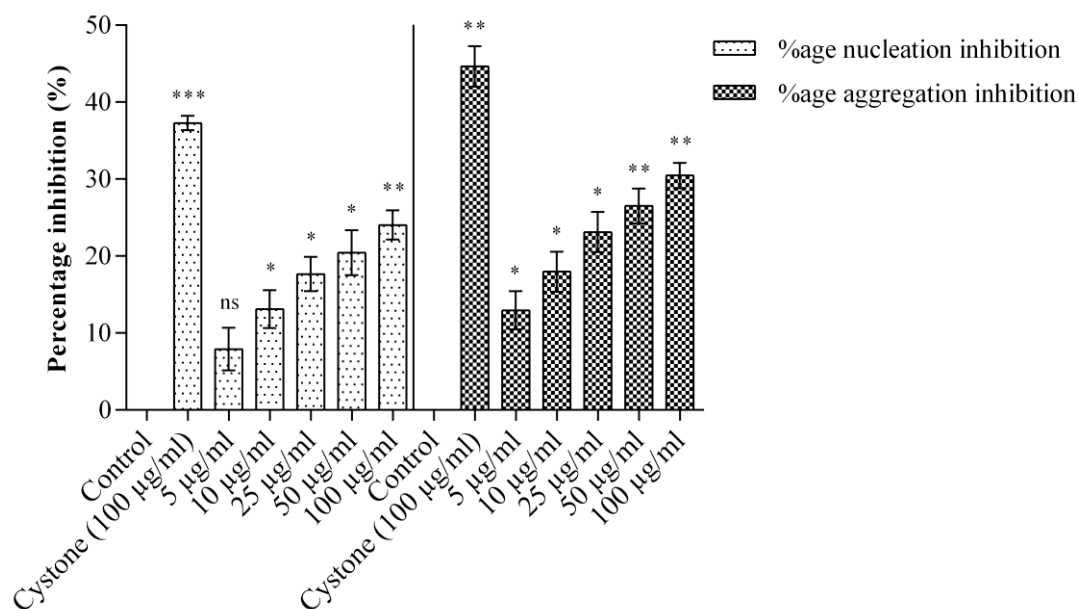


Figure 4.19 Effect of $<3 \text{ kDa}$ fraction of *T. arjuna* on nucleation and aggregation of calcium oxalate crystals. Data are mean \pm S.D of three independent observations. ns: not significant. * $p < 0.05$, ** $p < 0.01$, *** $p < 0.001$

4.3.4 Effect of $<3 \text{ kDa}$ fraction of *Terminalia arjuna* on the growth of calcium oxalate (CaOx) crystal

The $<3 \text{ kDa}$ fraction of *Terminalia arjuna* bark showed the inhibitory effect on the growth of CaOx crystals as shown in Figure 4.20. The cystone drug at a concentration of $100 \mu\text{g/mL}$ was used as a positive control. When compared to the control (with no plant extract), the percentage inhibition at $5 \mu\text{g/mL}$ was found to be $7.88 \pm 1.98\%$ which remained almost constant at $10 \mu\text{g/mL}$ with the percentage inhibition of $9.41 \pm 3.25\%$. As the concentration of $<3 \text{ kDa}$ fraction was increased to $25 \mu\text{g/mL}$, $50 \mu\text{g/mL}$ and $100 \mu\text{g/mL}$, the percentage inhibition increased to $15.06 \pm 1.84\%$, $19.07 \pm 2.65\%$ and $23.47 \pm 3.11\%$ respectively. Addition of $100 \mu\text{g/mL}$ cystone resulted in a growth percentage inhibition of $37.78 \pm 2.78\%$.

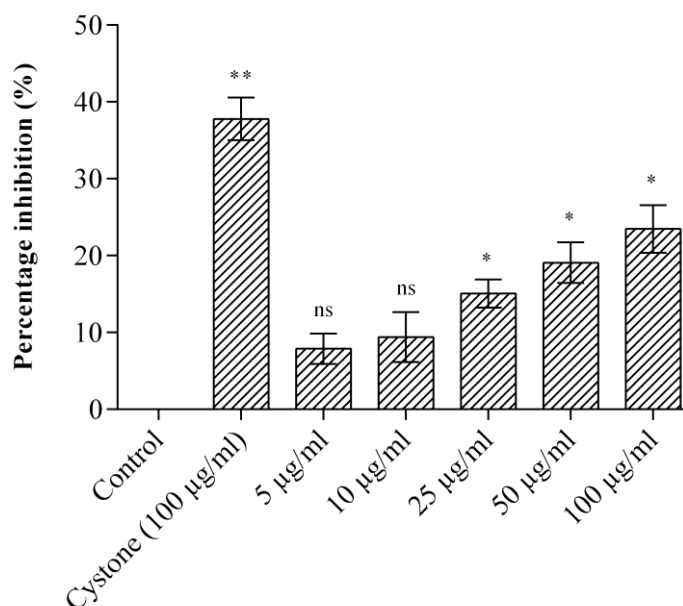


Figure 4.20 Effect of <3 kDa of *T. arjuna* on growth of calcium oxalate crystals. Data are mean \pm S.D of three independent observations. ns: not significant. * $p < 0.05$, ** $p < 0.005$

4.3.5 Effect of >3 kDa fraction of *Terminalia arjuna* on the calcium oxalate (CaOx) crystallization

At final concentrations of 5.0 mmol/L calcium and 0.5 mmol/L oxalate, the CaOx crystallization inhibitory activity of >3 kDa fraction of *Terminalia arjuna* increased with increasing concentrations of >3 kDa fraction in a dose-dependent manner from 5 µg/mL to 100 µg/mL as shown in Figure 4.21. The cystone drug at a concentration of 100 µg/mL was used as a positive control.

For CaOx crystal nucleation, the percentage inhibition shown by the *Terminalia arjuna* bark >3 kDa fraction at 5 µg/mL, 10 µg/mL and 25 µg/mL were found to be $40.48 \pm 1.41\%$, $58.48 \pm 1.06\%$ and $61.18 \pm 0.89\%$ respectively. As the concentration of >3 kDa fraction was increased to 50 µg/mL and 100 µg/mL, the percentage inhibition increased to $73.45 \pm 0.73\%$ and $74.49 \pm 1.59\%$ respectively when compared to the control (with no plant extract). Addition of 100 µg/mL cystone resulted in a nucleation percentage inhibition of $37.29 \pm 0.93\%$.

For CaOx crystal aggregation, the percentage inhibition shown by the *Terminalia arjuna* bark >3 kDa fraction at 5 µg/mL and 10 µg/mL was found to be $53.61 \pm 1.69\%$ and $58.96 \pm 1.86\%$. As the concentration of >3 kDa fraction was increased to 25

$\mu\text{g/mL}$, $50 \mu\text{g/mL}$ and $100 \mu\text{g/mL}$, the percentage inhibition significantly increased to $74.78 \pm 2.09\%$, $79.41 \pm 1.5\%$ and $82.89 \pm 1.34\%$ respectively when compared to the control (with no plant extract). Addition of $100 \mu\text{g/mL}$ cystone resulted in an aggregation percentage inhibition of $44.64 \pm 2.64\%$.

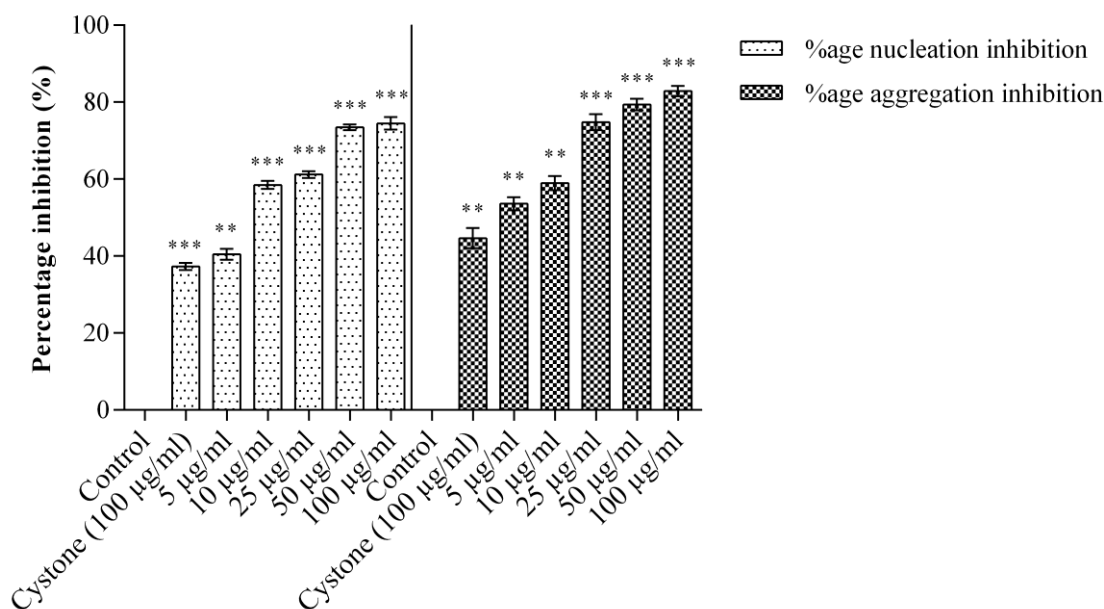


Figure 4.21 Effect of $>3 \text{ kDa}$ fraction of *T. arjuna* on nucleation and aggregation of calcium oxalate crystals. Data are mean \pm S.D of three independent observations. ** $p < 0.005$, *** $p < 0.001$

4.3.6 Effect of $>3 \text{ kDa}$ fraction of *Terminalia arjuna* on the growth of calcium oxalate (CaOx) crystal

The $>3 \text{ kDa}$ fraction of *Terminalia arjuna* bark showed the inhibitory effect on the growth of CaOx crystals as shown in Figure 4.22. The cystone drug at a concentration of $100 \mu\text{g/mL}$ was used as a positive control. When compared to the control (with no plant extract), the percentage inhibition at $5 \mu\text{g/mL}$ was found to be $24.42 \pm 4.28\%$ which remained almost constant at $10 \mu\text{g/mL}$ with the percentage inhibition of $23.43 \pm 4.43\%$. As the concentration of $>3 \text{ kDa}$ fraction was increased to $25 \mu\text{g/mL}$, $50 \mu\text{g/mL}$ and $100 \mu\text{g/mL}$, the percentage inhibition increased to $30.85 \pm 2.49\%$, $35.01 \pm 1.35\%$ and $51.25 \pm 3.25\%$ respectively. Addition of $100 \mu\text{g/mL}$ cystone resulted in a growth percentage inhibition of $37.78 \pm 2.78\%$.

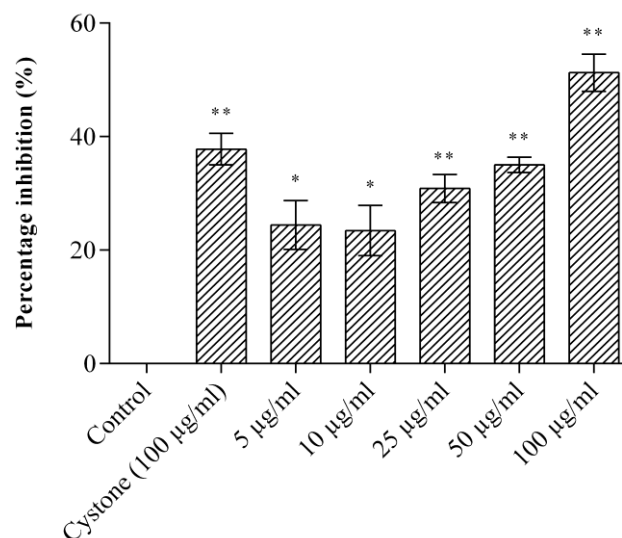


Figure 4.22 Effect of >3 kDa of *T. arjuna* on growth of calcium oxalate crystals. Data are mean \pm S.D of three independent observations. * $p < 0.05$, ** $p < 0.01$

4.3.7 SDS-PAGE of >3 kDa fraction of *Terminalia arjuna*

SDS-PAGE analysis of >3 kDa fraction of *Terminalia arjuna* was performed. A number of protein bands were visible in the >3 kDa fraction as shown in Figure 4.23. The gel was silver stained and plenty bands were visible in the >3 kDa fraction with a molecular weight in the range of 116 kDa to 3 kDa.

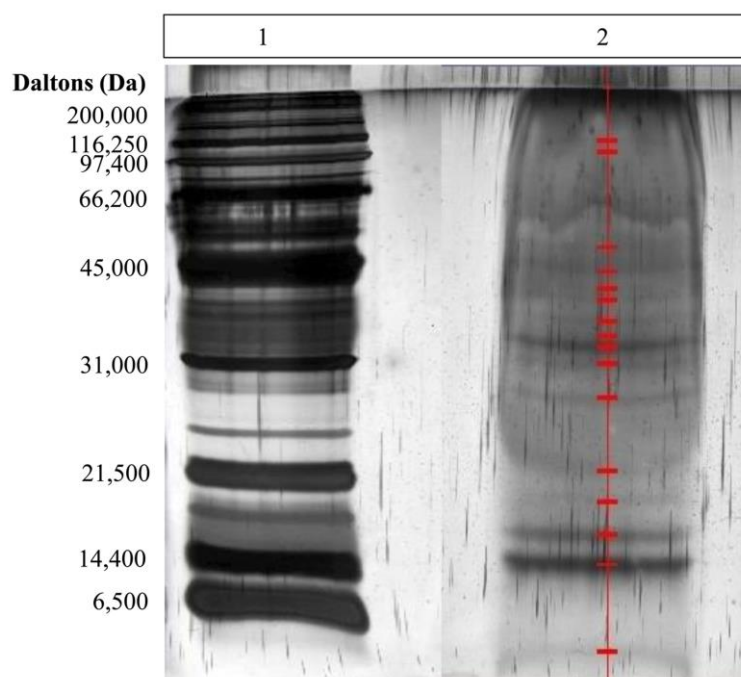


Figure 4.23 Separation of proteins. 12% SDS-PAGE of >3 kDa fraction of *T. arjuna*. Lane 1: Broad range marker (Biorad), Lane 2: >3 kDa fraction

4.4 Purification of antilithiatic proteins from *Terminalia arjuna*

4.4.1 Purification of potent proteins by anion exchange chromatography and their effect on the calcium oxalate (CaOx) crystallization and growth of calcium oxalate (CaOx) crystals

More than 3 kDa fraction exhibited maximum activity towards calcium oxalate crystal nucleation and growth assay system and hence was loaded on a strong anion exchanger Macro Prep® 25 Q column. Figure 4.24 illustrates the elution profile of anion exchange chromatography. The solid line represents the absorbance (mA.U.) of proteins at 280nm present in the sample and the dotted line represents the conductivity (mS/cm). Fractions were collected with increasing gradient, pooled under each peak and were named as P1 to P3. These peaks were dialyzed against 10 mM Tris-Cl buffer (pH 7.4) to remove the excess salt. These peaks were checked for their inhibitory activity towards calcium oxalate crystallization and crystal growth followed by SDS-PAGE. The peaks which showed maximum activity and few bands were then lyophilized and preserved for further purification.

It was observed that all the peaks (P1, P2 and P3) significantly inhibited CaOx crystallization and crystal growth as shown in Figure 4.25 and 4.26. For CaOx crystal nucleation, the percentage inhibition shown by the peaks P1, P2 and P3 at a concentration of 10 µg/mL were found to be $61.72 \pm 2.17\%$, $73.02 \pm 1.71\%$ and $70.34 \pm 1.69\%$ respectively. For CaOx crystal aggregation, the percentage inhibition shown by the peaks P1, P2 and P3 at a concentration of 10 µg/mL were found to be $60.18 \pm 3.17\%$, $75.79 \pm 3.45\%$ and $65.79 \pm 2.63\%$ respectively. For CaOx crystal growth, the percentage inhibition shown by the peaks P1, P2 and P3 at a concentration of 10 µg/mL were found to be $44.92 \pm 3.12\%$, $60.88 \pm 2.65\%$ and $50.49 \pm 3.72\%$ respectively.

SDS-PAGE analysis showed presence of few bands in each peak as represented in Figure 4.27. Peaks P1, P2 and P3 were further purified individually by molecular sieve chromatography.

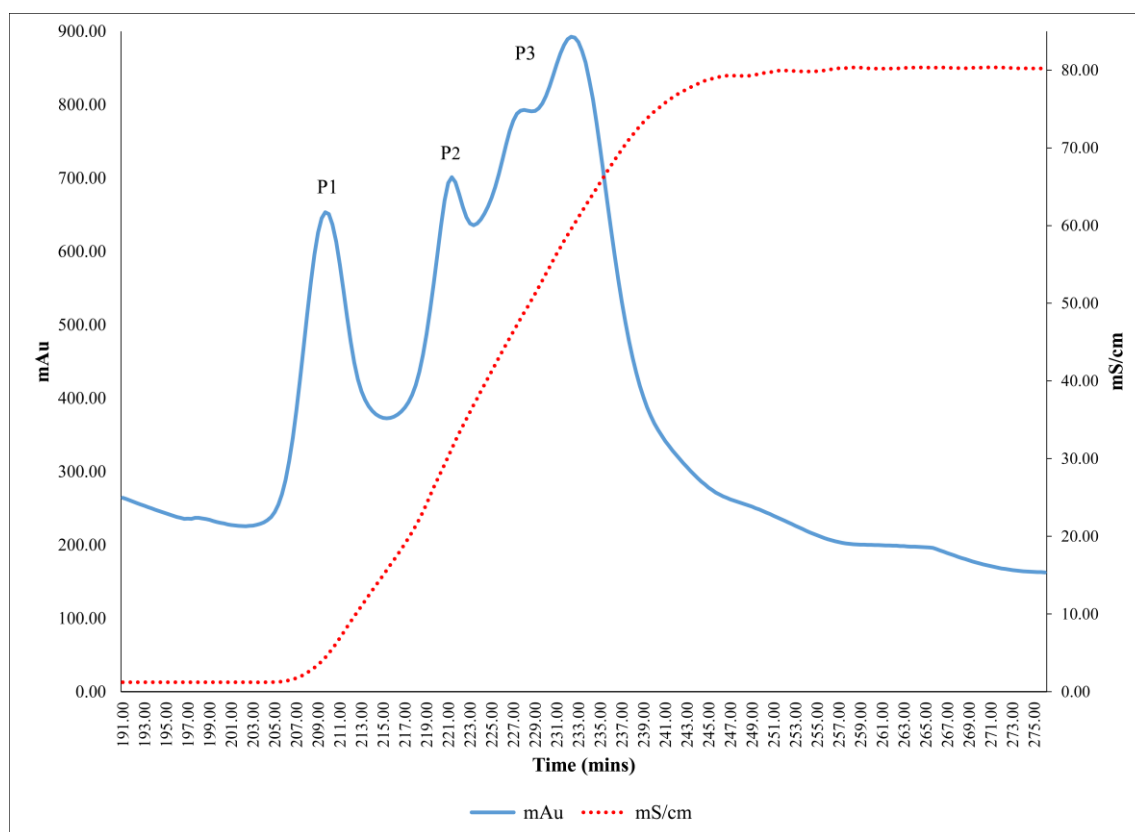


Figure 4.24 Elution profile of anion exchange chromatography. Elution profile of >3 kDa protein fraction of *T. arjuna* loaded on strong anion exchanger. P1, P2 and P3 peaks were collected with a linear gradient of NaCl

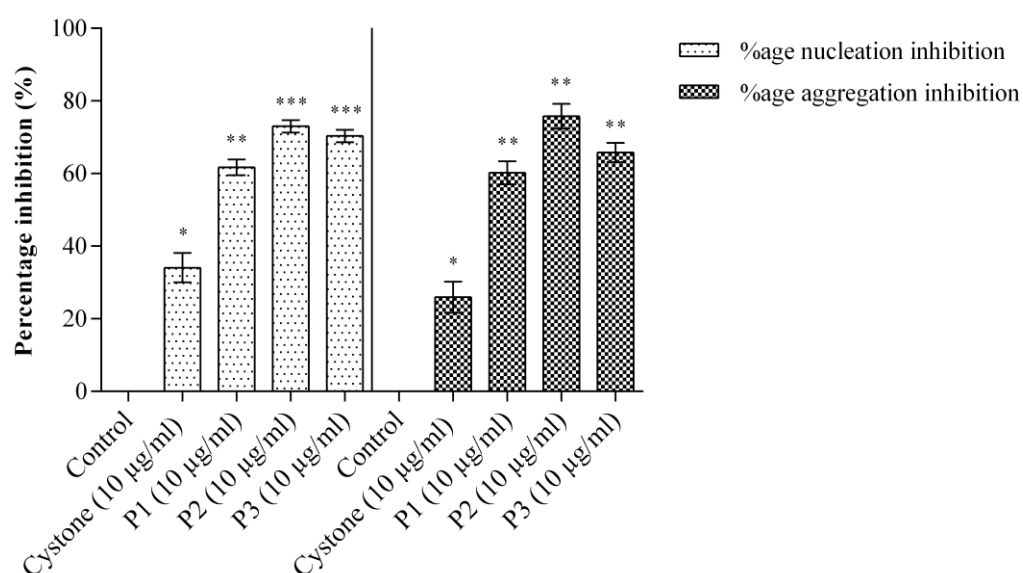


Figure 4.25 Percentage activity of peaks of anion exchange chromatography on nucleation and aggregation of calcium oxalate crystals. Data are mean \pm S.D of three independent observations. * $p < 0.05$, ** $p < 0.005$, *** $p < 0.001$

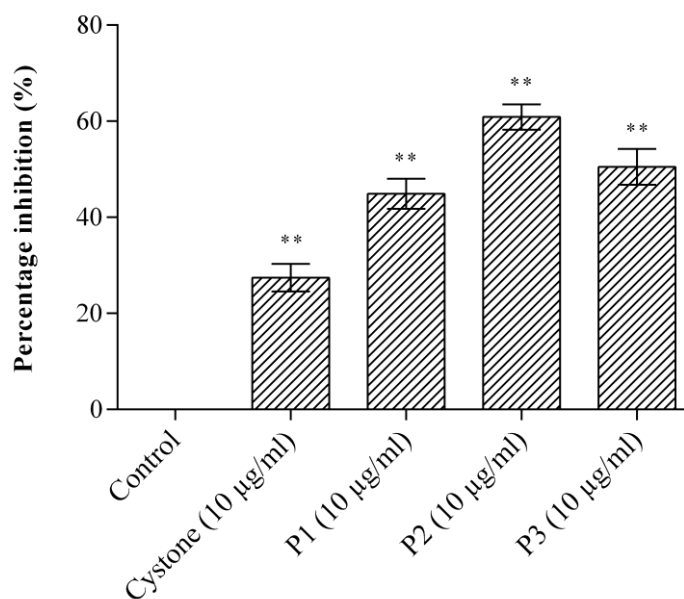


Figure 4.26 Percentage activity of peaks of anion exchange chromatography on growth of calcium oxalate crystals. Data are mean \pm S.D of three independent observations. ** $p < 0.01$

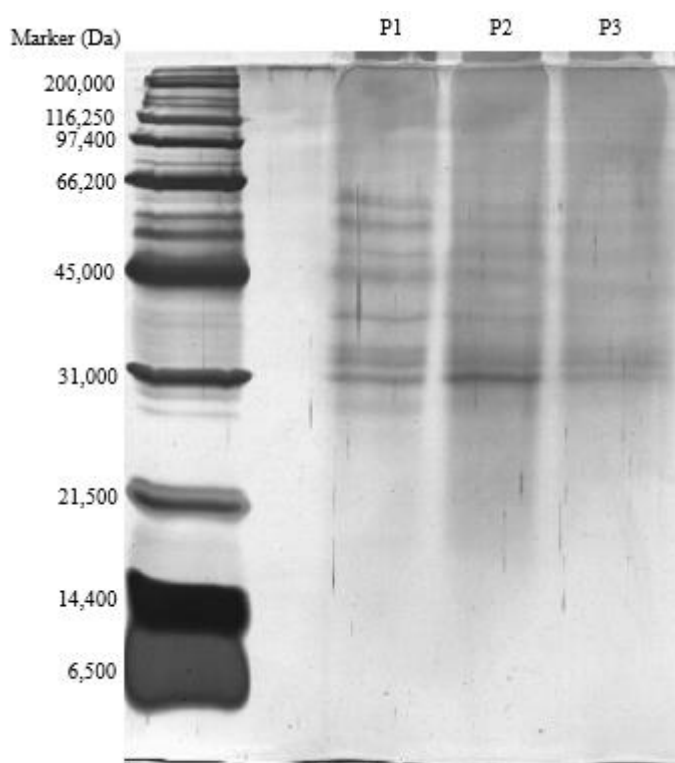


Figure 4.27 Separation of proteins. 12% SDS-PAGE of pooled fractions under each peak of *T. arjuna* after anion exchange chromatography. Lane 1: Broad range marker (Biorad), Lane 2: P1 (Peak1), Lane 3: P2 (Peak 2) and Lane 4: P3 (Peak 3)

4.4.2 Purification of potent proteins by molecular sieve chromatography and their effect on the calcium oxalate (CaOx) crystallization and growth of calcium oxalate (CaOx) crystals

Peaks P1, P2 and P3 were further purified individually by molecular sieve chromatography on a Bio gel® P-100 gel (Bio-Rad) molecular sieve column (XK 16/70, GE Healthcare) for which the elution profile is illustrated in Figure 4.28a, 4.28b and 4.28c respectively. Proteins are eluted isocratically with 10 mM Tris-Cl buffer (pH 7.4). Peaks collected after purification by molecular sieve chromatography of the peak P1 were collected as A1 to A4. Peaks collected after purification by molecular sieve chromatography of the peak P2 were collected as B1 to B3. Peaks collected after purification by molecular sieve chromatography of the peak P3 were collected as C1 to C2. The activity of these fractions were tested against CaOx crystal nucleation and growth assay systems.

All the peaks (A1 to A4, B1 to B3 and C1 to C2) obtained after molecular sieve chromatography of P1, P2 and P3 exhibited inhibitory activity against CaOx crystallization and crystal growth as represented in Figure 4.29 and 4.30. Four proteins viz. A1, B1, B2 and C1 exhibited highest inhibitory activity towards CaOx crystallization and CaOx crystal growth.

For CaOx crystal nucleation, the percentage inhibition shown by the peaks A1, B1, B2 and C1 at a concentration of 10 $\mu\text{g}/\text{mL}$ were found to be $60.03 \pm 1.59\%$, $73.31 \pm 3.19\%$, $70.28 \pm 2.63\%$ and $64.97 \pm 1.6\%$ respectively. For CaOx crystal aggregation, the percentage inhibition shown by the peaks A1, B1, B2 and C1 at a concentration of 10 $\mu\text{g}/\text{mL}$ were found to be $57.89 \pm 5.26\%$, $80.70 \pm 3.04\%$, $84.21 \pm 5.26\%$ and $64.91 \pm 3.04\%$ respectively. For CaOx crystal growth, the percentage inhibition shown by the peaks A1, B1, B2 and C1 at a concentration of 10 $\mu\text{g}/\text{mL}$ were found to be $41.18 \pm 2.94\%$, $63.24 \pm 1.47\%$, $62.5 \pm 0.74\%$ and $48.33 \pm 3.12\%$ respectively.

These four peaks were further analyzed by 12% SDS-PAGE and 12% Native-PAGE. SDS-PAGE of A1 showed the presence of 6 bands of molecular weight in the range of ~66 kDa to ~31 kDa (Figure 4.31). SDS-PAGE of B1 showed the presence of 6 bands of molecular weight in the range of ~65 kDa to ~31 kDa (Figure 4.31). SDS PAGE of B2 showed the presence of 5 bands of molecular weight in the range of ~65kDa to

~31kDa (Figure 4.31). SDS PAGE of C1 showed the presence of 4 bands of molecular weight of ~65 kDa to ~31kDa (Figure 4.31).

To ascertain that the protein in SDS-PAGE was a pure protein having multiple chains native PAGE was performed. Native-PAGE of A1 revealed the presence of a single band of molecular weight of ~190 kDa (Figure 4.32). Native-PAGE of B1 revealed the presence of a single band of molecular weight of ~130 kDa (Figure 4.32). Native-PAGE of B2 revealed the presence of a single band of molecular weight of ~90 kDa (Figure 4.32). Native-PAGE of C1 revealed the presence of a single band of molecular weight of ~90 kDa (Figure 4.32). The molecular weight of the purified proteins is represented in Table 4.2.

The homogeneity of the purified fractions A1, B1, B2 and C1 obtained after molecular-sieve chromatography was confirmed on RP-HPLC which showed a single peak as shown in Figure 4.33 a, b, c, d respectively.

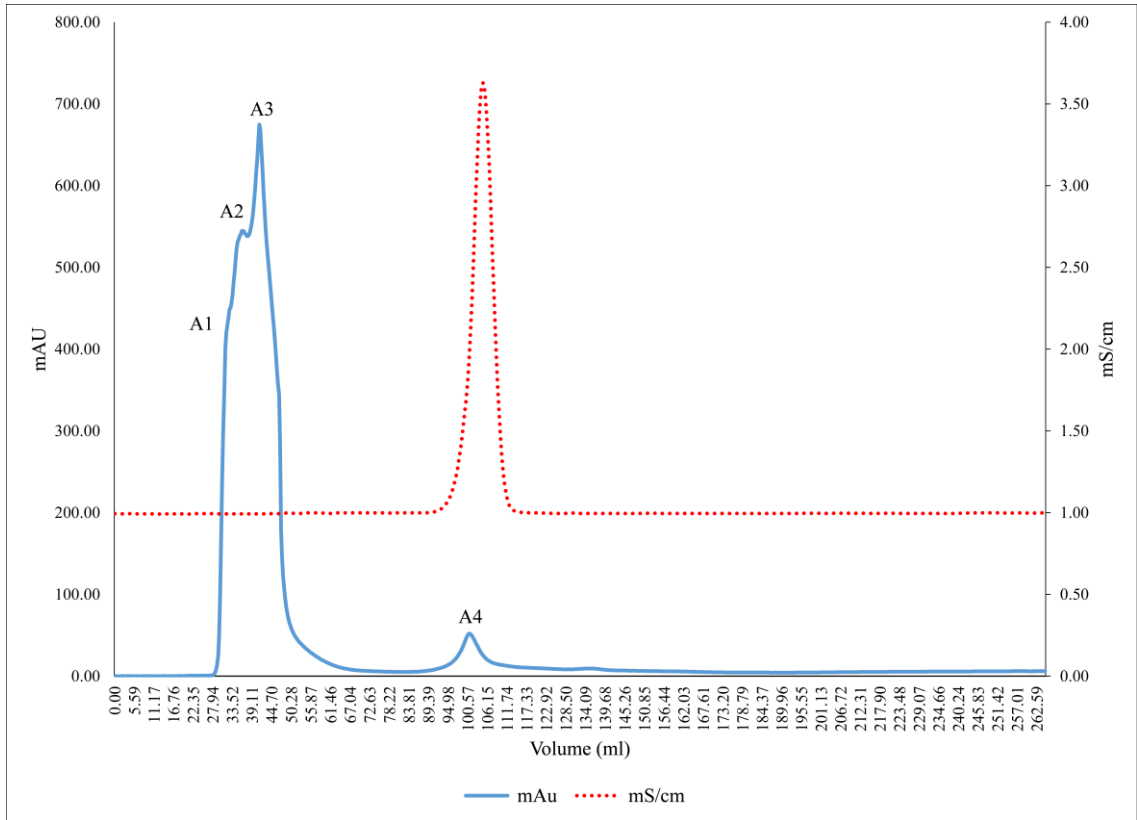


Figure 4.28 a

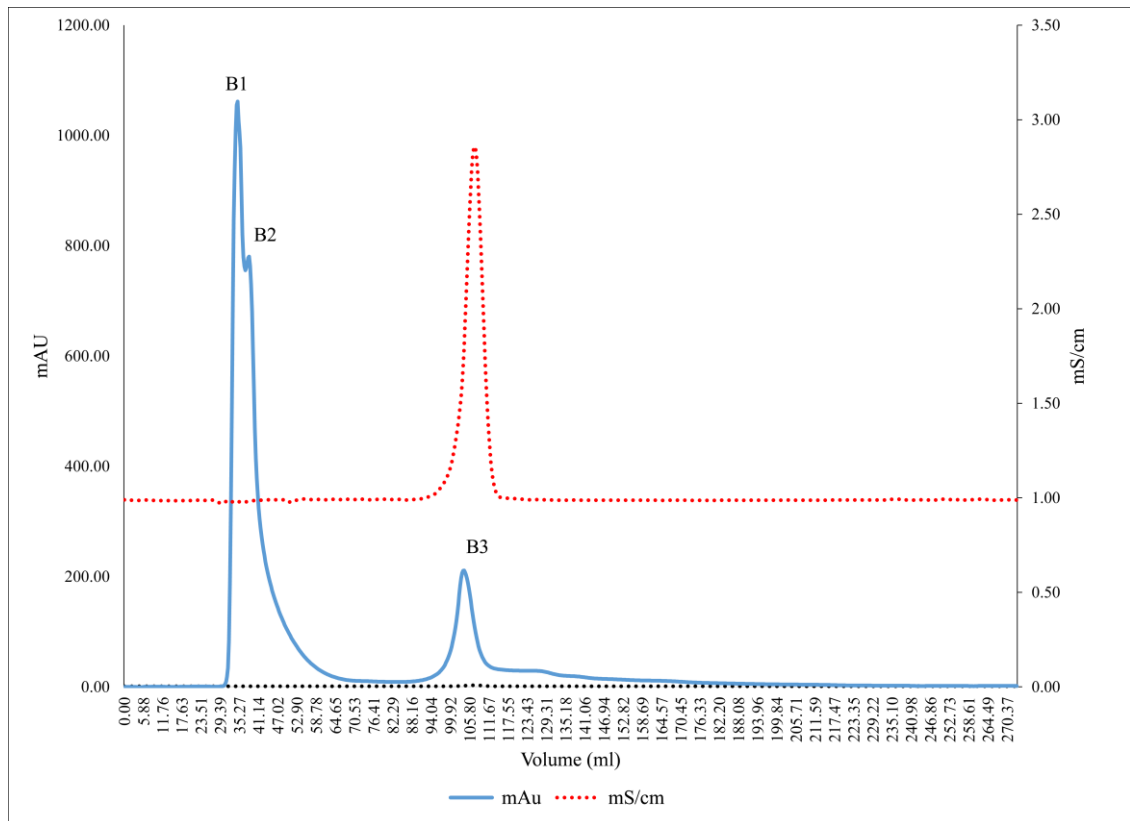


Figure 4.28 b

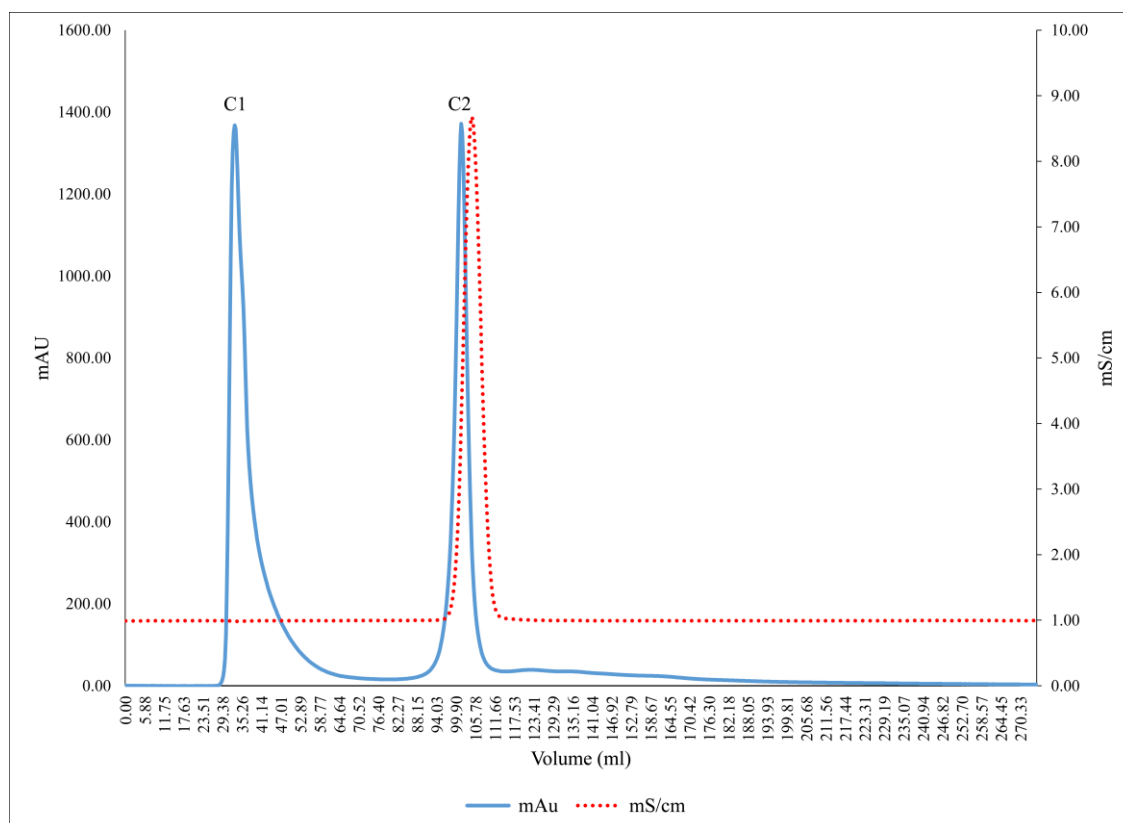


Figure 4.28 c

Figure 4.28 Purification by molecular sieve chromatography. a) Elution profile of fraction Peak 1 (P1) loaded on molecular-sieve chromatography column after anion exchange chromatography; b) Elution profile of fraction Peak 2 (P2) loaded on molecular-sieve chromatography column after anion exchange chromatography; c) Elution profile of fraction Peak 3 (P3) loaded on molecular-sieve chromatography column after anion exchange chromatography

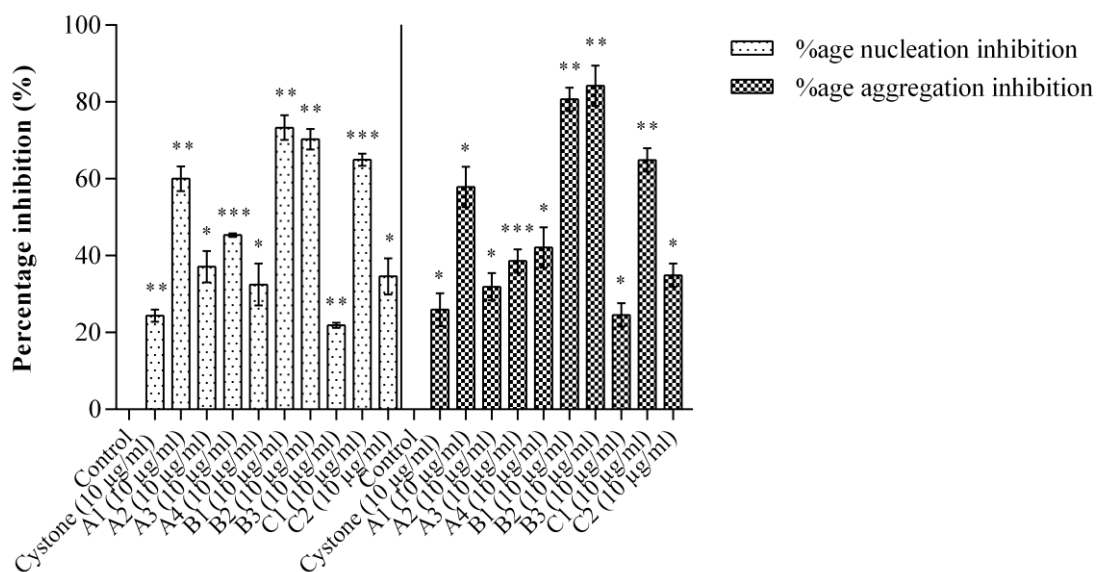


Figure 4.29 Bioactivity of eluted peaks of *T. arjuna*. a) Percentage activity of peaks of molecular sieve chromatography on nucleation and aggregation of calcium oxalate crystals. Data are mean \pm S.D of three independent observations. * $p < 0.05$, ** $p < 0.01$, *** $p < 0.001$

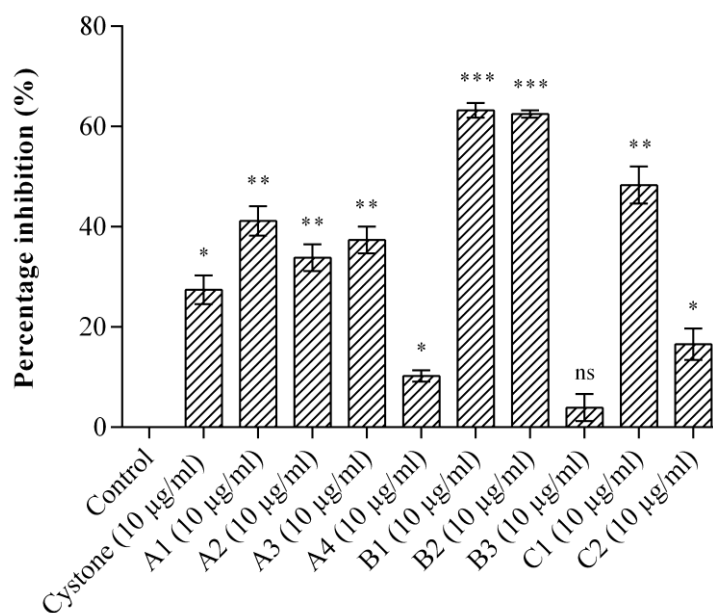


Figure 4.30 Percentage activity of peaks of molecular sieve chromatography on growth of calcium oxalate crystals. Data are mean \pm S.D of three independent observations. ns: not significant. * $p < 0.05$, ** $p < 0.01$, *** $p < 0.001$

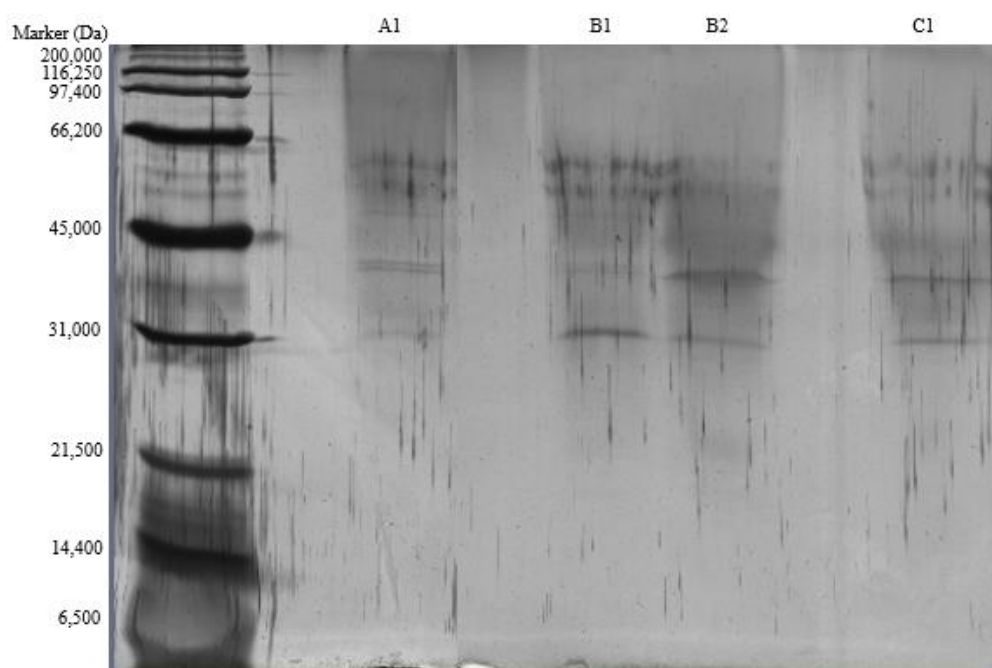


Figure 4.31 12% SDS-PAGE of pooled fractions under top 4 peaks with maximum activity of *T. arjuna* after molecular sieve chromatography. Lane 1: Broad range marker (Biorad), Lane 2: A1, Lane 3: B1, Lane 4: B2 and Lane: C1

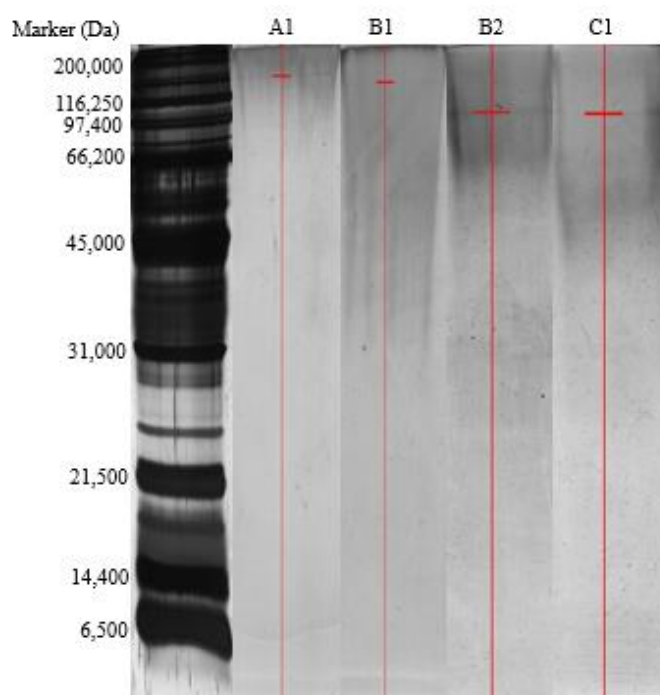
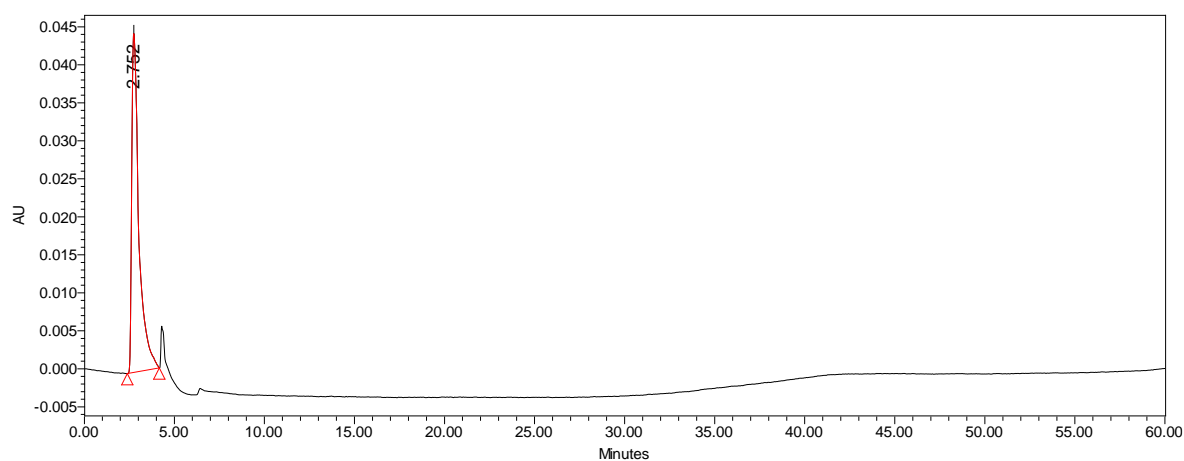
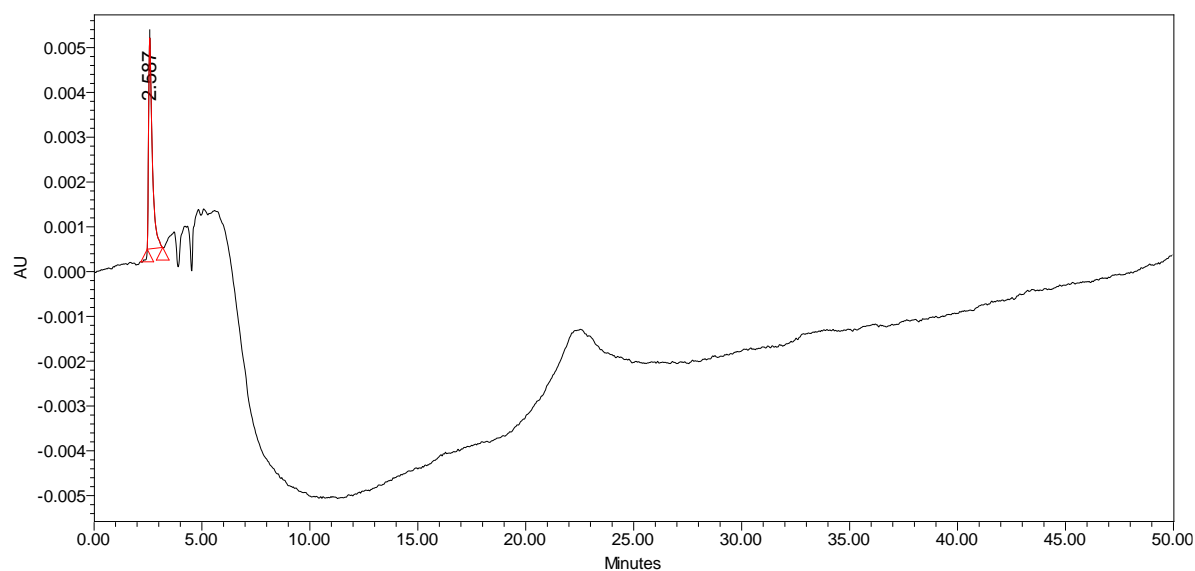


Figure 4.32 12% Native-PAGE of pooled fractions under top 4 peaks with maximum activity of *T. arjuna* after molecular sieve chromatography. Lane 1: Broad range marker (Biorad), Lane 2: A1, Lane 3: B1, Lane 4: B2 and Lane: C1

Table 4.2 Molecular weight of the anionic proteins

Peaks	SDS-PAGE	Native-PAGE (kDa)
A1	6 bands	~190
B1	6 bands	~130
B2	5 bands	~90
C1	4 bands	~90

**Figure 4.33 a****Figure 4.33 b**

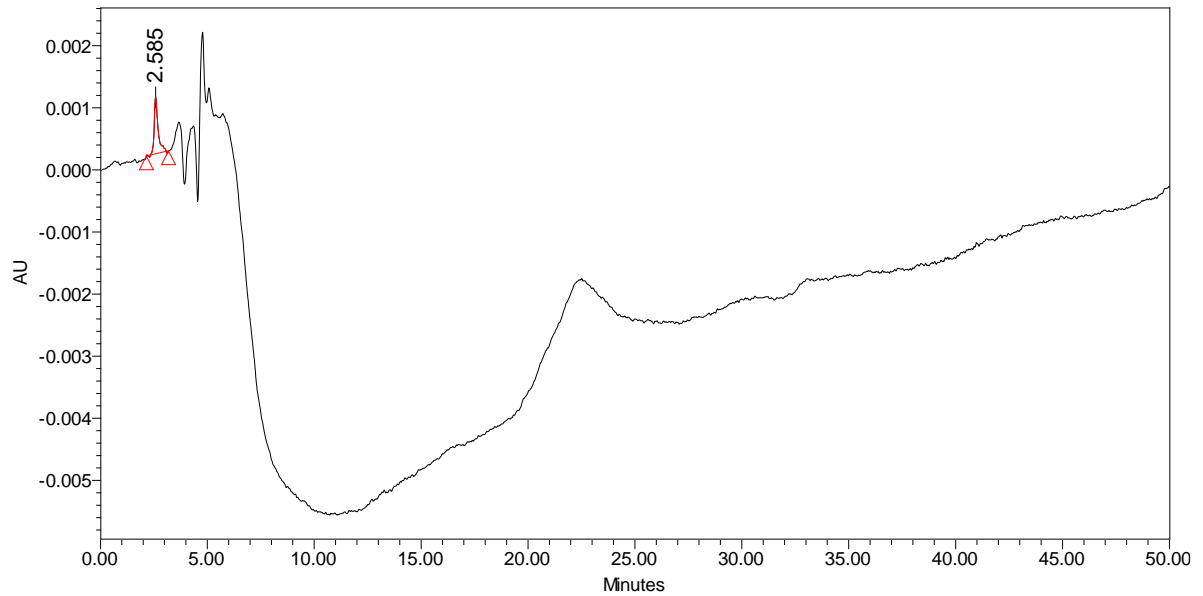
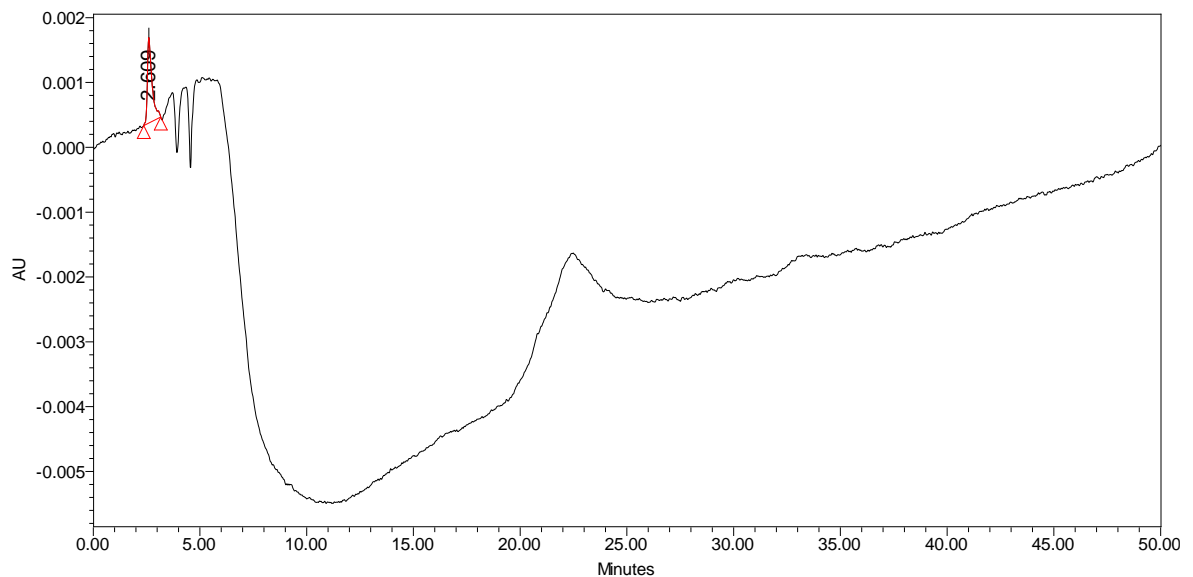
**Figure 4.33 c****Figure 4.33 d**

Figure 4.33 Homogeneity of protein from molecular sieve chromatography.

- (a) RP-HPLC of fraction A1 for homogeneity, showing a single peak at 3 min.
- (b) RP-HPLC of fraction B1 for homogeneity, showing a single peak at 3 min.
- (c) RP-HPLC of fraction B2 for homogeneity, showing a single peak at 3 min.
- (d) RP-HPLC of fraction C1 for homogeneity, showing a single peak at 3 min.

4.5 Characterization of purified antilithiatic proteins

The protein bands detected in peaks A1, B1, B2 and C1 were excised, in-gel tryptic digested and identified by matrix assisted laser desorption/ionization–time of flight (MALDI-TOF) MS. The MALDI-TOF-MS spectrum of purified protein A1, B1, B2 and C1 is shown in Figure 4.34 a, b, c, d respectively. Using the Mascot search engine (<http://www.matrixscience.com>), the MALDI-TOF data obtained from peaks A1, B1, B2 and C1 matched significantly with Nuclear pore anchor, DEAD Box ATP-dependent RNA helicase 45, Lon protease homolog 1 and Heat shock protein 90-3. The matching score of mascot search, nominal mass, pI and percentage sequence coverage is given in Table 4.3. The function of the identified proteins is given in Table 4.4.

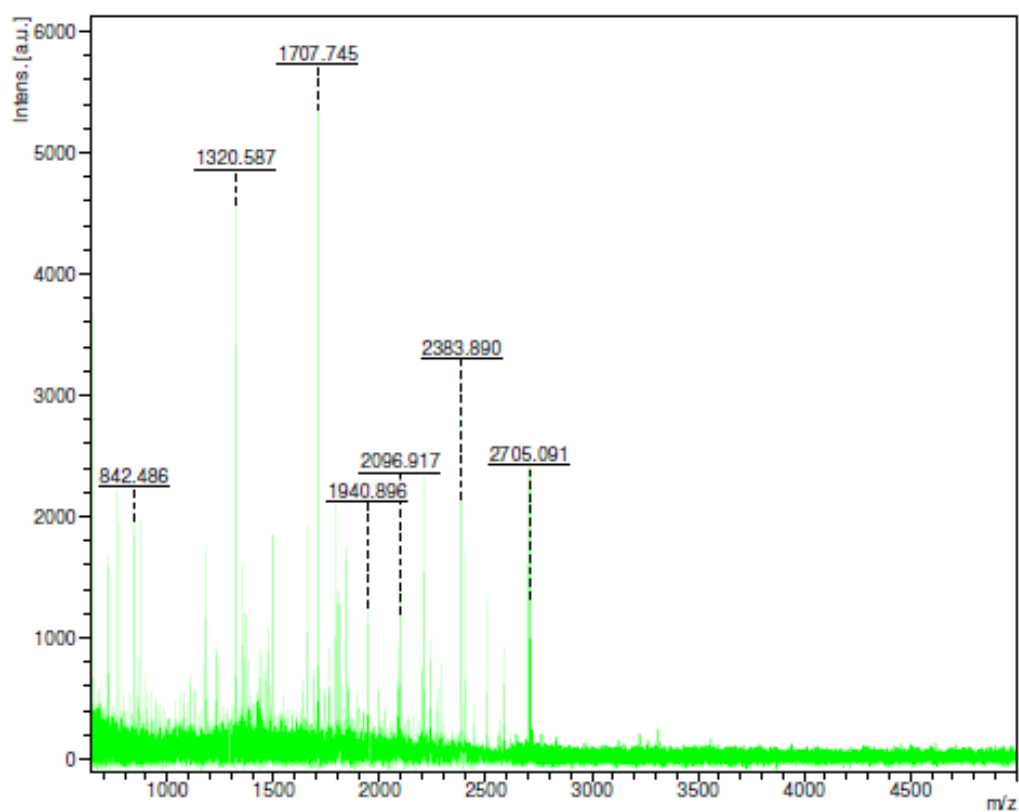


Figure 4.34 a

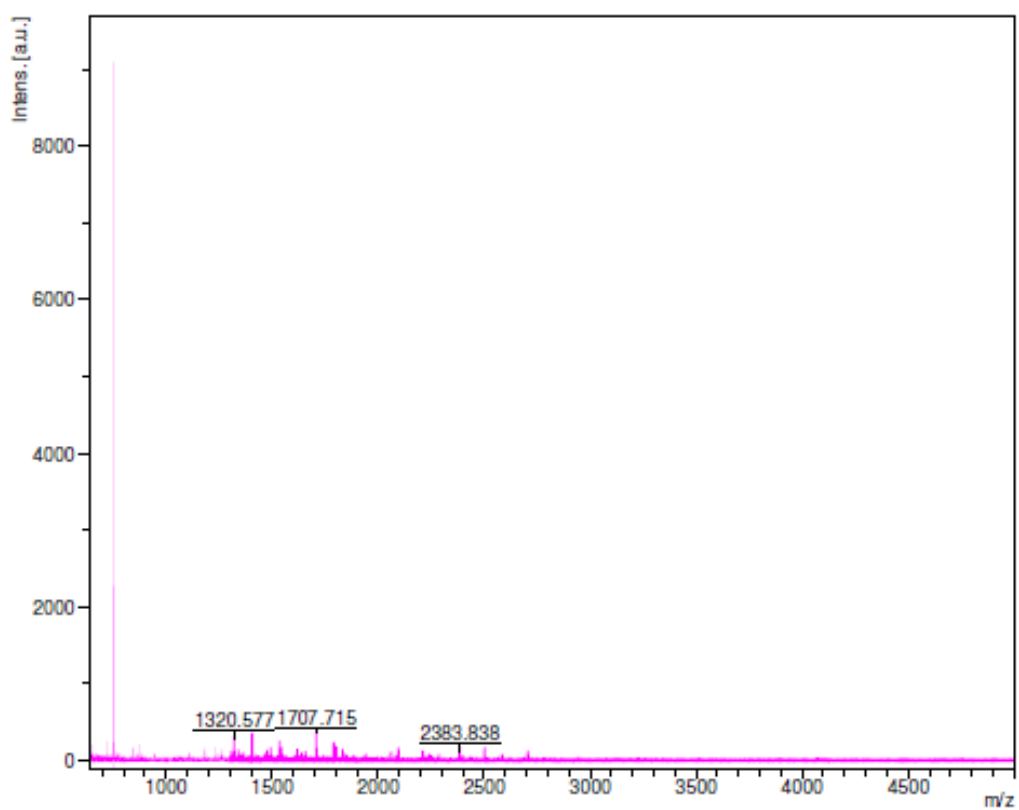


Figure 4.34 b

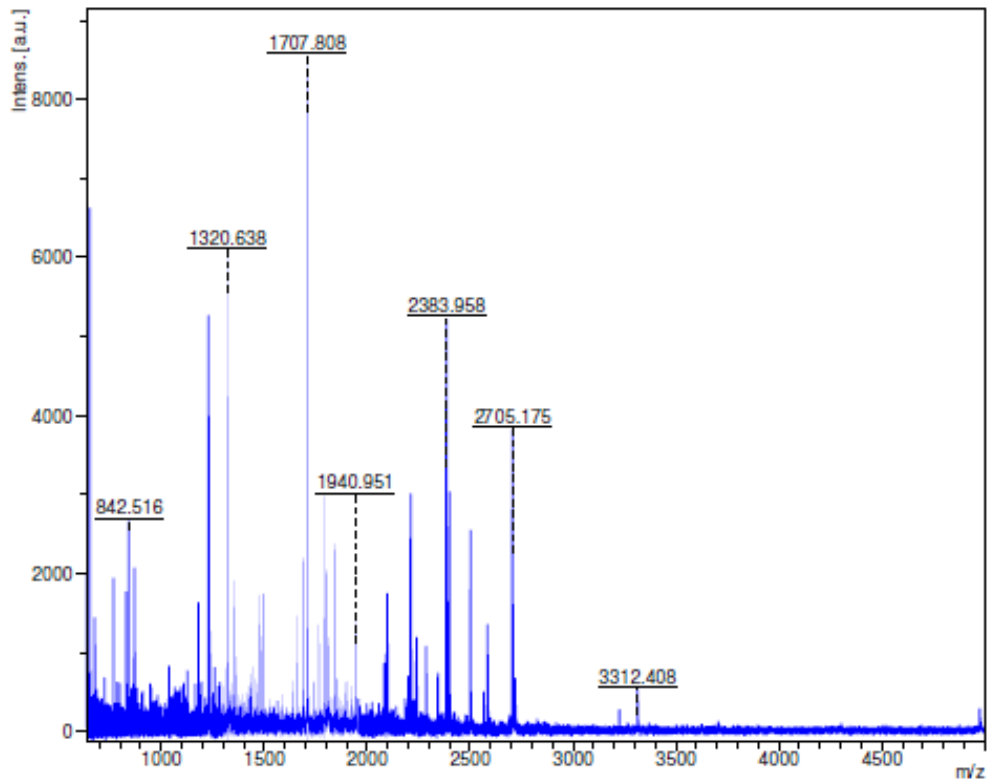


Figure 4.34 c

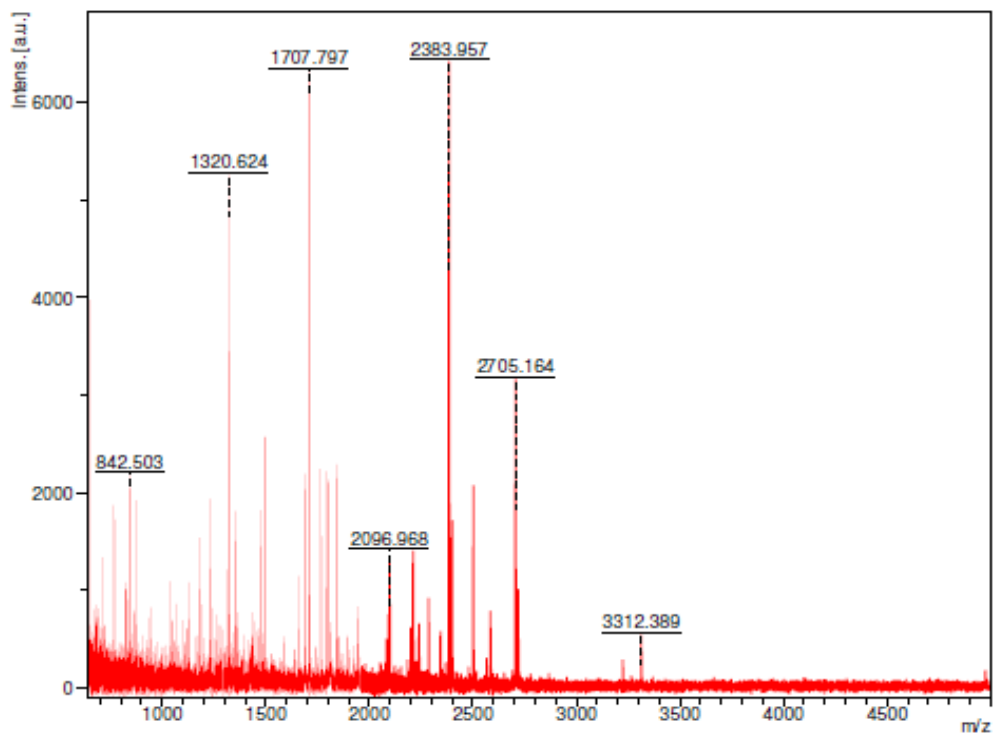


Figure 4.34 d

Figure 4.34 Identification of novel proteins by MALDI-TOF MS. Peptide mass fingerprinting by MALDI-TOF MS obtained from trypsinized fraction (a) A1 (b) B1 (c) B2 (d) C1

Table 4.3 Identified proteins using the Mascot search engine (<http://www.matrixscience.com>), from the data obtained from MALDI-TOF of the peaks A1, B1, B2, C1 and domains using online tool ScanProsite for domains and motifs

Peaks	Proteins	Matching score	Nominal Mass (Mr)	pI	Protein sequence coverage (%)	Domains/Motifs (Identified using ScanProsite)
A1	Nuclear pore anchor	50	237,637	5.01	15	Lysine rich region, Glutamic acid rich region
B1	DEAD Box ATP-dependent RNA helicase 45	33	105,223	5.14	14	Glutamic acid rich region, Aspartic acid rich region, Alanine rich region
B2	Lon protease homolog 1	49	104,379	5.42	22	Cell attachment sequence i.e. RGD (Arg-Gly-Asp)
C1	Heat shock protein 90-3	27	80,287	4.96	11	Glutamic acid rich region

Table 4.4 Biological functions and putative functions of purified proteins

Proteins	Functions
Nuclear pore anchor	<p>It is a 237 kDa protein encoded by the gene AT1G79280.2 and is localized to the inner surface of the nuclear envelope and is a component of the nuclear pore. The nuclear pore complex (NPC) is a large multiprotein complex that is the sole gateway of macromolecular trafficking between the cytoplasm and the nucleus [266].</p> <p>Nuclear membrane has oxalate binding at pH 7.4. The oxalate binding protein plays a vital role in the transport of oxalate. Oxalate transport across cellular membranes is mediated by anion-exchange transport proteins. Under physiological conditions, the NPC is an inhibitor of CaOx crystal nucleation, aggregation and growth. The expression of NPC increases in nephrolithiasis [267].</p> <p>Basic amino acid lysine is involved in oxalate binding which is evident by the fact that all oxalate binding proteins were sensitive to the transport inhibitor 4'-4' diisothiocyano stilbene-2-2 disulphonic acid (DIDS), which is known to interact with the lysine moiety of the proteins [267].</p>
DEAD Box ATP-dependent RNA helicase 45	<p>RNA helicases are prominent candidates as RNA chaperones because the energy derived from ATP hydrolysis can be used to promote the formation of optimal RNA structures via local RNA unwinding, or by mediating RNA–protein association/dissociation [268].</p> <p>DEAD-box proteins comprise the largest and most extensively characterized family of RNA helicases. These proteins are characterized by a core of 350 to 400 amino acids containing seven to nine conserved amino acid motifs. In the DEAD-box proteins, motif II includes the sequence D-E-A-D (Asp-Glu-Ala-Asp), from which the name was derived [268].</p> <p>Recent studies suggested some molecular mechanisms that enable DEAD/H RNA helicases to sustain cell survival, coordinate stress responses, and mediate cell death, by microbial pathogen-induced</p>

	<p>signaling cascades and stress granule formation triggered by various stress stimuli [269].</p> <p>Cell survival mechanism of Stress Granules is linked to reactive oxygen species (ROS) production. A recent study reported that Stress Granules harbor antioxidant activity, partly mediated by two Stress Granules components, G3BP1 (GTPase-activating protein SH3 domain binding protein 1) and USP10 (ubiquitin- specific protease 10). USP10 possesses an antioxidant activity. However, under steady-state conditions, its activity is suppressed by excess G3BP1. Upon stress, G3BP1 and USP10 cooperatively induce Stress Granules. Meanwhile, Stress Granules disrupt G3BP1-mediated inhibition against USP10, possibly by altering the conformation of USP10 and/or G3BP1, thereby uncovering the antioxidant activity of USP10 to reduce ROS production. The authors proposed that Stress Granules may act as rapidly inducible antioxidant machinery protecting cells from ROS-induced apoptosis [269].</p> <p>The role of Stress Granules in controlling apoptosis could be linked to sequestration of apoptosis-promoting factors, suppression of ROS production and reprogramming of mRNA expression upon stress [269].</p>
Lon protease homolog 1	<p>The Lon protease homolog 1 is an enzyme that in humans is encoded by the <i>LONP1</i> gene. This gene encoded a mitochondrial matrix protein that is the subunit of a barrel-shaped homo-oligometric protein complex, the Lon protease. In mitochondrial matrix, a majority of damaged proteins is removed via proteolysis led by Lon protease, which is an essential mechanism for mitochondrial protein quality control (PQC). This protein contains Arg-Gly-Asp (RGD) tripeptide, a cell attachment sequence which binds to integrin [270].</p> <p>Adhesion of urinary crystals to the apical surface of renal tubular cells could be a critical step in the formation of kidney stones. The negative regulators of CaOx crystal uptake include heparin, transforming growth factor-β2 (TGF-β2), and the tetrapeptide arginine-lycine-aspartic acid-serine (RGDS) [146]. Studies by Lieske and colleagues demonstrated an</p>

	<p>attenuation of crystal attachment in BSC-1 cells by treatment with arginine-glycine-aspartic acid-serine (RGDS, a tetrapeptide that bind to integrin), or by pretreatment with fibronectin, a connective tissue protein containing this peptide sequence [141,146]. Crystal endocytosis can be inhibited by agents that interact with cell adhesion sites including RGDS, fibronectin and heparin. The degree of CaOx crystal deposition was inhibited by 60-80% in the cyclic RGD pretreated MDCK cells [146].</p>
<p>Heat shock protein 90-3</p>	<p>Hsp90 is dependent on its inherent ATPase activity for chaperone function and is responsible for the refolding of denatured proteins as well as the three dimensional maturation and transport of more than 200 client proteins [271].</p> <p>Heat-shock proteins (HSPs) are a highly conserved family of molecular chaperones, some of which are induced by sublethal cellular stresses, including temperature elevation, hypoxia and oxidative damage. Heat-shock proteins negatively regulate apoptosis [272].</p> <p>Heat-shock protein 90 promotes cell survival by activation of NF-κB. Tumour necrosis factor-α activation recruits and stabilizes receptor interacting protein (RIP) at the TNF receptor-1 to maintain NF-κB activity. Key signaling molecules, such as VEGF, induces antiapoptotic protein Bcl-2 expression and stimulates HSP90 association with Bcl-2 and Apaf-1 to inhibit apoptosis [273].</p>

4.6 Cytoprotective effect of >3 kDa fraction and purified proteins of *Terminalia arjuna* on oxalate-induced renal tubular epithelial cell injury

4.6.1 Cell viability

The cytoprotective potential of >3 kDa fraction and purified proteins (A1, B1, B2 and C1) of *Terminalia arjuna* was assessed by cell viability using MTT assay.

4.6.1.1 Effect of >3 kDa fraction and purified proteins of *Terminalia arjuna* on oxalate-induced renal tubular epithelial cell injury by MTT assay

The protective effect of >3 kDa fraction and purified proteins of *Terminalia arjuna* towards the oxalate induced injury to renal tubular epithelial cells, NRK-52E is displayed in Figure 4.35. The oxalate induced a significant injury to the cells which could be ascertained by a decrease in viability from 100% in the untreated cells to $23.13 \pm 1.64\%$. The solvent system (1.44 mM Tris-Cl buffer pH 7.4), >3 kDa fraction and purified proteins A1, B1, B2 and C1 (10 $\mu\text{g}/\text{mL}$) had no effect on the cell with a viability percentage of $93.32 \pm 1.58\%$, $86.01 \pm 1.41\%$ and $89.49 \pm 2.67\%$, $92.40 \pm 1.94\%$, $91.47 \pm 1.9\%$ and $90.48 \pm 2.22\%$ respectively, indicating that there was no cytotoxicity to the cells. However, the viability was significantly improved in those cells treated with the >3 kDa fraction and purified proteins of *Terminalia arjuna* bark in a concentration dependent manner as the concentration of these proteins increased from 4 $\mu\text{g}/\text{mL}$ to 10 $\mu\text{g}/\text{mL}$. The percentage of viability with 4 $\mu\text{g}/\text{mL}$, 6 $\mu\text{g}/\text{mL}$, 8 $\mu\text{g}/\text{mL}$ and 10 $\mu\text{g}/\text{mL}$ of >3 kDa fraction was $35.03 \pm 2.51\%$, $46 \pm 1.66\%$, $54.78 \pm 2.1\%$ and $60.70 \pm 1.52\%$ respectively. The viability percentage of protein A1 at 4 $\mu\text{g}/\text{mL}$, 6 $\mu\text{g}/\text{mL}$, 8 $\mu\text{g}/\text{mL}$ and 10 $\mu\text{g}/\text{mL}$ was $24.40 \pm 1.16\%$, $34.08 \pm 1.66\%$, $41.52 \pm 1.87\%$ and $48.51 \pm 2.41\%$ respectively. The cell viability percentage with 4 $\mu\text{g}/\text{mL}$, 6 $\mu\text{g}/\text{mL}$, 8 $\mu\text{g}/\text{mL}$ and 10 $\mu\text{g}/\text{mL}$ of purified protein B1 was $33.27 \pm 2.26\%$, $42.05 \pm 1.2\%$, $54.11 \pm 2.49\%$ and $62.43 \pm 2.82\%$ respectively. The percentage of viability with 4 $\mu\text{g}/\text{mL}$, 6 $\mu\text{g}/\text{mL}$, 8 $\mu\text{g}/\text{mL}$ and 10 $\mu\text{g}/\text{mL}$ of purified protein B2 was $32.57 \pm 1.6\%$, $41.22 \pm 1.81\%$, $52.3 \pm 2.46\%$ and $60.49 \pm 1.69\%$ respectively. The viability percentage with 4 $\mu\text{g}/\text{mL}$, 6 $\mu\text{g}/\text{mL}$, 8 $\mu\text{g}/\text{mL}$ and 10 $\mu\text{g}/\text{mL}$ of purified proteins C1 was $27.08 \pm 2.24\%$, $35.54 \pm 1.19\%$, $43.23 \pm 2.24\%$ and $51.44 \pm 2.05\%$ respectively. Cystone drug at a concentration of 10 $\mu\text{g}/\text{mL}$ was used as a positive control. The addition of Cystone to oxalate treated NRK-52E cells also protected the cells from injury and increased cell viability to $36.15 \pm 1.22\%$ as compared to oxalate treated cells.

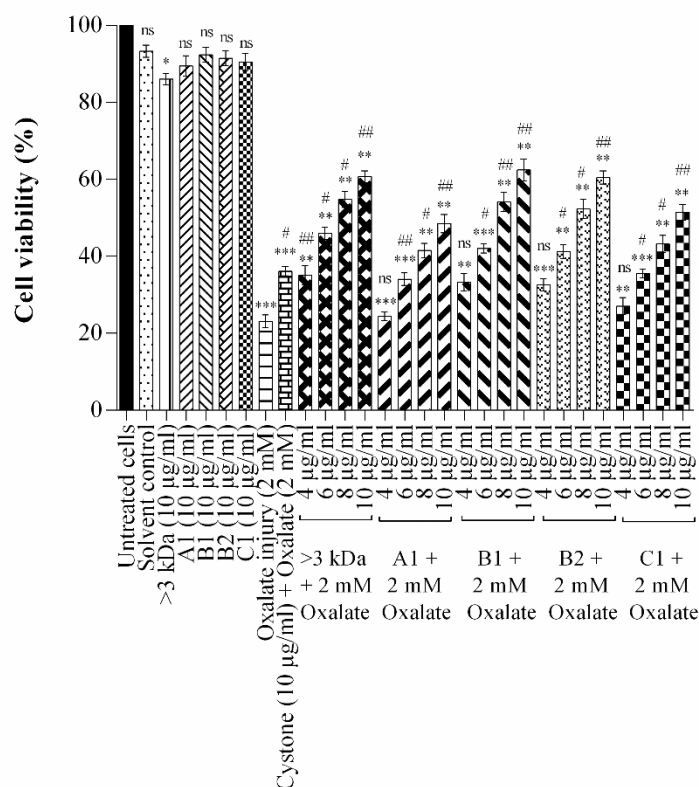


Figure 4.35 Effect of >3 kDa fraction and purified proteins of *T. arjuna* on NRK-52E cell viability assessed by MTT assay. Data are mean \pm S.D of three independent observations. ns: not significant. * $p < 0.05$, ** $p < 0.01$, *** $p < 0.001$ versus untreated control; and # $p < 0.05$, ## $p < 0.01$ versus oxalate injury control

The >3 kDa fraction and purified proteins (A1, B1, B2 and C1) of *Terminalia arjuna* protected the MDCK cells from oxalate induced injury as shown in Figure 4.36. The oxalate induced a significant injury to the cells which could be ascertained by a decrease in viability from 100% in the controls (untreated cells) to $24.36 \pm 0.97\%$. The solvent system (1.44 mM Tris-Cl buffer pH 7.4), >3 kDa fraction and purified proteins A1, B1, B2 and C1 at a concentration of $10 \mu\text{g/mL}$ had no cytotoxicity to the cell with a viability percentage of $93.04 \pm 2.18\%$, $87.31 \pm 1.81\%$ and $90.69 \pm 1.89\%$, $93.07 \pm 1.908\%$, $91.98 \pm 2.4\%$ and $90.72 \pm 2.33\%$ respectively. However, the injury due to oxalate was significantly reduced in those cells treated with the >3 kDa fraction and proteins of *Terminalia arjuna* bark. As the concentration of the plant proteins increased from $4 \mu\text{g/mL}$ to $10 \mu\text{g/mL}$, the percentage viability improved showing that the plant proteins reduced the injury caused to renal cells significantly in a concentration dependent manner. The percentage viability with $4 \mu\text{g/mL}$, $6 \mu\text{g/mL}$, $8 \mu\text{g/mL}$ and 10

$\mu\text{g/mL}$ of >3 kDa fraction was $37.47 \pm 2.03\%$, $46.25 \pm 2.93\%$, $55.42 \pm 2.08\%$ and $64.23 \pm 1.28\%$ respectively. The cell viability percentage of A1 protein at $4 \mu\text{g/mL}$, $6 \mu\text{g/mL}$, $8 \mu\text{g/mL}$ and $10 \mu\text{g/mL}$ was $27.65 \pm 1.98\%$, $35.85 \pm 1.44\%$, $44.11 \pm 1.32\%$ and $51.24 \pm 1.83\%$ respectively. The percentage of viability with $4 \mu\text{g/mL}$, $6 \mu\text{g/mL}$, $8 \mu\text{g/mL}$ and $10 \mu\text{g/mL}$ of protein B1 was $37.24 \pm 1.42\%$, $45.72 \pm 2.64\%$, $56.02 \pm 1.99\%$ and $67.15 \pm 1.45\%$ respectively. The viability percentage of protein B2 at $4 \mu\text{g/mL}$, $6 \mu\text{g/mL}$, $8 \mu\text{g/mL}$ and $10 \mu\text{g/mL}$ was $34.32 \pm 0.9\%$, $44.6 \pm 1.92\%$, $54.81 \pm 1.29\%$ and $62.46 \pm 2.39\%$ respectively. The percentage of viability with $4 \mu\text{g/mL}$, $6 \mu\text{g/mL}$, $8 \mu\text{g/mL}$ and $10 \mu\text{g/mL}$ of purified protein C1 was $27.89 \pm 2.11\%$, $36.26 \pm 1.16\%$, $45.51 \pm 2.21\%$ and $53.86 \pm 1.48\%$ respectively. Cystone drug at a concentration of $10 \mu\text{g/mL}$ was used as a positive control. The $10 \mu\text{g/mL}$ of Cystone on oxalate treated MDCK cells also exhibited cytoprotective effect with increased cell viability to $38.14 \pm 1.42\%$ as compared to oxalate treated cells.

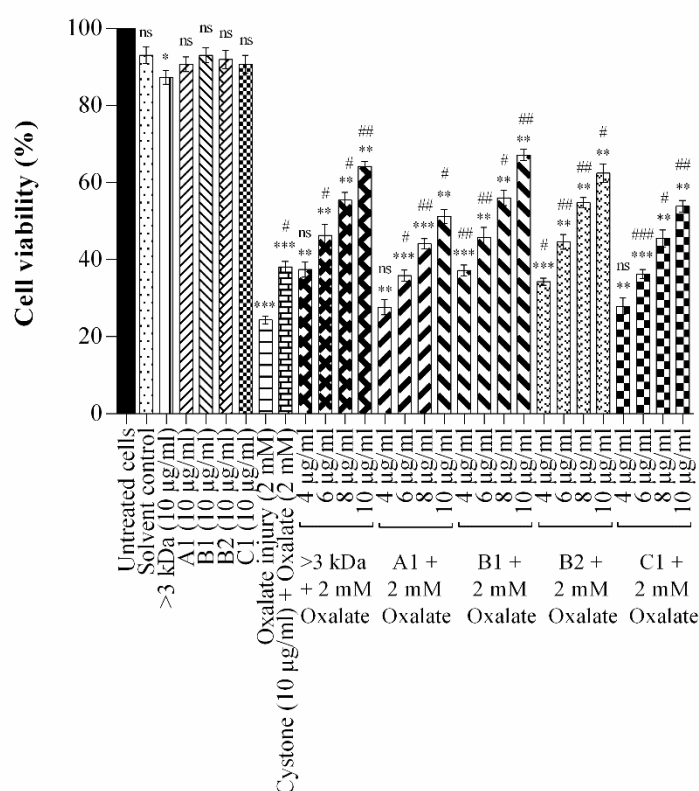


Figure 4.36 The effect of >3 kDa fraction and purified proteins of *T. arjuna* on MDCK cell viability assessed by MTT assay. Data are mean \pm S.D of three independent observations. ns: not significant. * $p < 0.05$, ** $p < 0.01$, *** $p < 0.001$ versus untreated control; and # $p < 0.05$, ## $p < 0.01$, ### $p < 0.0005$ versus oxalate injury control

4.6.1.2 Effect of >3 kDa fraction and purified proteins of *Terminalia arjuna* on calcium oxalate (CaOx) crystal adherence on oxalate-induced renal tubular epithelial cell injury

The NRK-52E and MDCK cells were microscopically studied for cell-crystal interactions under phase contrast polarized microscope to demonstrate crystal adhesion on the cell surface as shown in Figure 4.37 and 4.38.

After incubation of the NRK-52E cells with 2 mM oxalate for 48 hours at 37°C, hexagonal COM crystals and smaller granules were observed. These crystals adhered and some internalized to the cells even after several washes using PBS depicting that CaOx crystals adhered tightly to renal cells with subsequent harmful effects to the cells (Figure 4.37H). These crystals caused cell damage and cell death. Crystal adhesion and internalization into the cells were observed, showing the mechanism of renal cellular injury by CaOx. The cells treated with the solvent system (1.44 mM Tris-Cl buffer pH 7.4), >3 kDa fraction and purified proteins A1, B1, B2 and C1 (10 µg/mL) showed healthy cellular morphology (Figure 4.37B-G), indicating that there is no adverse effect to the cells. The effect of 10 µg/mL of >3 kDa fraction and plant proteins (A1, B1, B2, C1) on oxalate treated NRK-52E cells (Figure 4.37J-N) was assessed and compared to that of only oxalate treated cells (Figure 4.37H), more viable cells and smaller crystals were observed, showing loss of crystal adherence to cells and dissolution of crystals in presence of 10 µg/mL of >3 kDa fraction and purified proteins of *Terminalia arjuna* and thus, indicating cell-crystal interaction. Cystone drug at a concentration of 10 µg/mL was used as a positive control. The addition of Cystone on oxalate treated NRK-52E cells (Figure 4.37I) also exhibited protective potential to the cells from injury as observed with more viable cells and few loosely bound crystals as compared to oxalate treated cells.

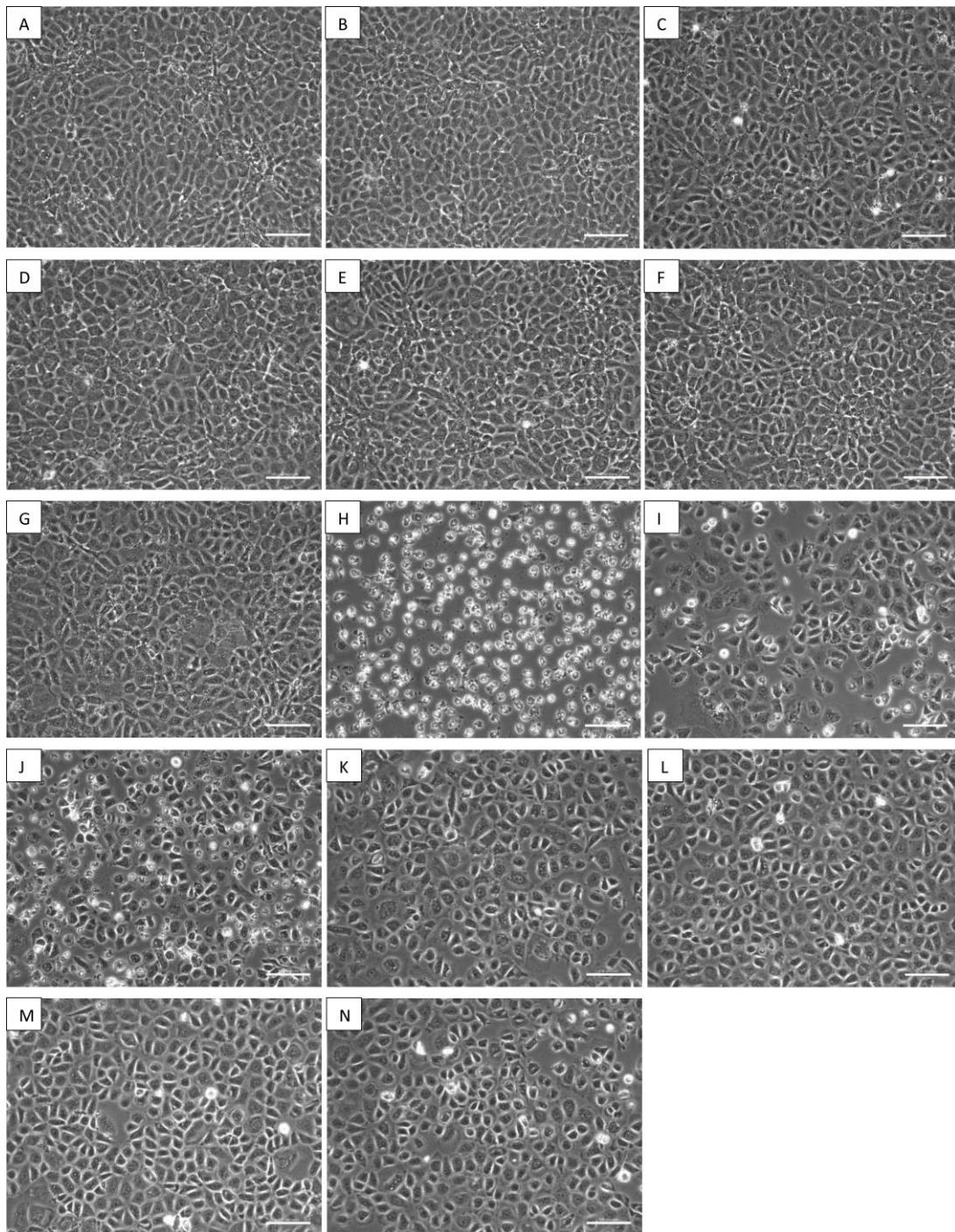


Figure 4.37 Effect of >3 kDa fraction and purified proteins of *T. arjuna* on CaOx crystal adherence in oxalate induced injury to NRK-52E cells, visualized under polarization and phase contrast at magnification 20X and scale bar 100 microns. Labels are as follow: A: Untreated cells; B: Solvent control (1.44 mM Tris-Cl buffer pH 7.4); C: Only 10 µg/mL >3 kDa fraction; D: Only 10 µg/mL A1; E: Only 10 µg/mL B1; F: Only 10 µg/mL B2; G: Only 10 µg/mL C1; H: 2 mM Oxalate injury; I: Positive control (10 µg/mL Cystone + 2 mM Oxalate); J: 10 µg/mL >3 kDa fraction + 2 mM Oxalate; K: 10 µg/mL A1 + 2 mM Oxalate; L: 10 µg/mL B1 + 2 mM Oxalate; M: 10 µg/mL B2 + 2 mM Oxalate and N: 10 µg/mL C1 + 2 mM Oxalate

When MDCK cells were exposed to 2 mM oxalate for 48 hours at 37°C, hexagonal COM, bipyramidal COD and aggregated crystals were observed. Some of these crystals internalized and some remained adhered to the cells even after several washes using PBS depicting that CaOx crystals adhered tightly to renal cells with subsequent detrimental effects to the cells (Figure 4.38H). These crystals had injurious effects to the cells leading to cell death; showing the mechanism of renal cellular injury by CaOx. The cells treated with the solvent system (1.44 mM Tris-Cl buffer pH 7.4), >3 kDa fraction and purified proteins A1, B1, B2 and C1 (10 µg/mL) showed healthy cellular morphology (Figure 4.38B-G), indicating that there is no adverse effect to the cells. The effect of 10 µg/mL of >3 kDa fraction and plant proteins (A1, B1, B2, C1) on oxalate treated MDCK cells (Figure 4.38J-N) was evaluated and compared to that of only oxalate treated cells (Figure 4.38H), more viable cells were observed showing loss of crystal adherence to cells and dissolution of crystals in presence of 10 µg/mL of >3 kDa fraction and purified proteins of *Terminalia arjuna* and thus, indicating cell-crystal interaction. Cystone drug at a concentration of 10 µg/mL was used as a positive control. The treatment of Cystone on oxalate exposed MDCK cells (Figure 4.38I) also exhibited cytoprotective effect with more viable cells and few loosely bound crystals as compared to oxalate treated cells.

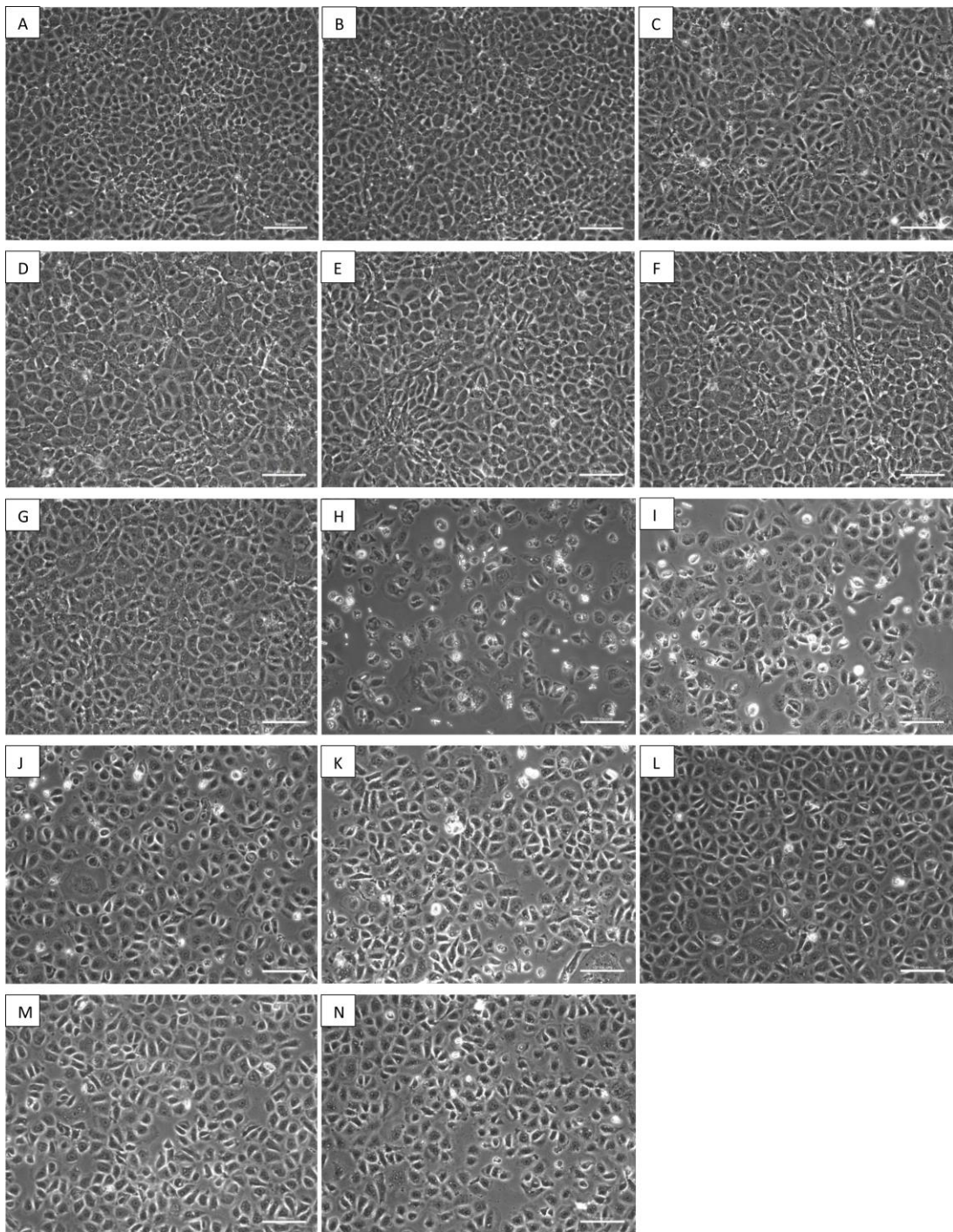


Figure 4.38 Effect of >3 kDa fraction and purified proteins of *T. arjuna* on CaOx crystal adherence in oxalate induced injury to MDCK cells, visualized under polarization and phase contrast at magnification 20X and scale bar 100 microns. Labels are as follow: A: Untreated cells; B: Solvent control (1.44 mM Tris-Cl buffer pH 7.4); C: Only 10 $\mu\text{g}/\text{mL}$ >3 kDa fraction; D: Only 10 $\mu\text{g}/\text{mL}$ A1; E: Only 10 $\mu\text{g}/\text{mL}$ B1; F: Only 10 $\mu\text{g}/\text{mL}$ B2; G: Only 10 $\mu\text{g}/\text{mL}$ C1; H: 2 mM Oxalate injury; I: Positive control (10 $\mu\text{g}/\text{mL}$ Cystone + 2 mM Oxalate); J: 10 $\mu\text{g}/\text{mL}$ >3 kDa fraction + 2 mM Oxalate; K: 10 $\mu\text{g}/\text{mL}$ A1 + 2 mM Oxalate; L: 10 $\mu\text{g}/\text{mL}$ B1 + 2 mM Oxalate; M: 10 $\mu\text{g}/\text{mL}$ B2 + 2 mM Oxalate and N: 10 $\mu\text{g}/\text{mL}$ C1 + 2 mM Oxalate

4.6.2 Detection of apoptosis

4.6.2.1 Effect of >3 kDa fraction and purified proteins of *Terminalia arjuna* on induction of apoptosis in oxalate induced renal cell injury by Hoechst staining

The morphological changes in cell nuclei were determined by fluorescence microscopy by staining NRK-52E and MDCK cells with Hoechst 33258 dye as shown in Figure 4.39 and 4.40 respectively.

The untreated NRK-52E cells appeared to be intact in healthy morphology and showed intact chromatin (Figure 4.39A), indicating that there was no apoptosis and/or necrosis in the untreated cells i.e. all the cells were live. The cells treated with the solvent system (1.44 mM Tris-Cl buffer pH 7.4), >3 kDa fraction and purified plant proteins A1, B1, B2 and C1 (10 µg/mL) showed healthy cellular morphology (Figure 4.39B-G), indicating that there was no adverse effect to the cells. After incubation of the NRK-52E cells with 2 mM oxalate for 48 hours at 37°C, a substantial level of cell death w.r.t. control was observed. The cells showed marked changes in morphology such as irregular shape, membrane blebbing, apoptotic bodies and condensed and fragmented chromatin (Figure 4.39H). The effect of 10 µg/mL of >3 kDa fraction and purified proteins (A1, B1, B2 and C1) on oxalate treated NRK-52E cells (Figure 4.39J-N) was assessed and compared to that of only oxalate treated cells (Figure 4.39H), more viable cells with intact cellular membrane and fewer apoptotic bodies were observed, showing reduced level of apoptosis and necrosis w.r.t. the oxalate injured cells. The B1 (Figure 4.39L) and B2 (Figure 4.39M) showed maximum protection followed by C1 (Figure 4.39N) and A1 (Figure 4.39K) from oxalate induced cellular damage and death. Cystone drug at a concentration of 10 µg/mL was used as a positive control. The treatment of Cystone on oxalate injured NRK-52E cells (Figure 4.39I) reduced injury and more viable cells with healthy morphology were observed as compared to oxalate treated cells.

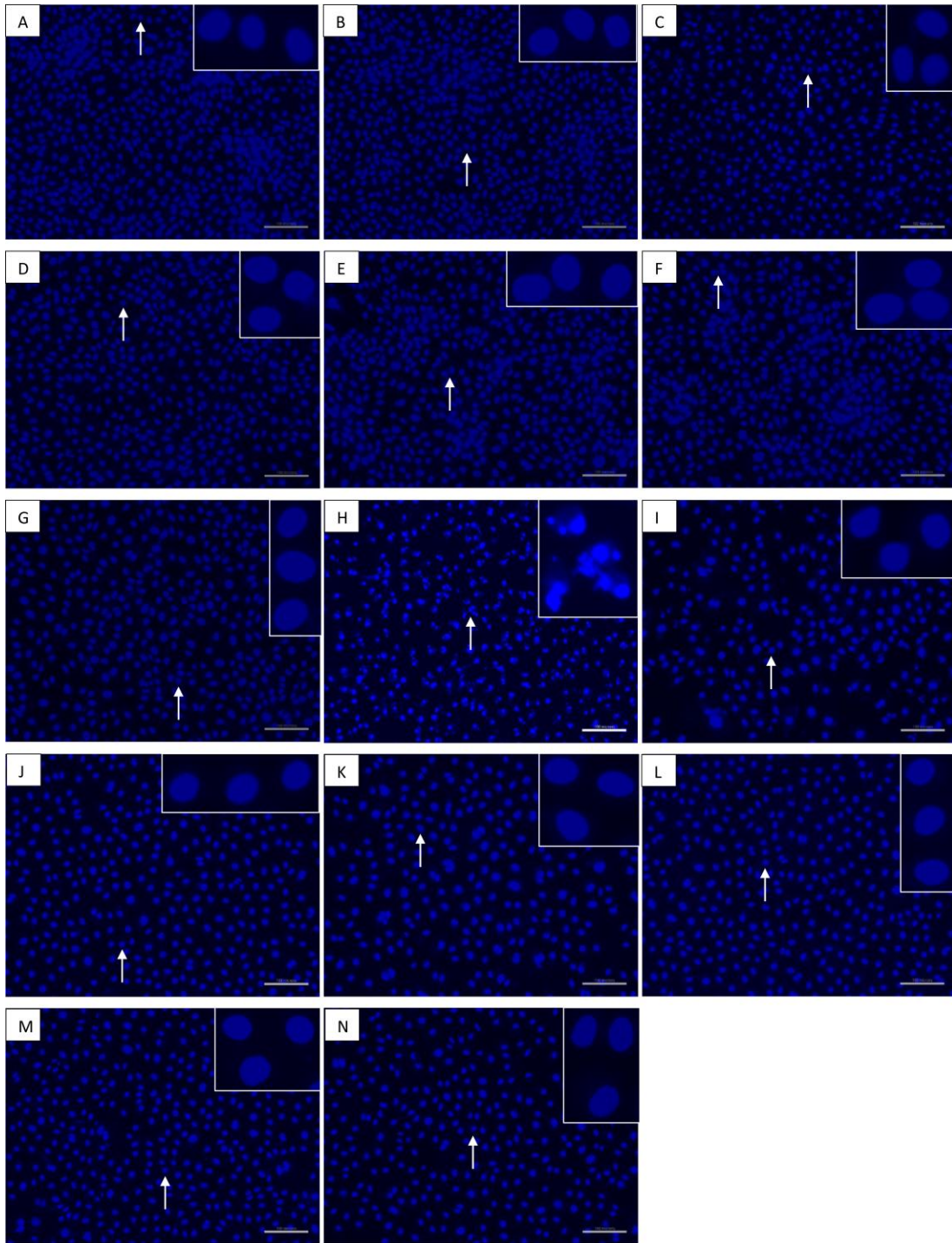


Figure 4.39 Effect of >3 kDa fraction and purified proteins of *T. arjuna* on induction of apoptosis in oxalate induced injury to NRK-52E cells, visualized under fluorescence microscopy at magnification 20X and scale bar 100 microns. Labels are as follow: A: Untreated cells; B: Solvent control (1.44 mM Tris-Cl buffer pH 7.4); C: Only 10 $\mu\text{g}/\text{mL}$ >3 kDa fraction; D: Only 10 $\mu\text{g}/\text{mL}$ A1; E: Only 10 $\mu\text{g}/\text{mL}$ B1; F: Only 10 $\mu\text{g}/\text{mL}$ B2; G: Only 10 $\mu\text{g}/\text{mL}$ C1; H: 2 mM Oxalate injury; I: Positive control (10 $\mu\text{g}/\text{mL}$ Cystone + 2 mM Oxalate); J: 10 $\mu\text{g}/\text{mL}$ >3 kDa fraction + 2 mM Oxalate; K: 10 $\mu\text{g}/\text{mL}$ A1 + 2 mM Oxalate; L: 10 $\mu\text{g}/\text{mL}$ B1 + 2 mM Oxalate; M: 10 $\mu\text{g}/\text{mL}$ B2 + 2 mM Oxalate and N: 10 $\mu\text{g}/\text{mL}$ C1 + 2 mM Oxalate

The untreated MDCK cells appeared to be intact in healthy morphology and showed intact chromatin (Figure 4.40A), indicating that there was no apoptosis and/or necrosis in the untreated cells i.e. all the cells were live. The cells treated with the solvent system (1.44 mM Tris-Cl buffer pH 7.4), >3 kDa fraction and purified plant proteins (A1, B1, B2, C1) alone (10 µg/mL) showed healthy cellular morphology (Figure 4.40B-G), indicating that there was no adverse effect to the cells. When MDCK cells were exposed to 2 mM oxalate for 48 hours at 37°C, a significant level of cell death w.r.t. untreated cells was observed. The cells showed marked changes in morphology such as irregular shape, membrane blebbing, apoptotic bodies and condensed and fragmented chromatin (Figure 4.40H). The effect of 10 µg/mL of >3 kDa fraction and plant proteins on oxalate treated MDCK cells (Figure 4.40J-N) was assessed and compared to oxalate injured cells (Figure 4.40H), more viable cells with intact cellular membrane and fewer apoptotic bodies were observed, showing reduced level of cell death either by apoptosis or necrosis w.r.t. the oxalate exposed cells. The B1 (Figure 4.40L) and B2 (Figure 4.40M) showed maximum protection followed by C1 (Figure 4.40N) and A1 (Figure 4.40K) from oxalate induced cellular damage and death. Cystone drug at a concentration of 10 µg/mL was used as a positive control. The cystone also protected renal cells from injury caused by oxalate (Figure 4.40I) with more viable cells and reduced number of apoptotic cells as compared to oxalate treated cells.

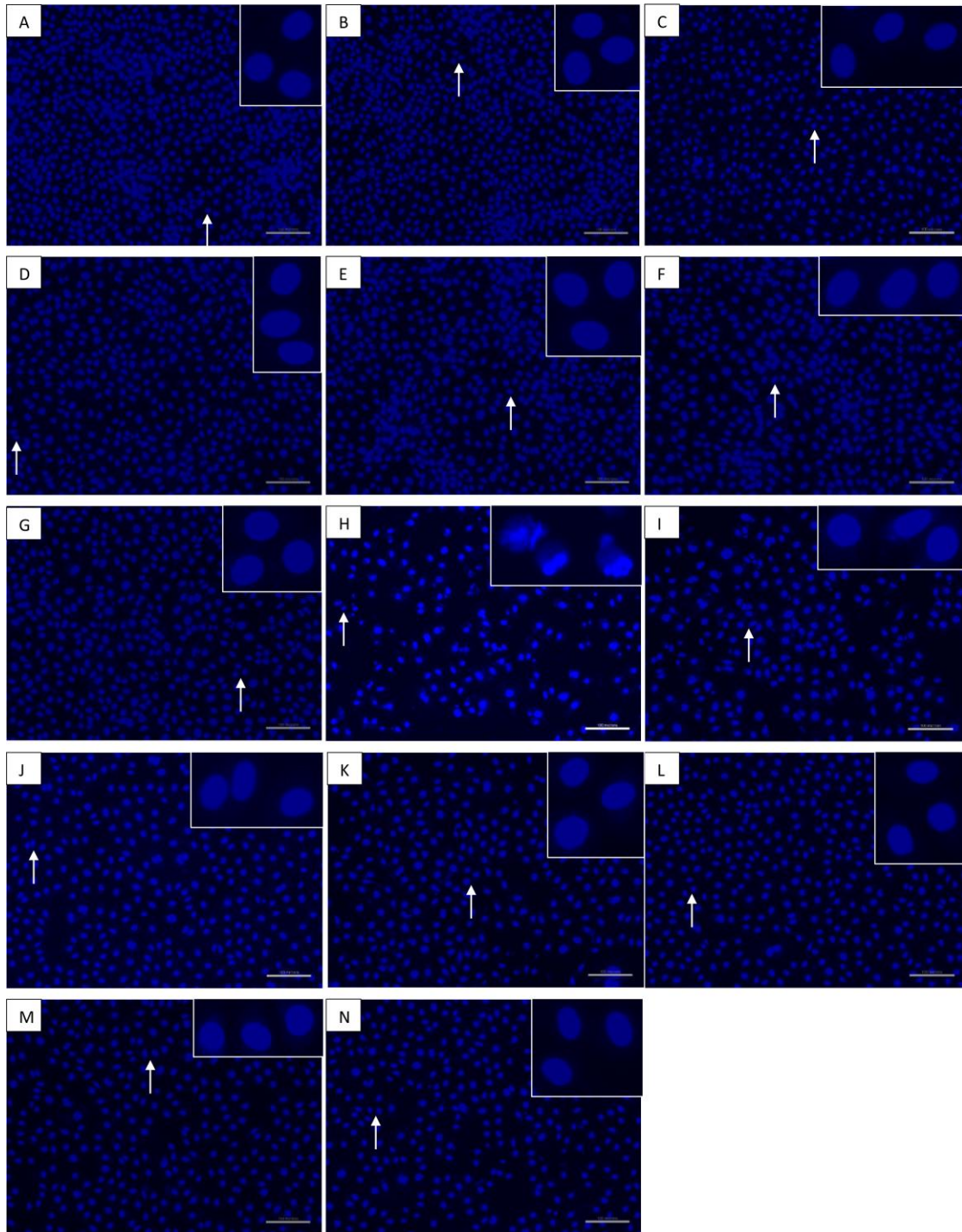
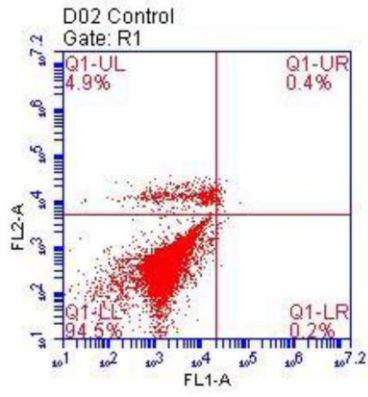


Figure 4.40 Effect of >3 kDa fraction and purified proteins of *T. arjuna* on induction of apoptosis in oxalate induced injury to MDCK cells, visualized under fluorescence microscopy at magnification 20X and scale bar 100 microns. Labels are as follow: A: Untreated cells; B: Solvent control (1.44 mM Tris-Cl buffer pH 7.4); C: Only 10 $\mu\text{g}/\text{mL}$ >3 kDa fraction; D: Only 10 $\mu\text{g}/\text{mL}$ A1; E: Only 10 $\mu\text{g}/\text{mL}$ B1; F: Only 10 $\mu\text{g}/\text{mL}$ B2; G: Only 10 $\mu\text{g}/\text{mL}$ C1; H: 2 mM Oxalate injury; I: Positive control (10 $\mu\text{g}/\text{mL}$ Cystone + 2 mM Oxalate); J: 10 $\mu\text{g}/\text{mL}$ >3 kDa fraction + 2 mM Oxalate; K: 10 $\mu\text{g}/\text{mL}$ A1 + 2 mM Oxalate; L: 10 $\mu\text{g}/\text{mL}$ B1 + 2 mM Oxalate; M: 10 $\mu\text{g}/\text{mL}$ B2 + 2 mM Oxalate and N: 10 $\mu\text{g}/\text{mL}$ C1 + 2 mM Oxalate

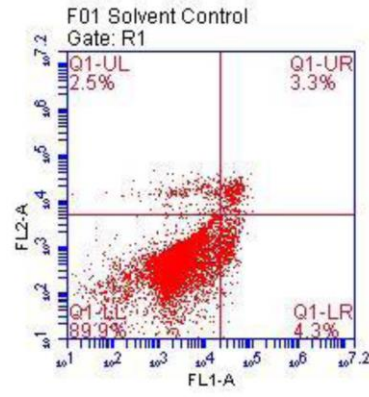
4.6.2.2 Effect of >3 kDa fraction and purified proteins of *Terminalia arjuna* on induction of apoptosis in oxalate induced renal cell injury by flow cytometry using Annexin/PI staining

Oxalate-induced apoptosis in NRK-52E and MDCK cells was analyzed by flow cytometry by identification of staining with annexin V and Propidium iodide (PI) as depicted in Figure 4.41 and 4.42 respectively.

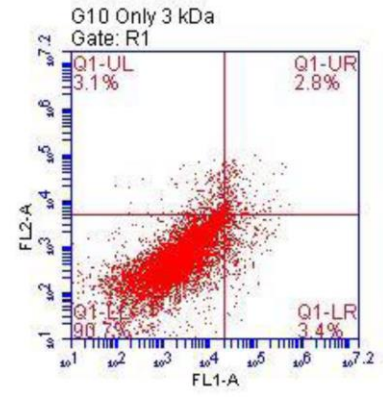
There was no significant apoptosis and necrosis in the untreated NRK-52E cells i.e. control with a cell viability of 94.5% (Figure 4.41A). Treatment of cells with the solvent system (1.44 mM Tris-Cl buffer pH 7.4), >3 kDa fraction and plant purified proteins A1, B1, B2 and C1 (10 µg/mL) cause no adverse effects to cells w.r.t. control with the percentage viability of 89.9%, 90.7% and 91.2%, 93.2%, 92.3% and 92.6% respectively (Figure 4.41B-G), indicating that there was no adverse effect to the cells. When NRK-52E cells were treated with 2 mM oxalate for 48 hours at 37°C, a considerable level of cell death w.r.t. untreated cells was observed (Figure 4.41H). Time-course cell death assay using annexin V/propidium iodide staining showed that percent cell death was gradually increased in cells exposed to oxalate from 0.2% in control to 58%. The effect of 10 µg/mL of >3 kDa fraction and purified proteins (A1, B1, B2, C1) on oxalate treated NRK-52E cells (Figure 4.41J-N) was evaluated and compared to that of only oxalate treated cells (Figure 4.41H), the number of apoptotic cells was significantly reduced to 35.9% and 32.2%, 13.9%, 22.2% and 26% respectively, indicating that >3 kDa fraction and plant based proteins protected the cells from oxalate induced apoptosis. Cystone drug at a concentration of 10 µg/mL was used as a positive control. The addition of Cystone on oxalate treated NRK-52E cells (Figure 4.41I) also exhibited cytoprotective effect with reduced level of apoptosis to 54.6% as compared to oxalate treated cells.



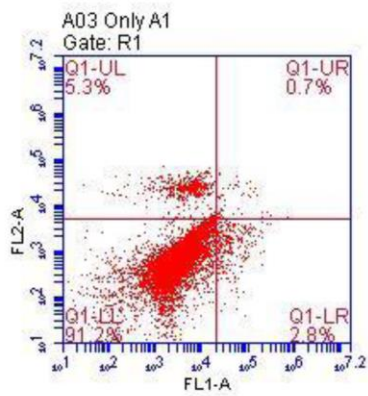
A



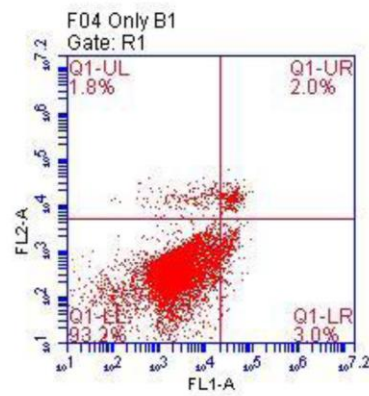
B



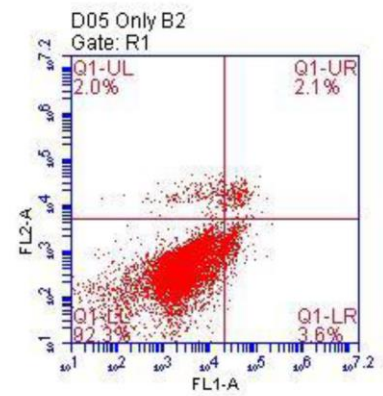
C



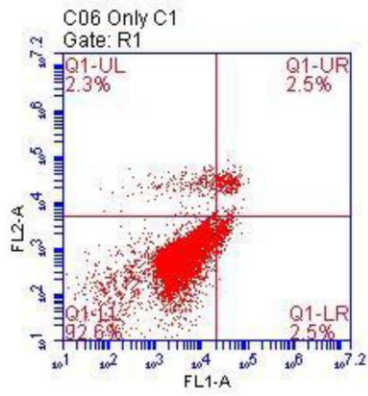
D



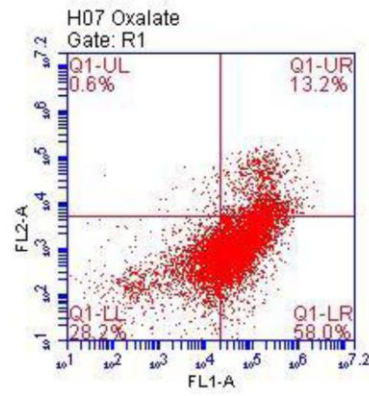
E



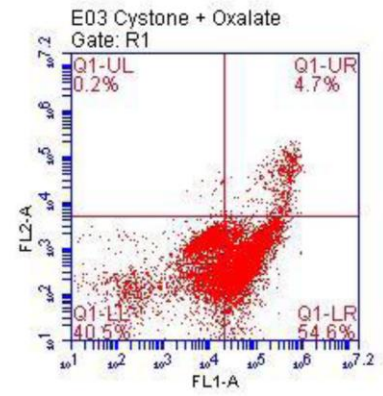
F



G



H



I

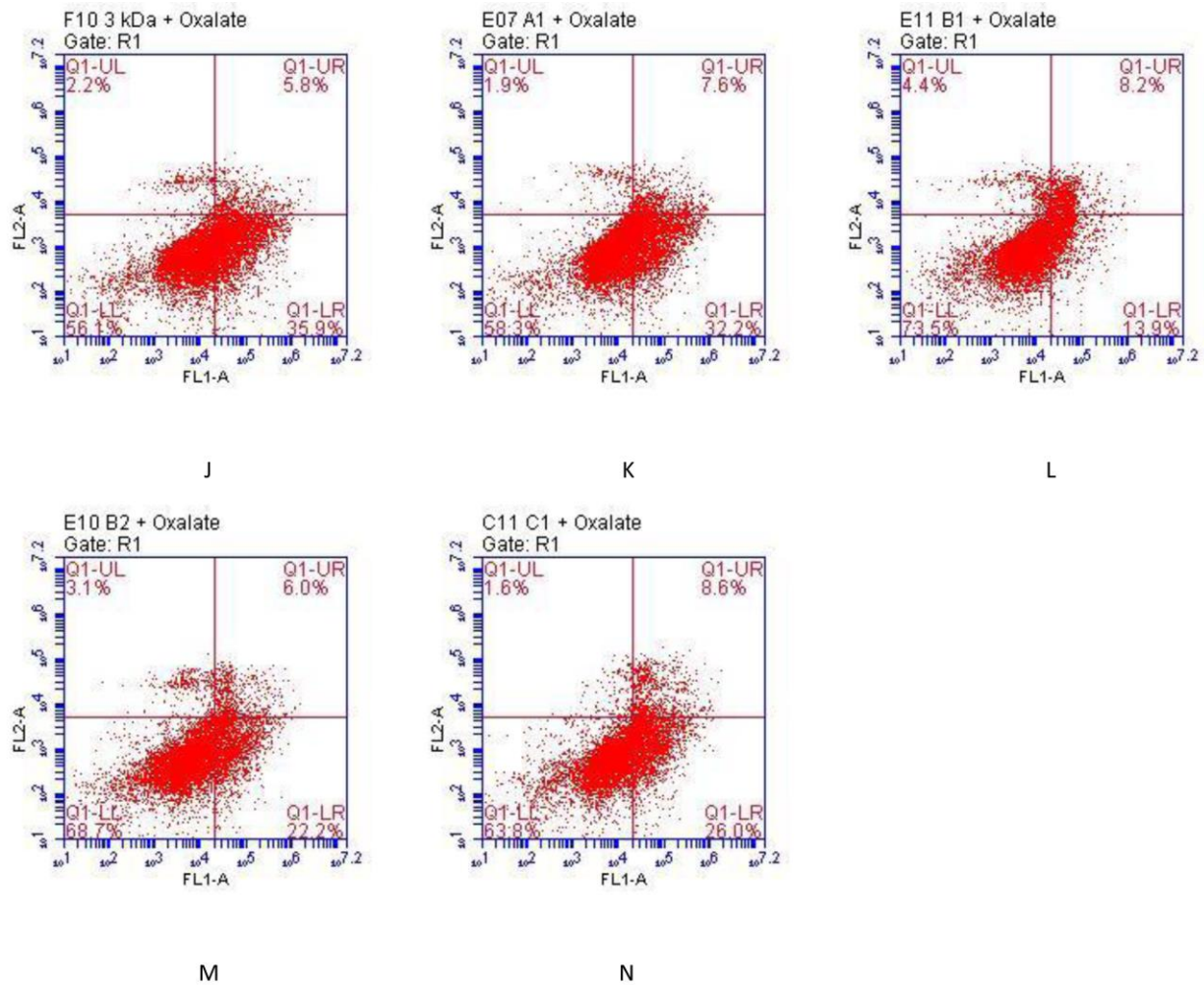
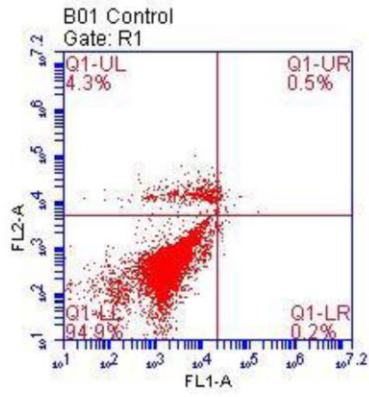
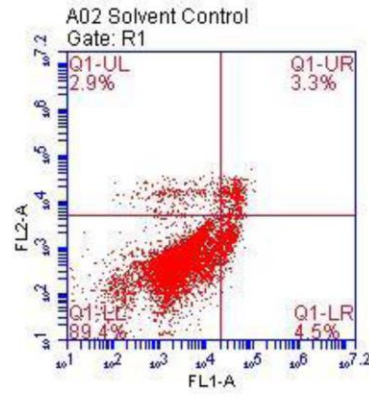


Figure 4.41 Flow cytometry analysis showing the effect of >3 kDa and purified proteins of *T. arjuna* on induction of apoptosis in oxalate induced injury to NRK-52E cells, visualized by AnnexinV/PI staining. Labels are as follow: A: Untreated cells; B: Solvent control (1.44 mM Tris-Cl buffer pH 7.4); C: Only 10 μ g/mL >3 kDa fraction; D: Only 10 μ g/mL A1; E: Only 10 μ g/mL B1; F: Only 10 μ g/mL B2; G: Only 10 μ g/mL C1; H: 2 mM Oxalate injury; I: Positive control (10 μ g/mL Cystone + 2 mM Oxalate); J: 10 μ g/mL >3 kDa fraction + 2 mM Oxalate; K: 10 μ g/mL A1 + 2 mM Oxalate; L: 10 μ g/mL B1 + 2 mM Oxalate; M: 10 μ g/mL B2 + 2 mM Oxalate and N: 10 μ g/mL C1 + 2 mM Oxalate

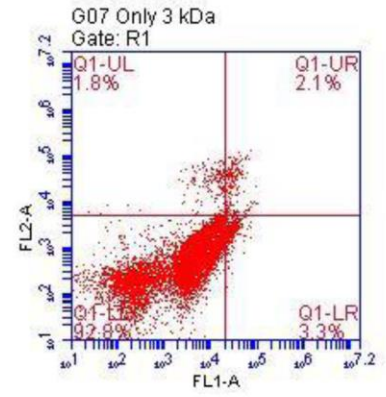
An insignificant percentage of apoptosis and necrosis was observed in the untreated MDCK cells i.e. control with a cell viability of 94.9% (Figure 4.42A). Treatment of cells with the solvent system (1.44 mM Tris-Cl buffer pH 7.4), >3 kDa fraction and purified proteins A1, B1, B2 and C1 (10 µg/mL) did not lead to any significant alteration in cell viability w.r.t. control with the percentage viability of 89.4%, 92.8% and 92.6%, 93.8%, 93.4% and 93.5% respectively (Figure 4.42B-G), indicating that there was no adverse effect to the cells. After incubation of the MDCK cells with 2 mM oxalate for 48 hours at 37°C, a substantial level of cell death w.r.t. control was observed (Figure 4.42H). Time-course cell death assay using annexin V/propidium iodide double staining showed that percent cell death by apoptosis was gradually increased in cells exposed to oxalate from 0.2% in control to 64%. The effect of 10 µg/mL of >3 kDa fraction and proteins (A1, B1, B2 and C1) on oxalate treated MDCK cells (Figure 4.42J-N) was assessed and compared to oxalate treated cells (Figure 4.42H), the number of apoptotic cells was significantly reduced to 32.4% and 31%, 17.2%, 16.3% and 22.3% respectively, indicating that >3 kDa fraction and proteins protected the cells from oxalate induced apoptosis. Cystone drug at a concentration of 10 µg/mL was used as a positive control. The treatment of Cystone on oxalate injured MDCK cells (Figure 4.42I) also exhibited protective potential with reduced level of apoptosis to 53.4% as compared to oxalate treated cells.



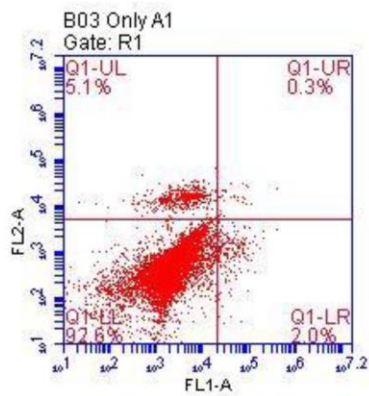
A



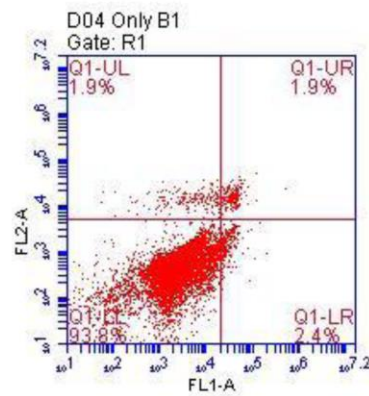
B



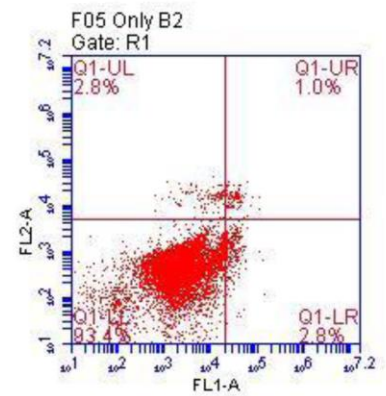
C



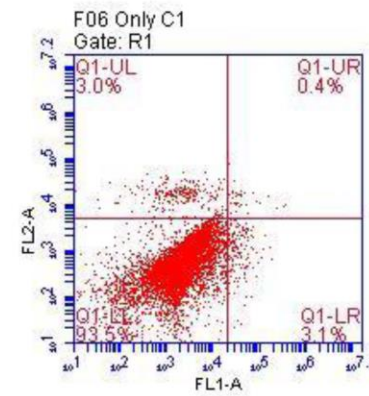
D



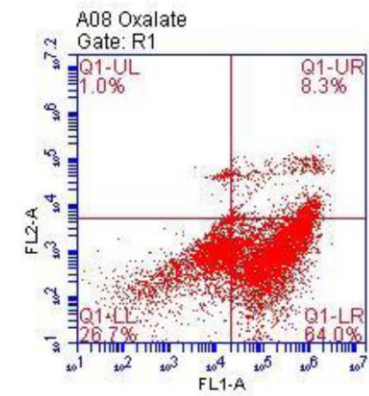
E



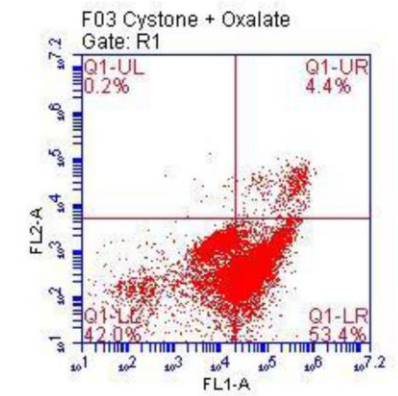
F



G



H



I

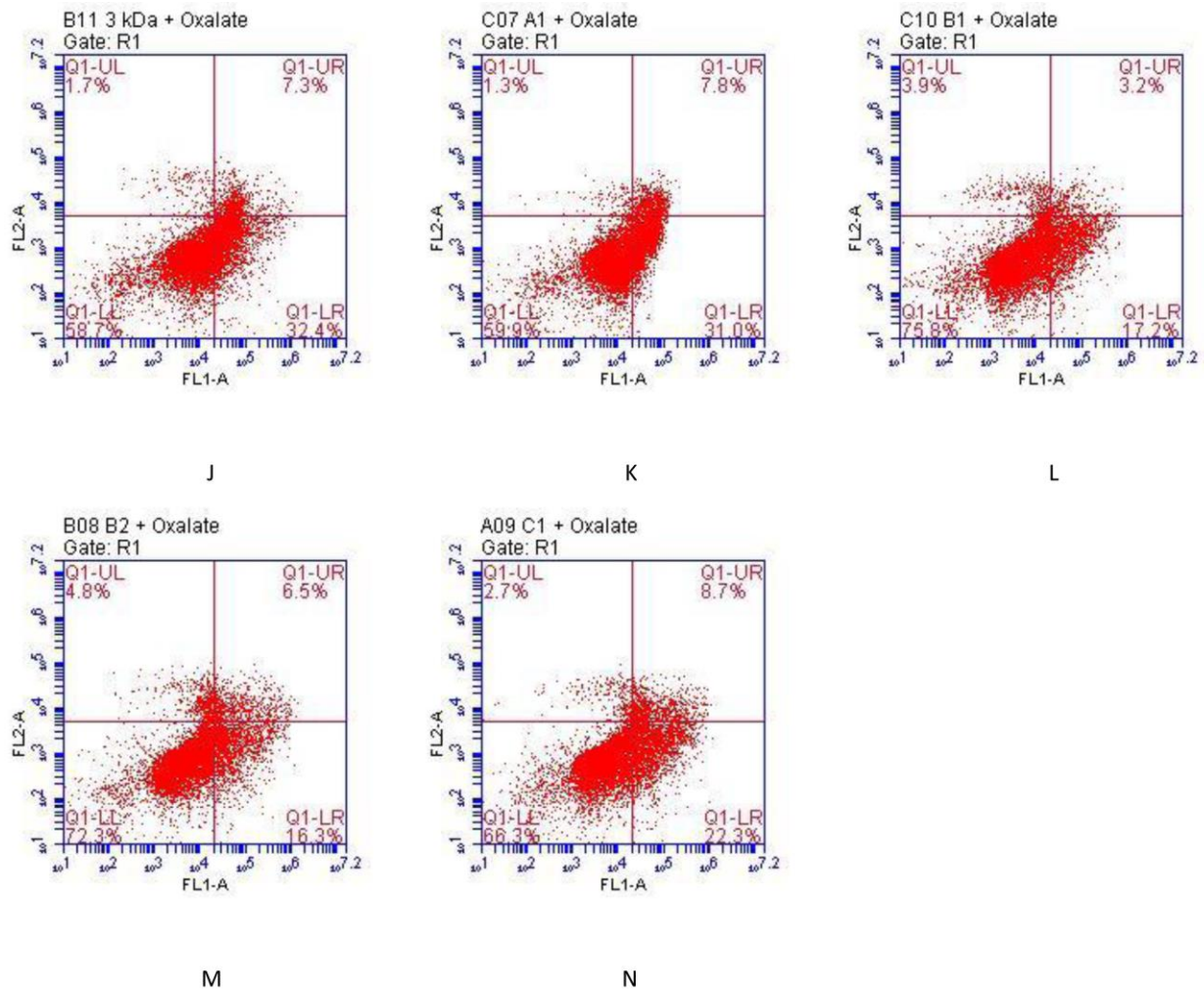
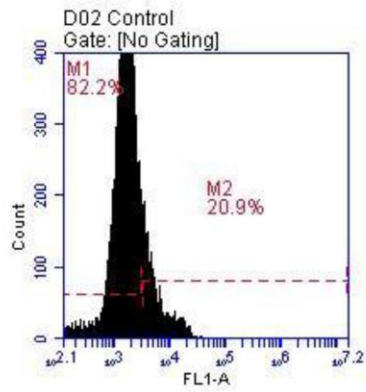


Figure 4.42 Flow cytometry analysis showing the effect of >3 kDa and purified proteins of *T. arjuna* on induction of apoptosis in oxalate induced injury to MDCK cells, visualized by AnnexinV/PI staining. Labels are as follow: A: Untreated cells; B: Solvent control (1.44 mM Tris-Cl buffer pH 7.4); C: Only 10 $\mu\text{g}/\text{mL}$ >3 kDa fraction; D: Only 10 $\mu\text{g}/\text{mL}$ A1; E: Only 10 $\mu\text{g}/\text{mL}$ B1; F: Only 10 $\mu\text{g}/\text{mL}$ B2; G: Only 10 $\mu\text{g}/\text{mL}$ C1; H: 2 mM Oxalate injury; I: Positive control (10 $\mu\text{g}/\text{mL}$ Cystone + 2 mM Oxalate); J: 10 $\mu\text{g}/\text{mL}$ >3 kDa fraction + 2 mM Oxalate; K: 10 $\mu\text{g}/\text{mL}$ A1 + 2 mM Oxalate; L: 10 $\mu\text{g}/\text{mL}$ B1 + 2 mM Oxalate; M: 10 $\mu\text{g}/\text{mL}$ B2 + 2 mM Oxalate and N: 10 $\mu\text{g}/\text{mL}$ C1 + 2 mM Oxalate

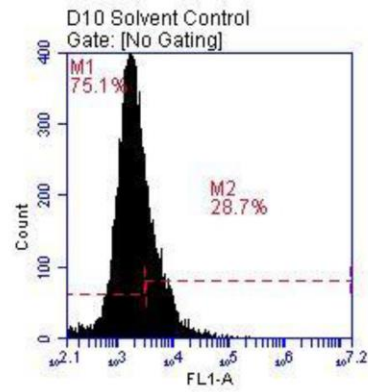
4.6.2.3 Effect of >3 kDa fraction and purified proteins of *Terminalia arjuna* on induction of apoptosis in oxalate induced renal cell injury by detecting Active Caspase-3 by flow cytometry

Oxalate-induced apoptosis in NRK-52E and MDCK cells was evaluated by flow cytometry by using Anti-Active Caspase-3 antibody staining as depicted in Figure 4.43 and 4.44 respectively.

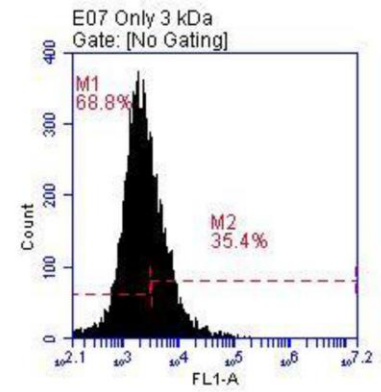
The untreated NRK-52E cells i.e. control showed no substantial cell death by apoptosis and necrosis with a cell viability of 82.2% (Figure 4.43A). Treatment of cells with the solvent system (1.44 mM Tris-Cl buffer pH 7.4), >3 kDa fraction and purified proteins A1, B1, B2 and C1 (10 µg/mL) did not lead to any significant alteration in cell viability w.r.t. control with the percentage viability of 75.1%, 68.5% and 66.3%, 72.8%, 70.9% and 69.9% respectively (Figure 4.43B-G), indicating that there was no adverse effect to the cells. After incubation of the NRK-52E cells with 2 mM oxalate for 48 hours at 37°C, a substantial level of cell death w.r.t. control was observed (Figure 4.43H). Time-course cell death assay using Anti-Active Caspase-3 antibody staining showed that percent of cells undergoing apoptosis was gradually increased in cells exposed to oxalate from 20.9% in control to 75.7%. The effect of 10 µg/mL of >3 kDa fraction and proteins A1, B1, B2 and C1 on oxalate injured NRK-52E cells (Figure 4.43J-N) was determined and compared to oxalate treated cells (Figure 4.43H), the number of cells with active caspase 3 enzyme was significantly reduced to 56.5% and 55.4%, 41%, 39.7% and 51.1% respectively, indicating that >3 kDa fraction and purified proteins reduced oxalate induced apoptosis to cells. Cystone drug at 10 µg/mL was used as a positive control and protected the NRK-52E cells (Figure 4.43I), thus, reducing the level of apoptosis to 64.9% as compared to oxalate treated cells.



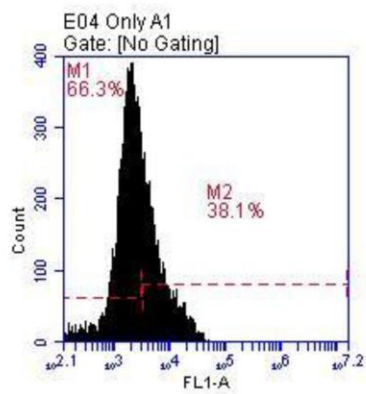
A



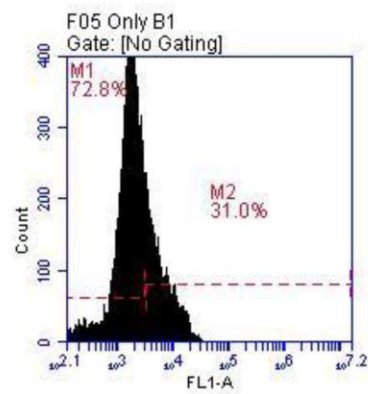
B



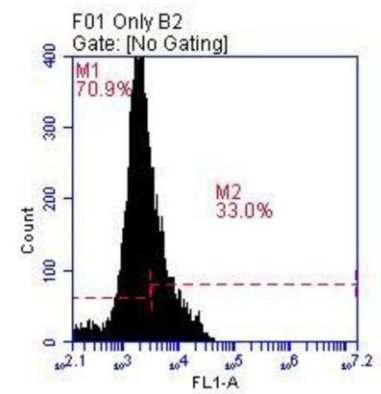
C



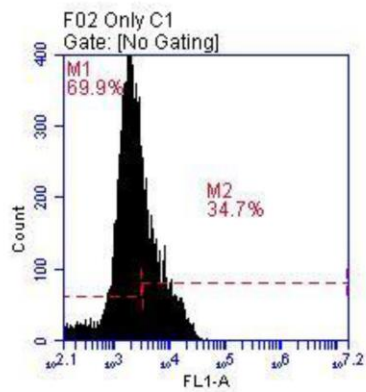
D



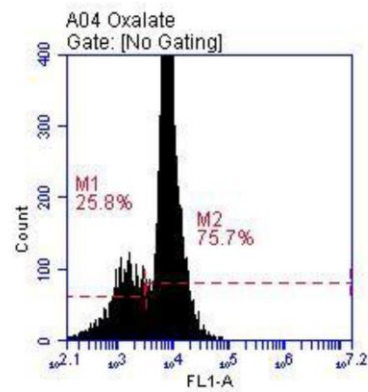
E



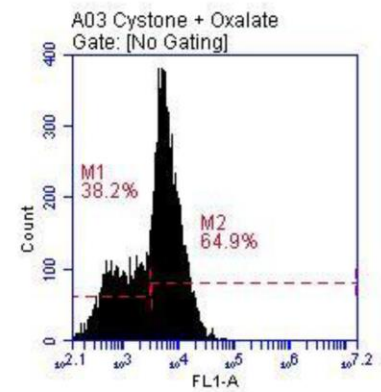
F



G



H



I

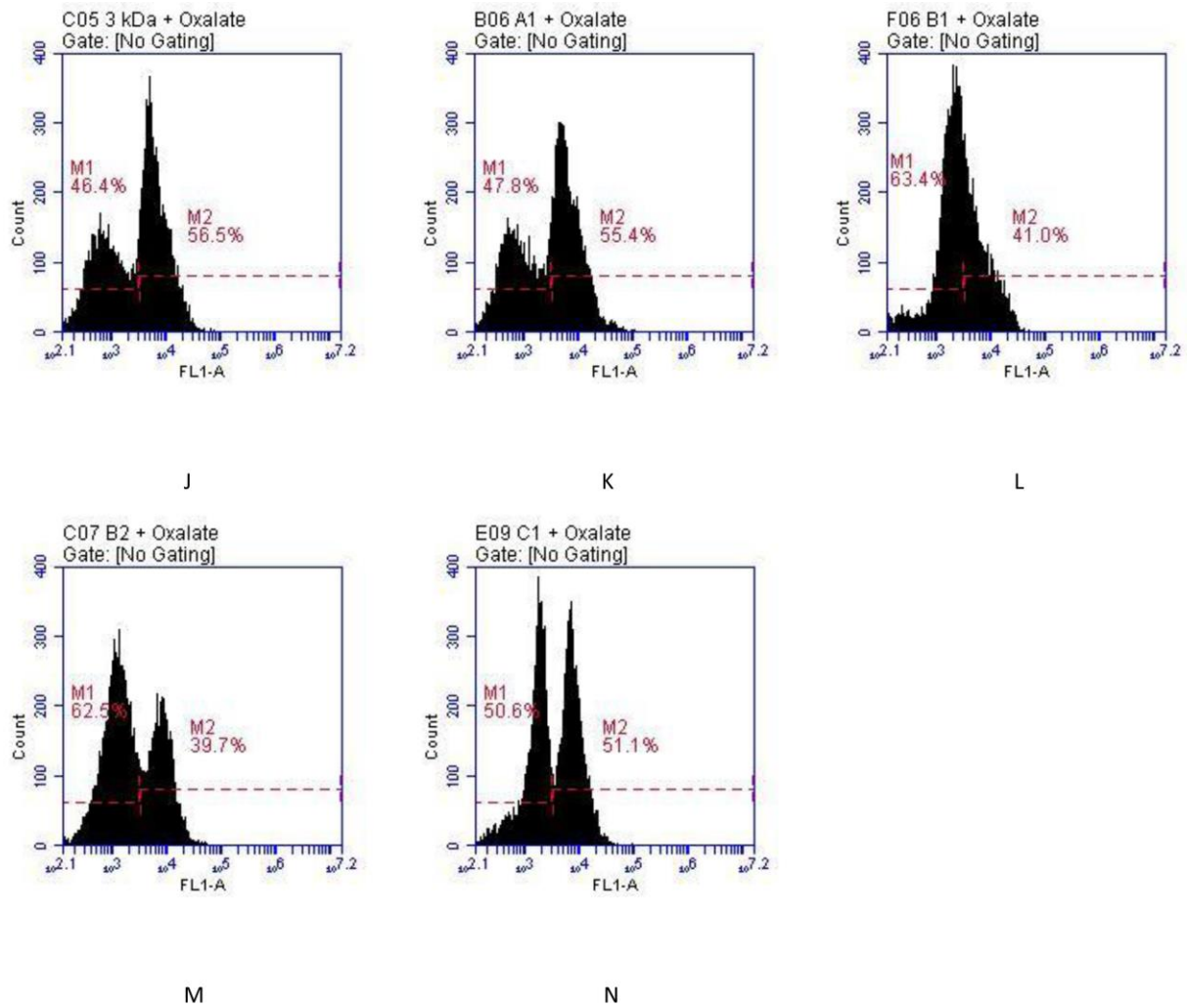
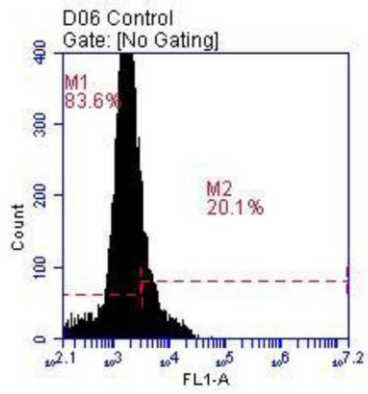
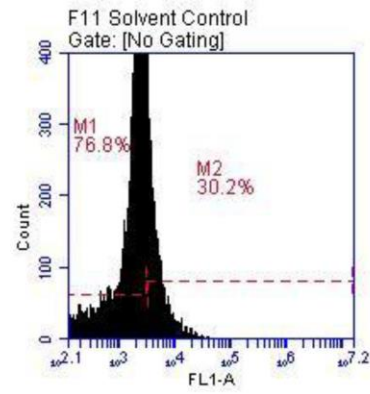


Figure 4.43 Flow cytometry analysis showing the effect of >3 kDa and purified proteins of *T. arjuna* on induction of apoptosis in oxalate induced injury to NRK-52E cells, visualized by Anti-Active Caspase-3 antibody staining. Labels are as follow: A: Untreated cells; B: Solvent control (1.44 mM Tris-Cl buffer pH 7.4); C: Only 10 $\mu\text{g}/\text{mL}$ >3 kDa fraction; D: Only 10 $\mu\text{g}/\text{mL}$ A1; E: Only 10 $\mu\text{g}/\text{mL}$ B1; F: Only 10 $\mu\text{g}/\text{mL}$ B2; G: Only 10 $\mu\text{g}/\text{mL}$ C1; H: 2 mM Oxalate injury; I: Positive control (10 $\mu\text{g}/\text{mL}$ Cystone + 2 mM Oxalate); J: 10 $\mu\text{g}/\text{mL}$ >3 kDa fraction + 2 mM Oxalate; K: 10 $\mu\text{g}/\text{mL}$ A1 + 2 mM Oxalate; L: 10 $\mu\text{g}/\text{mL}$ B1 + 2 mM Oxalate; M: 10 $\mu\text{g}/\text{mL}$ B2 + 2 mM Oxalate and N: 10 $\mu\text{g}/\text{mL}$ C1 + 2 mM Oxalate

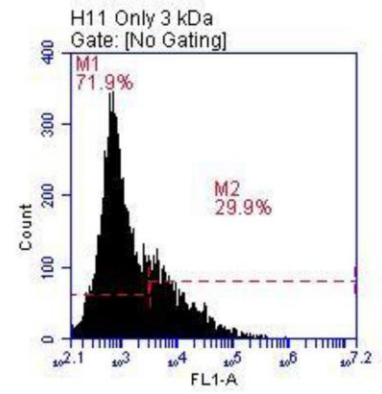
There was insignificant apoptosis and necrosis in the untreated MDCK cells i.e. control with a cell viability of 83.6% (Figure 4.44A). Treatment of cells with the solvent system (1.44 mM Tris-Cl buffer pH 7.4), >3 kDa fraction and purified proteins A1, B1, B2 and C1 (10 µg/mL) cause no harmful effects w.r.t. control with the percentage viability of 76.8%, 71.9% and 68.5%, 75.8%, 71.6% and 70% respectively (Figure 4.44B-G), indicating that there was no adverse effect to the cells. When MDCK cells were injured with 2 mM oxalate for 48 hours at 37°C, a substantial level of cell death w.r.t. control was observed (Figure 4.44H). Time-course cell death assay using Anti-Active Caspase-3 antibody staining showed that percent of cells with active caspase 3 enzyme was gradually increased in cells exposed to oxalate from 20.1% in control to 78.4%. The effect of 10 µg/mL of >3 kDa fraction and proteins A1, B1, B2 and C1 on oxalate treated MDCK cells (Figure 4.44J-N) was assessed and compared to oxalate treated cells (Figure 4.44H), the number of cells undergoing apoptosis was significantly reduced to 56.6% and 54.4%, 37.4%, 38.6% and 48.6% respectively, indicating that >3 kDa fraction and purified proteins protected the cells from oxalate induced apoptosis. Cystone drug at a concentration of 10 µg/mL was used as a positive control. The addition of Cystone on oxalate treated MDCK cells (Figure 4.44I) also exhibited cytoprotective effect with reduced level of apoptosis to 64.1% as compared to oxalate treated cells.



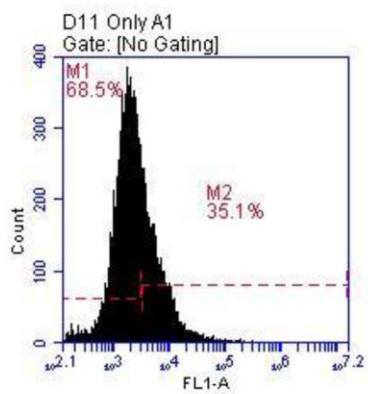
A



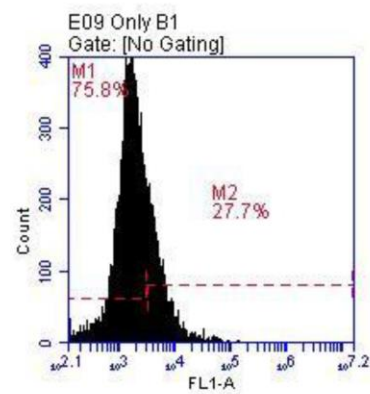
B



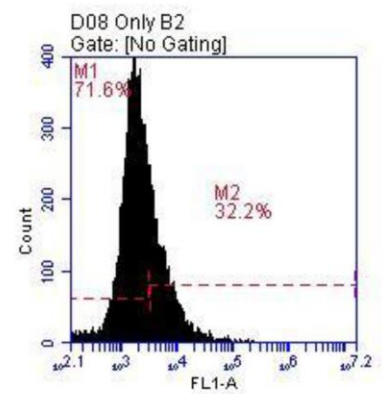
C



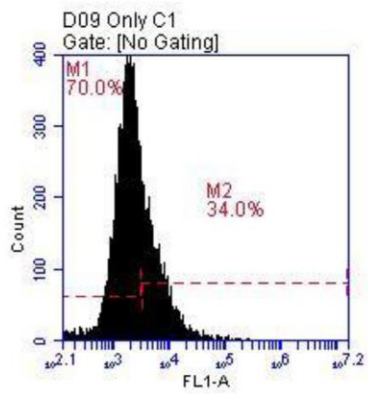
D



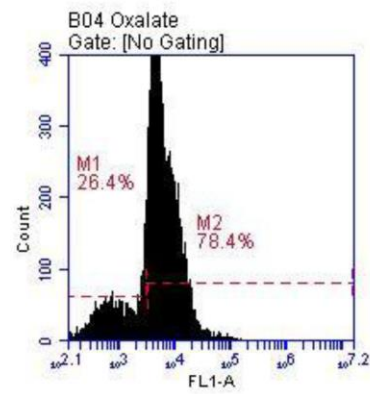
E



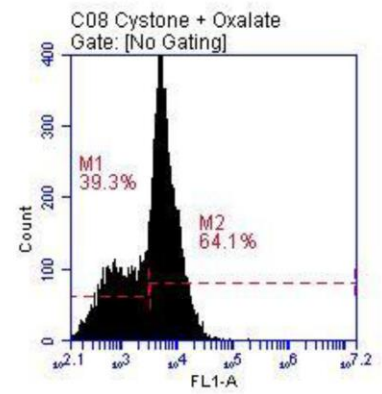
F



G



H



I

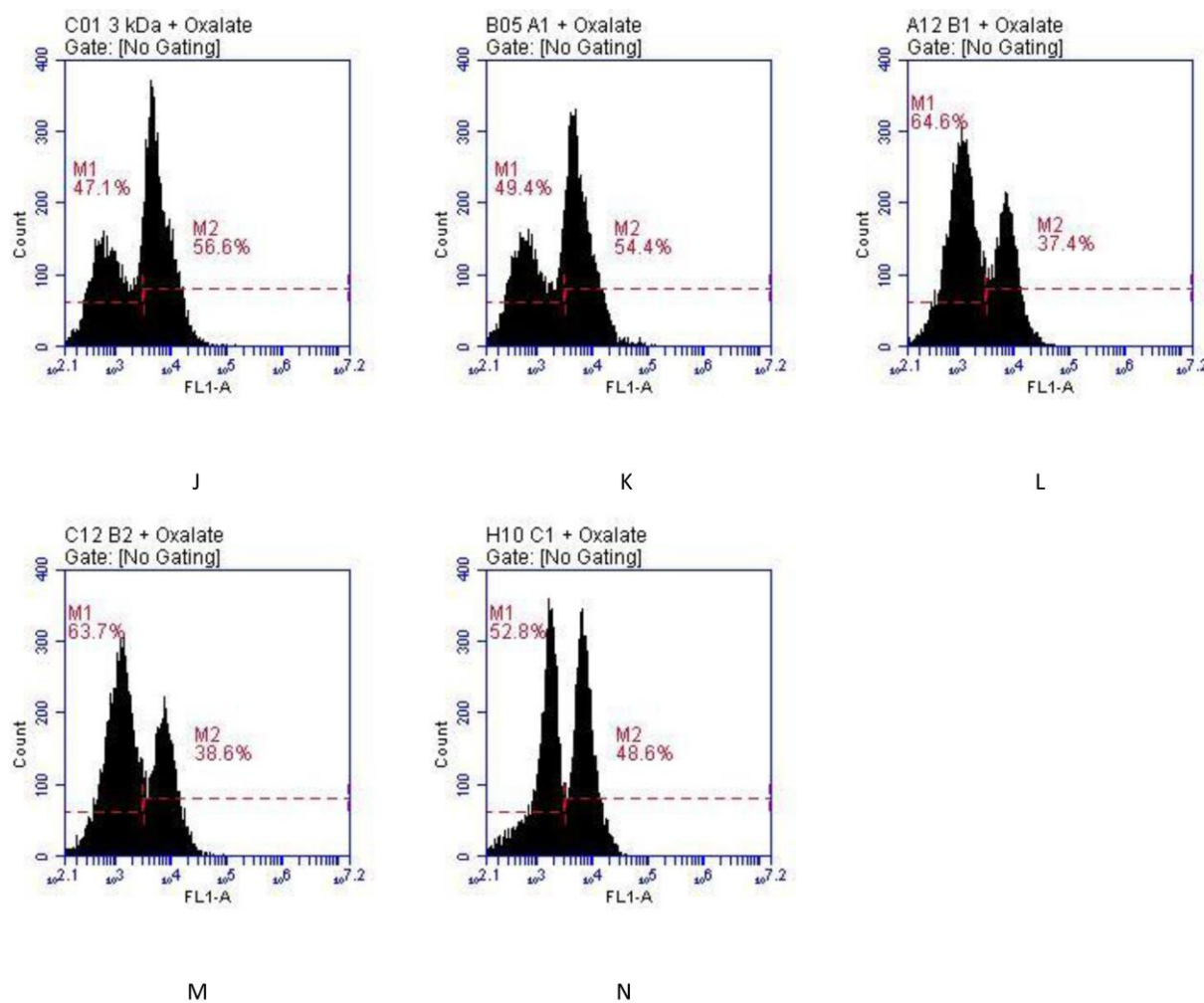


Figure 4.44 Flow cytometry analysis showing the effect of >3 kDa and purified proteins of *T. arjuna* on induction of apoptosis in oxalate induced injury to MDCK cells, visualized by Anti-Active Caspase-3 antibody staining. Labels are as follow: A: Untreated cells; B: Solvent control (1.44 mM Tris-Cl buffer pH 7.4); C: Only 10 μ g/mL >3 kDa fraction; D: Only 10 μ g/mL A1; E: Only 10 μ g/mL B1; F: Only 10 μ g/mL B2; G: Only 10 μ g/mL C1; H: 2 mM Oxalate injury; I: Positive control (10 μ g/mL Cystone + 2 mM Oxalate); J: 10 μ g/mL >3 kDa fraction + 2 mM Oxalate; K: 10 μ g/mL A1 + 2 mM Oxalate; L: 10 μ g/mL B1 + 2 mM Oxalate; M: 10 μ g/mL B2 + 2 mM Oxalate and N: 10 μ g/mL C1 + 2 mM Oxalate

CHAPTER 5

DISCUSSION

Renal stone disease has tormented people throughout the ages. Despite enormous developments in nephrology and urology, we still do not know exactly how kidney stones are formed and how to prevent them. Kidney stones are built from numerous tiny crystals that commonly are pasted together with organic material. The formation of crystals in the kidney is normal and harmless provided that they are excreted with the urine. The difference between stone formers and non-stone formers is that crystals stay behind in kidneys of stone formers. An acute renal colic that is caused by a tiny stone's passing down the ureter can be extremely painful. Small stones (≤ 5 mm) often pass without medical intervention, but larger stones (>5 mm) usually must be removed. With the advent of extracorporeal shock wave lithotripsy and improved surgical procedures, the removal of kidney stones no longer is as primitive as a few hundred years ago. Nevertheless, recurrent stone disease causes significant morbidity, and in patients with inborn errors in endogenous oxalate synthesis, pathologic renal calcifications ultimately may destroy the kidney. The human kidney concentrates the urine to preserve water and essential nutrients and to eliminate waste products [274].

The formation of renal stones is a consequence of increased urinary supersaturation with subsequent formation of crystalline particles. Since most of the solid particles crystallizing within the urinary tract will be excreted freely, particle formation is by no means equivalent to symptomatic stone disease. However, when solid particles are retained within the kidney, they can grow to become full-size stones [11]. Crystals can be retained at many sites in the kidneys and undergo the size-enhancing process of growth and aggregation. In order for stones to be formed, not only do crystals need to be retained within the kidney, but they must be located at sites from which crystals can cause ulceration at the papillary surface to form a stone nidus. It is thought that renal tubular injury plays an important role at this point. Khan hypothesized that renal tubular injury promotes crystal retention and the development of a stone nidus on the renal papillary surface [12]. In addition, renal tubular injury enhances crystal nucleation at low supersaturation [157].

The process of attachment or endocytosis of crystals to renal tubular cells is what is generally meant by crystal–cell interactions. Crystal–cell interaction is the next step, and is also promoted by renal tubular injury. Since crystal formation is a common phenomenon in human urine and crystalluria per se is harmless, abnormal retention of formed particles must occur when kidney stones form. Thus, crystal–cell interactions may be highly relevant. The crystals that are internalized in the interstitium undergo growth and aggregation, and develop into renal stones.

Experimental induction of CaOx urolithiasis starts with hyperoxaluria followed by crystalluria and deposition in the kidney [12, 148]. Many studies have focused on oxalate-induced changes in renal epithelial cells. Recent studies indicated that oxalate-induced death of renal epithelial cells exhibits characteristics of both apoptotic and necrotic cell death [196]. Several studies have provided evidence that oxalate-induced toxicity is related to superoxide [217] and lipid peroxidation [191, 197]. The oxalate-induced increase in free radical production and cell death appear to be linked in a concentration-dependent manner. Oxalate also causes activation of at least two lipid signaling cascades, one involving phospholipase A₂ (and resulting in increased release of arachidonic acid and formation of lysophospholipids [191] and the other involving sphingomyelinase (and resulting in increased levels of ceramide and decreased levels of sphingomyelin) [197]. Free radical mediators of inflammation have been shown to induce the production of chemokines and changes in gene expression [192].

Damaged or apoptotic renal cell monolayers present a number of binding sites for crystal attachment that are normally masked in intact epithelia, including sites enriched for PS, HA, sialic acid and/or matrix proteins [138]. Once attached, these crystals can serve as centers for the nucleation of new crystals, a process favoring stone development. Alternatively, crystals on the cell surface may be taken up by the renal cells (an active endocytic process) [146]. Once internalized, crystals may dissolve within lysosomes or re-emerge at the basolateral surface, providing centers for growth of stones in the renal interstitium [170]. Debris from damaged cells can also foster stone growth by providing centers for heterogeneous crystal nucleation. Human kidney stones contain an organic core whose composition resembles that of cellular membranes [275], and the addition of renal membrane fragments promotes heterogeneous nucleation of crystals in artificial urine [276].

It appears that the process of renal tubular cell injury is of key importance in renal stone formation. Though many aspects of the mechanism of renal stone formation remain

unclear, it is certain that renal tubular cell injury is a very important part of it. At present, though few substances useful for the prevention of urolithiasis are available, the development of medications that prevent renal tubular cell injury will provide a novel strategy for preventing this disease [112].

Hence, this study was aimed to conduct the detailed studies to assess the effect *Terminalia arjuna* on the adhesion of COM crystals to cultured renal cells to establish a scientific basis for their anti-urolithiatic property and characterization of the antilithiatic proteins from *Terminalia arjuna*. Since, *Terminalia arjuna*, belonging to the family Combretaceae, holds a reputed position in Ayurvedic system of medicine since ancient times [18]. Experimental and clinical studies revealed the beneficial effects of this plant against all sorts of conditions of cardiac failure [19]. It was found to be efficient in management of kidney stones not only *in vitro* but *in vivo* too. *Terminalia arjuna* bark extract is previously reported to inhibit CaOx crystal precipitation and growth [277]. Hence, characterization of antilithiatic proteins from *Terminalia arjuna* can open new vistas for the therapeutic proteins present in *Terminalia arjuna* for the treatment and cure of urolithiasis.

5.1 Antiurolithiatic potential of aqueous extract of *Terminalia arjuna* in vitro

In the present study, the inhibitory potential of *Terminalia arjuna* was evaluated *in vitro* on calcium oxalate crystallization and crystal growth. The supersaturation of urine with CaOx, the most common component of kidney stones, is an important factor in crystallization, with later factors being nucleation, growth and aggregation. Thus, if supersaturation or later steps in crystallization can be prevented, then lithiasis can be avoided [278]. The effect of *Terminalia arjuna* bark aqueous extract on CaOx crystallization and crystal growth kinetics was studied by the time course measurement of turbidity. With respect to calcium oxalate crystallization, the aqueous extract of the plant was effective in inhibiting both the nucleation and aggregation of CaOx crystals in a concentration-dependent manner. The aqueous extract of the plant also inhibited the CaOx crystal growth effectively. Moreover, a study was performed to evaluate the crystal dissolution potential of aqueous extract of *Terminalia arjuna* bark against CaOx monohydrate crystals. In the microscopic study, aqueous extract modified CaOx monohydrate crystal morphology. A similar change in the morphology of CaOx monohydrate crystals has been previously reported with citrate and Mg^{2+} [279]. Microphotography studies verified that aqueous extract of *Terminalia arjuna* resulted

in the formation of round CaOx crystals. COM and COD are the major forms found in most urinary calculi. Aqueous extract of *Terminalia arjuna* inhibited the growth of COM crystals, prevented the aggregation of COM crystals, and induced the formation of spherical COM crystals. These spherical COM crystals are thermodynamically less stable phase and have weaker affinity for cell membranes than hexagonal COM crystals. Both the positive control cystone drug (1000 µg/mL) and aqueous extract of *Terminalia arjuna* (1000 µg/mL) modified the morphology of hexagonal CaOx monohydrate crystals to more rounded edges and spherical shape, as shown in Figure 4.3B and 4.3C respectively. This shape may prevent the formation of kidney stones, because crystals with this shape are more easily excreted in the urine compared with the COM. Furthermore, *Terminalia arjuna* bark aqueous extract possess very high antioxidant activity due to the presence of Terpenoids. It has the ability to scavenge the free radicals with an IC₅₀ of 13.11 µg/mL. Thus, pretreatment with antioxidants can block oxalate induced increases in ceramide [197]. Antioxidant treatments also block oxalate-induced cell death [211], suggesting a role for oxidant stress in these responses.

5.2 Diminution of oxalate-induced renal tubular epithelial cell injury by aqueous extract of *Terminalia arjuna*

In recent years, evidence has emerged that the cells lining the renal tubules can have an active role in creating the conditions under which stones may develop. Since, these mechanisms are difficult to study *in vivo*, cultured renal tubular epithelial cells are a good option for the study of physiological and cell biological processes that are possibly linked to stone disease [280]. Since, it is known that hyperoxaluria is a major risk factor for CaOx nephrolithiasis, exposure to high levels of oxalate and/or COM crystals is injurious to renal epithelial cells and triggers serial responses related to stone formation. High level of oxalate causes a variety of changes in the renal epithelial cells, such as an increase in free radical production and a decrease in antioxidant status, followed by cell injury and cell death either by apoptosis or necrosis. These changes are significant predisposing factors for the facilitation of crystal adherence and retention [12, 196]. The duration of exposure and concentration of oxalate to which cells were exposed were selected based on results of earlier studies and the likelihood of occurrence inside the kidneys. The concentration of oxalate in the urine changes as it moves through the nephron and is 0.22 mM in normal excreted urine, 0.44 mM in

conditions of mild hyperoxaluria and 1.5 mM in primary hyperoxaluria. Various studies have used 0.1–4 mM oxalate [281] for exposure of renal epithelial cells *in vitro*.

In the *in vitro* cell culture study with NRK-52E and MDCK cells, *Terminalia arjuna* proved to have a protective effect towards the oxalate induced renal epithelial cell injury. When NRK-52E and MDCK cells were injured by exposure to 2 mM oxalate for 48 hours, the aqueous extract reduced the injury in a dose-dependent manner as verified by trypan blue exclusion and MTT viability assays. The adhesion and internalization of CaOx crystals to the cell surface of NRK-52E and MDCK was also studied in the absence and presence of aqueous extract of *Terminalia arjuna*. When the cells were exposed to oxalate, some of the CaOx crystals adhered tightly and some internalized into renal cells with subsequent detrimental effects to the cells [260]. These crystals caused cell damage and cell death either by apoptosis or necrosis which is evident by lesser number of cells. The aqueous extract reduced the injury to the renal cells by disrupting the interaction of CaOx crystals with the cells which was evident by increase in the number of viable cells. A study suggested that the adhesion of the radioactive CaOx crystals to the Madin Darby canine kidney (MDCK) cells was inhibited in the presence of the aqueous extract of *Herniaria hirsuta* in a concentration dependent manner [282].

We demonstrated that exposure to 2 mM oxalate for 48 hours caused induction of apoptosis leading to increased cell death. The morphological changes in cell nuclei were determined by fluorescence microscopy by staining cells with Hoechst 33258 dye. The cells treated with oxalate showed marked changes in morphology such as irregular shape, membrane blebbing, apoptotic bodies and condensed and fragmented chromatin. The aqueous extract exhibited cytoprotective potential which was apparent by larger number of viable cells with intact cellular membrane and fewer apoptotic bodies, showing reduced level of apoptosis. This was further confirmed by flow cytometry analysis using Annexin V/PI staining and Anti-Active Caspase-3 antibody staining. When renal cells were injured with oxalate and/or CaOx crystals, the number of cells that bind to annexinV increased, indicating that phosphatidylserine is exposed on the cell luminal surface. This observation is not only consistent with literature indicating that exposure to high concentration of oxalate results in the relocation of anionic phospholipids that are normally confined to the inner leaflet of the plasma membrane, but also firmly establishes the role of phosphatidylserine in crystal attachment. The

treatment with aqueous extract significantly reduced the number of apoptotic cells by disrupting the interaction of CaOx crystals with the cells.

In a recent study, it has also been shown that oxalate induces the exposure of phosphatidylserine on the surface of IMCD cells in culture and the exposure was temporal to the attachment of CaOx crystals to the cells [163]. Exposure to high levels of oxalate *in vitro* [196] and *in vivo* [203] leads to an increase in the abundance of apoptotic renal epithelial cells by a process involving increased oxidant stress [196]. ROS generated caused perturbations in mitochondrial function are often accompanied by an increase in mitochondrial permeability and a release of pro-apoptotic factors. These factors in turn trigger the activation of cellular caspases, serine proteases that have been linked to apoptotic cell death [204, 226]. Caspase-3 is a key protease that is activated during the early stages of apoptosis. We confirmed that when renal cells exposed to oxalate, the number of apoptotic cells significantly increased which were detected by anti-active caspase-3 antibody. The addition of aqueous extract reduced the number of apoptotic cells thus proving its ability to protect against oxalate induced renal cell injury. Our recent findings provide a possible explanation for these findings, e.g. oxalate actions at the cell membrane generate lipid signals that act on mitochondria to elicit an increase in oxidant stress and an increase in apoptotic death [197].

These data clearly indicate that oxalate and/or CaOx crystals are toxic to renal tubular epithelial cells. We postulated that the aqueous extract of *Terminalia arjuna* may contain substances that inhibit CaOx crystallization and crystal growth kinetics. Binding of the CaOx crystals to the renal epithelial surface and/or interaction of oxalate ions with calcium ions are blocked by active biomolecules of the plants [282]. Thus, *Terminalia arjuna* exhibited renoprotective role towards the oxalate induced cell injury. The mechanism of inhibition /reduction in the injury needs to be studied further. Hence, characterization of antilithiatic proteins from *Terminalia arjuna* can open new vistas for the therapeutic proteins present in *Terminalia arjuna* for the treatment and cure of urolithiasis.

5.3 Purification and characterization of antilithiatic proteins from *Terminalia arjuna*

Proteins were extracted from the bark of *Terminalia arjuna* to investigate the antilithiatic activity of plant proteins involved in the inhibition of calcium oxalate stone formation process. Protein estimation of the whole protein extract, separated into <3

kDa and >3 kDa fractions was done by Bradford assay. It was found that the protein concentration of the whole extract was 345.11 µg/mL, while that of <3 kDa and >3 kDa was 68.58 µg/mL and 273.44 µg/mL respectively. The bioactivity of whole protein extract, <3 kDa and >3 kDa fractions was investigated through CaOx crystallization and crystal growth assay systems. The whole extract possessed inhibitory activity against CaOx crystal nucleation, aggregation and growth kinetics. The <3 kDa fraction showed inhibitory activity towards CaOx crystal nucleation, aggregation and crystal growth assay system which was less than whole protein extract. The >3 kDa fraction showed inhibitory activity towards CaOx crystal nucleation, aggregation and growth assay system which was more than whole protein extract. SDS PAGE of >3 kDa proteins suggested that large number of proteins are present in the bark of *Terminalia arjuna*. A total of 16 bands were detected by silver staining. Based on the above observations, the >3 kDa fraction was thus chosen for further investigation of its bioactivity against oxalate injured NRK-52E and MDCK renal epithelial cells.

More than 3 kDa fraction exhibiting highest activity on CaOx crystal crystallization and growth assay was subjected to chromatography to purify proteins. The purification was performed systematically using anion exchange and molecular-sieve chromatography followed by bioactivity testing against CaOx crystal crystallization and growth assay and SDS-PAGE analysis after each purification step. After conducting anion exchange chromatography it was found that the eluted peaks P1, P2 and P3 exhibited inhibitory activity against CaOx crystal nucleation, aggregation and growth kinetics system. SDS-PAGE analysis showed presence of few bands in each peak. These peaks P1, P2 and P3 were then further purified individually by molecular-sieve chromatography, the purified proteins obtained from each peak were tested for their bioactivity against CaOx crystal crystallization and growth. The most potent fraction A1 obtained from purification of P1 possessed inhibitory activity against both CaOx crystal nucleation, aggregation and growth assay system. B1 and B2 were the most potent fractions obtained from purification of P2. B1 and B2 possessed inhibitory activity against CaOx crystal nucleation, aggregation and growth systems. The most potent fractions C1 obtained from purification of P3 possessed inhibitory activity against both CaOx crystal nucleation, aggregation and growth. The purified potent fractions A1, B1, B2 and C1 showed the presence of multiple bands when analyzed by 12% SDS-PAGE, but showed the presence of single bands of MW ~190 kDa, ~130 kDa, ~90 kDa and ~90 kDa respectively when further analyzed by 12% NATIVE-

PAGE. The homogeneity of the purified fractions was confirmed on RP-HPLC which showed a single peak. When the effect of these purified proteins was tested on oxalate injured NRK-52E and MDCK renal epithelial cells for their activity, it was found that A1, B1, B2 and C1 diminished the cellular injury caused by oxalate. Analysis of fractions A1, B1, B2 and C1 by MALDI-TOF-MS resulted in peptide mass fingerprint which when followed by database search on a MASCOT server matched significantly with Nuclear pore anchor, DEAD Box ATP-dependent RNA helicase 45, Lon protease homolog 1 and Heat shock protein 90-3. Our finding suggest presence of the above mentioned, as anionic proteins present in the bark of *Terminalia arjuna* with capability to modulate CaOx crystallization.

The identified Nuclear pore anchor (NUA) is an inhibitor protein which inhibits calcium oxalate crystal growth. It is a 237 kDa protein encoded by the gene AT1G79280.2 and is localized to the inner surface of the nuclear envelope and is a component of the nuclear pore. The nuclear pore complex (NPC) is a large multiprotein complex that is the sole gateway of macromolecular trafficking between the cytoplasm and the nucleus [266]. Nuclear membrane has oxalate binding at pH 7.4. The oxalate binding protein plays a vital role in the transport of oxalate. Oxalate transport across cellular membranes is mediated by anion-exchange transport proteins. Under physiological conditions, the NPC is an inhibitor of CaOx crystal nucleation, aggregation and growth. The expression of NPC increases in nephrolithiasis [267]. Also, it was observed that this protein has Lysine and glutamic acid rich region. Basic amino acid lysine is involved in oxalate binding which is evident by the fact that all oxalate binding proteins were sensitive to the transport inhibitor 4'-4' diisothiocyanostilbene-2-2 disulphonic acid (DIDS), which is known to interact with the lysine moiety of the proteins. Now there is an evidence of oxalate specific binding molecules with similar crystal growth modulating activity. They occur in the renal medulla and cortex and are differentially abundant in the subcellular organelles. All the oxalate binding proteins possess lysine in the active binding site. Lysine modification abolishes oxalate-binding activity [267]. In addition to lysine rich region, the presence of acidic polyglutamic acid residues may bind to calcium ions and thus, preventing the adhesion of COM crystals to the epithelial cell surface. Since COM and hydroxyapatite crystals adhered to negatively charged cell surface molecules by a process that could be inhibited by GAG, polyglutamic acid, polyaspartic acid, nephrocalcin, uropontin, and

citrate but not by THP. Anions that inhibited adhesion of crystals appeared to act on the crystal surface [149]. Hence, the exogenous supply of NUA protein may play a vital role in inhibiting the CaOx crystallization.

The second protein is a DEAD Box ATP-dependent RNA helicase 45. RNA helicases are prominent candidates as RNA chaperones because the energy derived from ATP hydrolysis can be used to promote the formation of optimal RNA structures via local RNA unwinding, or by mediating RNA–protein association/dissociation [268]. Helicases include six superfamilies (SF1 to SF6). The majority of known RNA helicases belong to the SF2 superfamily, which can be subdivided into several families including DEAD, DEAH and DExH/D. DEAD-box proteins comprise the largest and most extensively characterized family of RNA helicases. These proteins are characterized by a core of 350 to 400 amino acids containing seven to nine conserved amino acid motifs. In the DEAD-box proteins, motif II includes the sequence D-E-A-D (Asp-Glu-Ala-Asp), from which the name was derived [269]. Recent advances suggested some molecular mechanisms that enable DEAD/H RNA helicases to sustain cell survival, coordinate stress responses, and mediate cell death, by microbial pathogen-induced signaling cascades and stress granule formation triggered by various stress stimuli. Cell survival mechanism of Stress Granules is linked to reactive oxygen species (ROS) production. A recent study reported that Stress Granules harbor antioxidant activity, partly mediated by two Stress Granules components, G3BP1 (GTPase-activating protein SH3 domain binding protein 1) and USP10 (ubiquitin-specific protease 10). USP10 possesses an antioxidant activity. However, under steady-state conditions, its activity is suppressed by excess G3BP1. Upon stress, G3BP1 and USP10 cooperatively induce Stress Granules. Meanwhile, Stress Granules disrupt G3BP1-mediated inhibition against USP10, possibly by altering the conformation of USP10 and/or G3BP1, thereby uncovering the antioxidant activity of USP10 to reduce ROS production. The authors proposed that Stress Granules may act as rapidly inducible antioxidant machinery protecting cells from ROS-induced apoptosis [269]. The role of Stress Granules in controlling apoptosis could be linked to sequestration of apoptosis-promoting factors, suppression of ROS production and reprogramming of mRNA expression upon stress [269]. Since, this protein is rich in glutamic acid and aspartic acid amino acids, this protein may bind to calcium ions and thus, preventing the adhesion of COM crystals to the epithelial cell surface. Since COM and hydroxyapatite crystals adhered to negatively charged cell surface molecules by a

process that could be inhibited by GAG, polyglutamic acid, polyaspartic acid, nephrocalcin, uropontin, and citrate but not by THP. Anions that inhibited adhesion of crystals appeared to act on the crystal surface [149].

The third protein which is Lon protease homolog 1, is an enzyme that in humans is encoded by the *LONP1* gene. This gene encoded a mitochondrial matrix protein that is the subunit of a barrel-shaped homo-oligometric protein complex, the Lon protease. In mitochondrial matrix, a majority of damaged proteins are removed via proteolysis led by Lon protease, which is an essential mechanism for mitochondrial protein quality control (PQC). This protein contains Arg-Gly-Asp (RGD) tripeptide, a cell attachment sequence which binds to integrin [270]. Proteins that contain the RGD attachment site, together with the integrins that serve as receptors for them, constitute a major recognition system for cell adhesion [270]. RGD was originally identified as the sequence in fibronectin that engages *the fibronectin receptor*, integrin $\alpha 5\beta 1$. Although RGD peptides inhibit ligand binding to integrin with an RGD *recognition specificity* [283]. Adhesion of urinary crystals to the apical surface of renal tubular cells could be a critical step in the formation of kidney stones. The negative regulators of CaOx crystal uptake include heparin, transforming growth factor- $\beta 2$ (TGF- $\beta 2$), and the tetrapeptide arginine- lysine aspartic acid-serine (RGDS) [146]. Studies by Lieske and colleagues demonstrated an attenuation of crystal attachment in BSC-1 cells by treatment with arginine-glycine-aspartic acid-serine (RGDS, a tetrapeptide that bind to integrin), or by pretreatment with fibronectin, a connective tissue protein containing this peptide sequence [141, 146]. Crystal endocytosis can be inhibited by agents that interact with cell adhesion sites including RGDS, fibronectin and heparin. The degree of CaOx crystal deposition was inhibited by 60-80% in the cyclic RGD pretreated MDCK cells [146].

The fourth protein identified as Heat shock protein 90-3 is a molecular chaperone possessing antiapoptotic activity. Hsp90 is responsible for the refolding of denatured proteins as well as the three dimensional maturation and transport of more than 200 client proteins [271]. Heat-shock proteins (HSPs) are a highly conserved family of molecular chaperones, some of which are induced by sublethal cellular stresses, including temperature elevation, hypoxia and oxidative damage. Heat-shock proteins negatively regulate apoptosis [272]. Heat-shock protein 90 promotes cell survival by activation of NF- κ B. Tumour necrosis factor- α activation recruits and stabilises receptor interacting protein (RIP) at the TNF receptor-1 to maintain NF κ B activity. Key

signalling molecules, such as VEGF, induces antiapoptotic protein Bcl-2 expression and stimulates HSP90 association with Bcl-2 and Apaf-1 to inhibit apoptosis [273]. Also, Heat shock protein 90-3 has a glutamic rich region. The presence of acidic polyglutamic acid residues may bind to calcium ions and thus, preventing the adhesion of COM crystals to the epithelial cell surface. Since COM and hydroxyapatite crystals adhered to negatively charged cell surface molecules by a process that could be inhibited by GAG, polyglutamic acid, polyaspartic acid, nephrocalcin, uropontin, and citrate but not by THP. Anions that inhibited adhesion of crystals appeared to act on the crystal surface [149].

The working hypothesis that was confirmed in this study is that oxalate and/or COM crystals induce oxidative stress that contributes to renal tubular epithelial cell injury followed by death either by apoptosis and/or necrosis. Most of the cells underwent apoptotic cell death and few cells underwent necrotic cell death, may be in response to alterations in mitochondrial function that are characterized by initial increase in free-radical production, followed by a dissipation of the mitochondrial membrane potential and release of proapoptotic factors. Apoptosis of renal tubular cells in response to oxalate and CaOx crystals may play a significant role in CaOx urolithiasis. Apoptotic changes include exposure of annexin binding phosphatidylserine to the cell surface. Clusters of negatively charged head groups of phosphatidylserine attract calcium and can act as sites for attachment of calcific crystals to cell surfaces [284]. Such clusters on the surface of apoptotic bodies and membranous cellular degradation products can promote crystal nucleation [285]. Exposure of the basement membrane after detachment of cells or cellular debris, promoting calcium oxalate crystal adhesion and thus favoring crystal retention and lithogenesis, important in the pathogenesis of urolithiasis.

When renal epithelial cells are exposed to oxalate ions and CaOx crystals, there is an increase in expression of immediate early genes (*c-myc*, *Egr-1*, *c-jun* and *nur-77*) and production of several urinary macromolecules (Tamm-Horsfall protein, Osteopontin, Prothrombin fragment-1, Bikunin and inter- α -inhibitor, α_1 -Microglobulin, CD44, Calgranulin, Heparan sulfate, Osteonectin, Fibronectin, Matrix Gla Protein), which modulate the nucleation, growth, aggregation and retention of crystals in the kidneys [286]. The calcium binding property of these molecules enables them to interact with calcium containing crystals. Some of them, such as OPN, have specific domains to interact with cell membranes, which facilitate their immobilization and promotion of

crystal attachment. Almost all of the modulators are produced by the kidneys and excreted in the urine [222, 223].

In the present study Nuclear pore anchor, DEAD Box ATP-dependent RNA helicase 45, Lon protease homolog 1 and Heat shock protein 90-3 were identified as anionic inhibitors of CaOx crystallization from the bark of *Terminalia arjuna*. We observed that these anionic proteins possessed antilithiatic activity which was evident by the inhibition of CaOx crystallization and crystal growth kinetics. Also, these proteins protected the renal epithelial cells NRK-52E and MDCK from oxalate induced injury. Since, these proteins contain either polyglutamic acid, polyaspartic acid, polylysine rich regions and/or RGD sequence. Some of them also have anti-apoptotic activity and stimulates cell survival by inhibiting the proapoptotic factors.

Urinary Trefoil Factor 1 is an inhibitor of CaOx crystal growth. The 4C-terminal glutamic residues of TFF1 interact with calcium ions to prevent CaOx crystal growth [287]. The Fibronectin, a connective tissue protein containing this tripeptide sequence, is known as an inhibitor of CaOx [141, 146]. It has also been reported that FN protected against renal tubular cell injury caused by oxalate and COM crystals. The Osteopontin also containing this tripeptide sequence and rich in glutamic acid, arginine residues, inhibits nucleation, aggregation, growth and cellular attachment of CaOx crystals [288]. We postulated that exogenous supply of Nuclear pore anchor, DEAD Box ATP-dependent RNA helicase 45, Lon protease homolog 1 and Heat shock protein 90-3 proteins may play a vital role in inhibiting the CaOx crystallization and open new vistas to study therapeutic proteins from plants for the treatment of urolithiasis.

CHAPTER 6

CONCLUSION

Nephrolithiasis, or kidney stone, is the presence of renal calculi caused by a disruption in the balance between solubility and precipitation of salts in the urinary tract and in the kidneys. Kidney stones develop when urine becomes “supersaturated” with insoluble compounds containing calcium, oxalate (CaOx), and phosphate (CaP), resulting from dehydration or a genetic predisposition to over-excrete these ions in the urine. Approximately 70-80% of kidney stones are composed of calcium either in pure form or mixed with a majority of pure CaOx stones. CaOx kidney stones are found in two different varieties, COM or Whewellite, and COD or Weddellite. COM, the thermodynamically most stable form, is observed more frequently in clinical stones than COD and it has greater affinity for renal tubular cells, thus responsible for the formation of stones in kidney.

The problem of stone formation produces pain and obstruct the flow of urine as the stones formed are unable to travel through ureter. It also causes severe back ache (the worst pain known as colicky pain is produced in the lower back), bloody, cloudy, and smelly urine, sickness, urge for urination, burning sensation during urination, fever, chills etc., less urine volume, change in urinary pH, and infections [289]. Available standard pharmaceutical drugs used in preventing and curing renal calculi are not effective in all patients and may produce adverse effects on long term use [290]. The treatment of urolithiasis is mainly considered with the dissolution of existing stones and preventing the reoccurrence of stones. Standard pharmaceutical drugs used to prevent and cure urolithiasis are not effective in all cases. Surgical treatment causes some problems like long term renal damage, hypertension and reoccurrence of stones. Extracorporeal shock wave lithotripsy is considered as a revolution in treating renal stones, but this treatment also causes some problems like long term renal damage, hypertension and reoccurrence of stones [291].

Scientific studies are mostly focused on phytotherapy as it is proved to be vital in preventing reoccurrence of stones [292]. Herbal drugs are reported to be effective with no side effects. The drug for prevention of the disease or its reoccurrence is of great interest as no drug in clinical therapy is of satisfactory result [293]. Herbal agents act

by allowing spontaneous passage of small calculi in urine by increasing the urinary volume and pH. The herbs also act by regulating oxalate metabolism, by maintaining balance between inhibitors and promoters of crystallization, by producing anti-oxidant, anti-microbial, analgesic, anti-inflammatory activities [294]. Modern medicine are proved to target only one aspect of urolithiatic pathophysiology whereas herbal remedies have been shown to exert effectiveness at different stages of stone pathophysiology.

In the present research, *in vitro* antilithiatic properties of *Terminalia arjuna* have been evaluated. The bark of *Terminalia arjuna*, locally named as “Arjuna” in India, is known in Ayurveda for the treatment of cardiovascular disorders. Till date, various plant extracts have been studied to reduce the incidence of calcium stone deposition both *in vivo* and *in vitro* [282, 295, 296] but the identification of naturally occurring CaOx inhibitory biomolecules from plants was hampered in past by limitation in identification method. Initially *in vitro* antilithiatic potential of aqueous extract of *Terminalia arjuna* was assessed and its cytoprotective role was evaluated on oxalate induced renal tubular epithelial cell injury. Further, from the bark of *Terminalia arjuna* antilithiatic proteins were isolated and characterized. Finally, the efficacy of these purified proteins was evaluated on oxalate injured renal tubular epithelial cell lines NRK-52E and MDCK. The conclusions made from results obtained at every step of the study are summarized point wise.

1. *Terminalia arjuna* aqueous extract exhibited a concentration dependent inhibition of CaOx crystal nucleation and aggregation. The extract also inhibited the growth of CaOx crystals effectively. Moreover, the aqueous extract changed the morphology of COM crystals from hexagonal shape to spherical form with rounded edges which have weaker affinity for cell membranes than hexagonal COM crystals. Aqueous extract of *Terminalia arjuna* also possessed antilithiatic activity which may protect the renal cells from oxalate induced oxidative stress.
2. Reduction of oxalate induced injury by aqueous extracts of *Terminalia arjuna* was evaluated on NRK-52E and MDCK cells w.r.t. cell viability, CaOx crystal adherence and apoptotic changes wherein the extract of the plant protected renal cells from the injury caused by oxalate in a dose dependent manner. The antioxidant potential of *Terminalia arjuna* may contribute to the decrease in the free radicals

released due to injury caused by oxalate thus suggesting the protective potential of *Terminalia arjuna*. The plant may also coat the cells thereby blocking the interaction of the crystals with the renal epithelium thus preventing their adherence and further agglomeration.

3. Proteins were extracted from the bark of *Terminalia arjuna* and the bioactivity of whole protein extract, <3 kDa and >3 kDa fractions was investigated by CaOx crystallization and crystal growth kinetics assay systems. The whole extract possessed inhibitory activity against CaOx crystal nucleation, aggregation and growth kinetics. The <3 kDa fraction showed inhibitory activity towards CaOx crystal nucleation, aggregation and crystal growth assay system which was less than whole protein extract. The >3 kDa fraction showed inhibitory activity towards CaOx crystal nucleation, aggregation and growth assay system which was more than whole protein extract. SDS-PAGE of >3 kDa proteins suggests that plentiful proteins are present in the bark of *Terminalia arjuna*. A total of 16 bands were detected which are of both high and low molecular weight. Bioactivity of the >3 kDa fraction was investigated against oxalate injured NRK-52E and MDCK cells. >3 kDa fraction reflected inhibitory activity thereby leading to a decreased cell death in a dose dependent manner.
4. A total of four anionic inhibitors of CaOx crystallization were purified and identified from bark of *Terminalia arjuna* by bioactivity guided purification using anion exchange chromatography and molecular sieve chromatography along with validation with SDS-PAGE and Native-PAGE analysis. Finally, homogeneity of purified protein was confirmed by RP-HPLC. Further, the protein was in gel tryptic digested and characterized by MALDI-TOF-MS. Proteins were identified as Nuclear pore anchor, DEAD Box ATP-dependent RNA helicase 45, Lon protease homolog 1 and Heat shock protein 90-3 when m/z data obtained after MALDI-TOF-MS of digested protein was searched in MASCOT search engine. Proteins present in *Terminalia arjuna* were found to have an ability to inhibit CaOx crystallization and crystal growth it was observed that this inhibitory ability increased with successive protein purification steps.

5. Purified proteins from *Terminalia arjuna* also exhibited cytoprotective effect on NRK-52E and MDCK cells w.r.t. cell viability, CaOx crystal adherence to cells and apoptotic changes which was much more in comparison to the cytoprotective potential by aqueous extract. The protective potential of purified proteins from the bark of *Terminalia arjuna* in protecting renal cells from oxalate induced injury and cell death by apoptosis, thereby increasing the cell viability, was more profound even at a concentration of 10 µg/mL in comparison to 40 µg/mL of aqueous extract.

These results suggest that the purified proteins are inhibitors of CaOx crystallization and crystal growth and reduce the oxalate-induced renal cellular injury, thereby leading to enhanced cell viability. Polyanionic compounds coat the crystalline surface thus, inhibiting the binding of the crystals to the cells. The presence of specific cell attachment sequence also prevents the interaction and adhesion of CaOx crystals to the negatively charged head groups exposed on the cell surface as a result of oxalate exposure to renal cells. The purified proteins from the bark of *Terminalia arjuna* were anionic in nature due to presence of glutamic acid rich region and aspartic acid rich region and possessed cell attachment sequence (RGD, tripeptide that binds to integrins) thus, explaining the protective potential by increasing the cell viability, loss of CaOx crystal adherence to cells and reducing the induction of apoptosis in their presence. Our present results corroborate that this indigenous plant can be successfully used as an alternative treatment for urolithiasis. The data provides a rationale for the use of plant proteins as therapeutic agents to treat urolithiasis. The work presented here will open new vistas for protein therapeutics from medicinal plants for the management of urolithiasis.

REFERENCES

- [1] D. Prezioso, E. Illiano, G. Piccinocchi, C. Cricelli, R. Piccinocchi, A. Saita, C. Micheli and A. Trinchieri, “Urolithiasis in Italy: An epidemiology study”, *Archives of Italian Urology Andrology*, vol. 86, pp. 99-102, 2014.
- [2] M. Modlin, “A history of urinary stone”, *South African Medical Journal*, vol. 58, pp. 652–655, 1980.
- [3] N. Johri, B. Cooper, W. Robertson, S. Choong, D. Rickards and R. Unwin, “An update and practical guide to renal stone management”, *Nephron Clinical Practice*, vol. 116, pp. c159-c171, 2010.
- [4] S.A.H. Rizvi, S.A.A. Naqvi, Z. Hussain, A. Hashmi, M. Hussain, M.N. Zafar, H. Mehdi and R. Khalid, “The management of stone disease”, *BJU International*, vol. 89, pp. 62-68, 2002.
- [5] D. Spernat and J. Kourambas, “Urolithiasis - medical therapies”, *BJU International Supplements*, vol. 2, pp. 9-13, 2011.
- [6] M. Lopez and B. Hoppe, “History, epidemiology and regional diversities of urolithiasis”, *Pediatric Nephrology*, vol. 25, pp. 49 – 59, 2010.
- [7] C. Tandon, S.K. Singla, S.K. Singh and R.K. Jethi, “Urinary calculosis in man”, *Journal of Pan African Studies*, vol. 1, pp. 1-5, 1999.
- [8] G.E. Tasian and L. Copelovitch, “Evaluation and medical management of kidney stones in children”, *The Journal of Urology*, vol. 192, pp. 1329-1336, 2014.
- [9] M. Menon and M.I. Resnick, “Urinary lithiasis: etiology, diagnosis, and medical management”, In: *Campbell’s Urology*, 8th Ed., (Walsh PC, Retik AB, Vaughan ED, Jr, et al., eds.). Saunders, Philadelphia, PA, vol. 4, pp. 3229–3305, 2002.
- [10] S.R. Khan, “Role of Renal Epithelial Cells in the Initiation of Calcium Oxalate Stones”, *Nephron Experimental Nephrology*, vol. 98, pp. e55–e60, 2004.
- [11] B. Finlayson, S.R. Khan and R.L. Hackett, “Mechanisms of stone formation – an overview”, *Scanning Electron Microscopy*, vol. 3, pp. 1419–1425, 1984.

- [12] S.R. Khan, "Calcium oxalate crystal interaction with renal epithelium, mechanism of crystal adhesion and its impact on stone development", *Urological Research*, vol. 23, pp. 71-79, 1996.
- [13] J.M. Fasano and S.R. Khan, "Intratubular crystallization of calcium oxalate in the presence of membrane vesicles", *Kidney International*, vol. 59, pp. 169-178, 2001.
- [14] A. Choubey, A. Parasar, A. Choubey, D. Iyer, R.S. Pawar and U.K. Patil, "Potential of medicinal plants in kidney, gall and urinary stones", *International Journal of Drug Development & Research*, vol. 2, pp. 431-447, 2010.
- [15] C.Y.C. Pak, "Role of medical prevention", *Journal of Urology*, vol. 141, pp. 798-801, 1989.
- [16] R.K. Jethi, B. Duggal, R.S. Sahota, M. Gupta and I.B. Sofat, "Effect of the aqueous extract of an ayurvedic compound preparation on mineralization and demineralization reactions", *Indian Journal of Medical Research*, vol. 78, pp. 422-425, 1983.
- [17] D.J. Newman and G.M. Cragg, "Natural products as sources of new drugs over the last 25 years", *Journal of Natural Products*, vol. 70, pp. 461-477, 2007.
- [18] G. Scassellati-Sforzolini, L.M. Villarini, L.M. Moretti, L.M. Marcarelli, R. Pasquini, C. Fatigoni, L.S. Kaur, S. Kumar and I.S. Grover, "Antigenotoxic properties of *Terminalia arjuna* bark extracts", *Journal of Environmental Pathology Toxicology Oncology*, vol. 18, pp. 119-125, 1999.
- [19] H.Y. Cheng, C.C. Lin and T.C. Lin, "Antiherpes simplex virus type 2 activity of casuarinin from the bark of *Terminalia arjuna* Linn", *Antiviral Research*, vol. 55, pp. 447-455, 2002.
- [20] A. Nagpal, L.S. Meena, S. Kaur, I.S. Grover, R. Wadhwa and S.C. Kaul, "Growth of suppression human transformed cells by treatment with bark extracts from the medicinal plant *Terminalia arjuna*", *In Vitro Cellular & Development Biology Animal*, vol. 36, pp. 544-547, 2000.
- [21] A. Bharani, L.K. Ahirwar and N. Jain, "*Terminalia arjuna* reverses impaired endothelial function in chronic smokers", *Indian Heart Journal*, vol. 56, pp. 123-8, 2004.

- [22] A. Ali, G. Kaur, H. Hamid, T. Abdullah, M. Ali, M. Niwa and M.S. Alam, "Terminoside A, a new triterpene glycoside from the bark of *Terminalia arjuna* inhibits nitric oxide production in murine macrophages", *Journal of Asian Natural Products Research*, vol. 5, pp. 137-142, 2003.
- [23] P. Manna, M. Sinha and P.C. Sil, "Aqueous extract of *Terminalia arjuna* prevents carbon tetrachloride induced hepatic and renal disorders", *BMC Complementary and Alternative Medicine*, vol. 6, pp. 33-44, 2006.
- [24] C.H. Chen, T.Z. Liu, T.C. Kuo, F.J. Lu, Y.C. Chen, Y.W. Chang-Chien and C.C. Lin, "Casuarinin protects cultured MDCK cells from hydrogen peroxide-induced oxidative stress and DNA oxidative damage", *Planta Medica*, vol. 70, pp. 1022-1026, 2004.
- [25] W.G. Robertson, "Urinary calculi", (In: BEC Nordin, Need AG, Morros HA metabolic bone and stone disease, Churhill Livingstone, Newyork), pp. 249-311, 1993.
- [26] J.W. Sutherland, J.H. Parks and F.L. Coe, "Recurrence after a single renal stone in a community practice", *Mineral and Electrolyte Metabolism*, vol. 11, pp. 267-269, 1985.
- [27] R.J. Fakheri and D.S. Goldfarb, "Ambient Temperature as a Contributor to Kidney Stone Formation: Implications of Global Warming", *Kidney International*, vol. 79, pp. 1178-1185, 2011.
- [28] C. Kurts, U. Panzer, H.J. Anders and A.J. Rees, "The immune system and kidney disease: basic concepts and clinical implications", *Nature Reviews Immunology*, vol. 13, pp. 738-753, 2013.
- [29] H. Han, A.M. Segal, J.L. Seifter and J.T. Dwyer, "Nutritional management of kidney stones (Nephrolithiasis)", *Clinical Nutrition Research*, vol. 4, pp. 137-152, 2015.
- [30] J. Asplin, J. Parks, J. Lingeman, R. Kahnoski, H. Mardis, S. Lacey, D. Goldfarb, M. Grasso and F. Coe, "Supersaturation and stone composition in a network of dispersed treatment sites", *The Journal of Urology*, vol. 159, pp. 1821-1825, 1998.
- [31] J.R. Asplin, "Nephrolithiasis: introduction", *Seminars in Nephrology*, vol. 28, pp. 97-98, 2008.

- [32] F.L. Coe, H. Wise, J.H. Parks and J.R. Asplin, “Proportional reduction of urine supersaturation during nephrolithiasis treatment” *The Journal of Urology*, vol. 166, pp. 1247–1251, 2001.
- [33] L. Borghi, T. Meschi, U. Maggiore and B. Prati, “Dietary therapy in idiopathic nephrolithiasis”, *Nutritional Reviews*, vol. 64, pp. 301–312, 2006.
- [34] G.C. Curhan, “Dietary calcium, dietary protein, and kidney stone formation”, *Mineral and Electrolyte Metabolism*, vol. 23, pp. 261–264, 1997.
- [35] E.N. Taylor and G.C. Curhan, “Oxalate intake and the risk for nephrolithiasis”, *Journal of the American Society of Nephrology*, vol.18, pp. 2198–2204, 2007.
- [36] F.L. Coe, J.H. Parks and J.R. Asplin, “The pathogenesis and treatment of kidney stones”, *The New England Journal of Medicine*, vol. 327, pp. 1141–52, 1992.
- [37] J.H. Parks, E.M. Worcester, F.L. Coe, A.P. Evan and J.E. Lingerman, “Clinical implications of abundant calcium phosphate in routinely analyzed kidney stones”, *Kidney International*, vol. 66, pp. 777–85, 2004.
- [38] F.L. Coe, A. Evan and E. Worcester, “Pathophysiology-based treatment of idiopathic calcium kidney stones”, *Clinical Journal of the American Society of Nephrology*, vol. 6, pp. 2083–92, 2011.
- [39] A. Greischar, Y. Nakagawa and F.L. Coe, “Influence of urine pH and citrate concentration on the upper limit of metastability for calcium phosphate”, *The Journal of Urology*, vol. 169, pp. 867–70, 2003.
- [40] J.S. Rodman, “Struvite stones” *Nephron*, vol. 81, pp. 50–59, 1999.
- [41] R. Flannigan, W.H. Choy, B. Chew and D. Lange, “Renal struvite stones--pathogenesis, microbiology, and management strategies”, *Nature Reviews Urology*, vol. 11, pp. 333–341, 2014.
- [42] L. Romero-Vargas, A.J. Barba, C.D. Rosell and J.I.P. Pascual, “Staghorn stones in renal graft. Presentation on two cases report and review the bibliography”, *Archivos Espanoles de Urologia*, vol. 67, pp. 650–653, 2014.
- [43] A. Trinchieri, “Urinary calculi and infection”, *Urologia*, vol. 81, pp. 93–98, 2014.
- [44] J.E. Lingeman, Y.I. Siegel and B. Steele, “Metabolic evaluation of infected renal lithiasis: clinical relevance”, *Journal of Endourology*, vol. 9, pp. 51-54, 1995.

- [45] N.M. Maalouf, M.A. Cameron, O.W. Moe and K. Sakhaee, “Novel insights into the pathogenesis of uric acid nephrolithiasis”, *Current Opinion in Nephrology and Hypertension*, vol. 13, pp. 181–189, 2004.
- [46] K. Sakhaee, B. Adams-Huet, O.W. Moe and C.Y. Pak, “Pathophysiologic basis for normouricosuric uric acid nephrolithiasis”, *Kidney International*, vol. 62, pp. 971–9, 2002.
- [47] M.E. Moran, “Uric acid stone disease”, *Frontiers in Bioscience*, vol. 8, pp. s1339–s1355, 2003.
- [48] J.E. Kenny and D.S. Goldfarb, “Update on the pathophysiology and management of uric acid renal stones”, *Current Rheumatology Reports*, vol. 12, pp. 125–129, 2010.
- [49] P.M. Hall, “Nephrolithiasis: treatment, causes, and prevention”, *Cleveland Clinical Journal of Medicine*, vol. 76, pp. 583–91, 2009.
- [50] E.M. Worcester and F.L. Coe, “Nephrolithiasis”, *Primary Care*, vol. 35, pp. 369–91, 2008.
- [51] J.C. Crawhall, E.F. Scowen and R.W. Watts, “Effect of penicillamine on cystinuria”, *British Medical Journal*, vol. 1, pp. 588–90, 1963.
- [52] L.C. Herring, “Observations on the analysis of ten thousand urinary calculi”, *The Journal of Urology*, vol. 88, pp. 545–562, 1962.
- [53] N. Mandel, “Urinary tract calculi”, *Laboratory Medicine*, vol. 17, pp. 449–458, 1986.
- [54] R.A. Hiatt, L.G. Dales, G.D. Friedman and E.M. Hunkeler, “Frequency of urolithiasis in a prepaid medical care program”, *American Journal of Epidemiology*, vol. 115, pp. 255–265, 1982.
- [55] C.M. Johnson, D.M. Wilson, W.M. O’Fallon, R.S. Malek and L.T. Kurland, “Renal stone epidemiology: A 25 year study in Rochester, Minnesota”, *Kidney International*, vol. 16, pp. 624–631, 1979.
- [56] P.W. Baker, P. Coyle, R. Bais and A.M. Rofe, “Influence of season, age, and sex on renal stone formation in South Australia”, *The Medical Journal of Australia*, vol. 159, pp. 390–92, 1993.
- [57] J.M. Soucie, M.J. Thun, R.J. Coates, W. McClellan and H. Austin, “Demographic and geographic variability of kidney stones in the United States”, *Kidney International*, vol. 46, pp. 893–899, 1994.

- [58] K. Sternberg, S.P. Greenfield, P. Williot and J. Wan, “Pediatric stone disease: an evolving experience”, *The Journal of Urology*, vol. 174, pp. 1711–1714, 2005.
- [59] M. Hussain, M. Lal, S. Ahmed, N. Zafar, S.A. Naqvi and S.A.H. Rizvi, “Management of urinary calculi associated with renal failure”, *The Journal of the Pakistan Medical Association*, vol. 45, pp. 205-208, 1995.
- [60] G. Madhurambal, N. Prabha and S.P. Lakshmi, “Epidemiology of urinary stones”, *Research Journal of Pharmaceutical Biological and Chemical Sciences*, vol. 3, pp. 837-846, 2012.
- [61] Q.V. Nguyen, A. Kalin, U. Drouve, J.P. Casez and P. Jaeger, “Sensitivity to meat protein intake and hyperoxaluria in idiopathic calcium stone formers”, *Kidney International*, vol. 59, pp. 2273–81, 2001.
- [62] S.A. New, “Nutrition Society Medal lecture. The role of the skeleton in acid-base homeostasis”, *The Proceedings of the Nutrition Society*, vol. 61, pp. 151–164, 2002.
- [63] T.R. Arnett, “Extracellular pH regulates bone cell function”, *The Journal of Nutrition*, vol. 138, pp. 415S–418S, 2008.
- [64] S.A. Schuette, M.B. Zemel and H.M. Linkswiler, “Studies on the mechanism of protein-induced hypercalciuria in older men and women”, *The Journal of Nutrition*, vol. 110, pp. 305–315, 1980.
- [65] R. Pecoits-Filho, “Dietary protein intake and kidney disease in Western diet”, *Contributions to Nephrology*, vol. 155, pp. 102–112, 2007.
- [66] J. Lemann, “Relationship between urinary calcium and net acid excretion as determined by dietary protein and potassium: a review”, *Nephron*, vol. 81, pp. 18–25, 2007.
- [67] P.J. Osther, “Effect of acute acid loading on acid-base and calcium metabolism”, *Scandinavian Journal of Urology and Nephrology*, vol. 40, pp. 35–44, 2006.
- [68] A. Trinchieri, R. Lizzano, F. Marchesotti and G. Zanetti, “Effect of potential renal acid load of foods on urinary citrate excretion in calcium renal stone formers”, *Urological Research*, vol. 34, pp. 1–7, 2006.
- [69] R.P. Holmes, H.O. Goodman, L.J. Hart and D.G. Assimos, “Relationship of protein intake to urinary oxalate and glycolate excretion”, *Kidney International*, vol. 44, pp. 366–372, 1993.

- [70] M.R. Sowers, M. Jannausch, C. Wood, S.K. Pope, L.L. Lachance and B. Peterson, “Prevalence of renal stones in a population-based study with dietary calcium, oxalate, and medication exposures”, *American Journal of Epidemiology*, vol. 147, pp. 914–920, 1998.
- [71] G.C. Curhan, W.C. Willet, E.B. Rimm and M.J. Stampfer, “A prospective study of dietary calcium and other nutrients and the risk of symptomatic kidney stones”, *The New England Journal of Medicine*, vol. 328, pp. 833–838, 1993.
- [72] F.P. Cappuccio, R. Kalaitzidis, S. Duneclift and J.B. Eastwood, “Unraveling the links between calcium excretion, salt intake, hypertension, kidney stones, and bone metabolism”, *Journal of Nephrology*, vol. 13, pp. 169–177, 2000.
- [73] A.V. Osorio and U.S. Alon, “The relationship between urinary calcium, sodium, and potassium excretion and the role of potassium in treating idiopathic hypercalciuria”, *Pediatrics*, vol. 100, pp. 675–681, 1997.
- [74] P. Jaeger, P. Bonjour, B. Karlmark, B. Stanton, R.G. Kirk, T. Duplinsky and G. Giebisch, “Influence of acute potassium loading on renal phosphate transport in the rat kidney”, *The American Journal of Physiology*, vol. 245, pp. F601–F605, 1983.
- [75] G.C. Curhan, C.W. Willett and E.B. Rimm, “Prospective study of beverage use and the risk of kidney stones”, *American Journal of Epidemiology*, vol. 143, pp. 240–247, 1996.
- [76] T. Hirvonen, P. Pietinen, M. Virtanen, D. Albanes and J. Virtamo, “Nutrient intake and use of beverages and the risk of kidney stones among male smokers”, *American Journal of Epidemiology*, vol. 150, pp. 187–194, 1999.
- [77] B. Hess, “Tamm-Horsfall glycoprotein and calcium nephrolithiasis”, *Mineral and Electrolyte Metabolism*, vol. 20, pp. 393–398, 1994.
- [78] D.P. Simpson, “Citrate excretion: a window on renal metabolism”, *The American Journal of Physiology*, vol. 244, pp. F223–F234, 1983.
- [79] S. Abbagani, S.D. Gundimedda, S. Varre, D. Ponnala and H.P. Mundluru, “Kidney stone disease: Etiology and evaluation”, *International Journal of Applied Biology and Pharmaceutical Technology*, vol. 1, pp. 175–182, 2010.
- [80] F. Madore, M.J. Stampfer, W.C. Willett, F.E. Speizer and G.C. Curhan, “Nephrolithiasis and risk of hypertension in women”, *American Journal of Kidney Diseases*, vol. 32, pp. 802–807, 1998.

- [81] F. Madore, M.J. Stampfer, E.B. Rimm and G.C. Curhan, “Nephrolithiasis and risk of hypertension”, *American Journal of Hypertension*, vol. 11, pp. 46–53, 1998.
- [82] L. Borghi, T. Meschi, A. Guerra, A. Briganti, T. Schianchi, F. Allegri and A. Novarini, “Essential arterial hypertension and stone disease”, *Kidney International*, vol. 55, pp. 2397–2406, 1999.
- [83] F. Leonetti, B. Dussol, P. Berthezene, X. Thirion and Y. Berland, “Dietary and urinary risk factors for stones in idiopathic calcium stone formers compared to healthy subjects”, *Nephrology Dialysis Transplantation*, vol. 13, pp. 617–622, 1998.
- [84] G.C. Curhan, W.C. Willett, F.E. Speizer and M.J. Stampfer, “Twenty-four-hour urine chemistries and the risk of kidney stones among women and men”, *Kidney International*, vol. 59, pp. 2290–98, 2001.
- [85] M. Petrarulo, C. Vitale, P. Facchini, and M. Marangella, “Biochemical approach to diagnosis and differentiation of primary hyperoxalurias: an update”, *Journal of Nephrology*, vol. 11, pp. S23–S28, 1998.
- [86] T. Devuyst and Y. Pirson, “Genetics for hypercalciuric stone forming diseases”, *Kidney International*, vol. 72, pp. 1065–1072, 2007.
- [87] S. Park and M.S. Pearle, “Pathophysiology and Management of Calcium Stones”, *Urologic Clinics of North America*, vol. 34, pp. 323-334, 2007.
- [88] C.Y. Pak, M. Oata, E.C. Lawrence and W. Snyder, “The hypercalciurias. Causes, parathyroid functions, and diagnostic criteria”, *The Journal of Clinical Investigation*, vol. 54, pp. 387–400, 1974.
- [89] F.L. Coe, J.H. Parks and E.S. Moore, “Familial idiopathic hypercalciuria”, *The New England Journal of Medicine*, vol. 300, pp. 337–40, 1979.
- [90] C.Y.C. Pak, F. Britton, R. Peterson, D. Ward, C. Northcutt, N.A. Breslau, J. McGuire, K. Sakhaee, S. Bush, M. Nicar, D.A. Norman and P. Peters, “Ambulatory evaluation of nephrolithiasis: classification, clinical presentation and diagnostic criteria”, *The American Journal of Medicine*, vol. 69, pp. 19-30, 1980.
- [91] M. Cirillo, C. Ciacci, M. Laurenzi, M. Mellone, G. Mazzacca and N.G. De Santo, “Salt intake, urinary sodium, and Hypercalciuria”, *Mineral and Electrolyte Metabolism*, vol. 23, pp. 265–8, 1997.

- [92] J.M. Ruda, C.S. Hollenbeak and B.C.Jr. Stack, "A systematic review of the diagnosis and treatment of primary hyperparathyroidism from 1995 to 2003", *Otolaryngology Head and Neck Surgery*, vol. 132, pp. 359–72, 2005.
- [93] L.L. Hamm and K.S. Hering-Smith, "Pathophysiology of hypocitraturic nephrolithiasis", *Endocrinology and metabolism clinics of North America*, vol. 31, pp. 885–893, 2002.
- [94] C.Y. Pak, "Citrate and renal calculi: an update", *Mineral and Electrolyte Metabolism*, vol. 20, pp. 371–377, 1994.
- [95] C.M. Laing, A.M. Toye, G. Capasso and R.J. Unwin, "Renal tubular acidosis: developments in our understanding of the molecular basis", *The International Journal of Biochemistry and Cell Biology*, vol. 37, pp. 1151–61, 2005.
- [96] J. Amanzadeh, W.L. Gitomer, J.E. Zerwekh, P.A. Preisig, O.W. Moe, C.Y. Pak and M. Levi, "Effect of high protein diet on stone-forming propensity and bone loss in rats", *Kidney International*, vol. 64, pp. 2142–9, 2003.
- [97] K. Sakhaee, S. Nigam, P. Snell, M.C. Hsu and C.Y. Pak, "Assessment of the pathogenetic role of physical exercise in renal stone formation", *The Journal of Clinical Endocrinology and Metabolism*, vol. 65, pp. 974–9, 1987.
- [98] K. Mikami, K. Akakura, K. Takei, T. Ueda, K. Mizoguchi, M. Noda, M. Miyake and H. Ito, "Association of absence of intestinal oxalate degrading bacteria with urinary calcium oxalate stone formation", *International Journal of Urology*, vol. 10, pp. 293–296, 2003.
- [99] P.K. Grover, V.R. Marshall and R.L. Ryall, "Dissolved urate salts out calcium oxalate in undiluted human urine *in vitro*: implications for calcium oxalate stone genesis", *Chemistry and Biology*, vol. 10, pp. 271–8, 2003.
- [100] P.K. Grover and R.L. Ryall, "Urate and calcium oxalate stones: from repute to rhetoric to reality", *Mineral and Electrolyte Metabolism*, vol. 20, pp. 361–70, 1994.
- [101] C.Y. Pak, K. Holt and J.E. Zerwekh, "Attenuation by monosodium urate of the inhibitory effect of glycosaminoglycans on calcium oxalate nucleation", *Investigative Urology*, vol. 17, pp. 138–40, 1979.
- [102] F.L. Levy, B. Adams-Huet and C.Y. Pak, "Ambulatory evaluation of nephrolithiasis: an update of a 1980 protocol", *The American Journal of Medicines*, vol. 98, pp. 50–9, 1995.

- [103] S.R. Khan, P.N. Shevock and R. Hackett, "Urinary enzymes and CaOx urolithiasis", *The Journal of Urology*, vol. 142, pp. 846–849, 1989.
- [104] S.R. Khan, "Renal tubular damage/dysfunction: key to the formation of kidney stones", *Urological Research*, vol. 34, pp. 86-91, 2006.
- [105] D.J. Kok and S.E. Papapoulos, "Physicochemical considerations in the development and prevention of calcium oxalate urolithiasis", *Bone and Mineral*, vol. 20, pp. 1–15, 1993.
- [106] W.G. Robertson, M. Peacock and B.E. Nordin, "Activity products in stone-forming and non-stone forming urine", *Clinical Science*, vol. 34, pp. 579–94, 1968.
- [107] M. Marangella, P.G. Daniele, M. Ronzani, S. Sonega and F. Linari, "Urine saturation with calcium salts in normal subjects and idiopathic calcium stone formers *estimated* by an improved computer model system", *Urological Research*, vol. 13, pp. 189–193, 1985.
- [108] W.G. Robertson, D.S. Scurr and C.M. Bridge, "Factors influencing the crystallization of calcium oxalate in urine – critique", *Journal of Crystal Growth*, vol. 53, pp. 182–194, 1981.
- [109] I. Hojgaard and H.G. Tiselius, "Crystallization in the nephron", *Urological Research*, vol. 27, pp. 397-403, 1999.
- [110] D.J. Kok, "Intratubular crystallization events", *World Journal of Urology*, vol. 15, pp. 219-228, 1997.
- [111] N. Mandel, "Mechanism of stone formation", *Seminars in Nephrology*, vol. 16, pp. 364-374, 1996.
- [112] M. Tsujihata, "Mechanism of calcium oxalate renal stone formation and renal tubular cell injury", *International Journal of Urology*, vol. 15, pp. 115–120, 2008.
- [113] A.L. Boskey, "Current concepts of the physiology and biochemistry of calcification", *Clinical Orthopaedics and Related Research*, vol. 157, pp. 225–57, 1981.
- [114] B. Finlayson and F. Reid, "The expectation of free and fixed particles in urinary stone disease", *Investigative Urology*, vol. 15, pp. 442-448, 1978.
- [115] R. Hautmann and H. Osswald, "Concentration profiles of calcium and oxalate in urine, tubular fluid and renal tissue-some theoretical considerations", *The Journal of Urology*, vol. 129, pp. 433-436, 1983.

- [116] F. Coe and J.H. Parks, “Defenses of an unstable compromise: crystallization inhibitors and the kidney’s role in mineral regulation”, *Kidney International*, vol. 38, pp. 625-631, 1990.
- [117] S.R. Khan, P.N. Shevock and R.L. Hackett, “Membrane-associated crystallization of calcium oxalate”, *Calcified Tissue International*, vol. 46, pp. 116–120, 1990.
- [118] S.R. Khan, P.A. Glenton, R. Backov and D.R. Talham, “Presence of lipids in urine, crystals and stones: implications for the formation of kidney stones”, *Kidney International*, vol. 62, pp. 2062-2072, 2002.
- [119] J.C. Lieske and S. Deganello, “Nucleation, adhesion, and internalization of calcium-containing urinary crystals by renal cells”, *Journal of the American Society of Nephrology*, vol. 10, pp. S422-S429, 1999.
- [120] W. Wu, D.E. Gerard and G.H. Nancollas, “Nucleation at surfaces: the importance of interfacial energy”, *Journal of the American Society of Nephrology*, vol. 10, pp. S355-S358, 1999.
- [121] M.D. McKee, A. Nanci and S.R. Khan, “Ultrastructural immunodetection of osteopontin and osteocalcin as major matrix components of renal calculi”, *Journal of Bone and Mineral Research*, vol. 10, pp. 1913-1929, 1995.
- [122] F. Atmani, P.A. Glenton and S.R. Khan, “Identification of proteins extracted from calcium oxalate and calcium phosphate crystals induced in the urine of healthy and stone forming subjects”, *Urological Research*, vol. 26, pp. 201-207, 1998.
- [123] T. Tawada, K. Fujita, T. Sakakura, T. Shibutani, T. Nagata, M. Iguchi and K. Kohri, “Distribution of osteopontin and calprotectin as matrix protein in calcium-containing stone”, *Urological Research*, vol. 27, pp. 238-242, 1999.
- [124] R.L. Ryall, D.E. Fleming, P.K. Grover, M. Chauvet, C.J. Dean and V.R. Marshall, “The hole truth: intracrystalline proteins and calcium oxalate kidney stones”, *Molecular Urology*, vol. 4, pp. 391-402, 2000.
- [125] D.J. Kok, “Crystallization and stone formation inside the nephron”, *Scanning Microscopy*, vol. 10, pp. 484-486, 1996.
- [126] D.J. Kok, “Clinical implications of physicochemistry of stone formation”, *Endocrinology and Metabolism Clinics of North America*, vol. 31, pp. 855-867, 2002.

- [127] Y. Nakagawa, M. Ahmed, S.L. Hall, S. Deganello and F.L. Coe, "Isolation from human calcium oxalate renal stones of nephrocalcin, a glycoprotein inhibitor of calcium oxalate crystal growth. Evidence that nephrocalcin from patients with calcium oxalate nephrolithiasis is deficient in g-carboxyglutamic acid", *The Journal of Clinical Investigation*, vol. 79, pp. 1782-1787, 1987.
- [128] Y. Eguchi, M. Inoue, S. Iida, K. Matsuoka and S. Noda, "Heparan sulfate (HS)/heparan sulfate proteoglycan (HSPG) and bikunin are up-regulated during calcium oxalate nephrolithiasis in rat kidney", *The Kurume Medical Journal*, vol. 49, pp. 99-107, 2002.
- [129] F. Atmani, P.A. Glenton and S.R. Khan, "Role of inter-alpha- inhibitor and its related proteins in experimentally induced calcium oxalate urolithiasis. Localization of proteins and expression of bikunin gene in the rat kidney", *Urological Research*, vol. 27, pp. 63-67, 1999.
- [130] R.L. Ryall, "Glycosaminoglycans, proteins, and stone formation: adult themes and child's play", *Pediatric Nephrology*, vol. 10, pp. 656-666, 1996.
- [131] P.K. Grover, S.C. Dogra, B.P. Davidson, A.M. Stapleton and R.L. Ryall, "The prothrombin gene is expressed in the rat kidney: implications for urolithiasis research", *European Journal of Biochemistry*, vol. 267, pp. 61-67, 2000.
- [132] T. Umekawa, M. Iguchi, E. Konya, T. Yamate, N. Amasaki and T. Kurita, "Localization and inhibitory activity of alpha(2)HS-glycoprotein in the kidney", *Urological Research*, vol. 27, pp. 315-318, 1999.
- [133] V.A. Garten and R.B. Head, "Homogeneous nucleation and phenomenon of crystalloluminescence", *Philosophical Magazine*, vol. 14, pp. 1243-1253, 1966.
- [134] W.G. Robertson, M. Peacock and B.E. Nordin, "Calcium crystalluria in recurrent renal-stone formers", *Lancet*, vol. 2, pp. 21-24, 1969.
- [135] D.J. Kok, S.E. Papapoulos and O.L. Bijvoet, "Crystal agglomeration is a major element in calcium oxalate urinary stone formation", *Kidney International*, vol. 37, pp. 51-56, 1990.
- [136] R.K. Low and M.L. Stoller, "Endoscopic mapping of renal papillae for Randall's plaques in patients with urinary stone disease", *The Journal of Urology*, vol. 158, pp. 2062-2064, 1997.

- [137] C.L. Parsons, S.G. Mulholland and H. Anwar, "Antibacterial activity of bladder surface mucin duplicated by exogenous glycosaminoglycan (heparin)", *Infection and Immunity*, vol. 24, pp. 552-557, 1979.
- [138] M. Asselman and C.F. Verkoelen, "Crystal-cell interaction in the pathogenesis of kidney stone disease", *Current Opinion in Urology*, vol. 12, pp. 271-276, 2002.
- [139] M.W. Bigelow, J.H. Wiessner, J.G. Kleinman and N.S. Mandel, "Surface exposure of phosphatidylserine increases calcium oxalate crystal attachment to IMCD cells", *The American Journal of Physiology*, vol. 272, pp. F55-F62, 1997.
- [140] J.H. Wiessner, A.T. Hasegawa, L.Y. Hung, G.S. Mandel and N.S. Mandel, "Mechanisms of calcium oxalate crystal attachment to injured renal collecting duct cells", *Kidney International*, vol. 59, pp. 637-644, 2001.
- [141] J.C. Lieske, R. Leonard, H. Swift and F.G. Toback, "Adhesion of calcium oxalate monohydrate crystals to anionic sites on the surface of renal epithelial cells", *The American Journal of Physiology*, vol. 270, pp. F192-F199, 1996.
- [142] K. Kohri, M. Kodama, Y. Ishikawa, Y. Katayama, H. Matsuda, M. Imanishi, M. Takada, Y. Katoh, K. Kataoka and T. Akiyama, "Immunofluorescent study on the inter action between collagen and calcium oxalate crystals in the renal tubules", *European Urology*, vol. 19, pp. 249-252, 1991.
- [143] T. Yamate, K. Kohri, T. Umekawa, E. Konya, Y. Ishikawa, M. Iguchi and T. Kurita, "Interaction between osteopontin on madin darby canine kidney cell membrane and calcium oxalate crystal", *Urologia Internationalis*, vol. 62, pp. 81-86, 1999.
- [144] J.C. Lieske and F.G. Toback, "Interaction of urinary crystals with renal epithelial cells in the pathogenesis of nephrolithiasis", *Seminars in Nephrology*, vol. 16, pp. 458-473, 1996.
- [145] J.C. Lieske, B.H. Spargo and F.G. Toback, "Endocytosis of calcium oxalate crystals and proliferation of renal tubular epithelial cells in a patient with type 1 primary hyperoxaluria", *The Journal Urology*, vol. 148, pp. 1517-1519, 1992.

- [146] J.C. Lieske and F.G. Toback, "Regulation of renal epithelial cell endocytosis of calcium oxalate monohydrate crystals", *The American Journal of Physiology*, vol. 264, pp. F800-F807, 1993.
- [147] J.C. Lieske, M.M. Walsh-Reitz and F.G. Toback, "Calcium oxalate monohydrate crystals are endocytosed by renal epithelial cells and induce proliferation", *The American Journal of Physiology*, vol. 262, pp. F622-F630, 1992.
- [148] D.J. Kok and S.R. Khan, "Calcium oxalate nephrolithiasis, a free or fixed particle disease", *Kidney International*, vol. 46, pp. 847-854, 1994.
- [149] J.C. Lieske, R. Leonard and F.G. Toback, "Adhesion of calcium oxalate monohydrate crystals to renal epithelial cells is inhibited by specific anions", *The American Journal of Physiology*, vol. 268, pp. F604-F612, 1995.
- [150] J.C. Lieske, B.H. Spargo and F.G. Toback, "Endocytosis of calcium oxalate crystals and proliferation of renal epithelial cells in a patient with type 1 primary hyperoxaluria", *The Journal of Urology*, vol. 148, pp. 1517-1519, 1992.
- [151] A. Saxon, G.J. Bruschi, J.P. Merrill, V. Franco and R.E. Wilson, "Renal transplantation in primary hyperoxaluria", *Archives of Internal Medicine*, vol. 133, pp. 464-467, 1974.
- [152] I. Mandell, E. Krauss and J.C. Millan, "Oxalate-induced acute renal failure in Crohn's disease", *The American Journal of Medicine*, vol. 69, pp. 628-632, 1980.
- [153] R. Wharton, V. D'Agati, A.M. Magun, R. Whitlock, C.L. Kunis and G.B. Appel, "Acute deterioration of renal function associated with enteric Hyperoxaluria", *Clinical Nephrology*, vol. 34, pp. 116-121, 1990.
- [154] D.R. Gelbert, L.L. Brewer, L.F. Fajardo and A.B. Weinstein, "Oxalosis and chronic renal failure after intestinal bypass", *Archives of Internal Medicine*, vol. 137, pp. 239-243, 1977.
- [155] R.L. Hackett, P.N. Shevock and S.R. Khan, "Alterations in MDCK and LLC-PK1 cells exposed to Ox and CaOx monohydrate crystals", *Scanning Microscopy*, vol. 9, pp. 587-596, 1996.
- [156] S.R. Khan, K.J. Byer, S. Thamilselvan, R.L. Hackett, W.T. McCormack, N.A. Benson, K.L. Vaughn and G.W. Erdos, "Crystal-cell interaction and

- apoptosis in oxalate-associated injury of renal epithelial cells”, *Journal of the American Society of Nephrology*, vol. 10, pp. S457–S463, 1999.
- [157] J.M. Fasano and S.R. Khan, “Intratubular crystallization of calcium oxalate in the presence of membrane vesicles: an *in vitro* study”, *Kidney International*, vol. 59, pp. 169–178, 2001.
- [158] L.C. Cao, J. Jonassen, T.W. Honeyman and C. Scheid, “Oxalate-induced redistribution of phosphatidylserine in renal epithelial cells: Implications for kidney stone disease”, *American Journal of Nephrology*, vol. 21, pp. 69–77, 2001.
- [159] A.J. Verkleij and J.A. Post, “Membrane phospholipid asymmetry and signal transduction”, *The Journal of Membrane Biology*, vol. 178, pp. 1-10, 2000.
- [160] G.R. Sambrano and D. Steinberg, “Recognition of oxidatively damaged and apoptotic cells by an oxidized low density lipoprotein receptor on mouse peritoneal macrophages: role of membrane phosphatidylserine”, *Proceedings of the National Academy of Sciences of the United States of America*, vol. 92, pp. 1396-1400, 1995.
- [161] R.J. Riese, N.S. Mandel, J.H. Wiessner, G.S. Mandel, C.G. Becker and J.G. Kleinman, “Cell polarity and calcium oxalate crystal adherence to cultured collecting duct cells”, *The American Journal of Physiology*, vol. 262, pp. F177-F184, 1992.
- [162] N. Mandel, “Crystal-membrane interaction in kidney stone disease”, *Journal of the American Society of Nephrology*, vol. 5, pp. S37-S45, 1994.
- [163] J.H. Wiessner, A.T. Hasegawa, L.Y. Hung and N.S. Mandel, “Oxalate-induced exposure of phosphatidylserine on the surface of renal epithelial cells in culture”, *Journal of the American Society of Nephrology*, vol. 10, pp. S441-S445, 1999.
- [164] J.C. Lieske, R. Leonard and F.G. Toback, “Adhesion of calcium oxalate monohydrate crystals to renal epithelial cells is inhibited by specific anions”, *The American Journal of Physiology*, vol. 268, pp. F604–F612, 1995.
- [165] J.C. Lieske, S. Deganello and T.G. Toback, “Crystal–cell interactions and kidney stone formation”, *Nephron*, vol. 81, pp. 8–17, 1999.
- [166] C.F. Verkoelen, B.G. van der Boom, A.B. Houtsmuller, F.H. Schroder and J.C. Romijn, “Increased calcium oxalate monohydrate crystal binding to

- injured renal tubular epithelial cells in culture”, *The American Journal of Physiology*, vol. 274, pp. F958-F965, 1998.
- [167] C.F. Verkoelen, B.G. Van Der Boom and J.C. Romijn, “Identification of hyaluronan as a crystal-binding molecule at the surface of migrating and proliferating MDCK cells”, *Kidney International*, vol. 58, 1045-1054, 2000.
- [168] A. Verhulst, M. Asselman, V.P. Persy, M.S. Schepers, M.F. Helbert, C.F. Verkoelen and M.E. de Broe, “Crystal retention capacity of cells in the human nephron: involvement of CD44 and its ligands hyaluronic acid and osteopontin in the transition of a crystal binding into a nonadherent epithelium”, *Journal of the American Society of Nephrology*, vol. 13, pp. 107-115, 2003.
- [169] H. Koul, L. Kenington, T. Honeyman, J. Jonassen, M. Menon and C.R. Scheid, “Activation of the cmyc gene mediates the mitogenic effects of Ox in LLC-PK1 cells, a line of renal epithelial cells”, *Kidney International*, vol. 50, pp. 1525–1530, 1996.
- [170] S.R. Khan, “Calcium oxalate crystal interaction with renal tubular epithelium, mechanism of crystal adhesion and its impact on stone development”, *Urological Research*, vol. 23, pp. 71-79, 1995.
- [171] A. Goswami, P.C. Singhal, J.D. Wagner, M. Urivetzky, E. Valderrama and A.D. Smith, “Matrix modulates uptake of calcium oxalate crystals and cell growth of renal epithelial cells”, *The Journal of Urology*, vol. 153, pp. 206-211, 1995.
- [172] Y. Kohjimoto, S. Ebisuno, M. Tamura and T. Ohkawa, “Interactions between calcium oxalate monohydrate crystals and Madin-Darby canine kidney cells endocytosis and cell proliferation”, *Urological Research*, vol. 24, pp. 193-199, 1996.
- [173] A.H. Campos and N. Schor, “Mechanisms involved in calcium oxalate endocytosis by Madin-Darby canine kidney cells”, *Brazilian Journal of Medical Biological Research*, vol. 33, pp. 111-118, 2000.
- [174] N. Mandel and R. Riese, “Crystal-cell interactions: Crystal binding to rat renal papillary tip collecting duct cells in culture”, *American Journal of Kidney Diseases*, vol. 17, pp. 403–406, 1991.

- [175] J.C. Lieske, R. Norris, H. Swift and G. Toback, “Adhesion, internalization and metabolism of calcium oxalate monohydrate crystals by renal epithelial cells”, *Kidney International*, vol. 52, pp. 1291–1301, 1997.
- [176] A. Verhulst, M. Asselman, V.P. Persy, M.S. Schepers, M.F. Helbert, C.F. Verkoelen and M.E. de Broe, “Crystal retention capacity of cells in the human nephron: Involvement of CD 44 and its ligands hyaluronic acid and osteopontin in the transition to a crystal binding into a non-adherent epithelium”, *Journal of the American Society of Nephrology*, vol. 14, pp. 107–115, 2003.
- [177] T. Yamate, K. Kohri, T. Umekawa, Y. Ishikawa, M. Iguchi and T. Kurita, “Interaction between osteopontin on Madin-Darby canine kidney cell membrane and calcium oxalate crystals”, *Urologia Internationalis*, vol. 62, pp. 81–86, 1999.
- [178] J.H. Wiessner, A.T. Hasegawa, L.Y. Hung and N.S. Mandel, “Oxalate-induced exposure of PS on surface of renal epithelial cells in culture”, *Journal of the American Society of Nephrology*, vol. 10, pp. S441–S445, 1999.
- [179] J.C. Lieske and S. Deganello, “Nucleation, adhesion, and internalization of calcium containing urinary crystals by renal cells”, *Journal of the American Society of Nephrology*, vol. 10, pp. S422–S429, 1999.
- [180] R. deWater, C. Noordermeer, A.B. Houitsmuller, A.L. Nigg, T. Stinjen, F.H. Schroeder and D.J. Kok, “Role of macrophages in nephrolithiasis in rats: An analysis of the renal interstitium”, *American Journal of Kidney Disease*, vol. 36, pp. 615–625, 2000.
- [181] S. Katsuma, S. Shijima, A. Hirasawa, K. Takagaki, Y. Kaminishi, M. Koba, Y. Hagidai, M. Murai, T. Ohgi and G. Tsujimoto, “Global analysis of differentially expressed genes during progression of calcium oxalate nephrolithiasis”, *Biochemical and Biophysical Research Communications*, vol. 296, pp. 544–552, 2002.
- [182] T. Umekawa, N. Chegini and S.R. Khan, “Oxalate ions and calcium oxalate crystals stimulate MCP1 expression by renal epithelial cells”, *Kidney International*, vol. 61, pp. 105–112, 2002.
- [183] J.E. Toblli, L. Ferder, I. Stella, E.M. De Cavanaugh, M. Angerosa and F. Inserra, “Effects of angiotensin II subtype 1 receptor blockade by losartan on

- tubulointerstitial lesions caused by hyperoxaluria”, *The Journal of Urology*, 168, 1550–1555, 2002 .
- [184] J.E. Toblli, I. Stella, E. Cavanagh, M. Angerosa, F. Inserra and L. Feder, “Enalapril prevents tubulointerstitial lesions by hyperoxaluria”, *Hypertension*, vol. 33, pp. 225–231, 1999.
- [185] E.A. Dennis, “The growing phospholipase A2 superfamily of signal transduction enzymes”, *Trends in Biochemical Sciences*, vol. 22, pp. 1-2, 1997.
- [186] R.G. Schnellman, X. Yang and J.B. Carrick, “Arachidonic acid release in renal proximal tubule cell injuries and death”, *Journal of Biochemical Toxicology*, vol. 9, pp. 211-217, 1994.
- [187] C.L. Edelstein, H. Ling and R.W. Schrier, “The nature of renal cell injury”, *Kidney International*, vol. 51, pp. 1341-1351, 1997.
- [188] S.J. Shankland, “New insights into the pathogenesis of membranous nephropathy”, *Kidney International*, vol. 57, pp. 1204-1205, 2000.
- [189] B. Baggio and G. Gambaro, “Abnormal arachidonic acid content of membrane phospholipids -- the unifying hypothesis for the genesis of hypercalciuria and hyperoxaluria in idiopathic calcium nephrolithiasis”, *Nephrology Dialysis Transplantation*, 14, 553-555, 1999.
- [190] B. Baggio, A. Budakovic, M.A. Nassuato, G. Vezzoli, E. Manzato, G. Luisetto and M. Zaninotto, “Plasma phospholipid arachidonic acid content and calcium metabolism in idiopathic calcium nephrolithiasis”, *Kidney International*, vol. 58, pp. 1278-1284, 2000.
- [191] Y. Kohjimoto, L. Kennington, C.R. Scheid and T.W. Honeyman, “Role of phospholipase A2 in the cytotoxic effects of oxalate in cultured renal epithelial cells”, *Kidney International*, vol. 56, pp. 1432- 1441, 1999.
- [192] Y. Kohjimoto, T.W. Honeyman, J. Jonassen, K. Gravel, L. Kennington and C.R. Scheid, “Phospholipase A2 mediates immediate early genes in cultured renal epithelial cells: possible role of lysophospholipid”, *Kidney International*, vol. 58, pp. 638-646, 2000.
- [193] R.J. Dixon and N.J. Brunskill, “Lysophosphatidic acid induced proliferation in opossum kidney proximal tubular cells: role of PI3-kinase and ERK”, *Kidney International*, vol. 56, pp. 2064-2075, 1999.

- [194] Y. Chen, S. Morimoto, S. Kitano, E. Koh, K. Fukuo, B. Jiang, S. Chen, O. Yasuda, A. Hirotsu and T. Ogihara, "Lysophosphatidylcholine causes Ca²⁺ influx, enhanced DNA synthesis and cytotoxicity in cultured vascular smooth muscle cells", *Atherosclerosis*, vol. 112, pp. 69-76, 1995.
- [195] J.S. Levine, J.S. Koh, V. Triaca and W. Lieberthal, "Lysophosphatidic acid: a novel growth and survival factor for renal proximal tubular cells", *The American Journal of Physiology*, vol. 273, pp. F575-F585, 1997.
- [196] C. Miller, L. Kennington, R. Cooney, T. Honeyman, Y. Kohjimoto, L.C. Cao, J. Pullman, J. Jonassen and C.R. Scheid, "Oxalate toxicity in renal epithelial cells: characteristics of apoptosis and necrosis", *Toxicology and Applied Pharmacology*, vol. 162, pp. 132-141, 2000.
- [197] L.C. Cao, T. Honeyman, J. Jonassen and C. Scheid, "Oxalate-induced ceramide accumulation in Madin-Darby canine kidney and LLC-PK1 cells", *Kidney International*, vol. 57, pp. 2403-2411, 2000.
- [198] R.N. Kolesnick and M. Kronke, "Regulation of ceramide production and apoptosis", *Annual Review of Physiology*, vol. 60, pp. 643-665, 1998.
- [199] S. Jayadev, C.M. Linardic and Y.A. Hannun, "Identification of arachidonic acid as a mediator of sphingomyelin hydrolysis in response to tumor necrosis factor alpha", *The Journal of Biological Chemistry*, vol. 269, pp. 5757-5763, 1994.
- [200] L. Riboni, P. Viani, R. Bassi, A. Prinetti and G. Tettamanti, "The role of sphingolipids in the process of signal transduction", *Progress in Lipid Research*, vol. 36, pp. 153-195, 1997.
- [201] T. Hashizume, K. Kitatani, T. Kageura, M. Hayama, S. Akiba and T. Sato, "Ceramide enhances susceptibility of membrane phospholipids to phospholipase A2 through modification of lipid organization in platelet membranes", *Biological and Pharmaceutical Bulletin*, vol. 22, pp. 1275-1278, 1999.
- [202] Y.A. Hannun, "The sphingomyelin cycle and the second messenger function of ceramide", *The Journal of Biological Chemistry*, vol. 269, pp. 3125-3128, 1994.
- [203] K. Sarica, F. Yagci, K. Bakir, A. Erbagci, S. Erturhan and R. Ucak, "Renal tubular injury induced by hyperoxaluria: evaluation of apoptotic changes", *Urological Research*, vol. 29, pp. 34-37, 2001.

- [204] M. Crompton, "The mitochondrial permeability transition pore and its role in cell death", *The Biochemical Journal*, vol. 341, pp. 233-249, 1999.
- [205] A. Muthukumar and R. Selvam, "Renal injury mediated calcium oxalate nephrolithiasis: role of lipid peroxidation", *Renal Failure*, vol. 19, pp. 401-408, 1997.
- [206] S. Thamilselvan, R.L. Hackett and S.R. Khan, "Lipid peroxidation in ethylene glycol induced hyperoxaluria and calcium oxalate nephrolithiasis", *The Journal of Urology*, vol. 157, pp. 1059-1063, 1997.
- [207] R. Selvam, "Calcium oxalate stone disease: role of lipid peroxidation and antioxidants", *Urological Research*, vol. 30, pp. 35-47, 2002.
- [208] A. Muthukumar and R. Selvam, "Role of glutathione on renal mitochondrial status in hyperoxaluria", *Molecular and Cellular Biochemistry*, vol. 185, pp. 77-84, 1998.
- [209] H.S. Huang, M.C. Ma, J. Chen and C.F. Chen, "Changes in the oxidant-antioxidant balance in the kidney of rats with nephrolithiasis induced by ethylene glycol", *The Journal Urology*, vol. 167, pp. 2584- 2593, 2002.
- [210] F.D. Khand, M.P. Gordge, W.G. Robertson, A.A. Noronha-Dutra and J.S. Hothersall, "Mitochondrial superoxide production during oxalate-mediated oxidative stress in renal epithelial cells", *Free Radical Biology and Medicine*, vol. 32, pp. 1339-1350, 2002.
- [211] S. Thamilselvan, K.J. Byer, R.L. Hackett and S.R. Khan, "Free radical scavengers, catalase and superoxide dismutase provide protection from oxalate-associated injury to LLC-PK1 and MDCK cells", *The Journal Urology*, vol. 164, pp. 224-229, 2000.
- [212] S. Thamilselvan, S.R. Khan and M. Menon, "Oxalate and calcium oxalate mediated free radical toxicity in renal epithelial cells: effect of antioxidants", *Urological Research*, vol. 31, pp. 3-9, 2002.
- [213] N. Hsieh, C.H. Shih, H.Y. Chen, M.C. Wu, W.C. Chen and C.W. Li, "Effects of Tamm-Horsfall protein on the protection of MCDK cells from oxalate induced free radical injury", *Urological Research*, vol. 31, pp. 10-16, 2003.
- [214] P.P. Ruvolo, X. Deng, B.K. Carr and W.S. May, "A functional role for mitochondrial protein kinase Calpha in Bcl2 phosphorylation and suppression of apoptosis", *The Journal of Biological Chemistry*, vol. 273, pp. 25436-25442, 1998.

- [215] T. Strzelecki, B.R. McGraw, C.R. Scheid and M. Menon, "Effect of oxalate on function of kidney mitochondria", *The Journal of Urology*, vol. 141, pp. 423-427, 1989.
- [216] H. Koul, L. Kennington, G. Nair, T. Honeyman, M. Menon and C. Scheid, "Oxalate-induced initiation of DNA synthesis in LLC-PK1 cells, a line of renal epithelial cells", *Biochemical and Biophysical Research Communications*, vol. 205, pp. 1632-1637, 1994.
- [217] C.R. Scheid, H. Koul, W.A. Hill, J. Lubner-Narod, J. Jonassen, T. Honeyman, L. Kennington, R. Kohli, J. Hodapp, P. Ayvazian and M. Menon, "Oxalate toxicity in LLC-PK1 cells, a line of renal epithelial cells", *The Journal of Urology*, vol. 155, pp. 1112-1116, 1996.
- [218] R.L. Hackett, P.N. Shevock and S.R. Khan, "Madin-Darby canine kidney cells are injured by exposure to oxalate and to calcium oxalate crystals", *Urological Research*, vol. 22, pp. 197-204, 1994.
- [219] J.A. Jonassen, R. Cooney, L. Kennington, K. Gravel, T. Honeyman and C.R. Scheid, "Oxalate-induced changes in the viability and growth of human renal epithelial cells", *Journal of the American Society of Nephrology*, vol. 10, pp. S446-S451, 1999.
- [220] J.A. Jonassen, L.C. Cao, T. Honeyman and C.R. Scheid, "Mechanisms mediating oxalate-induced alterations in renal cell functions", *Critical reviews Eukaryotic Gene Expression*, vol. 13, pp. 55-72, 2003.
- [221] M.S. Hammes, J.C. Lieske, S. Pawar, B.H. Spargo and F.G. Toback, "Calcium oxalate monohydrate crystals stimulate gene expression in renal epithelial cells", *Kidney International*, vol. 48, pp. 501-509, 1995.
- [222] J.A. Wesson, R.J. Johnson, M. Mazzali, A.M. Beshensky, S. Stietz, C. Giachelli, L. Liaw, C.E. Alpers, W.G. Couser, J.G. Kleinman and J. Hughes, "Osteopontin is a critical inhibitor of calcium oxalate formation and retention in renal tubules", *Journal of the American Society of Nephrology*, vol. 14, pp. 139-147, 2003.
- [223] S.R. Khan, J.M. Johnson, A.B. Peck, J.G. Cornelious and P.A. Glenton, "Expression of osteopontin in rat kidneys: Induction during ethylene glycol induced calcium oxalate nephrolithiasis", *The Journal of Urology*, vol. 168, pp. 1173-1181, 2002.

- [224] M. Tsujihata, O. Miyake, K. Yoshimura, K. Kakimoto, S. Takahara and A. Okuyama, "Fibronectin as a potent inhibitor of calcium oxalate urolithiasis", *The Journal of Urology*, vol. 164, pp. 1718–1723, 2000.
- [225] M. Tsujihata, O. Miyake, K. Yoshimura, K. Tsujikawa, N. Tei and A. Okuyama, "Renal tubular cell injury and fibronectin", *Urological Research*, vol. 31, pp. 368–373, 2003.
- [226] V. Petronelli, D. Penzo, L. Scorrano, P. Bernardi and F. Di Lisa, "The mitochondrial permeability transition, release of cytochrome c and cell death. Correlation with the duration of pore openings in situ", *The Journal of Biological Chemistry*, vol. 276, pp. 12030-12034, 2001.
- [227] S.R. Khan, F. Atmani, P. Glenton, Z. Hou, D.R. Talham and M. Khurshid, "Lipids and membranes in the organic matrix of urinary calcific crystals and stones", *Calcified Tissue International*, vol. 59, pp. 357-365, 1996.
- [228] S.R. Khan, P.N. Shevock and R.L. Hackett, "Acute hyperoxaluria, renal injury and calcium oxalate urolithiasis", *The Journal Urology*, vol. 147, pp. 226-230, 1992.
- [229] N. Li, F.X. Yi, J.L. Spurrier, C.A. Bobrowitz and A.P. Zou, "Production of superoxide through NADH oxidase in thick ascending limb of the loop in rat kidney" *American Journal of Physiology Renal Physiology*, vol. 282, pp. F1111– F1119, 2002.
- [230] F.D. Khand, M.P. Gordge, W.G. Robertson, A.A. Noronha-Dutr and J.S. Hothersall, "Mitochondrial superoxide production during oxalate mediated oxidative stress in renal epithelial cells", *Free Radical Biological and Medicine*, vol. 32, pp. 1339–1350, 2002.
- [231] J.A. Jonassen, L.C. Cao, T. Honeyman and C.R. Scheid, "Intracellular events in the initiation of calcium oxalate stones", *Nephron Experimental Nephrology*, vol. 98, pp. e61–e64, 2004.
- [232] J.R. Asplin, "Evaluation of the kidney stone patient", *Seminars in Nephrology*, vol. 28, pp. 99-110, 2008.
- [233] J.H. Parks, E. Goldfisher, J.R. Asplin and F.L. Coe, "A single 24-hour urine collection is inadequate for the medical evaluation of nephrolithiasis", *The Journal of Urology*, vol. 167, pp. 1607-12, 2002.
- [234] J.M. Teichman, "Clinical practice. Acute renal colic from ureteral calculus" *The New England Journal of Medicine*, vol. 350, pp. 684-93, 2004.

- [235] J.A. McAteer, M.R. Bailey, J.C.Jr. Williams, R.O. Cleveland, and A.P. Evan, "Strategies for improved shock wave lithotripsy", *Minerva Urologica Nefrologica*, vol. 57, pp. 271-287, 2005.
- [236] L.R. Willis, A.P. Evan, B.A. Connors, Y. Shao, P.M. Blomgren, J.H. Pratt, N.S. Fineberg and J.E. Lingeman, "Shockwave lithotripsy: dose-related effects on renal structure, hemodynamics, and tubular function", *Journal of Endourology*, vol. 19, pp. 90-101, 2005.
- [237] G.M. Preminger, D.G. Assimos, J.E. Lingeman, S.Y. Nakada, M.S. Pearle and J.S.Jr. Wolf, "Chapter 1: AUA guideline on management of staghorn calculi: diagnosis and treatment recommendations", *The Journal of Urology*, vol. 173, pp. 1991-2000, 2005.
- [238] M.I. Paik, M.A. Wainsten, J.P. Spirnak, N. Hampel and M.I. Resnick, "Current indications for open stone surgery in the treatment of renal and ureteral calculi", *The Journal of Urology*, vol. 159, pp. 374-9, 1998.
- [239] C.Y. Pak and M.I. Resnick, "Medical therapy and new approaches to management of urolithiasis", *The Urologic Clinics of North America*, vol. 27, pp. 243-53, 2000.
- [240] C.L. Wabner and C.Y. Pak, "Effect of orange juice consumption on urinary stone risk factors", *The Journal of Urology*, vol. 149, pp. 1405-8, 1993.
- [241] S. Verma and S.P. Singh, "Current and future of herbal medicines", *Veterinary world*, vol, 1, pp. 347-350, 2008.
- [242] A. Aggarwal, S.K. Singla and C. Tandon, "Urolithiasis: Phytotherapy as an adjunct therapy", *Indian Journal of Experimental Biology*, vol. 53, pp. 103-111.
- [243] L.M. Sharma and R.K.D. Peterson, "The benefits and risks of producing pharmaceutical proteins in plants", *Risk Management Matters*, vol. 2, pp. 28-33, 2004.
- [244] M.M. Belovic, J.S. Mastilovic, A.M. Torbica, J.M. Tomic, D.R. Stanic and N.R. Dzinic, "Potential of Bioactive Proteins and Peptides for Prevention and Treatment of Mass Non-Communicable Diseases", *Food and Feed Research*, vol. 38, pp. 51-62, 2011.
- [245] S. Brien, G. Lewith, A. Walker, S.M. Hicks and D. Middleton, "Bromelain as a Treatment for Osteoarthritis: a Review of Clinical Studies", *Evidence-Based Complementary and Alternative Medicine*, vol. 1, pp. 251-257, 2004.

- [246] S. Lee-Huang, P.L. Huang, A.S. Bourinbaiar, H.C. Chen and H.F. Kung, "Inhibition of the Integrase of human immunodeficiency virus (HIV) type 1 by anti-HIV plant proteins MAP30 and GAP31", *Proceedings of the National Academy of Sciences of the United States of America*, vol. 92, pp. 8818-8822, 1995.
- [247] S.N. Pillay, J.R. Asplin and F.L. Coe, "Evidence that calgranulin is produced by kidney cells and is an inhibitor of calcium oxalate crystallization", *The American Journal of physiology*, vol. 44, pp. F255-61, 1998.
- [248] R.K. Bijarnia, T. Kaur, S.K. Singla and C. Tandon, "A novel calcium oxalate crystal growth inhibitory protein from the seeds of *Dolichos biflorus* (L.)", *Protein and Peptide Letters*, vol. 16, pp. 161-168, 2009.
- [249] T. Kaur, R.K. Bijarnia, S.K. Singla and C. Tandon, "Purification and characterization of an anticalcifying protein from the seeds of *Trachyspermum ammi* (L.)", *Protein and Peptide Letters*, vol. 16, pp. 173-181, 2009.
- [250] T. Kaur, R.K. Bijarnia, S.K. Singla and C. Tandon, "*In vivo* efficacy of *Trachyspermum ammi* anticalcifying protein in urolithiatic rat model", *Journal of Ethnopharmacology*, vol. 126, pp. 459-462, 2009.
- [251] A. Aggarwal, S. Tandon, S.K. Singla and C. Tandon, "A novel antilithiatic protein from *Tribulus terrestris* having cytoprotective potential", *Protein and Peptide Letters*, vol. 19, pp. 812-819, 2012.
- [252] S. Dwivedi and D. Chopra. "Revisiting *Terminalia arjuna* – An ancient Cardiovascular Drug", *Journal of Traditional and Complementary Medicine*, vol. 4, pp. 224-231, 2014.
- [253] A. Mittal, S. Tandon, S.K. Singla and C. Tandon (2015) "*In vitro* studies reveal antiurolithic effect of *Terminalia arjuna* using quantitative morphological information from computerized microscopy", *International Brazilian Journal Urology*, vol. 41, pp. 935-944, 2015.
- [254] N. Mago, I.B. Sofat and R.K. Jethi, "Effect of an Ayurvedic Compound Preparation on the Ability of Rat Urine to Influence Mineral Phase Formation", *The Indian Journal of Medical Research*, vol. 90, pp. 77-81, 1989.
- [255] B. Hess, U. Meinhardt, L. Zipperle, R. Giovanoli and P. Jaeger, "Simultaneous measurements of calcium oxalate crystal nucleation and

- aggregation: impact of various modifiers”, *Urological Research*, vol. 23, pp. 231-238, 1995.
- [256] S. Chutipogtanate, Y. Nakagawa, S. Sritippayawan, J. Pittayamateekul, P. Parichatikanond, B.R. Westley, F.E. May, P. Malasit and V. Thongboonkerd, “Identification of human urinary trefoil factor1 as a novel calcium oxalate crystal growth inhibitor”, *Journal of Clinical Investigation*, vol. 115, pp. 3613–3622, 2005.
- [257] C.Y. Zhang, W.H. Wu, J. Wang and M.B. Lan, “Antioxidant properties of polysaccharide from the Brown Seaweed *Sargassum graminifolium* (Turn.), and its effect on calcium oxalate crystallization”, *Marine Drugs*, vol. 10, pp. 119-130, 2012.
- [258] C.M. Liyana-Pathiranan and F. Shahidi, “Antioxidant activity of commercial soft and hard wheat (*Triticum aestivum* L) as affected by gastric pH conditions”, *Journal of Agricultural and Food Chemistry*, vol. 53, pp. 2433-2440, 2005.
- [259] A. Aggarwal, S. Tandon, S.K. Singla and C. Tandon, “Diminution of oxalate induced renal tubular epithelial cell injury and inhibition of calcium oxalate crystallization *in vitro* by aqueous extract of *Tribulus terrestris*”, *International Brazilian Journal of Urology*, vol. 36, pp. 480-488, 2010.
- [260] K.P. Aggarwal, S. Tandon, P.K. Naik, S.K. Singh and C. Tandon, “Peeping into human renal calcium oxalate stone matrix: characterization of novel proteins involved in the intricate mechanism of urolithiasis”, *PLoS ONE*, vol. 8, pp. e69916, 2013.
- [261] B.C. Jeong, C. Kwak, K.S. Cho, B.S. Kim, S.K. Hong, J.I. Kim, C. Lee and H.H. Kim, “Apoptosis induced by oxalate in human renal tubular epithelial HK-2 cells”, *Urological Research*, vol. 33, pp. 87-92, 2005.
- [262] R.M. Habibi, R.A. Mohammadi and J.A. Najafabadi, “Effects of Polygonum aviculare Herbal Extract on Proliferation and Apoptotic Gene Expression of MCF-7”, *DARU Journal of Pharmaceutical Sciences*, vol. 19, pp. 326-331, 2011.
- [263] T. Semangoen, S. Sinchaikul, S.T. Chen and V. Thongboonkerd, “Altered proteins in MDCK renal tubular cells in response to calcium oxalate dehydrate crystal adhesion: a proteomics approach”, *Journal of Proteome Research*, vol. 7, pp. 2889-2896, 2008.

- [264] S. Allen, J. Sotos, M.J. Sylte and C.J. Czuprynski, “Use of Hoechst 33342 Staining to Detect Apoptotic Changes in Bovine Mononuclear Phagocytes Infected with *Mycobacterium Avium* subsp. *Paratuberculosis*”, *Clinical and Diagnostic Laboratory Immunology*, vol. 8, pp. 460–464, 2001.
- [265] M. Bradford, “A rapid and sensitive method for the quantitation of microgram quantities of protein utilizing the principle of protein-dye binding”, *Analytical Biochemistry*, vol. 72, pp. 248-54, 1976.
- [266] X.m. Xu, A. Rose, S. Muthuswamy, S. Y. Jeong, S. Venkatakrishnan, Q. Zhao, and I. Meier, “NUCLEAR PORE ANCHOR, the Arabidopsis Homolog of Tpr/Mlp1/Mlp2/Megator, Is Involved in mRNA Export and SUMO Homeostasis and Affects Diverse Aspects of Plant Development”, *The Plant Cell*, vol. 19, pp. 1537–1548, 2007.
- [267] R. Selvam and P. Kalaiselvi, “Oxalate binding proteins in calcium oxalate nephrolithiasis”, *Urological Research*, vol. 31, pp. 242–256, 2003.
- [268] E. Jankowsky, C.H. Gross, S. Shuman and A.M. Pyle, “Active disruption of an RNA-protein interaction by a DExH/D RNA helicase”, *Science*, vol. 291, pp. 121–125, 2001.
- [269] M. Takahashi, M. Higuchi, H. Matsuki, M. Yoshita, T. Ohsawa, M. Oie and M. Fujii, “Stress granules inhibit apoptosis by reducing reactive oxygen species production”, *Molecular and Cellular Biology*, vol. 33, pp. 815–829, 2013.
- [270] B. Lu, T. Liu, J.A. Crosby, J. Thomas-Wohlever, I. Lee and C.K. Suzuki, “The ATP-dependent Lon protease of *Mus musculus* is a DNA-binding protein that is functionally conserved between yeast and mammals”, *Gene*, vol. 306, pp. 45–55, 2003.
- [271] L.H. Pearl and C. Prodromou, “Structure and mechanism of the Hsp90 molecular chaperone machinery”, *Annual Review of Biochemistry*, vol. 75, pp. 271–294, 2006.
- [272] J.C. Young, V.R. Agashe, K. Siegers and F.U. Hartl, “Pathways of chaperone-mediated protein folding in the cytosol”, *Nature Reviews Molecular Cell Biology*, vol. 5, pp. 781–791, 2004.
- [273] S. Dias, S.V. Shmelkov, G. Lam and S. Rafii, “VEGF(165) promotes survival of leukemic cells by Hsp90-mediated induction of Bcl-2 expression and apoptosis inhibition”, *Blood*, vol. 99, pp. 2532–2540, 2002.

- [274] C.F. Verkoelen, “Crystal retention in renal stone disease: A crucial role for the glycosaminoglycan hyaluronan?”, *Journal of the American Society of Nephrology*, vol. 17, pp 1673–1687, 2006.
- [275] S.R. Khan and R.L. Hackett, “Role of organic matrix in urinary stone formation: An ultrastructural study of crystal matrix interface of calcium oxalate monohydrate stones”, *The Journal of Urology*, vol. 150, pp. 239–245, 1993.
- [276] S.R. Khan, S.A. Maslamani, F. Atmani, P.A. Glenton, F.J. Opalko, S. Thamilselvan and C. Hammett- Stabler, “Membranes and their constituents as promoters of calcium oxalate crystal formation in human urine”, *Calcified Tissue International*, vol. 66, pp. 90– 96, 2000.
- [277] A. Chaudhary, S.K. Singla and C. Tandon, “*In vitro* evaluation of *Terminalia arjuna* on calcium phosphate and calcium oxalate crystallization”, *Indian Journal of Pharmaceutical Sciences*, vol. 72, pp. 340-345, 2010.
- [278] M. Beghalia, S. Ghalem, H. Allali, A. Belouatek and A. Marouf, “Inhibition of calcium oxalate monohydrate crystal growth using Algerian medicinal plants”, *Journal of Medicinal Plants Research*, vol. 2, pp. 066-070, 2008.
- [279] A. Guerra, T. Meschi, F. Allegri, B. Prati, A. Nouvenne, E. Fiaccadori and L. Borghi, “Concentrated urine and diluted urine: the effects of citrate and magnesium on the crystallization of calcium oxalate induced *in vitro* by an oxalate load”, *Urological Research*, vol. 34, pp. 359–364, 2006.
- [280] C.F. Verkoelen, B.G. Van der Boom, F.H. Schroder and J.C. Romijn, “Cell cultures and nephrolithiasis”, *World Journal of Urology*, vol. 15, pp. 229-235, 1997.
- [281] Y. Kohjimoto, L. Kennington, C.R. Scheid and T.W. Honeyman, “Role of phospholipase A2 in the cytotoxic effects of oxalate in cultured renal epithelial cells”, *Kidney International*, vol. 56, pp. 1432–1441, 1999.
- [282] F. Atmani, G. Farell and J.C. Lieske, “Extract from *Herniaria hirsuta* coats calcium oxalate monohydrate crystals and blocks their adhesion to renal epithelial cells”, *The Journal of Urology*, vol. 172, pp. 1510-1514, 2004.
- [283] E.F. Plow, T.A. Haas, L. Zhang, J. Loftus and J.W. Smith, “Ligand binding to integrins”, *The journal of biological chemistry*, vol. 275, pp. 21785-21788, 2000.

- [284] M.W. Bigelow, J.H. Wiessner, J.G. Kleinman and N.S. Mandel, “Calcium oxalate crystal membrane interactions: dependence on membrane lipid composition”, *The Journal of Urology*, vol. 155, pp. 1094–8, 1996.
- [285] S.R. Khan, “Interactions between stone forming calcific crystals and macromolecules”, *Urologia Internationalis*, vol. 59, pp. 59–71. 1997.
- [286] S.R. Khan and D.J. Kok, “Modulators of stone formation”, *Frontiers in Bioscience*, vol. 9, pp. 1450–1482, 2004.
- [287] S. Chutipongtanate, Y. Nakagawa, S. Sritippayawan, J. Pittayamateekul, P. Parichatikanond, B.R. Westley, F.E. May, P. Malasit and V. Thongboonkerd, “Identification of human urinary trefoil factor 1 as a novel calcium oxalate crystal growth inhibitor”, *The Journal of Clinical Investigation*, vol. 115, pp. 3613–3622, 2005.
- [288] M. Mazzali, T. Kipari, V. Ophascharoensuk, J.A. Wesson, R. Johnson and J. Hughes, “Osteopontin – a molecule for all seasons”, *QJM*, vol. 95, pp. 3–13, 2002.
- [289] V.K. Devi, R. Baskar and P. Varalakshmi, “Biochemical effects in normal and stone forming rats treated with the ripe kernel juice of Plantain (*Musa Paradisiaca*)”, *Ancient Science of Life*, vol. 3-4, 1993, pp. 451 – 461, 1993.
- [290] R. Mayee and A. Thosar, “Evaluation of *Lantana camara* Linn. (*Verbenaceae*) for antiurolithiatic and antioxidant activities in rats”, *International Journal of Pharmaceutical and Clinical Research*, vol. 3, pp. 10-14, 2011.
- [291] L. Samal, A.K. Pattanaik, C. Mishra, B.R. Maharana, L.N. Sarangi and R.K. Baithalu, “Nutritional strategies to prevent urolithiasis in animals”, *Veterinary World*, vol. 4, pp. 142-144, 2011.
- [292] K.R.U. Gilhotra and A.J.M. Christina, “Effect of *Rotula aquatica* Lour. on ethylene-glycol induced urolithiasis in rats”, *International Journal Drug Development and Research*, vol. 3, pp. 273-280, 2011.
- [293] P. Soundararajan, R. Mahesh, T. Ramesh and V.H. Begum, “Effect of *Aerva Lanata* on calcium oxalate urolithiasis in rats”, *Indian journal of experimental biology*, vol. 44, pp. 981-986, 2006.
- [294] K.J. Kore, R.V. Shete, P.J. Jadhav and M.P. Kabra, “Antiuro lithiatic effects of hydroalcoholic extract of *lawsonia inermis* L leaves”, *International Journal of Universal Pharmacy and Life Sciences*, vol. 1, pp. 81-95, 2011.

- [295] A.J. Christina, K. Ashok, M. Packialakshmi, G.C. Tobin, J. Preethi and N. Muruges, "Antilithiatic effect of *Asparagus racemosus* Wild on ethylene glycol-induced lithiasis in male albino Wistar rats", *Methods and Findings in Experimental and Clinical Pharmacology*, vol. 27, 633-8. 2005.
- [296] V.S. Joshi, B.B. Parekh, M.J. Joshi and A.D. Vaidya, "Inhibition of the growth of urinary calcium hydrogen phosphate dehydrate crystals with aqueous extracts of *Tribulus terrestris* and *Bergenia ligulata*", *Urological Research*, vol. 33, pp. 80-6, 2005.

LIST OF PUBLICATIONS

- Mittal A, Tandon S, Singla SK and Tandon C (2016). *In vitro* inhibition of calcium oxalate crystallization and crystal adherence to renal tubular epithelial cells by *Terminalia arjuna*. *Urolithiasis*. 44(2):117-125 (IF: 1.454)
- Mittal A, Tandon S, Singla SK and Tandon C (2015). *In vitro* studies reveal antiurolithic effect of *Terminalia arjuna* using quantitative morphological information from computerized microscopy. *Int Braz J Urol*. 41(5):935-944 (IF: 1.2)

PUBLICATIONS IN CONFERENCES

- Mittal A, Tandon S, Singla SK and Tandon C (2015). *In vitro* assessment of antilithiatic property of *Terminalia arjuna* on calcium oxalate crystallization and its cytoprotective role on renal epithelial cells. *Canadian urological association journal supplement* 9(5-6Suppl2):S58. (Impact factor: 1.92) [Ottawa, Canada, 27-30 June 2015]
- Mittal A, Tandon S, Singla SK and Tandon C (2015). Inhibition of Calcium Oxalate Crystallization and Diminution of Oxalate Induced Renal Tubular Epithelial Cell Injury *in vitro* by *Terminalia arjuna*. *The journal of urology supplement* 193(4): e415-e416. (Impact factor: 3.753) [New Orleans, USA 15-19 May 2015]
- Mittal A, Singla SK and Tandon C (2014) Inhibition of calcium oxalate crystallization *in vitro* by aqueous extract of *Terminalia arjuna*. *Indian Journal of Urology supplement* 30(5):172. [New Delhi, India, 30 January-2 February 2014]

LIST OF CONFERENCES ATTENDED

- 70th Canadian Urological Association (CUA) Annual meeting from. 27-30 June 2015, Ottawa, Ontario, Canada. Unmoderated Poster presentation on “*In vitro* assessment of antilithiatic property of *Terminalia arjuna* on calcium oxalate crystallization and its cytoprotective role on renal epithelial cells”.
- 110th American Urological Association (AUA) Annual meeting. 15 – 19 May 2015, New Orleans, LA, USA. Moderated poster presentation on “Inhibition of Calcium Oxalate Crystallization and Diminution of Oxalate Induced Renal Tubular Epithelial Cell Injury *in vitro* by *Terminalia arjuna*”.
- 47th Annual Conference of Urological society of India (USICON). 30th January – 2nd February 2014, New Delhi, India. Moderated poster presentation on “Inhibition of calcium oxalate crystallization *in vitro* by aqueous extract of *Terminalia arjuna*”.